ADDIS ABABA UNIVERSITY

COLLEGE OF TECHNOLOGY AND BUILT ENVIRONMENT (CTBE)

SCHOOL OF CIVIL AND ENVIRONMENTAL ENGINEERING

PhD DISSERTATION ON:

SEDIMENT YIELD PREDICTION IN UNGAUGED CATCHMENT AND ITS IMPACT ON RESERVOIR DEVELOPMENT IN ETHIOPIA HIGHLANDS

BY

BAYU GETA BIHONEGN

ADVISOR: Dr. ADMASU GEBEYEHU

March, 2026

SEDIMENT YIELD PREDICTION IN UNGAUGED CATCHMENT AND ITS IMPACT ON RESERVOIR DEVELOPMENT IN ETHIOPIA HIGHLAND'S

PhD Dissertation

By:

Bayu Geta Bihonegn

Under the supervision of:

Dr. Admasu Gebeyehu (Professor of Practice, Addis Ababa University)

A Dissertation Submitted to the Graduate School of Addis Ababa University, Addis Ababa Institute of Technology, School of Civil and Environmental Engineering, in partial fulfillment of the requirements for the degree of

Doctor of Philosophy

in

Civil Engineering (Specialization in Hydraulic Engineering)

Addis Ababa, Ethiopia

March 2026

APPROVAL SHEET

Addis Ababa University (AAU)

College Of Technology and Built Environment (CTBE)

Doctoral Dissertation Approval Sheet

This is to certify that the dissertation presented by Bayu Geta entitled, **Sediment Yield Prediction in Ungauged Catchment and Its Impact on Reservoir Development in Ethiopia Highland's,** and submitted in partial fulfillment of the requirements for the degree of Doctor of Philosophy in Civil Engineering (Hydraulic Engineering) complies with the regulation of the university and meets the accepted standards with respect to quality and originality.

Professor Admasu Gebeyehu		23-03-26
Supervisor	Signature	Date

APPROVED BY BOARD OF EXAMINERS:

Professor Mekonen Ayana External Examiner	Signature	18.3.2026 Date
Dr. Bayou Chanie Internal Examiner	Signature	24/03/2026 Date
Dr. Yenesew Mengestie Chairperson	Signature	26 Mar. 26. Date
Dr. Yenesew Mengestie (Dean, SCEE)	Signature	26 Mar. 26 Date

DECLARATION OF AUTHORSHIP

I, the undersigned, do hereby solemnly declare that this PhD dissertation is my original work and has not been submitted in part or whole for any academic qualification or degree at this or any other university. I also declare that this dissertation is of the highest ethical standards of research scholarship, with no cases of plagiarism, fabrication, or misrepresentation.

DEDICATION

This work is dedicated to:

- My father, Geta Bihonegn, my mother, Workie Megabayaw, and Fasika Tsehaw, without your support, this chapter of my life would not have been possible. We love you deeply.
- I also want to honour the wise woman who stands by me: my wife, Mahilet, and my little one, Yonatan.

Bayu Geta Bihonegn _____ _____

Name of the Author Signature Date

ACKNOWLEDGEMENTS

First and foremost, I would like to thank Almighty God for His never-ending love, divine grace, and perpetual guidance in my studies and life. This work is a manifestation of His blessings, without which all this could not have been possible.

I am profoundly indebted to my supervisor, Dr. Admasu Gebeyehu, whose exceptional guidance, intellectual reflexivity, and unwavering encouragement were the pillars of my Ph.D. journey. His expertise, patience, and willingness to engage in discussions of my research problems at every stage were integral to the development of this work. I consider myself extremely fortunate to have had such a dedicated supervisor who not only nurtured my academic skills but also inspired me to strive for excellence.

I would like to extend my heartfelt gratitude to the Ethiopian Ministry of Water and Energy (MoWE), National Meteorological Agency (NMA), and the Ethiopian Mapping Agency for their unconditional support in facilitating essential hydro-meteorological, soil, and geospatial data. These datasets formed the foundation of this research. I also highly value the Ministry of Education (MoE) and Wollo University for providing me with the chance to continue my academic career in a friendly atmosphere where innovation and knowledge flourish.

To my parents, Geta Bihonegn, Workie Megabayaw, and Fasika Tsehaw, I have a debt of gratitude for life for their unwavering love, sacrifices, and faith in me. They have been my inspiration and rock in every adversity. My siblings, Genzeb Geta, Temesgen Geta, Habtam Geta, and Ketemaw Geta, thank you for backing me with unfailing support.

Last but not least, to my dear wife, Mahilet Tesfay, and my dear baby, Yonatan Bayu, words cannot convey how thankful I am for your boundless patience, sacrifice, and love. This success is yours as much as it is mine, and I dedicate it to you both.

To everyone who supported this journey, either directly or indirectly, thank you. Your support has left an indelible imprint on my work and life.

ABSTRACT

Predicting sediment load for ungauged catchments remains the most uncertain and complex problem in hydrology. A clear understanding of sediment yield, transport, and deposition processes in river basins is critical to developing efficient measures for mitigating reservoir sedimentation and predicting reservoir lifespans. Sedimentation, a major issue, significantly affects the sustainability and operational efficiency of reservoirs and deteriorates dam operation. Reservoir sedimentation is heavily influenced by the supply of sediments from catchments in the upper reaches, influencing riverbank deposition of sediments as well.

Although reliable sediment data is vital for the planning of effective dams and water resource systems, most parts of the world, especially in developing countries like Ethiopia, lack hydrological monitoring and sediment data. This is especially true in the highlands of the Awash and Abbay (Blue Nile) river basins, where sediment measurements are limited. Meanwhile, these basins are home to important water-related projects such as the Grand Ethiopian Renaissance Dam (GERD) and several proposed irrigation and hydropower initiatives. Given this gap, there is a pressing need to develop viable alternative models for estimating suspended sediment output.

The main objective of this study was to estimate suspended sediment yield in the ungauged Abbay and Awash catchments. To achieve this, the research specifically aimed to (1) assess the effects of land use and land cover changes (LULC) on sediment yield dynamics in the Upper Awash River Basin using the QGIS-based Soil and Water Assessment Tool PLUS model (QSWATPLUS), (2) analyze the spatial and temporal variability of suspended sediment yield in the Upper Blue Nile Basin using QSWATPLUS, (3) develop an alternative empirical model for estimating suspended sediment yield using conceptual model, and (4) compare different modeling approaches used for suspended sediment yield prediction.

In this study, the Quantum Geography Information System Interference Soil and Water Assessment Tool Plus (QSWAT-PLUS) model was used to assess the impacts of land use and land cover (LULC) on sediment load in the Upper Awash River Basin (UARB), which is experiencing sedimentation issues in the Koka reservoir. The Modified Universal Soil Loss Equation within the SWAT Plus model was employed to simulate streamflow and sediment yield, thereby identifying spatiotemporal hotspots of sediment variability across various reservoir catchments. The QSWAT Plus model incorporated digital elevation models, climate data, land use, soil types, and slope characteristics of the Upper Blue Nile Basin (UBNB). The calibration and validation of monthly

streamflow and sediment yield were conducted using the Sobol tool algorithm from the SWAT Toolbox. Furthermore, the QSWAT+ model divided the Kessie watershed into 18 sub-basins in order to analyze each catchment's characteristics. The performance testing of the alternative model utilized a data set spanning 11 years from six watersheds, the assessment of which was conducted through the utilization of model statistics. Principal component analysis (PCA) was used to identify significant variables affecting sediment yield. In addition, data reduction techniques, including the Gamma test (GT), classification and regression trees (CART), and stepwise regression (SR), were used to select the most influential factors on suspended sediment output. Finally, multiple linear regression (MLR) and artificial neural networks (ANN) were used to develop a regional model for estimating suspended sediment yield (SSY) in ungauged catchments.

Results indicated that the mean annual sediment yield entering the Koka reservoir under the 2005, 2010, and 2015 LULC scenarios was about 26.03, 26.34, and 28.33 t/ha/yr, respectively. In general, streamflow, surface runoff, and sediment output increased by 4.5%, 12.68%, and 8.84%, respectively, due to the rapid change of LULC from 2000 to 2015. Temporally, the sediment yield at the upstream side of the Koka Dam watershed was 60.8% during the wet season. The upward trend indicates that changes in LULC bring increased sediment loads, which may endanger reservoir sustainability and watershed health. Simulation outputs revealed that filter strips, contour farming, and terracing best management practices (BMPs) decreased sediment yield by 60%, 65%, and 80%, respectively. Terraces were most effective in controlling erosion in the priority Sub-basin upstream of the Koka Dam.

Spatial variability in sediment yield within the Kessie Sub-basin was observed to range extensively from 0 to 67.6 t/ha/yr. A further analysis revealed that 42.04% of the watershed falls within the critical erosion zone and 39.48% falls within the sub-critical zone. This spatial variability is attributed to a combination of environmental factors and human activities. It is imperative to note that this critical amount of sediment yield has the potential to impact the service life of the reservoir. It is estimated that approximately 90% of the annual sediment load was transported during the wet season. These BMPs can be effectively used to minimize sediment transport, which controls reservoir sedimentation in the Upper Blue Nile Basin.

Out of 24 variables screened, seven were found to be the most dominant significant factors: drainage area, stream slope, main channel length, rainfall, agricultural land cover, forest cover,

and streamflow. Collectively, climatic, geomorphological, and hydrological variables were found to be major drivers of suspended sediment yield (SSY). Following calibration and validation of streamflow and suspended sediment yield data at the Kessie gauge station using the QSWATPLUS model, a new empirical model was developed to estimate suspended sediment yield in the ungauged catchment. The new empirical model developed was verified based on three statistical performance metrics, proving to be highly accurate and versatile in varying environmental conditions, even in areas where data are limited. This improves its credibility in sediment management and watershed conservation planning.

In all the tested models, the Genetic Algorithm-based Artificial Neural Network (GT-ANN) achieved superior performance compared to the ANN and Multiple Linear Regression (MLR) models. GT-ANN model under calibration (R^2 = 99.9%, RMSE = 12,631.6 t/yr, and MAE = 10,354.9 t/yr) and under validation (R^2 = 82%, RMSE = 139,944 t/yr, and MAE = 136,036 t/yr) demonstrated that this model is effective in estimating sediment yield.

Overall, determining influential SSY drivers and using AI-driven modeling can empower water resource managers to effectively estimate SSY amounts in ungauged basins, promoting improved sediment management and conservation plans.

Keywords: Sediment Yield, Ungauged Catchment, Empirical Model, Suspended sediment yield, Physical Model, Artificial Niral Network, Data Reduction Technique

List of Original Papers

This dissertation is based on the following four original papers, which are listed from paper 1 to 4.

Paper 1: Bihonegn, B.G., Awoke, A.G., 2023. Evaluating the impact of land use and land cover changes on sediment yield dynamics in the upper Awash basin, Ethiopia, the case of Koka reservoir. Heliyon 9, e23049. https://doi.org/10.1016/j.heliyon.2023.e23049

Paper2: Bihonegn BG, Awoke AG (2025) Spatiotemporal sediment yield variability in the Upper Blue Nile Basin, Ethiopia. Earth Sci Informatics 18:1 22. https://doi.org/10.1007/s12145-025-01821-0

Paper 3: Bihonegn, B. G. & Awoke, A. G. (2025) Developing an empirical model for estimating suspended sediment yield in ungauged watersheds of the Ethiopian Highlands. *Model. Earth Syst. Environ.* **11**(6), 1–19. https://doi.org/10.1007/s40808-025-02608-4

Paper 4: Bihonegn, B. G., & Awoke, A. G. (2025). Developing an alternative regional suspended sediment yield estimation model for ungauged catchments: Ethiopia Highlands. Hydrological Sciences Journal, 1–19. https://doi.org/10.1080/02626667.2025.2555850

TABLE OF CONTENTS

Contents

LIST OF TABLES

LIST OF FIGURES

LIST OF ACRONYMS

AI	Artificial Intelligence
ANN	Artificial Neural Network
ASSY	Area Specific Suspended Sediment Yield
BNB	Blue Nile Basin
BMPs	Best Management Practices
BS	Baseline scenarios
CART	Classification and Regression Trees
DEM	Digital Elevation Model
DRT	Data Reduction Techniques
ENMA	Ethiopian National Meteorological Institute
EROS	Earth Resources Observation and Science
ETM	Enhanced Thematic Mapper
FS	Filter Strip
GERD	Grand Ethiopian Renaissance Dam
GT	Gamma Test
HRUs	Hydrological Response Unit
KMO	Kaiser-Meyer-Olkin
LULC	Land Use and Land Cover
LSTM	Long Short-Term Memory
MAE	Mean Absolute Error
MLR	Multiple Linear Regression
MoWE	Ministry of Water and Energy
MUSLE	Modified Universal Loss Equation
NMA	National Meteorological Agency
NSE	Nash Sutcliffe Efficiency
OLI	Operational Land Imager
ORG	Original
PBIAS	Percent Bias
PCA	Principal Component Analysis
QGIS	Quantum Geography Information System
QSWATPLUS	QGIS-based Soil and Water Assessment Tool PLUS
R^2	Coefficient of Determination
RMSE	Root Mean Square Error
RUSLE	Revised Universal Loss Equation
SDR	Sediment Delivery Ratio
SL	Sediment Load
SY	Sediment Yield
SSL	Suspended Sediment Load
SR	Stepwise Regression

SRC	Sediment Rating Curve
SSC	Suspended Sediment Concentration
SSY	Suspended Sediment Yield
SWAT	Soil and Water Assessment Tool
UARB	Upper Awash River Basin
UBNB	Upper Blue Nile Basin
USGS	United States Geological Survey
USLE	Universal Soil Loss Equation
WALRC	Water and Land Resource Center

1. INTRODUCTION

1.1 Background of the study

Ethiopia has twelve major river basins with an amount of 124.4 billion m^3 of river water and 30 billion m^3 of groundwater potential sources (Melesse et al., 2013). Among them, the Abbay River is the longest river and the most utilized river in Ethiopia, which is used for irrigation, water supply, hydropower, and other purposes. Numerous large-scale projects are being planned, designed, and built in the Abbay River basin. The Grand Ethiopian Renaissance Dam (GERD) is one of the largest projects that built in the Abbay River basin for hydropower generation to solve power outages for above 65 million Ethiopian people. Proper and cost-effective design is required to guarantee that those projects are functional for a long period. Predicting streamflow and sediment yield variables is crucial for the economic design of reservoirs.

Sediment yield is defined as the end product of soil erosion, which is the discharge of sediment load from the catchment or the concentration of sediment delivered to the point of interest in the river network over a stated period of time (Melesse et al., 2011) and the net result of the soil erosion and sediment deposition process (Haregeweyn et al., 2013). In a watershed, sediment yield includes erosion from the land surface, slopes, gullies, streams, and mass wasting minus sediment that is deposited after it is eroded but before it reaches the point of interest. Sediment erosion, transport, and deposition in fluvial systems are complex processes. It is governed by topography, hydrometeorology, catchment characteristics, channel hydraulic characteristics, sediment characteristics, and geology and land use /cover (Arnold et al., 2018). In the planning and designing of water-related development projects, the estimation of watershed sediment yield is critical.

Sediment sources have conventionally been assumed to as fields, hillsides, forests, construction sites, and so on, a range of spatially distributed sources around the river basin whose capacity to supply sediment varies with both climate inputs and how these areas are managed. It is necessary to identify sediment sources to implement appropriate strategies to control sediment mobilization and subsequent siltation of river channels and reservoirs (Carter et al., 2003). Mainly, sedimentation originates from the catchment area and the river system, then gradually settles in the reservoir.

Sediment has a major effect on the operation of dams and reservoir capacity. It is a major problem that affects several water resources engineering projects, such as reducing the reservoir capacity, obstructing the inlet of the dam intakes, and decreasing the discharge capacity of channels (Buyukyildiz and Kumcu, 2017), (Calsamiglia et al., 2018). Besides its impact on the design and management of hydro-systems, sedimentation has undesirable effects on water quality in rivers by decreasing the concentration of dissolved oxygen (Olyaie et al., 2015), (Shiau and Chen, 2015).

Sedimentation of reservoirs has direct and indirect effects on irrigation practices. The susceptibility of a reservoir to sedimentation depends on the sediment delivery of the source watercourse, the retention characteristics of the watershed, and the manner in which the flow is delivered from the natural source to the reservoir.

Reservoir sedimentation is a gradual accumulation of the incoming sediment load from a river. It is a universal and natural phenomenon. The eroded soil from the upper catchment area is carried into watercourses by flood and storm waters, resulting in tremendous sediment movement. Uncontrolled deforestation, forest fires, overgrazing, improper methods of tillage, and unwise agricultural and land use practices accelerate soil erosion, resulting in a large increase in sediment inflow into streams.

All reservoirs, which are manmade and natural lakes, are subjected to sediment inflow and deposition (Duru, 2015). Sediment accumulation in a reservoir is a serious problem that threatens the sustainability of the reservoir and has severe consequences on reservoir productivity during its operation time. It is also a serious off-site consequence of soil erosion that threatens the sustainability of dams built for various purposes throughout Ethiopia (N. Haregeweyn et al., 2008) as well as in other parts of the world. Though the ultimate destiny of all reservoirs is to become filled with sediment, the length of time that this takes depends on the sedimentation rate and how well the problem is addressed both during the planning stage and while reservoir sedimentation is occurring. To predict the reservoir sediment deposition pattern, evaluate its consequences on the reservoir yield, and identify an appropriate reservoir sediment management strategy, accurate quantification of long-term average sediment yield is needed.

Sedimentation is a problem for many dams around the world and is considered an invisible enemy. For each year, 0.5 to 1% reservoir capacity is lost due to sediment deposition in the world (Bachiller et al., 2019). The gradual loss of reservoir capacity reduces the effective life of dams. It also has tremendous economic and environmental impacts.

The existing and the newly constructed reservoirs of Ethiopia are under a similar threat of sedimentation problems (Haregeweyn et al., 2012a). Previous studies on sediment yield and impacts, conducted mainly in the northern parts of Ethiopia, have shown that the spatial variability of sediment yield in that region is generally high. The frequent power cuts and rationing-based electric power distribution recently experienced in the country are partially attributed to storage losses due to sedimentation (Haregeweyn et al., 2008). A number of efforts have been made to estimate sediment yield throughout the world, though few in Ethiopia. (Ermias et al., 2014) reported that the lifespan of dams in Ethiopia, specifically in two schemes, is almost five times shorter than originally anticipated. (Tamene and Vlek, 2008) studied reservoir siltation and siltation rate on 11 small reservoirs in the Tigray region, which is in the north of Ethiopia. He found that the annual average rate of capacity loss varies from 0.1 to 7.4% due to the wide contrast in environmental variables of catchments. In addition to this, his results showed that most of the reservoirs would be filled with sediment within less than 50% of their projected service time.

Long-term sediment yield data are required for the design of reservoir life and its storage capacity. It is important to know the problem of the design of reservoirs and dams, transport of sediment and pollutants in rivers, lakes, and estuaries, design of stable channels and dams, protection of fish and wildlife habitats, determination of the effects of watershed management, and environmental impact assessment (Cigizoglu, 2004). However, observed sediment yield data for all major river basins are limited in Ethiopia. This lack of suspended yield data has an impact on quantifying the actual suspended sediment load to the dam reservoirs while planning new reservoirs, which leads to the risky or non-economical design of reservoirs (Haregeweyn et al., 2013).

There are different methods that are used to predict erosion and sediment yield of the catchment. No single catchment sediment yield prediction method can be assumed to be applicable to all possible conditions. All methods have limitations and advantages, and the choice of the method to apply should consider a number of influencing factors (Basson, 2009). These influencing factors are catchment characteristics, site conditions, hydrologic, geomorphologic, and topographic factors, dam engineering requirements, availability of time, economics, data requirements, and data availability.

Sediment yield can be predicted using a range of approaches, from simple empirical models to detailed process-based simulations, as well as various watershed models that estimate runoff and other hydrological processes. Traditional regression-based methods relate sediment delivery to catchment characteristics such as drainage area, topography, climate, and vegetation in a straightforward manner. However, these methods have significant drawbacks: they cannot effectively identify the dominant controls on spatial variations in suspended sediment yield, have limited applicability beyond the regions where they were developed, and do not produce spatially detailed outputs needed for targeted erosion control. To address these limitations, current research integrates advanced physics-based models with machine learning techniques to achieve higher accuracy, broader applicability, and spatially distributed results essential elements for effective sediment management and prioritizing conservation efforts across different watersheds.

The Upper Awash and Blue Nile regions face significant challenges related to sediment management, primarily due to increased sedimentation driven by deforestation, agricultural practices, and urbanization. These factors contribute to decreased reservoir capacity and deteriorating water quality, worsening water resource management problems.

The main objective of this study is to estimate suspended sediment yield in ungauged catchments of the Abay and Awash River basins. In order to achieve this objective, the research focuses on several key methods: The impact of land use and land cover changes (LULC) on sediment dynamics in the Upper Awash River Basin was assessed using the QGIS-based Soil and Water Assessment Tool PLUS (SWATPLUS) model. The spatial and temporal variability of suspended sediment yield in the Upper Blue Nile Basin was analyzed using SWATPLUS. An alternative empirical model for estimating suspended sediment yield was developed, and various modelling approaches for sediment yield prediction were compared.

1.2 Statement of the problem

Sediment yield is also an immense problem that has threatened water resource development in the river basin. An insight into soil erosion/sedimentation mechanisms and mitigation methods plays an imperative role in the sustainable water resources development in the region. The majority of rivers, stream reaches, and tributaries in the world are ungauged or poorly gauged, as it is a costly, difficult, and time-consuming task, especially in remote water courses and developing countries

(M. Atieh et al., 2015). In developing countries like Ethiopia, a decreasing trend in the number of gauges is observed. In total, there are 409 river gauging stations spread over the 12 major river basins of the country. However, only 28 of these stations have relatively well-recorded data on sediment concentration and runoff discharge (Haregeweyn et al., 2013).

Lack of flow and sediment records increases the difficulty of developing efficient water strategies at different levels including: irrigation allocation and agricultural expansion (Atieh et al., 2015), hydropower generation (Amasi et al., 2021), and (Kuma et al., 2024), dam operation (Lee and Du, 2025), and (Kuma et al., 2024), flood and drought analysis (Houghton-Carr and Matt, 2006), and (Ward et al., 2020), climate change assessment (Ferdowsi et al., 2024), (Yasarer and Sturm, 2016), and ecological assessment (Praskievicz and Luo, 2020), and (Zinabu et al., 2019). Accordingly, there is a pivotal need for proper methods of sediment prediction at ungauged catchments.

Ethiopia loses 1.5 billion tons of topsoil in every year. It shows that soil erosion is a serious issue in Ethiopia (Tamene and Vlek, 2008). As a result, some reservoirs had sediment deposition issues and reduced their functions. Good examples of power generation and water supply reservoirs that are affected by sediment deposition problems are Koka (Adugna and Cherie, 2023), Gilgel Gibe I (Devi, 2008), MelkaWakena (Hayicho et al., 2019), Angreb (E. and M., 2012), and Legedadi (Adugna and Cherie, 2023).

1.3 Gaps in current sediment yield prediction methods

Different methods are used to predict sediment yield that are applicable depending on the type and availability of data, time frame, and availability of funds. One of the most applicable methods for estimating sediment yield in ungauged catchments is the regionalization method, which involves transferring information from a gauged catchment to an ungauged one (Heng and Suetsugi, 2014a);(Roth et al., 2016), (Ang et al., 2023);(MYermolaev and Mukharamova, 2023); (Jackisch et al., 2014). Hydrological models developed for sediment yield prediction include: physical based models (Gull and Shah, 2022); (Aga et al., 2020);(Ramsankaran et al., 2013); (Nkwasa et al., 2022),(Roba et al., 2021)and (Anamika et al., 2021), conceptual-based models (Gwapedza et al., 2021); (Haque et al., 2024); (Gwapedza et al., 2023), and data-driven models that may either be linear regression-based (Keshtegar et al., 2023); (Francke et al., 2008), or more recently use nonlinear regression-based approaches such as neural networks (Nda et al., 2023).

Data-driven models require less time for processing and have proven to give accurate estimations, especially at locations where the underlying physical processes are not well understood (Bezak et al., 2025). Applications of artificial neural network (ANN) models in hydrology have been numerous and diverse, covering quality and quantity, surface water and groundwater (Daliakopoulos et al., 2005); (Bezak et al., 2025); (Chen et al., 2020);(Sušanj Čule et al., 2025). The majority of studies using ANN models for sediment prediction have addressed forecasting cases (M. Atieh et al., 2015); (Heng and Suetsugi, 2013a); (Cigizoglu, 2004) and (Kisi and Shiri, 2012).

AI-based models play a crucial role in estimating sediment characteristics in ungauged catchment. This research has been developed in response to recognition of a need for models that (1) describe key physio-climatic characteristics that influence sediment parameters using an extensive list of characteristics and a regional dataset (2) incorporate spatial and temporal variability of suspended sediment, (3) develop an alternative empirical model for prediction of suspended sediment yield, and (4) compare conceptual model and data driven model artificial neural network for prediction of suspended sediment yield. The overall intent of this research was to gain a better understanding of sediment yield statistics at ungauged catchments. The major motivator for developing this study was the need for simple, reliable, and comprehensive models for the prediction of sediment in ungauged catchments.

1.4 Research questions

The output of this research will be achieved by designing this study to answer the following major research questions.

Question 1. How do land use and land cover (LULC) changes influence sediment yield dynamics in the Upper Awash River Basin?

Question 2. What are the spatial and temporal variations of suspended sediment yield in the Upper Blue Nile Basin?

Question 3. How can an alternative empirical model be developed to estimate suspended sediment yield?

Question 4. How can a regional model be developed to estimate suspended sediment yield in ungauged catchments?

1.5 Objectives of the study

The general objective of this research is to predict suspended sediment yield in ungagged catchments that impact reservoir development in the Ethiopian highlands.

1.5.1 Specific Objectives

To achieve the above main objective the following specific objectives were proposed:

- ⊗ To evaluate the effects of land use and land cover changes (LULC) on sediment yield dynamics in the Upper Awash River Basin using the QGIS-based Soil and Water Assessment Tool PLUS model (QSWATPLUS)
- ⊗ To analyze the spatial and temporal variability of suspended sediment yield in the Upper Blue Nile Basin using the QSWATPLUS model
- ⊗ To develop an alternative empirical model for estimating suspended sediment yield using physical model output parameters
- ⊗ To Develop an alternative regional suspended sediment yield estimation model for ungauged Catchments

1.6 Organization and structure of the dissertation

This dissertation is organized into seven chapters, which consist of four research outputs from chapters three to six. A brief description of the outline of the content is presented to simplify the understanding of the connection between the chapters.

- The first chapter provides a comprehensive overview of the dissertation. This includes the research background, the problem statement, the current gaps, particularly the study area, the research questions, and the dissertation objectives.
- Chapter 2 provides a comprehensive overview of the study area, encompassing its geographical location, climatic conditions, soil characteristics, land use patterns, and current land cover.
- The third chapter of this study focuses on the evaluation of the impact of alterations in land use and land cover on the dynamics of sediment yield in the upper Awash basin in Ethiopia, with particular reference to the Koka reservoir.
- The fourth chapter of this study investigates the spatiotemporal variability of suspended sediment yield in the upper Blue Nile basin.
- In Chapter Five, an alternative empirical model is proposed for the estimation of suspended sediment yield in ungauged catchments.
- In Chapter Six, a comparative analysis is presented of the various modelling approaches that have been employed to predict suspended sediment yield in ungauged catchments located within the Ethiopian highlands.
- Chapter seven offers a comprehensive conclusion and a set of recommendations for future research.

2. DESCRIPTION OF STUDY AREA

2.1 Location and topography

There are 12 major river basins in Ethiopia: eight are perennial river basins, one is a lake basin, and three (Danakil, Aysha, and Ogaden basins) are intermittent river basins with almost no or insignificant flow. This study was carried out in the Awash and Blue Nile (Abbay) river basins, with a particular focus on the Koka and Kessie watersheds.

The Blue Nile (Abbay) basin lies in the western part of Ethiopia between 7^0 45'-12^0 45' N and 34^0 05'-39^0 45' E (figure 2.1). It is the largest of the 12 major river basins in Ethiopia, with an area of about I76918 km^2 at the border point with Sudan. It is the largest river basin and covers about 33.2 % of the total area of the country. It contributes about 62% of the discharge to the main Nile River (Ahmed et al., 2010). The entire Abbay basin may be partitioned into 16 sub-basins. The Blue Nile sub-basins, which contribute to the Kessie watershed, are Tana, Jemma, Beshilo, North Gojjam, Weleka, and Mugger. Mean streamflow at the border amounts to 1540 m^3/s, which translates to an annual runoff volume of 49 billion m^3.

The Awash Basin is Ethiopia's second-largest basin, with a length of around 1200 kilometers and a catchment area of 110,000 km^2. It is located between $8^0$16' and $9^0$18' latitude and between $37^0$57' and $39^0$17' longitude with the elevation varies between 215 to 4185 m a.m.s.l (above mean sea level) (Daba and You, 2020). The study area is located on the upstream side of the Koka dam, which covers 10,371.43 km^2 watershed area with an altitude varying between 1503 to 3388m. Koka Dam was built in 1960 for hydropower generation on the Awash River's upstream section, with a reservoir capacity of 1180 Mm^3. The area is recognized as a prominent location where rapid population growth, agricultural practice, urbanization, and industry expansion occur, resulting in changes in the LULC from time to time. The Koka Dam watershed area is bounded to the south by the Rift Valley Basin, to the northwest by the Abbay Basin, to the west by the Omo-Gibe, and to the east by the Middle Awash. The detailed geographical location of the research area is presented below (Figure 2.1).

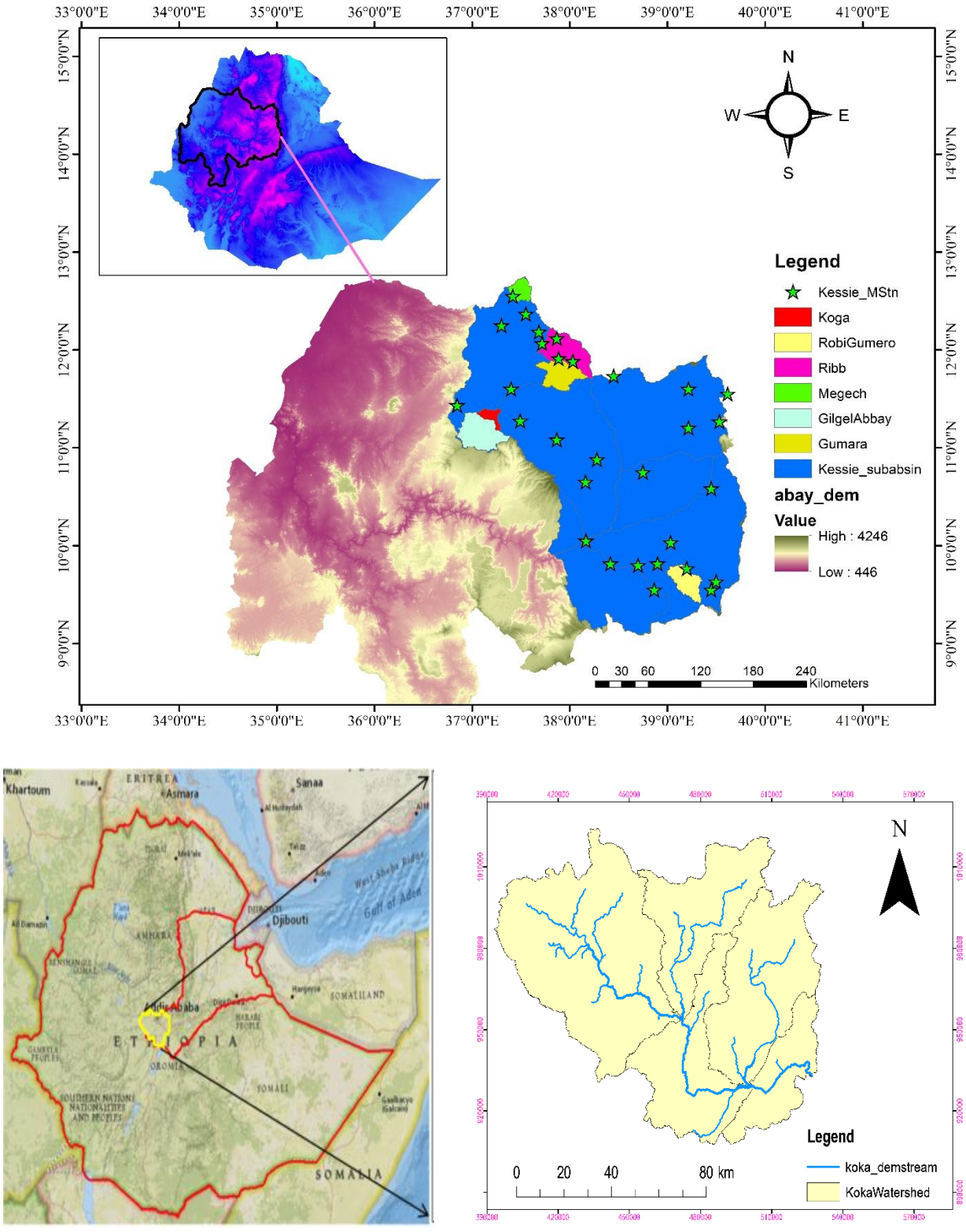

Figure 2-1 Location of Kesse and Koka watersheds

2.2 Climate and hydrology

The climate of the Abbay basin is largely controlled by two factors: its proximity to the equator and a wide elevation range, from about 590 meters to over 4,000 meters above sea level. The influence of these factors determines the rich variety of local climates, ranging from hot and desert-like along the Sudan border, to temperate on the high plateau, and cold on the mountain peaks.

Twenty-nine meteorological observation stations were used, where the stations are located within and around the Upper Kessie Watershed Annual rainfall varies between about 665 mm to 1,645 mm, with a mean annual rainfall over the Kessie watershed of about 1,420 mm, and a mean evapotranspiration of about 1,300 mm (Figure 2.2). The mean temperature of the basin is 18.5 °C, with minimum and maximum average daily temperatures of 11.4 °C and 25.5^0C respectively. Temperatures generally decrease with altitude (about 0.7°C per 100 m). In contrast, rainfall tends to increase with altitude while also being greatly affected by local rain-shadow and related effects.

Thirteen meteorological observation stations were used, where the stations are located within and around the Koka Dam watershed. Climate data such as daily precipitation, temperature, wind, sunlight hours, and humidity were obtained from the Ethiopian National Meteorological Institute (ENMI) from 2000 to 2015.

The mean annual rainfall of Addis Ababa, Adama, KokaDam, Asgori, Hombole, Beshefito, Mojo, Sendafa, Tulo Bolo, Addis Alem, Akaki, Ginchi, and Ejere meteorological stations for the period of 2000 to 2015 are shown below in Figure 2.3.

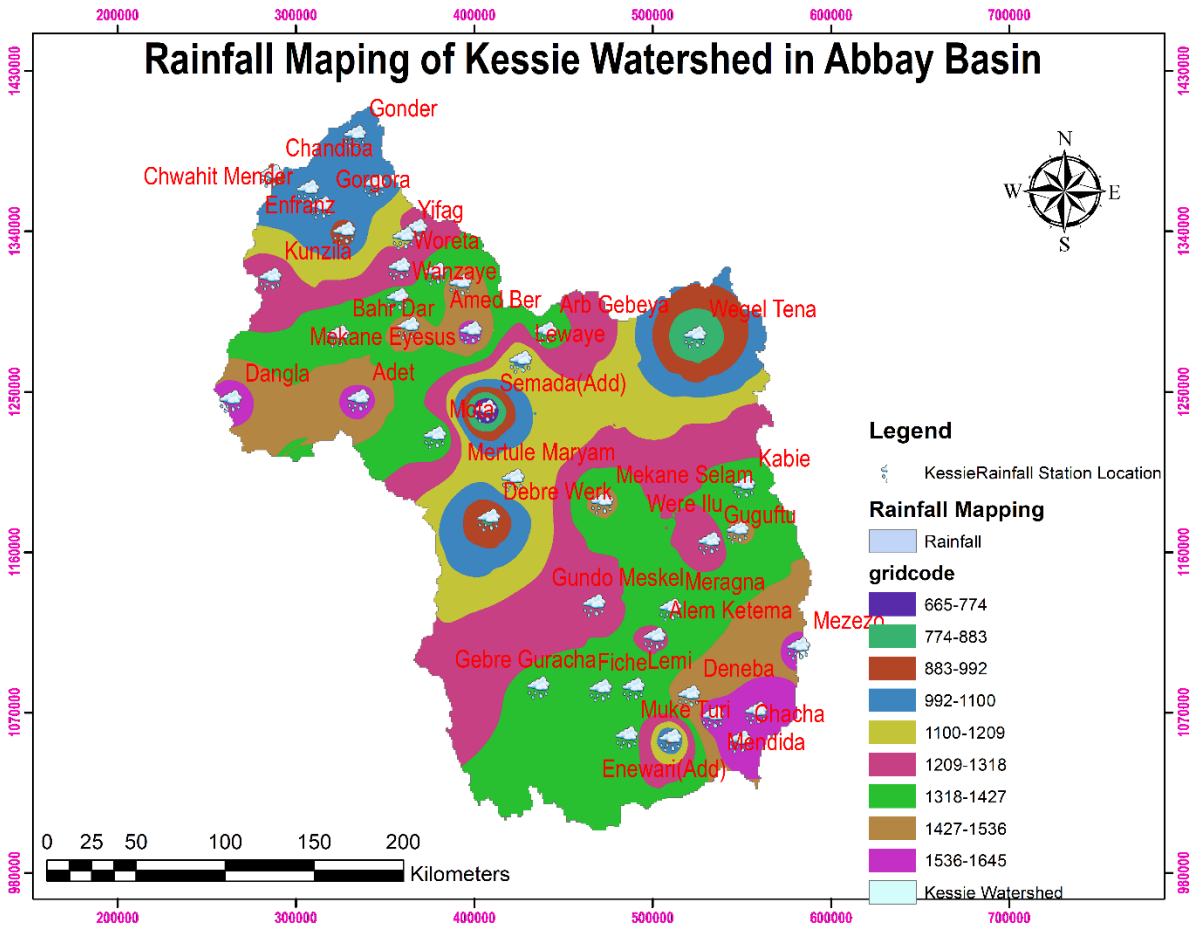

Figure 2-2Average annual rainfall depth (2000–2015) in Abbay Kessie Sub Basin based on inverse distance square interpolation method (IDW)- interpolation of data for near meteorological rain stations

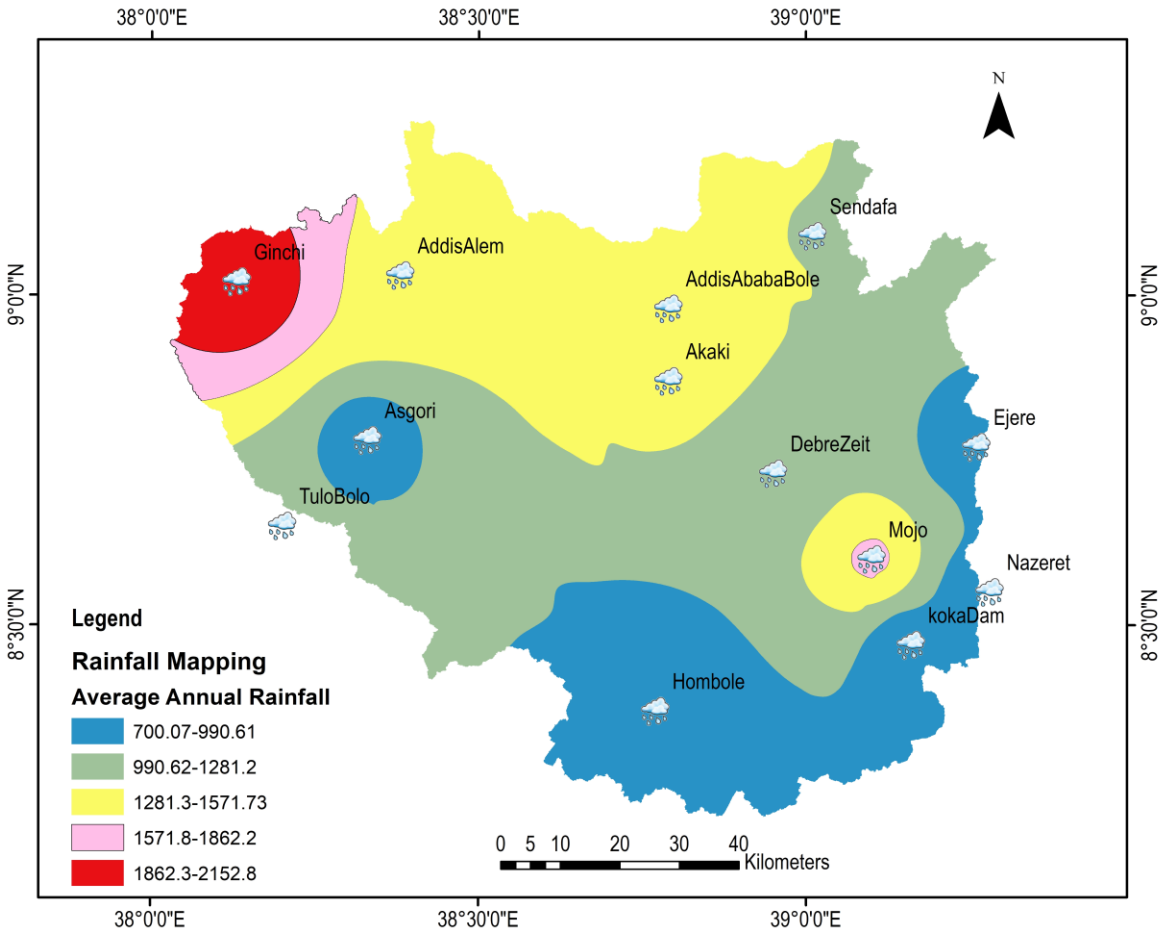

Figure 2-3Average annual rainfall depth (2000–2015) in Awash Koka Sub Basin based on inverse distance square interpolation method (IDW)- interpolation of data for near meteorological rain stations

2.3 Soil types and land use

The predominant soils of the UBNB are characterized as vertisols, luvisols, and leptisols (Easton et al., 2010). Majorly, the main soil groups of the Kessie watershed are Lithic Leptosols, Eutric Vertisols, and Chromic Luvisols, which cover 44%, 24%, and 14%, respectively (Figure **2.4**). Commonly, the types of LULC in the upper Awash River basin are agricultural land (rainfed and irrigation crops), water bodies, forests, shrubs, woodland, and bare land. Crop land is the dominant LULC in the watershed. The principal crops grown in this region include teff, maize, barley, vegetables, wheat, beans, and sugarcane. In general, irrigation farms, sugar plants, wetlands, Addis Abeba (Ethiopia's capital city), and other small urban regions are found in the watershed. Because

of fast population growth, human activity in this watershed is increasing, and natural resources are being depleted in unanticipated and unsuitable ways.

The catchment is dominated by Vertisols and Cambisols. Other prevalent soils include Calcic Fluvisols, Lithic Leptosols, Eutric Nitisols, Calcic Xerosols, and Vertic Cambisols. The predominant soil textures across the study area are sandy loam and silt-clay loam.

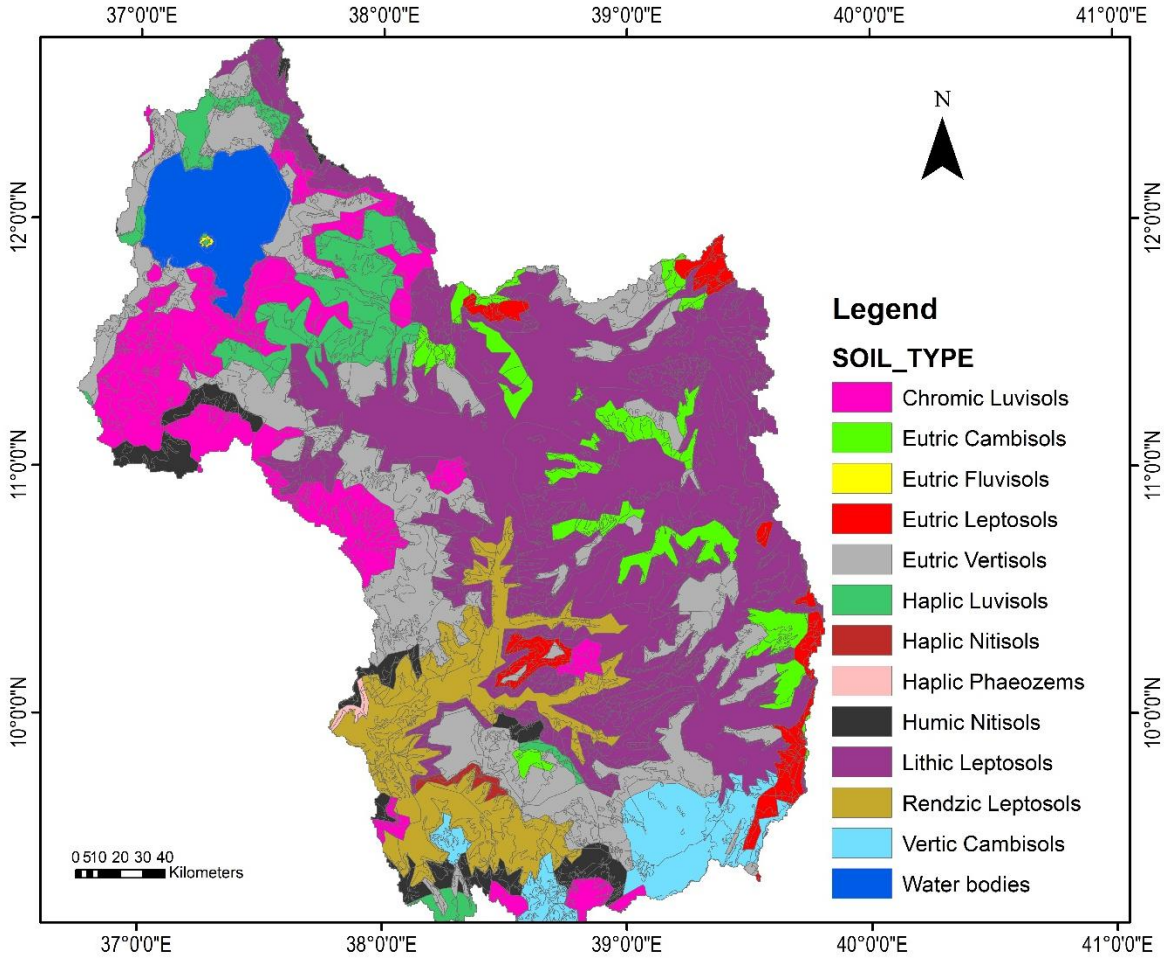

Figure 2-4 Soil types

The dominant LULC categories found within the Kessie watershed include farmland, grassland, barren terrain, bushland, and woodland. Based on the Water and Land Resource Center (WALRC), around half of the watershed area is covered by farmland. The dominant LULC in this watershed was farmland, which covered 50.69% of the watershed. Following agricultural land, the grassland and the bare land cover 12.41% and 10.50%, respectively. The area occupied by urban development is insignificant compared to the total LULC area, accounting for only 0.39% (Figure 2.5).

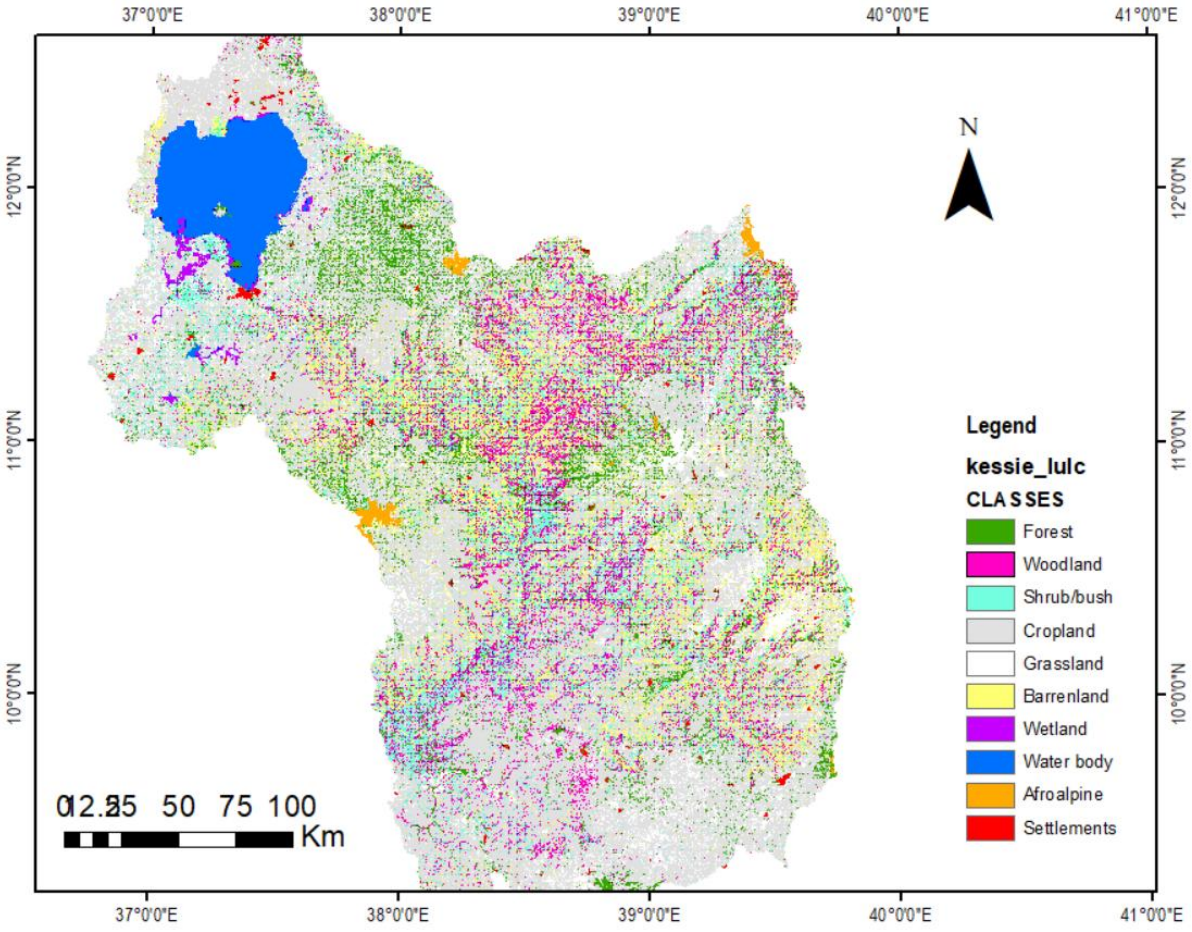

Figure 2-5 LULC map

2.4 Water Resources Potential

Utilization of the water resources of the country is focused on the eight river basins, as they are located in a climate zone favorable for human settlement. Awash and Blue Nile (Abbay) River basins are the most widely utilized and are being developed for water resources projects, mainly for hydropower and irrigation purposes. For instance, the Awash basin covers 70% of the irrigated agriculture area of the country and provides hydropower with an installed power of 46 megawatt (MW). Renewable groundwater resources are estimated to be about 2.6 billion cubic meters while gross hydro-electric potential about 45,000 MW (160,000GWh/year) within 299 potential sites and the potentially irrigable land in the country has been estimated at 3.7 million hectares **(Awulachew et al., 2007)**.

From many constructed and proposed dams in the Awash and Blue Nile basins, GERD, Megech, Rib, and Koka are the main sources of water for irrigation and hydropower purposes. Nevertheless,

the Koka dam has lost 40 % of its storage capacity due to sedimentation problems in the 30 years of its service period (Hathaway, 2008). Specifically, the Ribb and Koka watersheds, which are found in the upper Blue Nile and upper Awash River basins, are the selected area to investigate the impact of land use/ cover changes on sediment yield dynamics and to assess the variability of sediment yield.

In summary, Ethiopia has 124.4 billion cubic meters of surface water potential, 30 billion cubic meters of groundwater resources, and 80 billion cubic meters of lake water. The country also has an irrigation potential of 3.8 million hectares and a hydropower generation capacity of 45,000 MW. The Awash River Basin notably accounts for 3.95% of the total surface water potential, while the Abbay, Baro-Akobo, Mereb, and Tekeze rivers collectively cover 69.83% of the country's surface water resources (Melesse et al., 2013).

.

3. Evaluating the Impact of Land Use and Land Cover Changes on Sediment Yield Dynamics in the Upper Awash Basin, Ethiopia: The Case of Koka Reservoir

ABSTRACT

Land Use and Land Cover changes (LULC) are the driving forces behind changes in the hydrological response of the watershed. In this study, the Quantum Geography Information System Interface Soil and Water Assessment Tool Plus (QSWAT-PLUS) model was applied to evaluate the effects of LULC on sediment load at the Upper Awash River Basin (UARB), which is causing sedimentation problems in the Koka reservoir. The LULC data for 2005, 2010, and 2015 were obtained from historical satellite images using Earth Resources Observation and Science (ERDAS) 2014. The classification of LULC changes showed that the agricultural practice and the settlement land both increased by 6.7% and 6.3%, respectively. In contrast, the forest area, woodland, shrubland, and water bodies decreased by 5.47%,0.93%,0.96%, and 1.34% from 2000 to 2015, respectively. The model evaluation results were satisfactory for the three LULC scenarios. The average annual surface runoff volume for the 2005 LULC data was 182.2 mm, which increased to 193.29 mm in 2010 and 205.3 mm in 2015. Similarly, the average annual sediment yield that would enter the Koka reservoir under the 2005, 2010, and 2015 LULC scenarios was 26.03 t/ha/yr, 26.34 t/ha/yr, and 28.33 t/ha/yr, respectively. In general, streamflow, surface runoff, and sediment output increased by 4.55%, 12.68%, and 8.84%, respectively, due to the rapid change of LULC from 2000 to 2015. Temporarily, the sediment load at the upstream side of the Koka Dam watershed was 60.8% during the wet season. The southwest direction of the watershed was identified as the primary erosion-prone area. Based on the simulation results, the filter strip, contour, and terraces reduced the watershed sediment yield by up to 60%, 65%, and 80%, respectively. Therefore, the selected best management practices are highly effective in reducing silt along the entire upstream side of the Koka Dam watershed.

Keywords: Hydrological Response, Koka Dam, Land Use Change, QSWATPLUS Model

3.1 INTRODUCTION

Land use and land cover changes have a great impact on global environmental dynamics. It significantly affected the hydrological response, the hydrological cycle, and climate processes (Welde and Gebremariam, 2017),(Aneseyee et al., 2020), and (Tamene and Vlek, 2008).

One of the effects of altering land use and land cover changes is soil erosion, which causes more silt to enter into dam reservoirs, reducing their capacity and endangering their performance (Tamene and Vlek, 2007). In the World, many reservoirs have lost one-half of a percent of their storage capacity per annum due to sedimentation problems, which is causing serious problems for hydropower, irrigation, water supply, and flood control (Ayele et al., 2021).

In developing countries like Ethiopia, the highland areas are categorized as regions with high rates of soil erosion and land degradation problems (Tamene et al., 2017),(Haregeweyn et al., 2015a), and (Contador L.F.J., Schnabel S., 2009). The soil erosion and land degradation problems of the highland areas increased due to rapid LULC change. The rapid LULC changes are the results of expanded agricultural land, fast population growth, deforestation, and poor afforestation practices in the sloping area which are the main factors to accelerate soil erosion and land degradation in Ethiopia resulting in reservoir sedimentation problems (Tamene and Vlek, 2007), and (Ayele et al., 2021). Ethiopia loses 1.5 billion tons of topsoil in every year. It shows that soil erosion is a serious issue in Ethiopia (Tamene and Vlek, 2008). As a result, some reservoirs had sediment deposition issues and reduced their functions. Good examples of power generation and water supply reservoirs that are affected by sediment deposition problems are Koka (Adugna and Cherie, 2023), Gilgel Gibe I (Devi, 2008), MelkaWakena (Hayicho et al., 2019), Angreb (E. and M., 2012), and Legedadi (Adugna and Cherie, 2023). Moreover, in downstream countries like Egypt and Sudan, infrastructures such as Aswan, Rossier, and other storage reservoirs and irrigation canals have experienced serious sedimentation problems due to excessive sediment loads that originate from Ethiopian highlands (Betrie et al., 2011), and (Easton et al., 2010).

Particularly, the UARB is severely affected by poor watershed management problems due to dense population, expansion of urbanization, poor forestation, deforestation, and overgrazing, resulting in perceptible loss of soil fertility, and rapid degradation of natural resources (Shawul and Chakma, 2019),(Mariye et al., 2022),(Bekele et al., 2018), and (Mersha et al., 2018).

The result of soil erosion and sediment transportation into some dam reservoirs, particularly in this area, accelerated the sediment deposition and reduced the reservoir capacity, resulting in difficulty in using the reservoirs for hydropower, flood control, irrigation, and water supply. For example, the Koka Dam reservoir lost 17 million cubic meters of storage capacity per year. Due to this, the generated power capacity of the dam reservoir reduced in 2014 (Haregeweyn et al., 2012b). In addition to this, the Awash Melkessa reservoir stopped its service due to heavy siltation problems,

and the Methara sugar factory was also challenged due to the high siltation of the canal and difficulty in irrigating the sugarcane plants (Tessema et al., 2021).

Land use/land cover, rainfall, topography, soil properties, and geological formation are some of the many variables that affect the hydrological processes. Among such, the primary cause of the hydrologic process in watersheds is human-induced LULC change (Kuma et al., 2023). Alterations of LULC dynamics have been a major source of soil erosion and sediment yield in recent times (Belay and Mengistu, 2019), (Abiye et al., 2023). The significant change in LULC is a cause of surface runoff and sediment yield variation at seasonal and spatial scales. To understand this, the change of the Angerb watershed LULC from 1985 to 2011 is an explanatory example. This watershed changed the land use type from forest plantations to agricultural practices between 1985 to 2011. As a result, the runoff was increased by 39% (Getachew and Melesse, 2012). In the Tekeze Dam watershed, the LULC type has changed from grass and bare land to agricultural land. Because of this, the average annual stream flow has increased by 6.02%, while the amount of sediment yield increased by 17.39% during the time interval from 1986 to 2008 (Welde and Gebremariam, 2017).

Many researchers have investigated the impact of LULC change on sediment yield dynamics in the UARB. According to their findings, the LULC changes in Ethiopia's highlands are a significant issue that endangers natural ecosystems (Bekele et al., 2018). Therefore, understanding the effects of LULC change in the watershed is essential for planning and managing land use and water resources (Daba and You, 2022). According to Shawl and Chakma's findings in the upper Awash watershed, LULC changed dramatically from shrubland to crop area (Shawul and Chakma, 2019). This result showed how much the agricultural practice in this area has expanded from 1972 to 2014. This led to an increase in the annual sediment production in the Koka Dam reservoir. According to the average annual sediment product entering the Koka Dam reservoir is 21.43 t/ha/yr. 106,352.59 tons of average annual sediment output entered the Merti intake structure, which was built in the Awash River (Bishaw and Kedir, 2015). The sediment yield of the UARB varies from time to time. During the wet season, 70.8% of the yearly sediment yield occurs in the middle Awash catchments (Tesema et al., 2021). Even though the issue of evaluating the effects of LULC changes on sediment yield dynamics in the UARB has been the subject of numerous studies, it is necessary to urgently and seriously assess the impact of LULC changes on sediment load at Koka dam reservoirs to extend reservoir life through the application of practical land use

and watershed management techniques. Furthermore, most studies were limited to small watersheds and landscapes, and calibration and validation were carried out at the Hombole gauge station, which had a coverage area of around 7,000 km^2. But the calibration and validation for this study were performed at the upstream side of the dam, which covered 10,000 km^2 watershed area.

Unlikely the previous studies, in this study, the new version of the QSWATPLUS model was used to evaluate the effects of land use change on sediment variation by using different years of LULC data and to evaluate the best watershed management strategies.

The Awash River basin is the backbone of economic development in Ethiopia. Large sugar and hydro-power plants have been found in this basin, and they are vital to the country's economy. However, the UARB is currently suffering from a land degradation problem caused by urbanization, dense population, agricultural development, and poor watershed management (Daba and You, 2022). On top of that, the basin is environmentally vulnerable (Hailemariam, 1999),(Edossa et al., 2010), and (Mersha et al., 2018), and the river is characterized by high flash floods, which carry a high amount of silt that significantly affects the capacity of the Koka reservoir. Due to sediment deposition in the reservoir, Koka's power generation capability was reduced from the expected power output. In general, most reservoirs have major sedimentation problems (Bashar et al., 2010). Therefore, evaluating the impact of LULC change on sediment yield dynamics in the upper Awash River basin is critical for providing useful information to water resource and land use planners in developing subbasin management strategies and reducing sediment deposition at Koka Reservoir using effective watershed management strategies.

Various physical-based soil erosion models have been developed worldwide to anticipate soil loss and sediment load and to assess the impact of LULC change on watersheds (Koneti et al., 2018). They also help to identify the erosion-prone area and to determine the optimum management approach for the erosion-prone area in a timely and cost-effective manner. For instance, Annualized Agricultural Non-Point Source (AnnAGNPS) (Zema et al., 2010), SWAT (Setegn et al., 2010), Water Erosion Prediction Project (WEPP) (Singh et al., 2011), QSWATPlus (Bieger et al., 2019), (Wu et al., 2020), and European soil erosion model (EUROSEM) (Pandey et al., 2016), such physical models have been used in recent years to evaluate the impact of LULC change on soil erosion and its control mechanism. Among those models, the AnnAGNPS model requires extensive data input and no mass balance equation (Bingner et al., 2018), the WEPP model also

requires a large number of input data and parameters, and cannot accurately simulate the process occurring in permanent channels and streams. EUROSED is relying on a single storm and is suitable for small catchments (Pandey et al., 2016). Whereas the SWAT model requires relatively small input data and is used to simulate long-term hydrologic, soil erosion, and sediment yield in large and complex watersheds using daily time steps. It is the most applicable model worldwide to estimate sediment yield on a daily and monthly basis and to predict the long-term impact of land use activities in complicated and large watersheds (Cooper, 2010), and (Liu et al., 2015). It was applicable for predicting sediment load, identifying the erosion area, and evaluating the best management strategies in Ethiopia's watersheds under different scenarios (Zantet et al., 2023),(Anteneh et al., 2023), and (Dibaba et al., 2021). The fundamental issue of SWAT model over the other hydrological models is its capacity to predict sediment load if the observed streamflow and sediment data are not sufficient and unreliable in the watershed (Zalaki-badil et al., 2017). Therefore, the QSWATPLUS model was used in this study to assess the impacts of LULC variations on sediment load in the Koka reservoir. It is the upgraded version of the SWAT model, a time-continuous semi-distributed model that works on the principle of hydrologic response units. The uniqueness of the QSWAT plus model from the previous version added the landscape units beside to sub-catchment. The importance of using the QSWAT plus model over other physical models is to understand the basic catchment characteristics when the data are not accessible and to evaluate the long-term effects of LULC change on the hydrological response that are difficult to simulate (El-Sayed and Zumwalt, 1991).

In this study, it was hypothesized that major changes in the LULC in the UARB are related to human activities that provide for the needs of the fast-rising population in terms of food security by utilizing improper and ill-planned natural resource management practices.

The particular aims of this study are as follows:

i) To assess the impact of land use and land cover changes on sediment yield dynamics in the upper Koka Dam watershed using the 2000,2005,2010, and 2015 LULC maps

ii) To estimate the mean annual sediment yield loading to the Koka reservoir

iii) To evaluate the spatial and temporal variability of sediment yield and identify the erosion-prone area.

3.2 MATERIALS AND METHODS

3.2.1 Description of the Study Area

The Awash Basin is Ethiopia's second-largest basin, with a length of around 1200 kilometers and a catchment area of 110,000 km^2. It is located between $8^0 16'$ and $9^0 18'$ latitude and between $37^0 57'$ and $39^0 17'$ longitude with altitude varying between 215 to 4185 m a.m.s.l (above mean sea level) (Daba and You, 2020). The study area is located on the upstream side of the Koka dam, which covers 10,371.43 km^2 watershed area with an altitude varying between 1503 to 3388m. Koka Dam was built in 1960 for hydropower generation on the Awash River's upstream section, with a reservoir capacity of 1180Mm^3. The area is recognized as a prominent location where rapid population growth, agricultural practice, urbanization, and industry expansion occur, resulting in changes in the LULC from time to time. The Koka Dam watershed area is bounded to the south by the Rift Valley Basin, to the northwest by the Abbay Basin, to the west by the Omo-Gibe, and to the east by the Middle Awash. The detailed geographical location of the research area is presented below (Figure 3.1).

The upstream of the Koka dam catchment got an annual mean rainfall of 1199.56mm from 2000 to 2015. The maximum, minimum, and average values of temperature observed at the watershed during the period 2000-2015 were 25 ^{0}C, 10 °C, and 17.5 ^{0}C, respectively.

Commonly, the types of LULC in the UARB are Agricultural land (rainfed and irrigation crops), water bodies, forests, shrubs, woodland, and bare land. Crop land is the dominant LULC in the watershed. The principal crops grown in this region include teff, maize, barley, vegetables, wheat, beans, and sugarcane. In general, irrigation farms, sugar plants, wetlands, Addis Abeba (Ethiopia's capital city), and other small urban regions are found in the watershed. Because of fast population growth, human activity in this watershed is increasing, and natural resources are being depleted in unanticipated and unsuitable ways.

The most dominant soil groups in the catchment are Vertosols and Cambisols. Calcic Fluvisols, Lithic Leptosols, Eutric Nitosols, Calcic Xerosols, and Vertic Cambisols are the most common types of soil in this watershed. The most common soil texture of the research area is sandy and silt-clay loam.

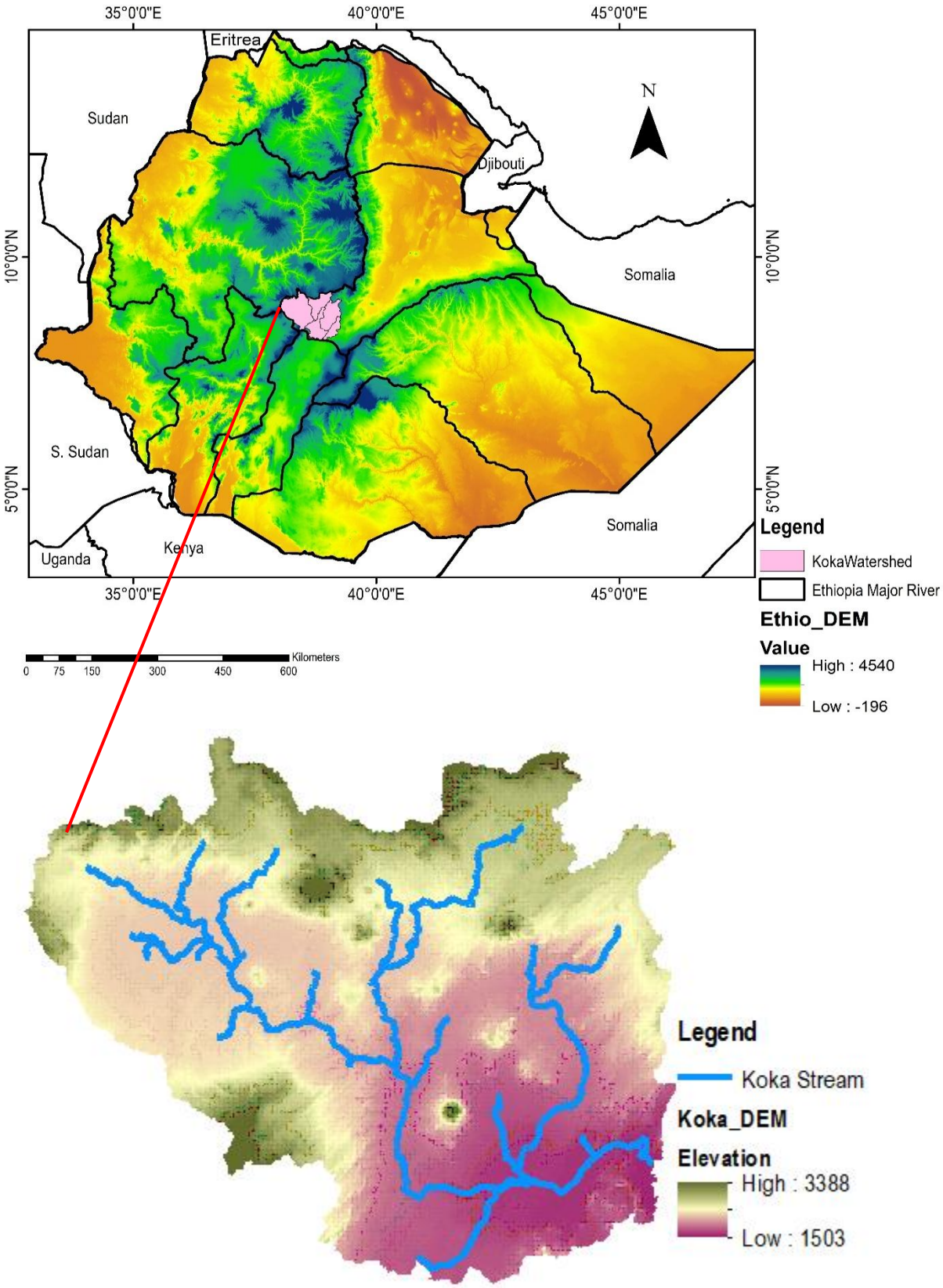

Figure 3-1 Location of the study area

3.2.2 Model Input and Data Acquisition

The QSWATPLUS model requires spatial inputs (topography, DEM, soil, and land use maps) as well as meteorological data (precipitation, temperature, relative humidity, wind speed, and solar radiation). The hydrological data (streamflow and sediment concentration) were collected from the Ministry of Water and Energy and used to calibrate and validate. The spatial, vector, climate, and hydrological data were collected from different sources to use in this study. The following are the model inputs that were used for the QSWATPLUS Model.

3.2.2.1 Meteorological Data

Thirteen meteorological observation stations were used, where the stations are located within and around the Koka Dam watershed. Climate data such as daily precipitation, temperature, wind, sunlight hours, and humidity were obtained from the Ethiopian National Meteorological Institute (ENMI) from 2000 to 2015.

The mean annual rainfall of Addis Ababa, Adama (Nazeret), KokaDam, Asgori, Hombole, Beshefito (Debrezeit), Mojo, Sendafa, Tulo Bolo, Addis Alem, Akaki, Ginchi, and Ejere meteorological stations for the period of 2000 to 2015 are shown below in Figure 3.2.

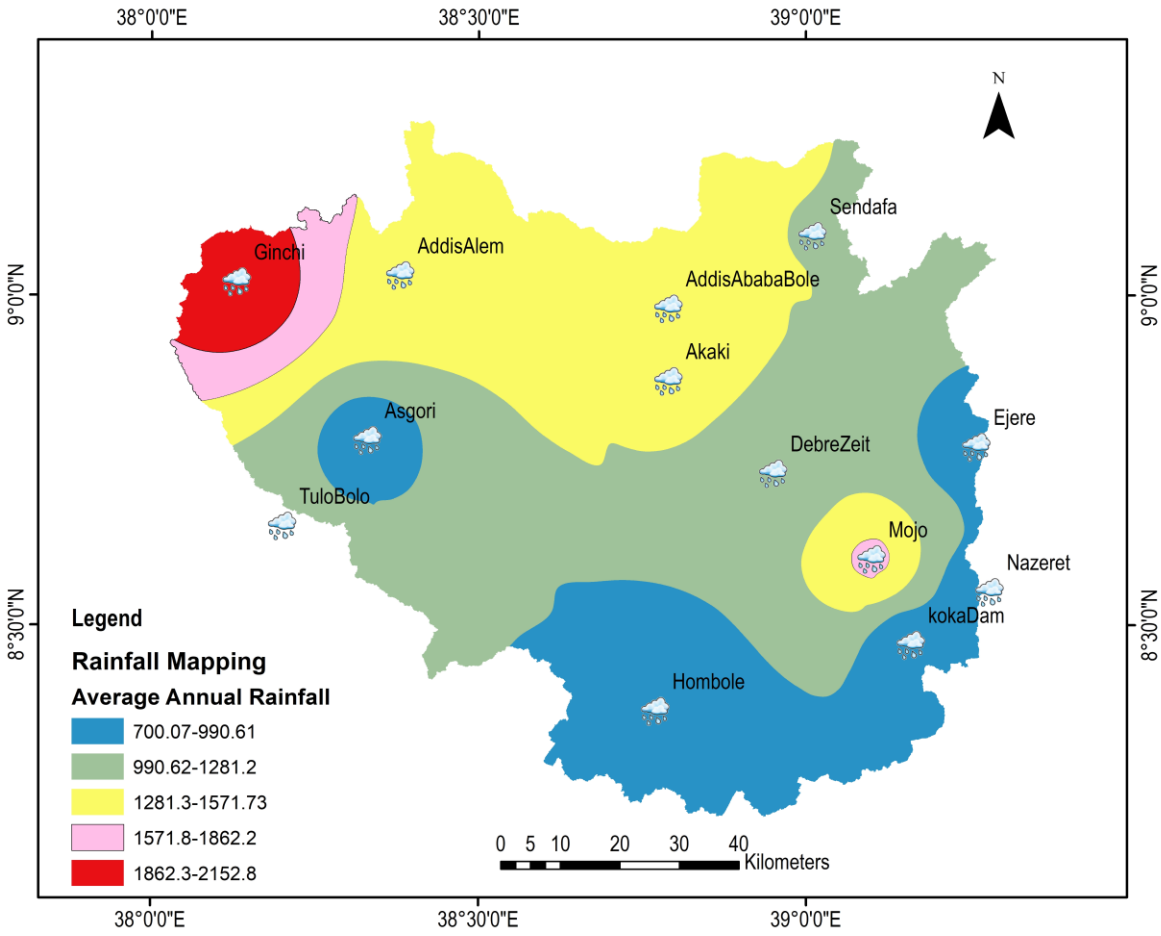

Figure 3-2 Average annual rainfall depth (2000-2015) of upper Awash metrological stations using inverse distance Weighted Interpolation Method

3.2.2.2 Observed Streamflow and Sediment Data

The hydrological data, such as daily observed streamflow and suspended sediment sample data, were obtained from the Ministry of Water and Energy to calibrate and validate the QSWATPLUS model at the Koka Dam gauging station. The calibration and validation were performed using 16 years of observed data (2000-2015). The sediment concentration data is a non-continuous time step that was collected from the Ministry of Water and Energy. A sediment rating curve should be developed using observed sediment data as a function of the related stream flow data to obtain the continuous time-step sediment data (Assfaw, 2020).

The following equations can be used to express the relationship between streamflow and suspended sediment concentration (Equations 3.1 and 3.2):

$$Q_s = a * Qw^b \quad (3.1)$$

$$Qs = 0.0864 * Qw * C \quad (3.2)$$

Where C is the suspended sediment concentration (mg/lit), Qs is the suspended sediment load (ton/day), a and b are constants, and Qw is the streamflow (m^3/sec).

It is obtained from the empirical relationship between observed sediment data and associated streamflow data (Zhang and Lu, 2004) and is equated as(Equation 3.3):

$$Log(Q_S) = a + b * \text{Log}\,(Q_W) \quad (3.3)$$

The bias correction factor was used to improve the accuracy of the sediment rating curve, which calculates the sediment load. The equation is as follows (Equation 3.4) (Ferguson, 1986)

$$Log(Q_S) = a + b * \text{Log}\,(Q_W) + \text{CF} \quad (3.4)$$

Based on Ferguson's (1986) study, a statistical bias correction factor is the exponent of ($2.65S^2$), which is used to minimize the error estimation using the sediment rating curve, and the variance is equal to (Equation):

$$S^2 = \frac{\sum_{i=1}^{n} \langle Log(Ci) - Log(\hat{C}i) \rangle^2}{n-2} \quad (3.5)$$

Where Ci is the observed value, $\hat{C}$i is the predicted value, and n is the total sample of data, S^2 is the variance.

For this particular study, three rating curve development methods were used to derive the suspended sediment rating curve using non-continuous time step sediment data and corresponding measured streamflow data, such as normal linear log-log relationships, normal linear log-log relationships with a bias correction factor, and non-linear log-log relationships. The non-linear log-log relationship is calculated using the Microsoft Excel Solver Tool (Equation 3.6) (Asselman, 2000).

$$Log(Q_S) = a + b * \text{Log}\,(Q_W)^C \quad (3.6)$$

Where a and b are constants and c is the exponent coefficient

For the Koka gauge and Hombole stations, a sediment rating curve is developed using the three equations mentioned above (Equations (3.3), (3.4), and (3.6)). Using goodness-of-fit, the optimal sediment rating curve was identified. The goodness of fit of the sediment rating curve is assessed using the coefficient of determination (R^2), Nash-Sutcliffe efficiency (NSE), root mean square error (RMSE), observed standard deviation ratio (RSR), and percent bias (PBIAS). Based on the above statistical model performance indicator value, the equation was selected (Moriasi et al., 2012). The Koka dam gauging station's sediment rating curve results are shown in the charts below (Figures 3.3 and 3.4).

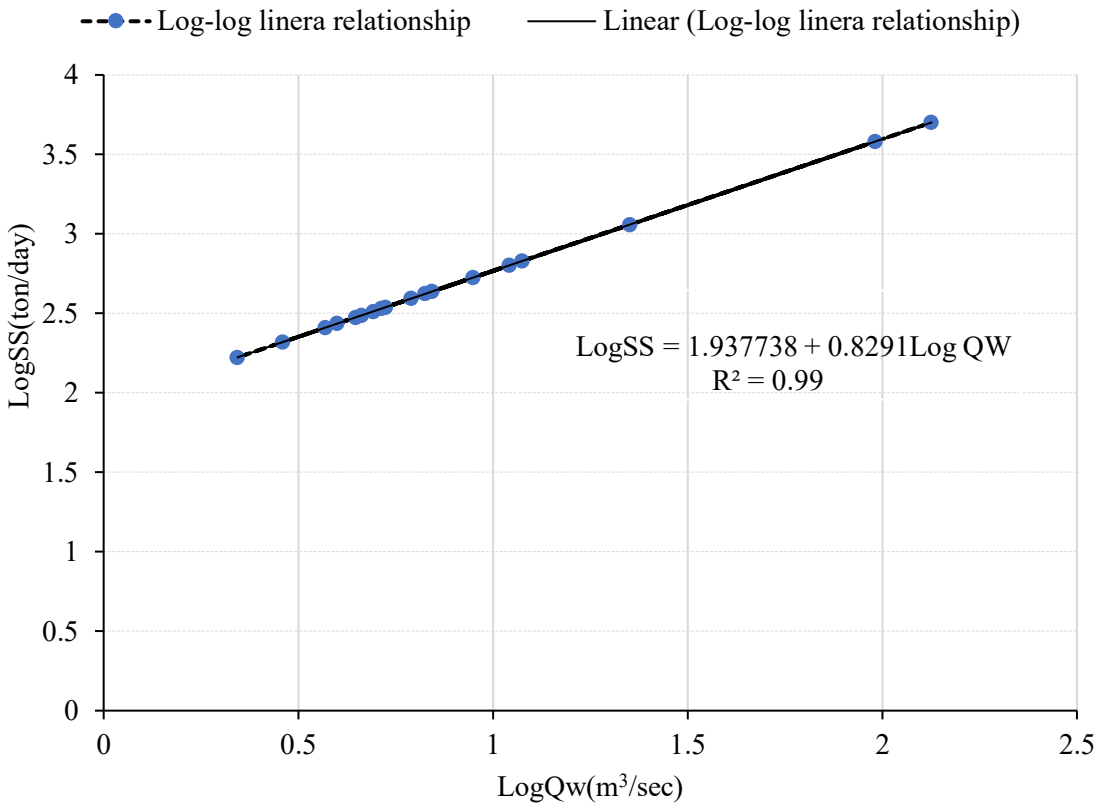

Figure 3-3: Log-Log linear relationship sediment rating curve developed at Koka dam station

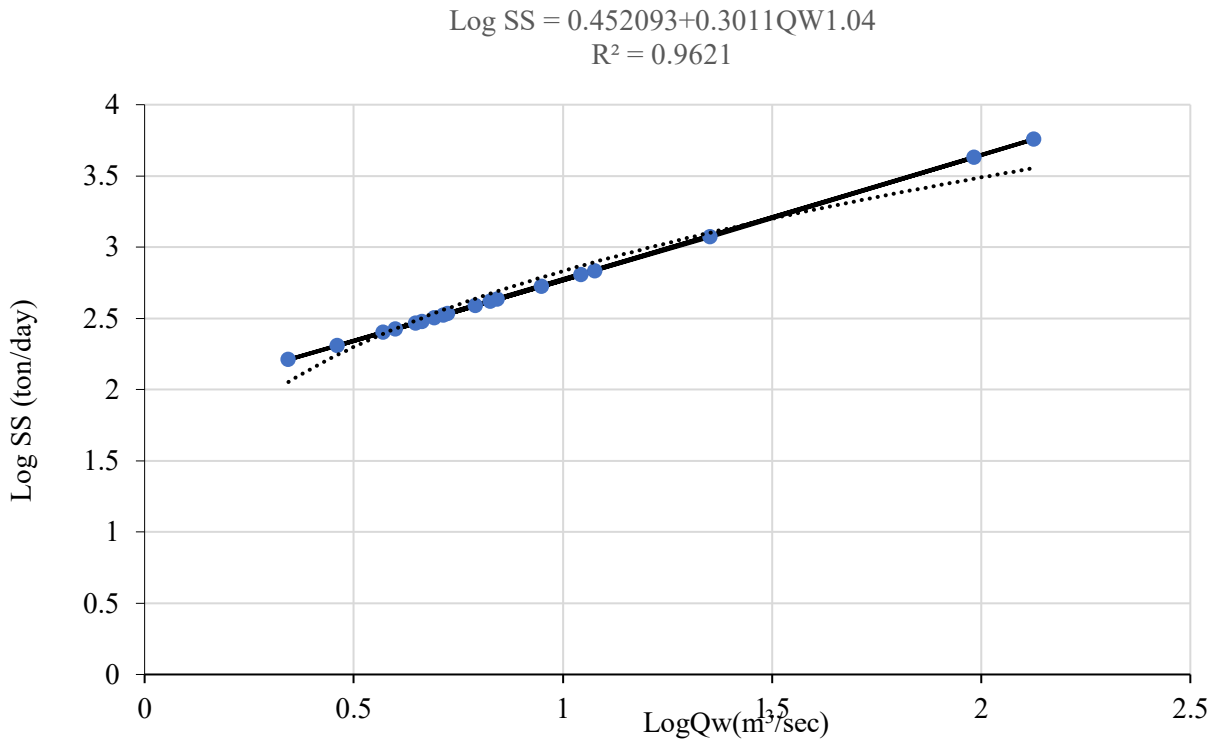

Figure 3-4 Log-Log nonlinear relationship sediment rating curve developed at Koka dam station.

3.2.2.3 Spatial Data

The spatial data, including land sat images (remote sensing satellite), DEM, soil map, and vector data, were obtained from the Earth Resources Observation and Science (EROS) data center of the United States Geological Survey (USGS) (http://espa.cr.usgs.gov) and the Ethiopian Geospatial Map Institute. Three historical satellite images were used to assess the impact of LULC change on watershed hydrology and sediment production, and a five-year gap was taken into account for the years 2005, 2010, and 2015. In addition, field observation and ground truth data were collected to validate the LULC classification.

3.2.2.4 Landsat Image Data Sources

Multi-variety satellite pictures in terms of spatial and temporal data were gathered to simulate and assess the effects of LULC change on sediment yield dynamics. The historical 2005,2010, and 2015 cloud-free satellite images were downloaded using Landsat-7 ETM+(Enhanced Thematic Mapper), and Landsat-8 OLI (Operational Land Imager) satellite. The Landsat7 ETM+ images (2005,2010) with Worldwide Reference System (WRS) Path 169 and Row 52 were acquired on May 20/2005, and March 2010, respectively, while the Landsat-8OLI satellite image was acquired

on February 13/2015. The images of February, March, and May were used because of the best period of minimum cloud and sense cover images in Ethiopia, which is the summer season starting from February up to May. The satellite image data has a 30m-by-30m resolution.

3.2.3 Land Use and Land Cover Classification

The image processing, such as layer stack, mosaic, merge, and clip image, was performed using Quantum GIS and ERDAS-14 software. After image pre-processing, the satellite raster image is changed into a polygon shape using the signature editor, then the LULC classification is done using the combination of the ERDAS supervise image technique and Google Earth. The supervised classification was performed using 536 training sampling locations obtained from georeferenced data and applied to the Landsat image using the maximum likelihood classification technique and the area covered by each LULC class. The supervised classification method outperforms other image classification methods currently in use. It is verified by using ground truth data.

3.2.4 Accuracy Assessment

The accuracy assessment was done using information which is collected from ground surveying data for each type of LULC. The survey data was collected using the Global Position System from February 1, 2022, to May 2022 time interval. Visual observations were made from 536 training locations where 110,40, 60,54,65,69,70, and 68 were taken from cultivated land, urban areas, bare land, shrubland, bushland, woodland, water bodies, and forest, respectively. The majority of the observation data (384 sample points) were utilized for classification, while the remaining data (152) were used to evaluate the accuracy. Out of 384 sample training points, 78,28,42,38,46,50, 51, and 51 were taken from cultivated land, urban area, bare land, shrubland, bushland, woodland, water bodies, and forest, respectively. Besides collecting data, a discussion was held with community elders to check the similarity between the classification of the LULC type and the ground LULC type.

The accuracy assessment efficiency was calculated using the Kappa coefficient, and the overall accuracy efficiency value is 0.81. Majorly, the LULC types in the Koka Dam watershed are cultivated land, woodland, shrubs, urban areas, bare ground, forest, woodland, and aquatic bodies (Figure 3.5). During the classification of LULC, the following descriptions of LULC were considered (see Table 3.1).

Table 3-1 Classification of LULC change type from 2000 to 2015

Classification of LULC type	Descriptions
Forest	Areas covered by natural high forests and large man-made trees
Woody land	Mainly, the woodland falls next to the forest and is found in hill areas and along the riverside, and it consists of medium-sized bushes.
Cultivate land	The area includes all agricultural practices, like state farms and holder farms
Bushland	areas dominated by small bushes and shrubby plants, and sized plant species (less than 3m)
Bare land	Areas of the exposed surface
Water Bodies	The water bodies include lakes, rivers, and other water bodies.

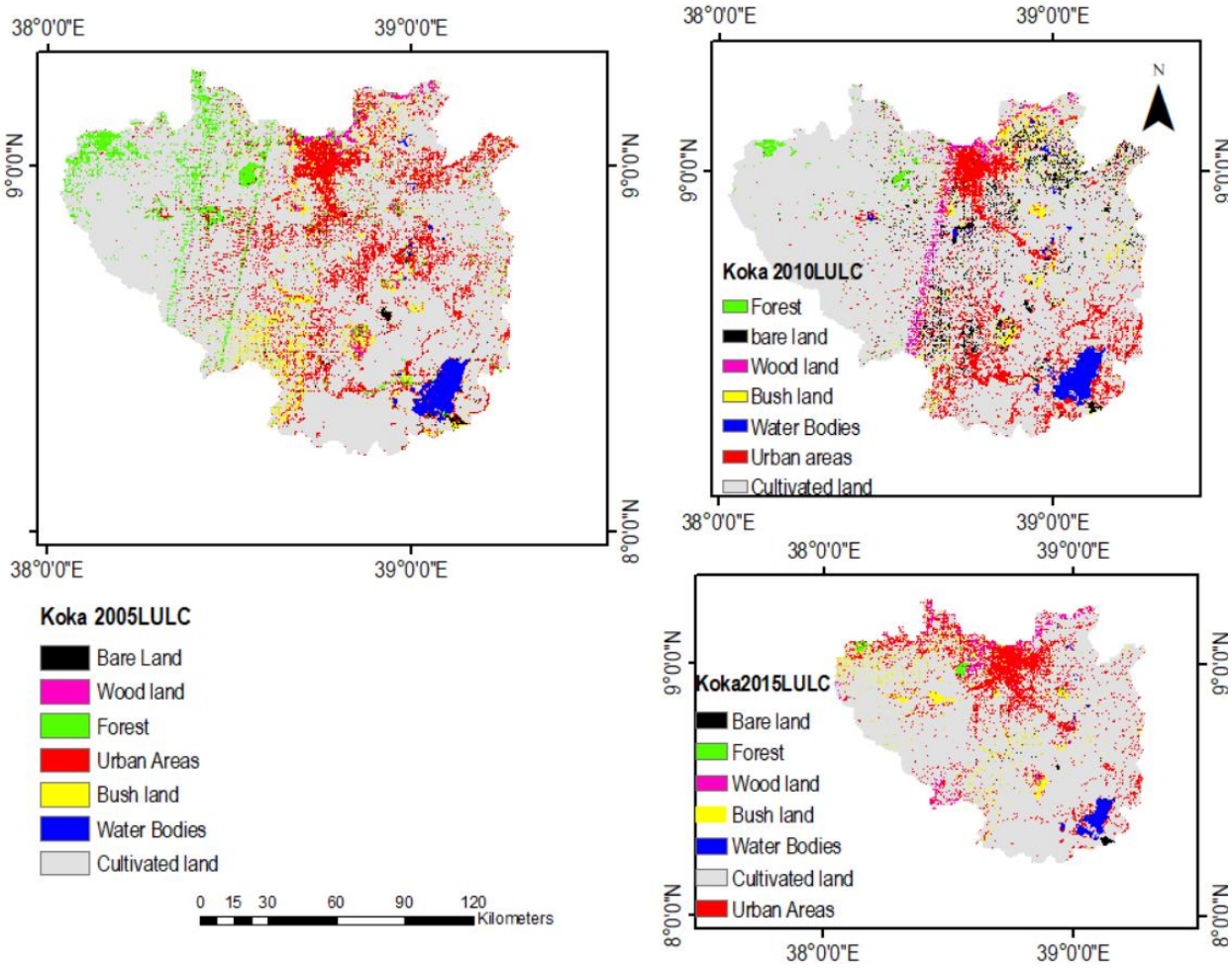

Figure 3-5 LULC classification 2005,2010, and 2015 LULC data using the supervised technique

3.2.5 QSWATPLUS model

SWAT+ is the most recently rebuilt version of the SWAT model, and it is based on the concept of the hydrological response unit of watersheds. The hydrological response unit shows the catchment characteristics by identifying the soil type, land use type, and slope of watersheds.

Similar to the SWAT model, the SWATPlus model uses an equation to predict various aspects of the hydrological cycle, including surface runoff, infiltration, evapotranspiration, plant growth, sediment yield, routing, and many more. However, the SWATPlus model has significant advantages over the original SWAT model. It is suitable for large models and has virtually no size restriction. It is very flexible compared to SWAT. It also adds some features like landscape units. It is a semi-distributed hydrological model that simulates the response of the hydrology and the output of suspended sediment by using the dynamics of LULC (Farhan and Nawaiseh, 2015). The QSWATPlus model, which is also the most recent version, simulates surface runoff and sediment yield using the water balance equation (3.7) (S.L. Neitsch, J.G. Arnold, J.R. Kiniry, 2009).

$$SW_t = SW_0 + \sum_{j=1}^{t}(R_{day} - Q_{surf} - E_a - W_{seep} - Q_{gw}) \qquad (3.7)$$

Where SWt is the final depth of soil and water content (mm), SWo is the initial soil and water content on the time j (mm), t is the period (days), Rday is the measurement of the amount of rainfall on day j (in millimeters), Qsurf is the measurement of the amount of runoff on day j (in millimeters), Wseep is the measurement of the amount of water seeping into the soil layer on day j (in millimeters), Ea is the measurement of the amount of evapotranspiration on day j (in millimeters), and Qgw is the measurement of the return flow amount on the day (mm)

A modified universal soil loss equation (MUSLE) can be used to estimate sediment production (Equation 3.8):

$$S_{ed} = 11.8(Q_{surf} * q_{peak} * area_{hru})^{0.56} * K_{USLE} * C_{USLE} * P_{USLE} * LS_{USLE} * CFGR \qquad (3.8)$$

Where K_{USLE} is the soil erosion factor, C_{USLE} is crop management, P_{USLE} is plant management practice, LS_{USLE} is a topographic factor, CFRG is the coarse fragment factor, and Sed is the sediment yield from the catchment (tons). Qsurf is the amount of surface runoff volume (mm/ha), qpeak is the peak flow rate (m^3/sec), and $area_{hru}$ is the area of the hydrological response unit (ha).

3.2.6 Sensitivity analysis, model calibration, and validation

The model calibration process is complex, and it needs iteration of the calibration process for all model parameters (Gupta et al., 1999). Under such cases, sensitivity analysis should be carried out

to identify which parameters had a high impact on changing model results. The data used for calibration cover January 2000 through December 31, 2010, and the data used for validation span January 1, 2011 through December 31, 2025.

Both automatic and manual techniques were used to calibrate the simulated and measured values. By changing the parameter value, the corresponding model statistical values were computed, and the calibration continued until the acceptable model performance statistical indicator value, which was recommended by the QSWAT+ developer. The recommended value for calibration of streamflow and sediment is a coefficient determination (R^2) >0.6 and Nash Sutcliffe Efficiency (ENS) >0.5 (Santhi et al., 2001).

Model validation is the testing of the capability of the model to simulate the variable without any calibration adjustment parameters at different periods and spaces (Aumann, 2007).

3.2.7 Statistical indicators for model performance evaluation

Model performance statistical indicators are used to evaluate the model's prediction capability. The performance indicator is important to examine the relationship between the simulation output and the measured value. The statistical indicators are Nash Sutcliffe Efficiency (NSE), coefficient of determination(R^2), and percent bias. They were used to evaluate the capability of model simulation (Nash and Sutcliffe, 1970), (Moriasi et al., 2007a), and (S.L. Neitsch, J.G. Arnold, J.R. Kiniry, 2009).

3.2.8 Evaluation of land use change on sediment yield

The temporal and spatial effects of LULC alteration on sediment output were assessed using 2005,2010, and 2015 LULC scenarios. The temporal variance was analyzed using four time frames, namely 2000-2005, 2005-2010, 2010-2015, and 2000-2015, which reflect different LULC regimes in the watershed. Between 2000 and 2015, the spatial hydrological responses at the subbasin scale were evaluated.

3.2.9 Mapping erosion-prone areas and sediment reduction methods

Watershed management practices cannot be adopted over the entire watershed due to financial constraints, human resources, time constraints, and land availability in the targeted area. Identifying erosion-prone areas is essential for effective and efficient watershed management practices. In general, mapping the spatial distribution of sediment yield is critical for watershed management planning and strategies (Betrie et al., 2011). Generally, the overall methodology approach is shown below (Figure 3.6).

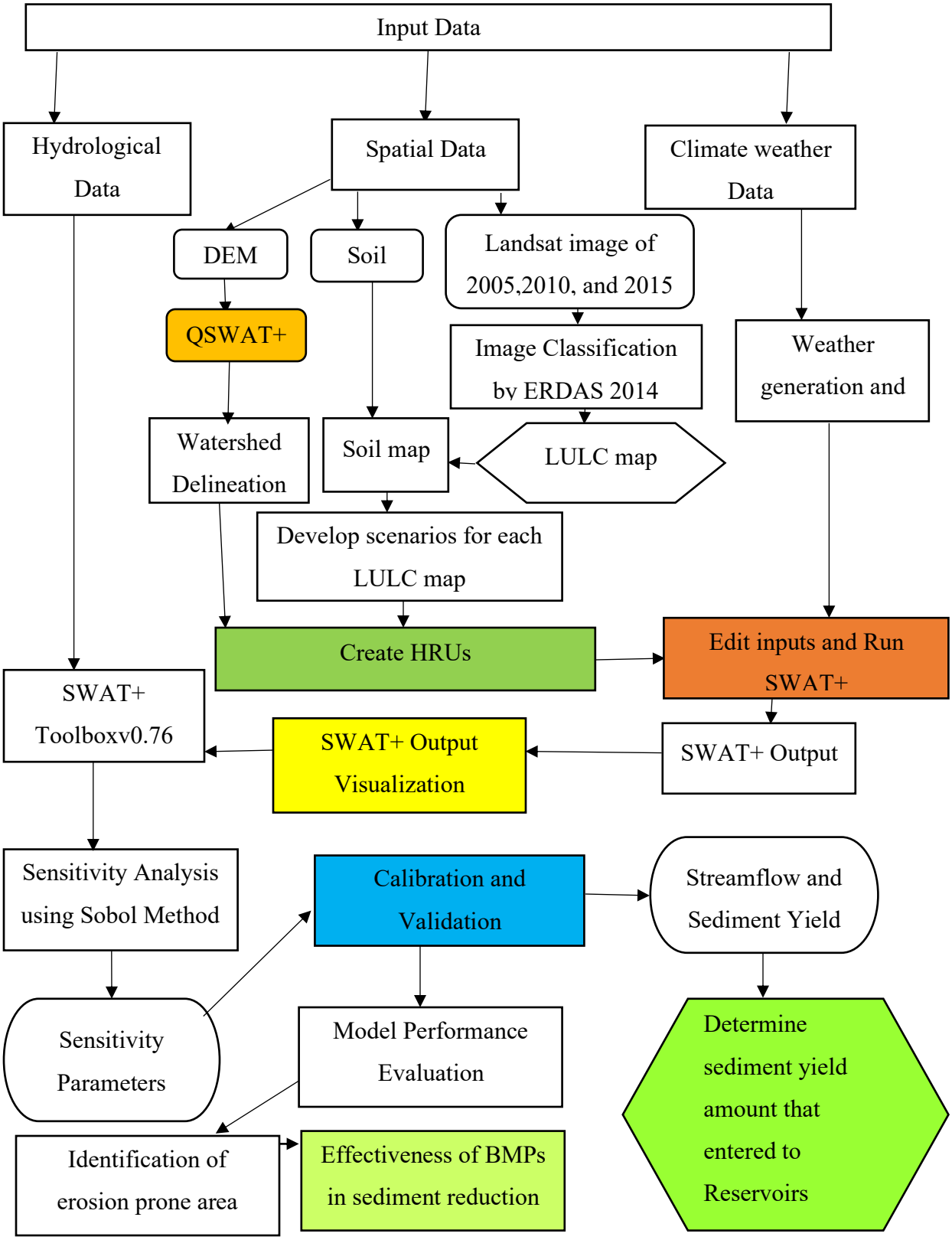

Figure 3-6 The overall methodology layout

In this work, the best management practices adopted in various land use management scenarios were analyzed based on the efficiency of sediment reduction in the upper Awash basin. The development of BMPs in watersheds (critical subbasins) has been identified as an efficient technique to significantly reduce sediment erosion. The best management practices (BMP) scenarios were applied by adjusting QSWATPLUS parameters to understand the effects of practice on simulated results within the model. The selection of BMPs and the values of their parameters are site-specific and should represent the reality of the research area (Abdelwahab et al., 2014). The best management strategies chosen are filter strips, terracing, and contour, which are utilized to manage sediment erosion areas in the upper Awash River basin. In this context, the best management practices were taken from a community-based Ethiopian watershed management guideline, and the selected best scenarios were similar to different findings involving catchments in Ethiopia (Guideline, 2005), (Haregeweyn et al., 2015a),(Ayele et al., 2017),(Nadew' et al., 2019), and (Lemma et al., 2019b). The detailed discussion for each scenario is presented below.

Baseline Scenario (1): This scenario shows the existing condition of the watershed without any implementation of best management practices. In this simulation, the calibration and verification of the model were performed without changing any calibration parameters.

Filter strips Scenario (2): Different widths of filter strips were applied on all hydrological response units based on soil types, land use types, and slope classes. The filter strips are used to trap silt in a particular area. The filter width value was assigned based on local research experience in the Ethiopian highlands, and the value of width is 1m to 30m (Gashaw et al., 2021). As a result, a 5m wide filter strip is used for this study.

Terrace Scenario (3): The application of terracing in a watershed reduces the slope of the HR and the slope length of the subbasin. Terracing in QSWAT is simulated by adjusting both erosion and runoff parameters. The simulation of the effect of terracing on sediment reduction, USLE support practice factor (USLE-P), SCS curve number (CN2), and slope length of the hillside (SLSUBBSN) are the parameters to be adjusted based on the land slope. In general, parallel terraces with different slope lengths and stone bunds were placed on agricultural HRUs that are a combination of farmed land, all soil types, and slope classes. As a result, we chose a 30% reduction in slope length for this investigation.

Contour Scenario (4): Contour planting parameters were modified in QSWAT by changing the curve number (CONT-CN) for surface storage and infiltration and the USLE practice factor (CONT_P) for erosion.

Combination Scenario (5): This scenario is implemented by adjusting the curve number, management practice, average sloping length, and basin slope.

3.2.10 RESULTS

3.2.11 Land Use and Land Cover Change

Cultivated land was the most dominant LULC type in the Koka Dam watershed, and it covered 75.51% in 2000, 78.61% in 2005, 81.66 % in 2010, and 82.82 % in 2015 (Table 3.2). In 2015, the urban area expanded by 6.34%, and the coverage of cultivated or agricultural land increased by 7.31%. Whereas the forest land coverage decreased by 5.47 % in 2015. The significant expansion of cultivated land and urbanization areas has occurred in the upper Awash River basin since 1985. Based on Shawl and Chakma's study, the future LULC change scenarios of the years 2025 and 2035 will have a significant expansion of cropland and urban areas in the upper Awash River basin. They concluded that an expansive area covered in woodland and shrubland had been replaced by agricultural land and urban areas (Shawul and Chakma, 2019). The LULC dynamics dramatically shifted from forest and shrubland to agricultural land, according to other studies (Daba and You, 2022),(Chelkeba Tumsa, 2023). The outcome is similar to those previous findings in the case of incremental agricultural land and urbanization area, but the incremental rate is different from the previous findings. This study revealed that the forest area declined by 5.47% between 2000 and 2015, although previous studies did not show the deforestation rate.

Table 3-2 LULC change in (2000-2015years)

Land use type	**LULC (%)**				**Changes in LULC (%)**		
	2000	2005	2010	2015	2000-2005	2005-2010	2010-2015
Cultivate land	75.51	78.61	81.66	82.82	3.1	3.05	1.16
Woodland	2.33	1.31	1.43	1.4	-1.02	0.12	-0.03
Urban Areas	5.4	9.9	10.52	11.74	4.5	0.62	1.22
Forest	5.92	4.92	4.77	0.45	-1	-0.15	-4.32
Water Body	2.65	1.67	1.89	1.31	-0.98	0.22	-0.58
Shrub land	4.32	3.28	2.57	3.36	-1.04	-0.71	0.79
Bare land	0.8	0.27	2.92	0.24	-0.53	2.65	-2.68

3.2.12 Sensitivity Analysis

The SWAT Toolbox was used to conduct the sensitivity analysis. The parameters were ranked based on their impact on hydrological model simulation results. The most responsive parameters for flow simulation were curve number, saturated soil hydraulic conductivity, soil depth, available water capacity, and base flow recession coefficient. The most sensitive parameters for sediment yield simulation were the soil erosion factor, sediment concentration for lateral, Manning's "n" for overland, the parameter for sediment routing, and the curve number. The sensitivity parameters were determined based on a high correlation between the ground observed data and the simulated value, as well as recommendations from several literature sources in the Awash River basin (Daba and You, 2022),(Jilo et al., 2019), and (Tessema et al., 2021). The sensitive parameters used to calibrate and validate streamflow and sediment yield were consistent with previous research in the Awash River basin (Jilo et al., 2019), (Santhi et al., 2001). The calibration flow and sediment parameters are shown below in Table 3.3.

Table 3-3 Sensitivity analysis for streamflow and sediment calibration

List Parameters	Description	Ranks		Parameters range
		Flow	Sediment	
ALPHA_BF	Base flow recession coefficient	5		0.0 -1.0
CN2	Initial curve number	1	5	35-95
CH_K	Channel hydraulic conductivity	6	6	0.0-150.0
ESCO	Soil evaporation compensation factor	7	7	0.0-1.00
Soil_Z	Soil depth	3		0.0-3500.0
Soil_k	Saturate the soil's hydraulic permeability	2	8	0.0-2000.0
SOL_AWC	Soil storage capacity or content	4		0.0-1.00
SLOPE	Slope rank		9	0.0-0.9
SPCON	Parameter for sediment routing		4	0.0001-0.01
USLE_P	Cover factor	8	10	0.1-1.0
REVAP_MIN	Percolation into the deep aquifer is to occur	9		0.0-500
OVN	Manning's value for Overland	10	3	0.01-30

USLE_K	Soil loss factor	1	0.0-0.65
LAT_SED	Lateral sediment concentration	2	0.0-5000

3.2.13 Calibration and validation

Calibration and validation were performed using monthly measured flow and sediment yield data at the outlet of the Koka Dam watershed. The simulated values of streamflow and sediment yield for the three LULC scenarios have a good match to the ground observed values, as shown in Figures 3.7 to 3.12. However, the streamflow and sediment yield simulations are higher than the actual values. This demonstrated that the model overpredicted the streamflow and sediment. This could be due to data quality and a lack of sediment data. The hydrograph of streamflow, which is indicated in Figures 3.7 to 3.9, showed that the simulated flow and observed flow for the 2005 LULC scenario had a better relationship when compared to the 2010 LULC and 2015 LULC map results. The statistical values of (R^2) for the 2005 LULC, 2010 LULC, and 2015 LULC data were 0.91, 0.89, 0.89, and 0.77,0.81,0.79 during calibration and validation, respectively (Table 3.4). This result showed that the model's efficiency was at a good level. This ensured a high correlation between the predicted and observed flow. The model performance results for this study were consistent with findings from prior research projects carried out in the upper Awash River basin (Boru et al., 2022).

Table 3-4 Model performance result for streamflow calibration and validation at Koka dam

Model Performance Indicators	2005 Historical LULC		2010 Historical LULC		2015 Historical LULC	
	Calibration (2000-2010)	Validation (2011-2015)	Calibration (2000-2010)	Validation (2011-2015)	Calibration (2000-2010)	Validation (2011-2015)
R2	0.91	0.77	0.89	0.81	0.89	0.79
NSE	0.89	0.7	0.88	0.77	0.87	0.67
Percent Bias	-16.70	-18.11	-14.86	-21.12	-12.74	-28.77

The simulated and observed monthly flow at the Koka Dam watershed outlet was plotted for visual comparison (Figure 3.7,3.8,3.9). The hydrograph of the calibration and validation period of observed and simulated streamflow showed that the model slightly overestimated the peak value during the rainy season. As displayed in Figures (3.7,3.8,3.9), the simulated peak flow during the

rainy season exceeded the measured values in three LULC scenarios. The average annual measured stream flow was 59.99m^3/sec, whereas the mean annual simulated stream flow was 70.3m^3/sec, 72.3m^3/sec, and 73.5m^3/sec for the 2005, 2010, and 2015 LULC data, respectively. This demonstrated that the change in LULC was the reason for the increase in mean annual stream flow, which increased from 70.3 m^3/sec to 73.5 m^3/sec between the years 2005 and 2015.

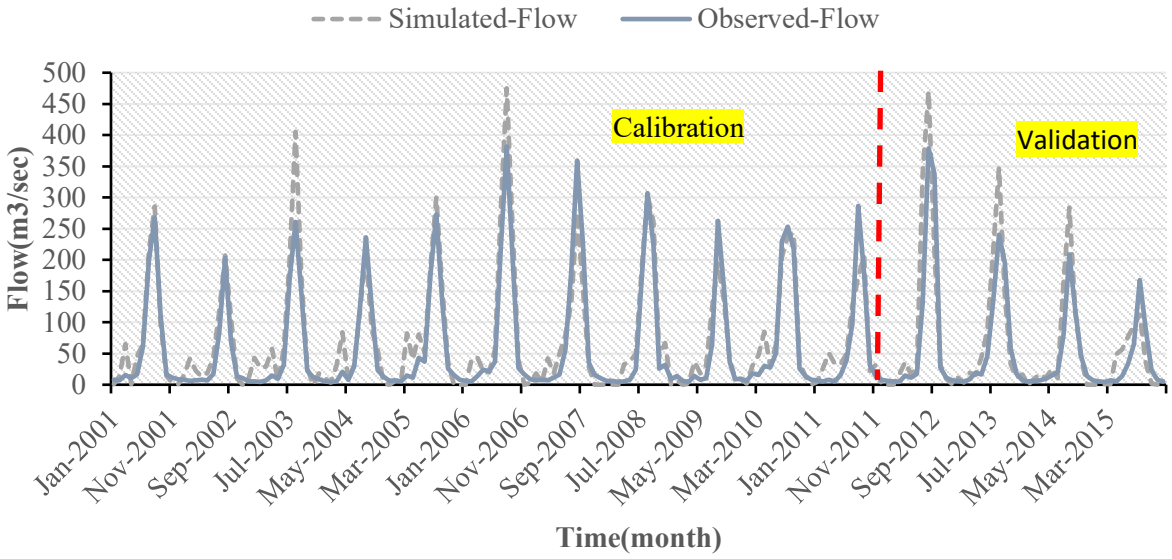

Figure 3-7 Streamflow calibration and validation at Koka dam stations for 2005 LULC

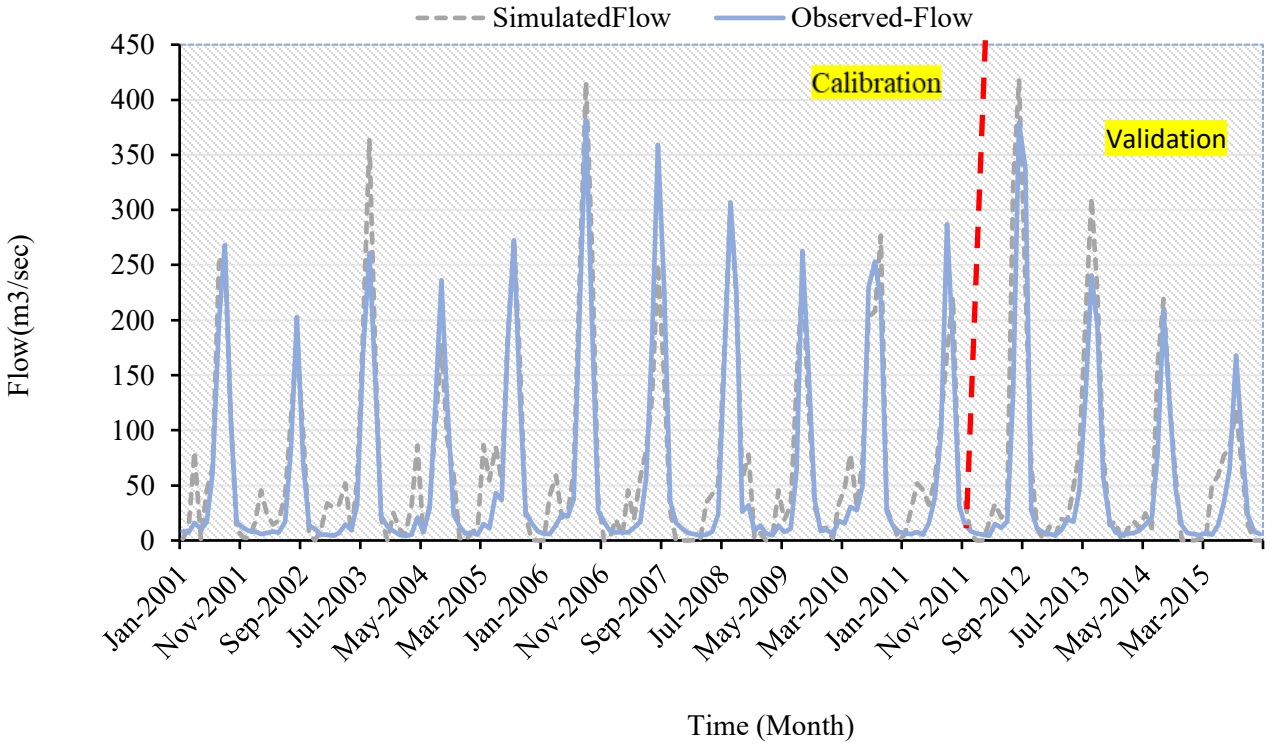

Figure 3-8 Streamflow calibration and validation at Koka dam stations for 2010 LULC

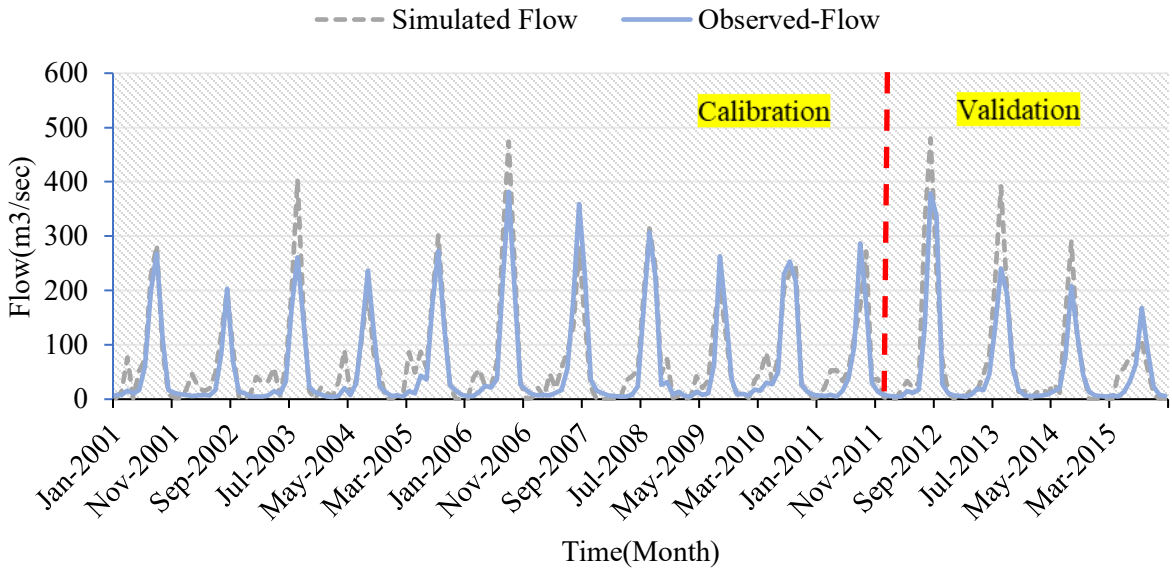

Figure 3-9 Streamflow calibration and validation at Koka dam stations for 2015 LULC

The monthly time-step sediment yield hydrograph was developed to show the simulated and actual sediment load values (2000-2015) during the calibration period. Figures 3.10, 3.11, and 3.12 depict the sediment yield hydrograph for measured and simulated values between 2000 and 2015.

The result of calibration and validation revealed an excellent correlation between simulated and observed sediment values. The model performance result also showed a satisfactory result. As shown in Figures 3.10, 3.11, and 3.12, the simulated sediment value exceeds the observed sediment values. This showed that the model overpredicted the sediment value. R^2, NSE, and percent bias during calibration for the 2005 LULC data were 0.81, 0.68, and -66.18, respectively (Table 3.5). The model performance result is better than the previous study results in this area (Boru et al., 2022).

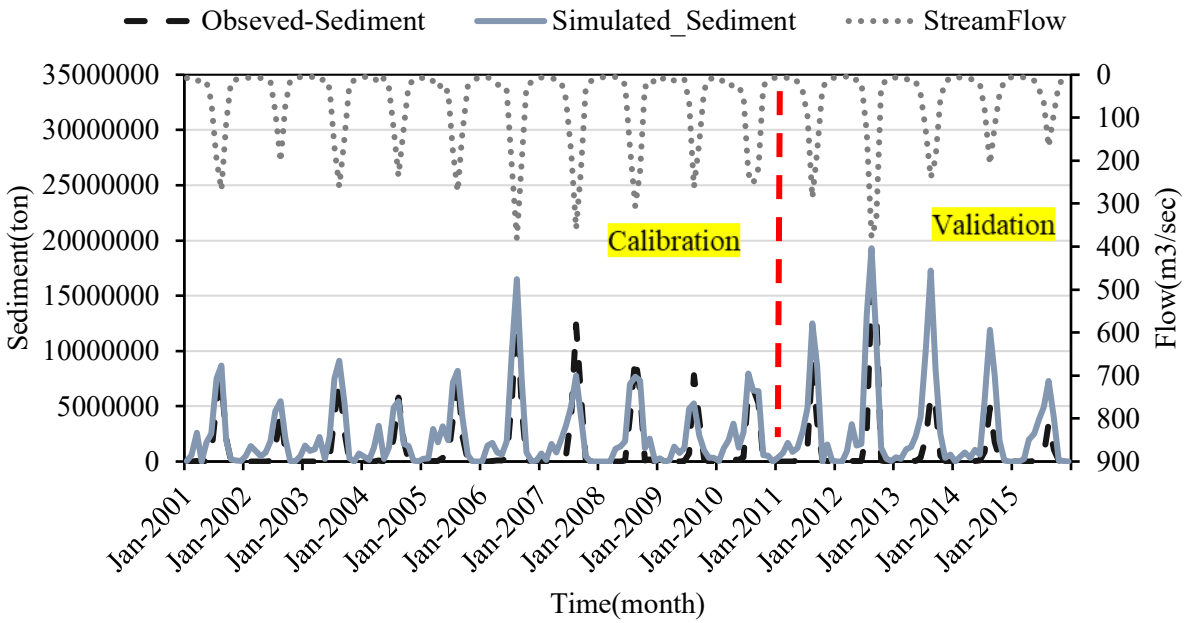

Figure 3-10 Sediment calibration and validation at Koka dam stations for 2005 LULC

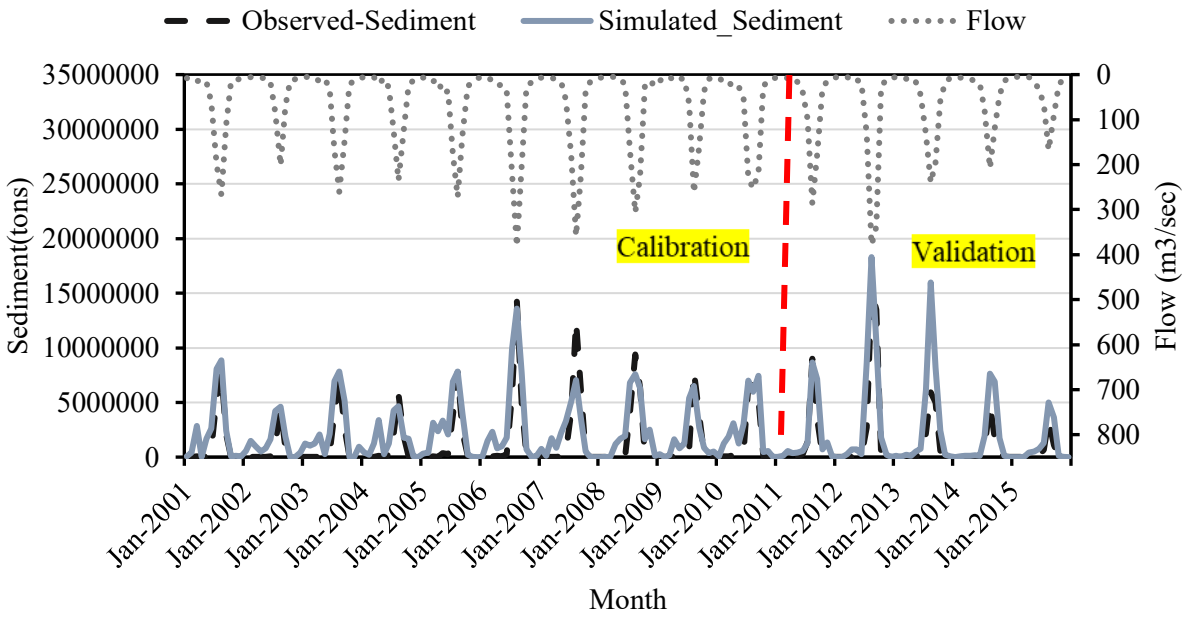

Figure 3-11 Sediment calibration and validation at Koka dam stations for 2010 LULC

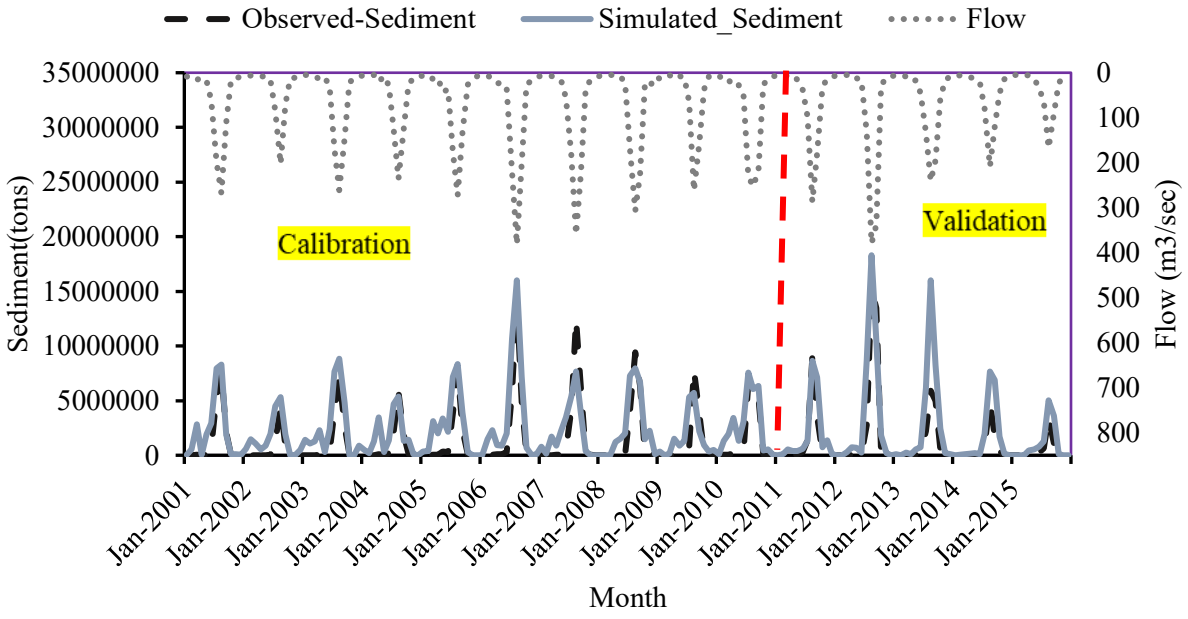

Figure 3-12 Sediment calibration and validation at Koka dam stations for 2015 LULC

Table 3-5 Model efficiency for sediment calibration and validation at Koka Dam gauge station

Model Performance Indicators	2005 Historical LULC		2010 Historical LULC		2015 Historical LULC	
	Calibration (2000-2010)	Validation (2011-2015)	Calibration (2000-2010)	Validation (2011-2015)	Calibration (2000-2010)	Validation (2011-2015)
R^2	0.81	0.71	0.78	0.79	0.78	0.68
NSE	0.68	0.61	0.66	0.6	0.64	0.6
Percent Bias	-66.5	-75.5	-64.23	-53.5	-68.9	-54.6

3.2.14 Temporal Variability of Sediment Yield, Evaporation, and Surface Runoff

The three LULC scenarios were used to evaluate the temporal effects of LULC changes on surface runoff, evaporation, peak flow, and sediment yield. As shown in Figure 3.13, the amount of surface runoff volume, peak flow, and evaporation during the period between 2006 and 2010 is greater than the values of the period between 2000 and 2005. The hydrological responses with different periods of LULC change scenarios are prepared and shown in Table 3-6. The mean annual

streamflow and sediment yield of the Koka Dam watershed increased year to year due to LULC effects. This was due to an increase in agricultural practice areas. The Koka Dam watershed changed from forest plantations to agricultural land between 2000 and 2015. As a result, the runoff and sediment yield increased by 12.68% and 8.84% respectively. These findings are similar to other studies conducted in different catchments. For example, M.choto et al. (2019) described the sediment yield of the Gojeb watershed increasing over time due to an increase in agricultural land area (Choto and Fetene, 2019). Similarly, the surface runoff of the Andassa watershed increased due to changes in land use and land cover (Gashaw et al., 2017).

		2005LULC	2010LULC	2015LULC
Surface Runoff(mm)	2001-2005	212.2	179.4	143.08
	2006-2010	243	209.2	169.96
ET (mm)	2001-2005	686.2	690.6	707.11
	2006-2010	721.4	724.4	749.16
PeakFlow(m3/sec)	2001-2005	2170	2030	1590
	2006-2010	2560	2430	1900

Figure 3-13: Temporal variations of hydrological response under land use change

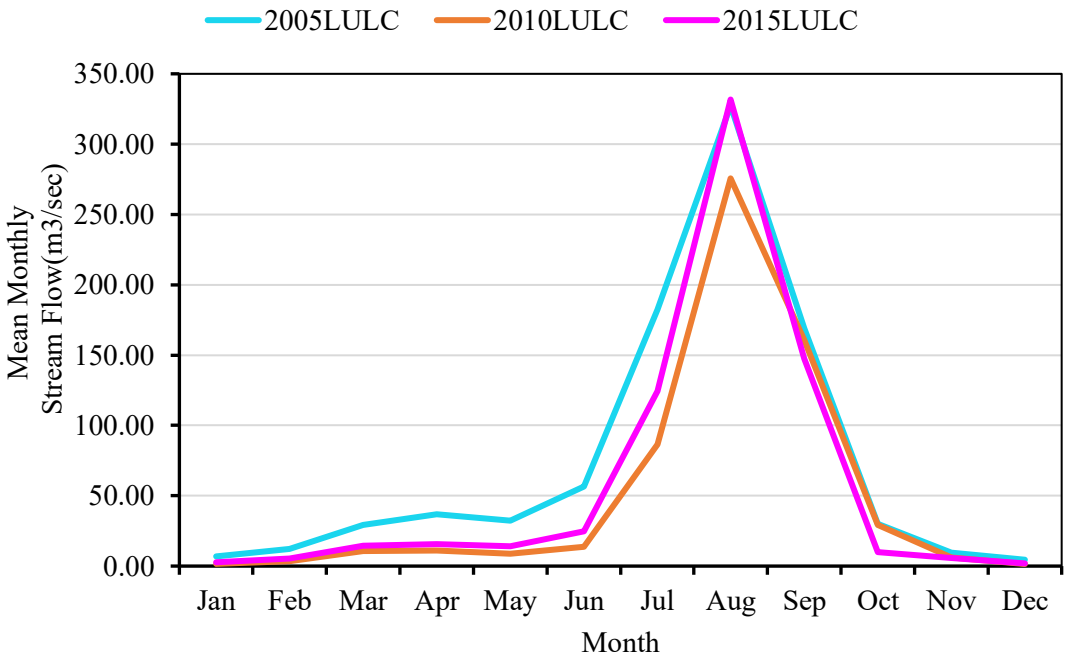

Figure 3-14 Monthly average streamflow comparison under three land use reference data (2001-2015)

3.2.15 Spatial Variability of Sediment Yield, Surface Runoff, and Evaporation at Subbasin Scale

The QSWAT-Plus model was used to evaluate the impact of LULC changes on hydrological responses at the subbasin level using 2005,2010,2015 LULC data. The hydrological responses vary from subbasin to subbasin due to land use/cover change, DEM, soil type, rainfall distribution, slope classes, and management practice. Subbasin 2 has the largest change in surface runoff, water yield, and evaporation when compared to the other subbasins (Table 3.6).

Table 3-6 The spatial variation of surface runoff due to LULC change

Subbasin	2005LULC			2010LULC			2015LULC		
	Surface Runoff(mm)	Water Yield(mm)	Evaporation(mm)	Surface Runoff(mm)	Water Yield(mm)	Evaporation(mm)	Surface Runoff(mm)	Water Yield(mm)	Evaporation(mm)
1	166.58	224.96	736.59	163.46	196.13	756.68	177.84	204.66	753.48
2	281.16	357.56	765.37	283.46	333.98	768.55	314.84	358.01	762.81
3	202.58	237.98	668.63	199.33	224.12	686.29	215.24	241.04	720.64
4	117.26	129.72	554.37	133.60	142.99	561.63	135.53	143.69	561.30
5	162.71	177.16	634.53	176.58	185.36	627.71	214.16	221.48	623.99

3.2.16 Spatial Mapping of Sediment Yield at Subbasin Scale

The spatial mapping of sediment yield over the entire watershed is displayed in Figure 3.15. The simulated mean annual sediment yield of the watershed ranged from 0.02 to 47.31 t/ha/yr, with a mean value of 28.33 t/ha/yr in the baseline scenario. Figure 3.15 indicates that subbasin 2 was the most erosion-prone area with an average value of 29.03-47.31t/ha/yr. In the Koka Dam watershed, 18.93% of the areas are classified as very high erosion-prone, 28.4% and 35.1% as high and moderate erosion-prone, 11.5% as lowly prone to erosion, and 7.8% as very low prone to erosion.

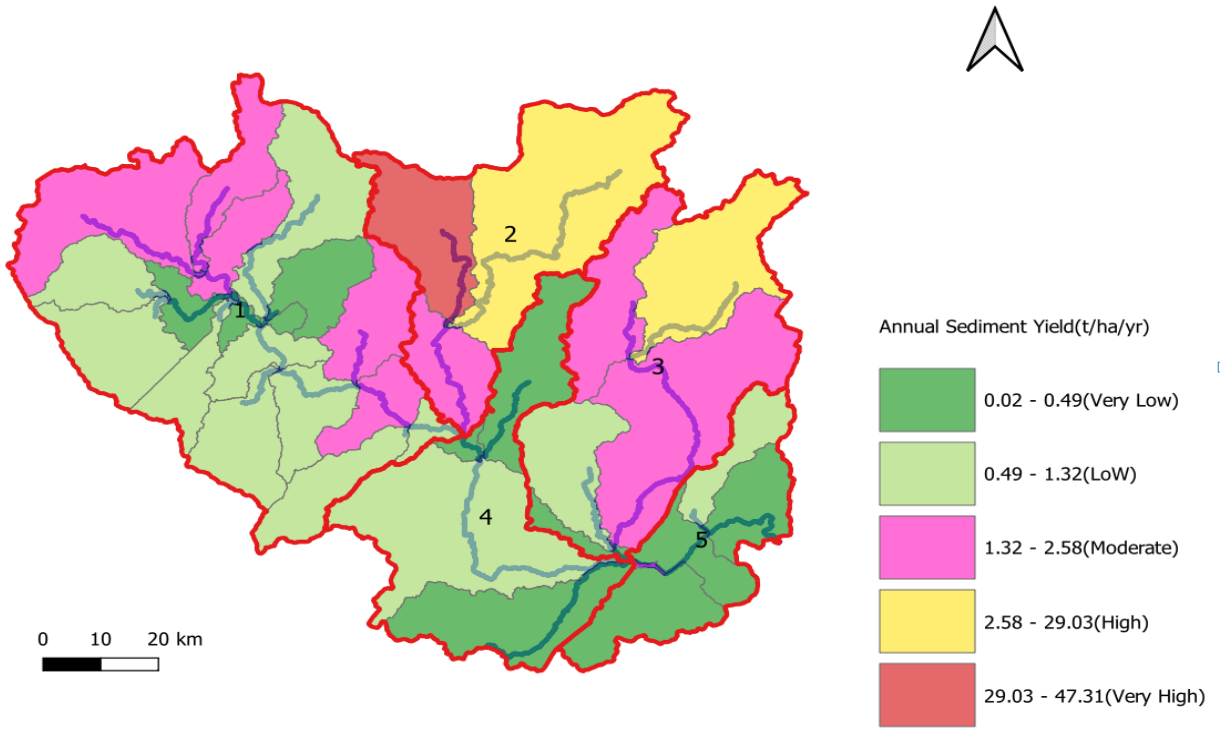

Figure 3-15 Spatial mapping of mean annual sediment yield using 2015 LULC (Base-line)

Subbasin 2 is dominantly covered by agricultural and urban land, which has caused to increased erosion rate. Agricultural practice contributed the most sediment yield in subbasin two. Based on Estifano's reported sediment yield increased due to an increase in agricultural land and a decrease in forest land (Hailu Estifanos and Gebremariam, 2019). Another study also described that cultivated or agricultural land contributed more sediment yield to the Megech reservoir (Assfaw, 2020).

3.2.17 Identifying Best Management Practices (BMPs)

It was identified that subbasins 2 and 3 are categorized as high erosion-prone areas. These subbasins contribute to the Koka Dam reservoir with an average annual sediment yield of ≥29.031t/ha/year. As a result, this watershed underwent the implementation of three chosen management approaches. As shown in Figure 3.16 terrace was the best sediment reduction scenario method among the selected methods, which was tested in three LULC scenarios. This finding differed from other studies in this study area. For instance, N. Boru et al., study (2022) found that terraces, grass waterways, and filter strips were the best management practices, and the sediment reduction scenario was done using one specific year of LULC data. However, in this particular

study, the sediment reduction method was evaluated using three LULC scenarios. According to their findings, the terrace application reduced the amount of sediment yield compared to the grass waterway and filter strip. This finding also indicated that the terrace had better sediment reduction than the contour and filter strip. A similar discovery has been made in the Kesem Dam watershed (Tesema and Leta, 2020). They found that applying terracing in watershed management was the best option to reduce sediment that would enter reservoirs.

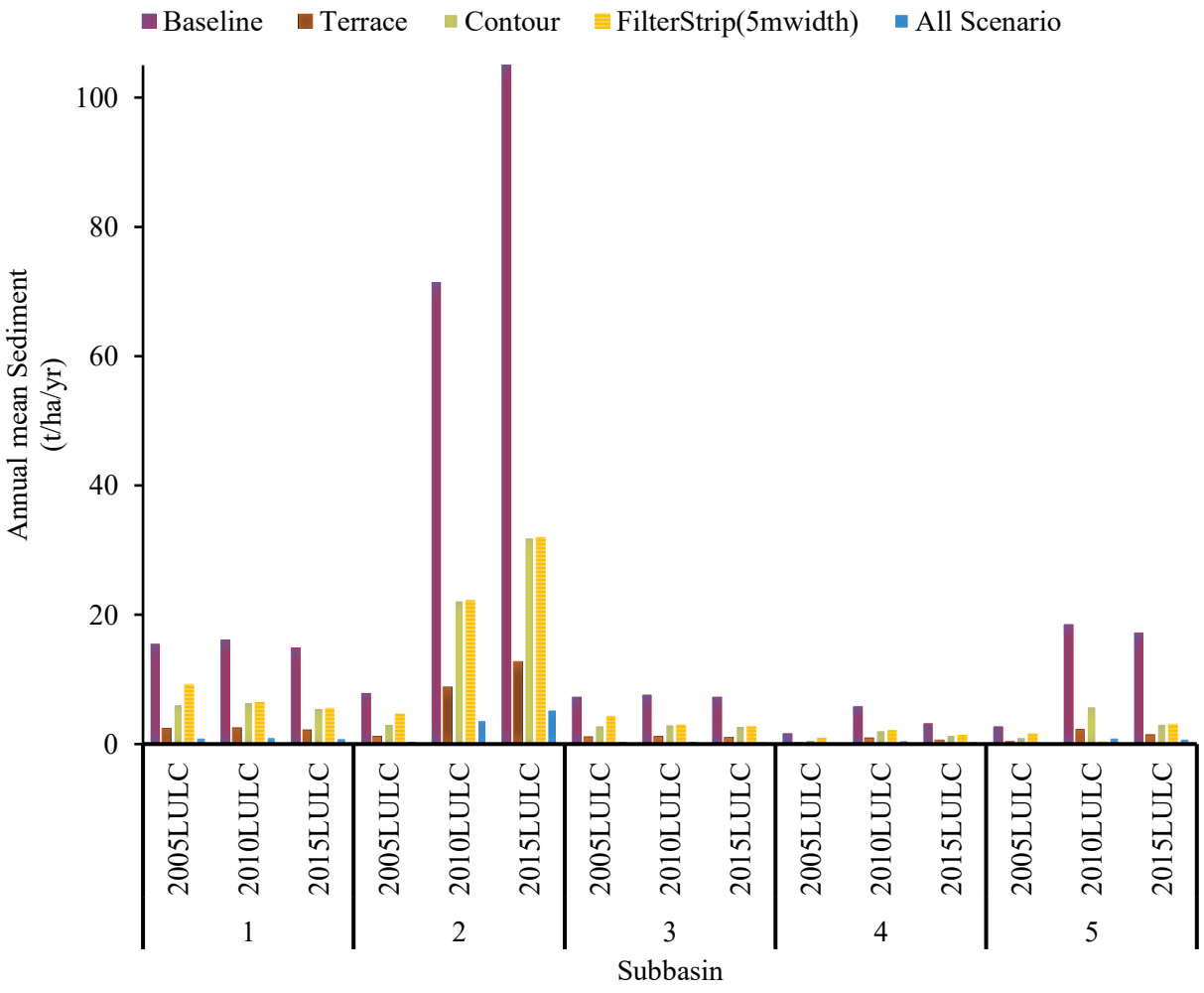

Figure 3-16 Mean annual simulated sediment yield for each scenario

3.3 DISCUSSION

3.3.1 Impact of land use and land cover change on Streamflow

The impact of LULC change in the Koka Dam watershed significantly affected the hydrological response. For instance, the average annual surface runoff for the recent 2015 land use/cover was

increased by 12.65% from the 2005 historical land cover. The mean annual streamflow of the Awash River at the outlet of the Koka Dam watershed increased by 3.2 m^3/sec within 16 years. These changes in streamflow were due to the majority area of forest and woodland being converted to urban areas and agricultural land. The increase in surface runoff is primarily caused by a decrease in the infiltration rate when forest land is converted to other land uses. In general, surface runoff has increased in the study area within 16 years. These findings support previous studies that found surface runoff increased as a result of LULC changes (Chelkeba Tumsa, 2023). Furthermore, these results are comparable to those of other research carried out in various catchments. For example, Kuma et al. (2023) reported an increase in surface runoff in the Bilate catchment as a result of LULC alterations (Kuma et al., 2023). Similarly, changes in LULC in the Megech Dam watershed were found to increase surface runoff (Assfaw, 2020).

3.3.2 Effect of land use and land cover change on sediment yield

The effects of LULC changes on sediment yield dynamics in the Koka dam reservoir are higher when compared from time to time. Because the LULC drastically changed from forest and shrubland to agricultural land and urban areas. The amount of mean annual sediment load entering the Koka Dam reservoir was 26.03 t/ha/year in 2005 and increased to 26.34 t/ha/year in 2010, and 28.33 t/ha/year in 2015. Due to the woodland and forest land converted to agricultural land, the contribution of mean annual sediment yield increased by 2.3 t/ha/year from 2000 to 2015. Moreover, over 16 16-year period (2000-2015), there was an increase of cultivated land area by 7.31% causing an increase of sediment yield by 47.31 t/km^2/year in the study area. This led to increased soil erosion in this watershed and increased sediment supply in the reservoirs of the Koka dam. As a result, the capacity of hydropower generation of the reservoir has decreased from the expected design capacity. Similar results have been noted in this research region; the Koka reservoir's silt accumulation reached 481 million cubic meters, resulting in an estimated 60 million Ethiopian Birr in economic losses and 128 million kWh of energy loss(Adugna and Cherie, 2023). Similar findings have also been reported in other studies conducted in different parts of Ethiopia. For instance, Boru et al. (2022)(Boru et al., 2022) reported that the average annual sediment yield of the Melka Werer watershed is 21.43t/ha/year. According to Kidane et al. (2019) (Kidane et al., 2019), the mean annual soil erosion rate of the Guder watershed ranges between 25 and 30 t/ha/year.

3.3.3 Temporal Land Use Effects on Streamflow and Sediment Yield

The amount of surface runoff, evapotranspiration, peak flow, and sediment yield varied throughout the time as LULC altered. The simulated hydrological responses using the three LULC scenario data were divided into two-time frames (2001-2005) and (2006-2010) to understand the effect of LULC change over time series. The periods from 2006 to 2010 showed the maximum variation in hydrological responses, while the periods from 2001 to 2005 showed the minimum variation. The maximum variation of hydrological response occurred between the 2005 LULC and 2015 LULC models, where the surface runoff volume and peak flow rate values were 48.6 mm and 115 m^3/s, respectively. Surface runoff, peak flow, and sediment yield values in the 2015 LULC model are higher than those in the 2010 LULC and 2005 LULC models. Every year, the sediment yield increased during the month of high precipitation occurrences. About 60.8% of the total annual sediment yield occurred during the rainy season. It implies that the surface runoff is greater in the months of July, August, and September (Goaba, 2022). Similar research revealed that July, August, and September recorded 70.8% of the overall sediment production (Tesema et al., 2021).

3.3.4 Sediment Yields Spatial Variability

The variability of sediment yield for each subbasin in the watershed was identified using three LULC scenarios, and the simulated values range from 0.02 to 47.03 t/ha/yr. Sediment yields from each subbasin varied due to the combined effects of LULC, soil type, slope, weather, and runoff conditions. The areas of high sediment yield are located in cultivated land, shrub/bushland, urban areas, and bare land with steep slopes. Consequently, the annual sediment yield rate from each subbasin region was used to obtain a map of the spatial variability of sediment yield in the watershed, which showed the subbasins with the worst erosion severity classes. The severity of soil erosion in the watershed points to the need for careful control of sediment reduction in the subbasins, especially in susceptible sections, which was also concluded by the authors of (Boru et al., 2022).

According to Hurni's (1985) study, the tolerable soil loss rate in different agroecological zones of Ethiopia is estimated to be between 2 and 18 t/ha/y. However, subbasins 2 and 3 showed that annual mean sediment yields significantly exceeded the allowable rate of soil loss. Maximum sediment yields were recorded in subbasins 2 and 3, with amounts of 105.1 and 71.8 t/ha/yr, respectively. These outcomes are obtained under the 2015 LULC scenario. The main sources of high sediment yield are agricultural land, bare land, shrubland, and steep slopes. This demonstrates

that the regional variance in sediment yield can be linked to the type of land use, soil, and slope classes. A similar study conducted in the Kesem dam watershed indicated that shrubland, agricultural, forest, bare land, and pasture land covers contributed a significant amount of sediment yield in catchments, and slope had an impact of the highest sediment yield in the subbasins(Tessema et al., 2021). Therefore, the spatial variability of sediment output in the catchment and subbasin is crucial for the implementation of optimum management techniques of soil erosion in the upper Awash River basin.

3.3.5 Effective Management Options on Soil Loss

It was identified that subbasins 2 and 3 were classified as high erosion source areas. The subbasins contribute an annual average sediment yield of ≥ 28.33 t/ha/year. After identifying the hotspots in subbasins, BMPs will be implemented to reduce sediment output from the watershed. Several factors, such as the source of sediment, the cost of implementation, sustainability, the efficiency of BMPs in reducing sediment yield, the amount of rainfall, land use, and the slope of the sub-basins, should be considered while selecting appropriate management practices. Consequently, in this study, inexpensive and more effective BMPs for reducing sediment yield were applied to those sub-basins greater than 28.33 tons/ha/year. The comparison was done using three LULC scenarios. Following the establishment of terracing in the UARB, the mean annual sediment yields of AWRB in 2005 LULC, 2010 LULC, and 2015 LULC data were 1.87, 5.37, and 6.1t/ha/yr, respectively. In this scenario, the mean annual sediment yield of the catchment reduced by 84%,86.5%, and 87.5% in 2005,2010, and 2015 LULC data, respectively. Terraces can substantially reduce sediment yield, especially during high rainfall events and natural hillslopes. Similar findings have been observed in the Upper and Middle Awash River Basin (UAMRB) and the Kesem Dam watershed. According to the author(Boru et al., 2022), the use of terracing resulted in a reduction of sediment yield of 19.56% from the baseline scenario. They conclude that the area covered by agriculture and bare land achieved the maximum silt decrease.

Implementing a 5m filter strip reduces sediment yield by 40%, 71%, and 69.6% for the 2005, 2010, and 2015 LULC scenarios, with mean annual sediment yields of 7.01, 11.43, and 14.98 t/ha/yr, respectively. When the 10m filter strip was used, the sediment was reduced by 60%, 81%, and 80% for the 2005,2010, and 2015 LULC scenarios. These findings indicate that increasing the width of the filter strip can increase the reduction efficiency of the sediment yield-prone subbasins. This is attributed to the fact that about 63% of the study area has a slope of less than 20%. Since

the effectiveness of filter strips increases as the slope of a field is kept less than 20%, the simulation result for this scenario was found to be higher than the simulation result reported by Sisay. This study's findings are consistent with prior findings in Ethiopia (Tessema et al., 2021) and (Abebe and Gebremariam, 2019).

The simulation result of contour reduced the average annual sediment output for the 2005 LULC,2010 LULC, and 2015 LULC data by 60%,66.8%, and 69.6% from the baseline simulation of 11.69,39.87, and 47.03 t/ha/yr, respectively.

During the combination of filter strips, Contour, and terrace scenarios, the amount of sediment yield in UARB reduced by 93.3 %, 94.2%, and 94.6% for the 2005,2010, and 2015 LULC data, respectively. The average annual sediment yield of the watershed for the 2005,2010, and 2015 LULC data was 11.69,39.87, and 47.31 t/ha/yr, respectively.

3.4 Limitations of the Study

This study helps to understand the impact of land use and land cover changes on sediment yield dynamics in the Koka Dam watershed using three LULC scenarios. However, other important physical variables such as phosphorus and nitrates were not considered in this study due to a lack of reliable data. In addition to this, this study showed the efficiency of BMP implementation in reducing sediment yield, but the economic feasibility of these implementations was not evaluated due to the absence of data.

3.5 CONCLUSION

Changes in land use and land cover are key sources of soil erosion at the watershed, basin, regional, and global levels. The QSWAT Plus model was used to assess the effects of LULC changes on sediment yield dynamics in the Koka Dam watershed. The analysis of LULC change between the three references LULC (2005,2010, and 2015) revealed that over the past 16 years, LULC change had a significant impact on the upper Koka Dam watershed. Over 16 years, these were shown by increases of 7.31% and 6.34% in agricultural land and urban area, respectively. In contrast, the coverage of plantation forests, water bodies, and woodlands decreased by 5.47%, 5.7%, and 3%, respectively. Runoff and sediment yield variables significantly changed when the Upper Koka Dam watershed's LULC map was changed, keeping the catchment variables constant. Over sixteen years, streamflow, surface runoff, and sediment yield have all increased by 4.55%, 12.68%, and 8.84% respectively. The simulated mean annual sediment yields of the Koka Dam watershed for the three LULC scenarios (2005,2010,2015) were 26.03, 26.34, and 28.33 t/ha/yr, respectively.

Some subbasins produced larger sediment output, ranging from 71.8 to 105.1 t/ha/yr. Therefore, identifying and mapping the spatial distribution of sediment yield is critical to minimizing the erosion rate. Three management scenarios (filter strip, contour, and terraces) are used to reduce sediment yield. Filter strip, contour, and terrace reduced sediment yield by 60%, 65%, and 86%, respectively, when compared to the baseline situation. Overall, the combination of filter strip, contour, and terrace, the amount of sediment yield in UARB was reduced by 94%. Based on the research findings, it is recommended that the terrace scenario be implemented on the upper side of the Koka Dam watershed for efficient sediment reduction. Areas like steep slopes and extensive agricultural practices have a high risk of erosion, categorized as high and very high. The differences in erosion risk among sub-basins help planners identify and prioritize certain catchment areas that require immediate soil conservation measures. The modeling technique may be valuable to decision-makers in determining potential soil erosion causes and identifying hotspot areas. The study's findings will assist policymakers in making land and water management decisions and can be utilized as a model for land use implementation in other watersheds. The simulated effective BMPs can be used to reduce soil erosion in the Ethiopian highlands and other similar watershed zones across the world.

4. Spatiotemporal Sediment Yield Variability in the Upper Blue Nile Basin, Ethiopia

Abstract

Soil erosion and silt deposition have caused significant problems in the Ethiopian highlands, particularly in the Upper Blue Nile Basin (UBNB), reducing the service life of reservoirs in the region. To develop effective mitigation strategies, it is essential to understand the sediment yield in the region and identify the hotspot areas. The Modified Universal Soil Loss Equation in Soil and Water Assessment Tool Plus (SWAT Plus) was used to simulate streamflow and sediment yield and identify the hotspot spatiotemporal variability of sediment yield in the UBNB at different reservoir catchments. The QSWAT Plus model is implemented by utilizing the digital elevation model, climate and weather generation data, land use, soil type, and slope of the UBNB. The Sobol tool algorithm, part of the SWAT Toolbox's calibration and uncertainty analysis programs, is used to calibrate and verify streamflow and sediment yield monthly. The model exhibited satisfactory performance across all the watersheds studied. The Kessie watershed exhibited significant spatiotemporal variation in sediment yield. The spatial variation of sediment output across different catchments within the watershed ranged from 0 to 67.6t/ha/yr. 42.04 % of the watershed area is a critical erosion region, and 39.48 % of the watershed is a subcritical region. This significant spatial variability in sediment yield is attributed to a combination of human activities and environmental factors in the region. The extremely high sediment yield values observed in parts of the watershed have serious negative consequences for the longevity and functioning of numerous reservoirs located in the Ethiopian highlands. Approximately 90% of the total yearly sediment load was recorded during the winter season. According to the simulation results, implementing filter strips, terraces, and contour procedures within the watershed could drastically lower watershed sediment yield by 58.67%, 93.685%, and 64.46%, respectively. The chosen best management practices (BMPs) have proven to be very effective in reducing sediment discharge in watershed-vulnerable areas. Based on the percentage reduction in sediment, it was concluded that terracing was the most effective strategy for the affected subbasins compared to other watershed management approaches. This study found that BMPs are effective at reducing sediment transport and could be used to reduce reservoir sedimentation in the UBNB.

Keywords: Sediment Yield, Spatio-temporal variability, Best Management Practice, Upper Blue Nile Basin, QSWAT+

4.1 Introduction

Soil erosion is a challenge that has spread quickly over the years due to land degradation caused by human factors, activities, and inappropriate management practices. The storage capacity of reservoirs is, therefore, reduced due to sediment deposition (Ayele et al., 2021). In recent years, sedimentation has been a worrying issue and is becoming a topic for discussion by researchers due to the adverse effects that this process exerts on water storage capacity, design, and operational techniques in global dam reservoirs (Briak et al., 2016). This is a problem that plagues many dams all over the world, and it has often been referred to as an invisible enemy. For instance, (Perera et al., 2023), it is projected that reservoirs worldwide will experience a 26% reduction in their storage capacity by the year 2050. By now, significant regions across the globe have lost 13–19% of their originally available water storage. Each year, 0.5 to 1% of reservoir capacity is lost in the world due to sediment deposition (Bachiller et al., 2019). For instance, the gradual decrease in reservoir capacity over time diminishes the useful lifespan of dams. As a result, it has tremendous economic and environmental problems. ("An overview of reservoir sedimentation in some African river basins," 1993) highlighted reservoir sedimentation as a serious issue in African river basins, pointing out that the usable storage capacity of these reservoirs is declining.

Previous studies showed that several dams in Ethiopia are prone to sediment deposition. For example,(Tessema et al., 2024) found that the storage capacity of Angreb dam reservoirs decreased by 62.28% in 16 years of operation and caused an average annual volume reduction of 3.9%. In addition to this,(Haregeweyn et al., 2006) found that the operational lifespan of small-scale irrigation dam reservoirs in the Tigray area has been drastically diminished owing to high levels of silt accumulation. Seventy percent of the examined reservoirs exhibited severe siltation problems, suggesting they will cease to be functional long before their anticipated design lifespan. The Koka reservoir was reported to be losing 17 million cubic meters of storage capacity each year because of siltation. This swift decline in capacity is expected to considerably shorten the projected lifespan of the reservoir (Bihonegn and Awoke, 2023). Dams located in the Amhara region have fully silted up much earlier than their intended design lifespan. For example, the Shumburit reservoirs found in the East Gojjam area will likely not be functional for more than 15 years if the current rate of sediment deposition continues at the same pace as the previous 6 years throughout

the operational period (Endalew and Mulu, 2022). Additionally, some dams in this area are at risk of accelerated sedimentation buildup. For instance, the Borkena intake structure in the Awash River basin, as well as the Adrako dams in this same region, had already failed before the completion of their construction (Mekonnen et al., 2015).

The principal cause of silt buildup in Ethiopian reservoirs is soil erosion caused by rainfall, which is a critical concern in Ethiopia's highland regions (Hurni et al., 2005). In the highland regions of Ethiopia, the main causes of land degradation and soil erosion are the topography, long-standing agricultural practices, climate, land use patterns, and changes in land cover (Chelkeba Tumsa, 2023), (Hurni et al., 2005). Specifically, the UBNB has experienced significant soil erosion due to heavy rainfall in the region's steep and uneven terrain. This soil loss has been exacerbated by agricultural practices that diminish the natural and human-maintained vegetation cover, which would otherwise help protect the soil layer (Nyssen et al., 2004). Based on Haregeweyn's study, 39 % of the UBNB is subjected to a higher erosivity rate (more than 30 t/ha/yr), which could potentially threaten downstream reservoirs like the Grand Ethiopia Renaissance Dam(Haregeweyn et al., 2017).

Ethiopia has been allocating significant financial resources towards the planning and construction of dams in the UBNB region. However, there is a risk that half of the dam reservoirs may lose their expected economic lifespan within half of the design period (Haregeweyn et al., 2015b). This is the result of improper reservoir design without properly identifying sediment sources and the amount of sediment yield. This is due to the lack of a comprehensive local database on sediment yield and the absence of an appropriate sediment yield model, which has been a challenge for reservoir designers (Billi, 2015).

The amount of sediment transported in the upper region of the UBNB exhibits significant spatial variability or unevenness across the landscape. For example, the catchment areas showed a wide range in their specific suspended sediment yields, varying from as low as 4 t/km^2/yr to as high as 4,935 t/km^2/ yr (Fazzini et al., 2015). According to a previous study (Haregeweyn et al., 2008), the average spatially specific sediment yield for 11 reservoirs in the Tigray region was 9.89 t/ha /yr. Recent bathymetric surveys conducted on a reservoir located in the Upper Blue Nile Basin (UBNB) have revealed that the average sediment yield in the surrounding watershed area is more than 120 metric tons per hectare per year. Additionally, this high rate of sedimentation is leading to an annual capacity loss of 11% for this specific reservoir, known as the Anjeb Reservoir. This

showed a large spatial variation in suspended sediment yield (SSY) among the different catchments, with the magnitude being high both regionally and globally. This implies that land degradation, especially soil erosion, and its resulting on-site and off-site impacts, is a severe problem in the Ethiopian highland region. Therefore, it is crucial to understand the degree of sediment variability and the total amount of sediment that will be transported to water infrastructure projects, such as dams and irrigation facilities, over the planned operational lifetime of these structures.

Erosion can adversely affect ecosystems onsite and offsite. Before implementing any conservation measures, it is important to first assess the areas that are experiencing rapid erosion, which can be considered erosion "hotspots". Specifically, estimating the spatial distribution of sediment load within the catchment areas has become crucial information needed for effective soil conservation and management efforts (Easton et al., 2010). Determining the spatial distribution of sediment yield across an entire watershed through field surveys, which has been done before, is a complex, expensive, and time-intensive process. This approach only provides a rough approximation of the actual erosion patterns due to the high degree of spatial variation within the watershed. Additionally, many of the parameters related to sediment yield are still obtained through estimates rather than direct measurements (Bai et al., 2017). Erosion and sediment transport are intricate processes that are influenced by a variety of factors, including the underlying geology, topography, climate, and vegetation cover, both natural vegetation and human-driven land use patterns. While erosion processes are complex, various physically based models have been developed to address this issue. These models operate at different spatial scales and utilize different conceptual approaches.

Due to inadequate or improper watershed management practices being implemented in the upstream areas of the Genale Dawa catchment, the majority of reservoirs located in this area are experiencing significant losses in their overall capacity. This is caused by excessive sediment deposition and buildup within these water bodies, originating from the upstream watersheds (Feyissa Negewo and Kumar Sarma, 2021). In the Ethiopian highlands, the absence of an effective watershed management system, as well as changes in land use patterns across the landscape, have played a significant role in driving land degradation (Tebebu et al., 2010).

Physically based distributed models have the ability to more accurately identify critical erosion areas and represent the spatial variability within a catchment, in comparison to empirical or

conceptual modeling approaches(Pandey et al., 2016). Agricultural Non-Point Source, Limburg Soil Erosion Model, and Soil and Water Assessment Tool (SWAT) are some of the physically-based hydrological models used in the UBNB to evaluate the hydrological response and soil erosion process (Betrie et al., 2011); (Easton et al., 2010). The QSWAT+ model is a valuable tool for simulating hydrological responses, including runoff and sediment production. This is because the model focuses on capturing the interconnected spatial relationships between the various components of the watershed system. By accounting for these spatial relationships, the QSWAT+ model can provide a more comprehensive and accurate representation of the watershed system (Bieger et al., 2017). Furthermore, it has been proven to make reliable forecasts of water flow and sediment transport in streams and rivers. It has been calibrated using observed data for runoff and sediment data at multiple sites, and this calibration process has yielded satisfactory results. The insights provided by the QSWAT+ model can assist decision-makers and planners in increasing awareness about the problems of soil loss in the basin and sedimentation occurring in Lake Tana (Lemma et al., 2019a). The purpose of this study is to utilize the QSWAT+ model to identify the most severe erosion hotspots and evaluate the spatial differences in SSY within the UBNB. While the QSWAT+ model is new, the standard SWAT model has been more widely used and applied across the world in various sediment yield research studies (Betrie et al., 2011), (Tibebe and Bewket, 2011), (Vigiak et al., 2017), (Dutta and Sen, 2018), and (Mosbahi and Benabdallah, 2020). The QSWAT Plus model represents an advancement over previous versions, as it incorporates landscape units in addition to sub-catchments. The key advantage of using the QSWAT Plus model over other physical models is its ability to provide insights into basic catchment characteristics, even when comprehensive data may not be readily accessible. Additionally, the QSWAT Plus model can be used to assess hydrological responses that are typically challenging to simulate accurately using other modeling approaches (Bieger et al., 2017). In general, the choice between QSWAT+ and the InVEST SDR model depends on the specific needs and constraints of the study. QSWAT+ is ideal for detailed, process-based hydrological and sediment transport modeling, particularly in data-rich environments where high-resolution analysis is required. In contrast, the InVEST SDR model is better suited for rapid, user-friendly assessments of sediment delivery, especially in scenarios where data availability and computational resources are limited.

It stands out that this study used sophisticated modeling and calibration methods like QSWAT Plus with MUSLE and the Sobol method, which analyzed the spatial and seasonal variation of

sediment yield in the UBNB and recommended suitable BMPs. These aspects not only set our study apart from other studies but also substantially enhanced our understanding of sediment processes within the Upper Blue Nile Basin. By providing actionable insights and practical solutions, this study contributes to improved water resource management and reservoir life span in the region, making it a valuable addition to the existing body of knowledge.

The primary objectives of the study are to: 1) calibrate and validate the model at various gauged stations while identifying sensitive parameters; 2) analyze spatial and temporal variations in sediment yield throughout the UBNB; 3) identify critical erosion-prone areas within the basin; and 4) evaluate these erosion hotspots and the prioritized watersheds.

4.2 Materials and methodological approaches

4.2.1 Description of the study area

This study is conducted in the Upper Blue Nile Basin (UBNB), which is in the northwestern part of Ethiopia. The Blue Nile basin plays a crucial role in the hydrology of the entire Nile River system, as it generates more than 60% of the total Nile River runoff that reaches Sudan and Egypt. It is the largest tributary of the Nile River, covering a drainage area of 175,000 km^2. Specifically, the research area encompasses seven nested watersheds within the UBNB: Megech, Koga, Robigumero, Ribb, Gilgel Abbay, Gumara, and Kessie watersheds. The location of the study area is provided below in Figure 4.1 and Table 4.1.

Table 4-1 Information on the location and size (area) of different watersheds

Name of watershed	Lat &Long of outlet	Area(km^2)
Kessie	11: 4: 0 N &38:11: 0 E	65784
Koga	11:22: 0 N&37: 3: 0 E	244
Megech	12:29: 0 N& 37:27: 0 E	462
Ribb	12: 0: 0 N&37:43: 0 E	1592
Robi Gumero	9:45: 0 N&39: 0: 0 E	887
Gumara	11:50: 0 N&37:38: 0 E	1394
Gilgel Abbay	11:22: 0 N&37: 2: 0 E	1664

The mean annual rainfall of the Koga watershed is 1475 mm from 2000 to 2015, and the mean annual temperatures range from 7 °C to 30 °C. The mean annual rainfall of the Kessie watershed is 1145 mm in the range of 2000–2015. The mean annual rainfall of the Megech, Ribb, `Gilgel Abbay, Robigumero, and Gumara watersheds is 1177mm, 1428mm, 1821mm, 1266mm, and 1443mm, respectively.

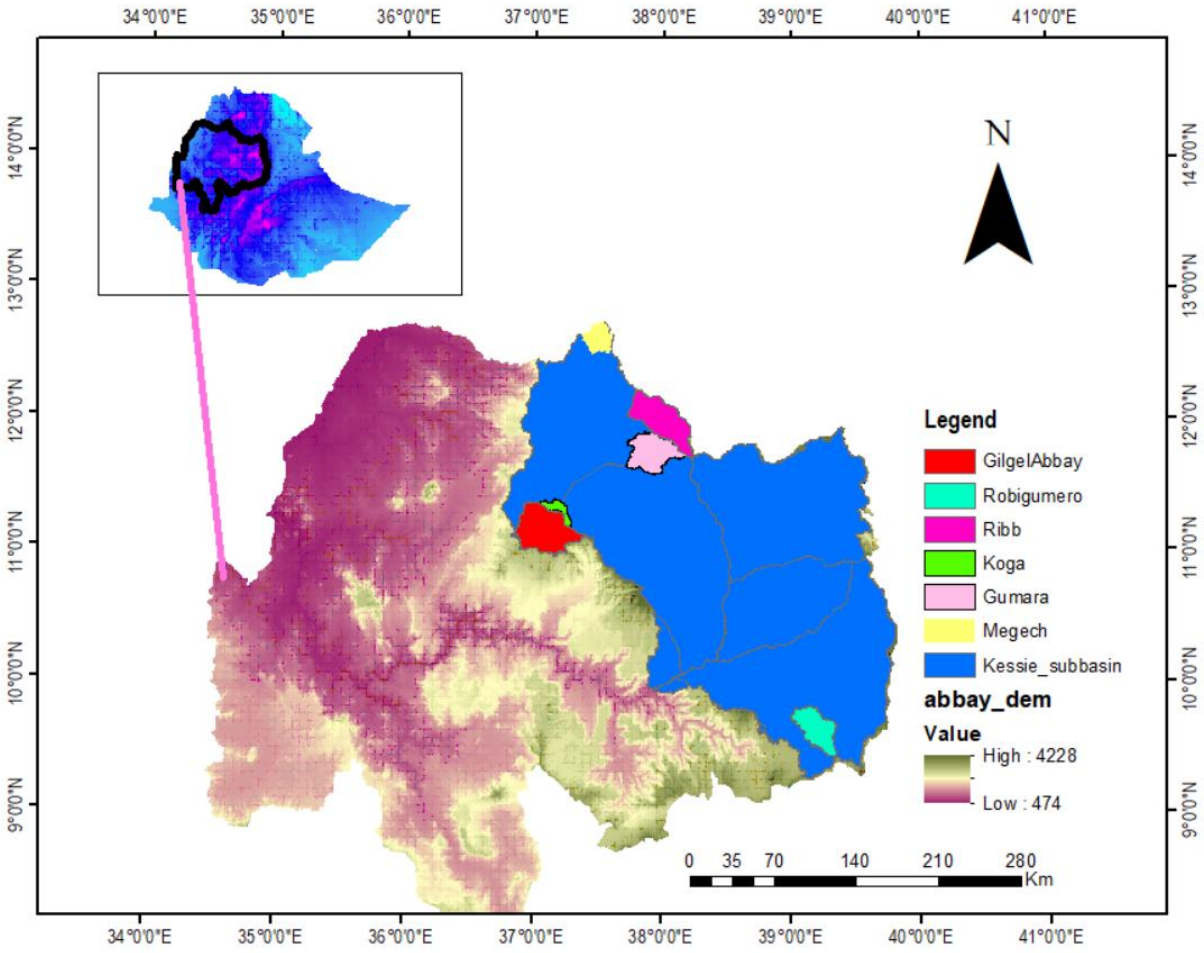

Figure 4-1 The location of the Kessie watershed area

The predominant soils of the UBNB are characterized as vertisols, luvisols, and leptisols (Easton et al., 2010). Majorly, the main soil groups of the Kessie watershed are Lithic Leptosols, Eutric Vertisols, and Chromic Luvisols, which cover 44%, 24%, and 14%, respectively (Figure 4.2).

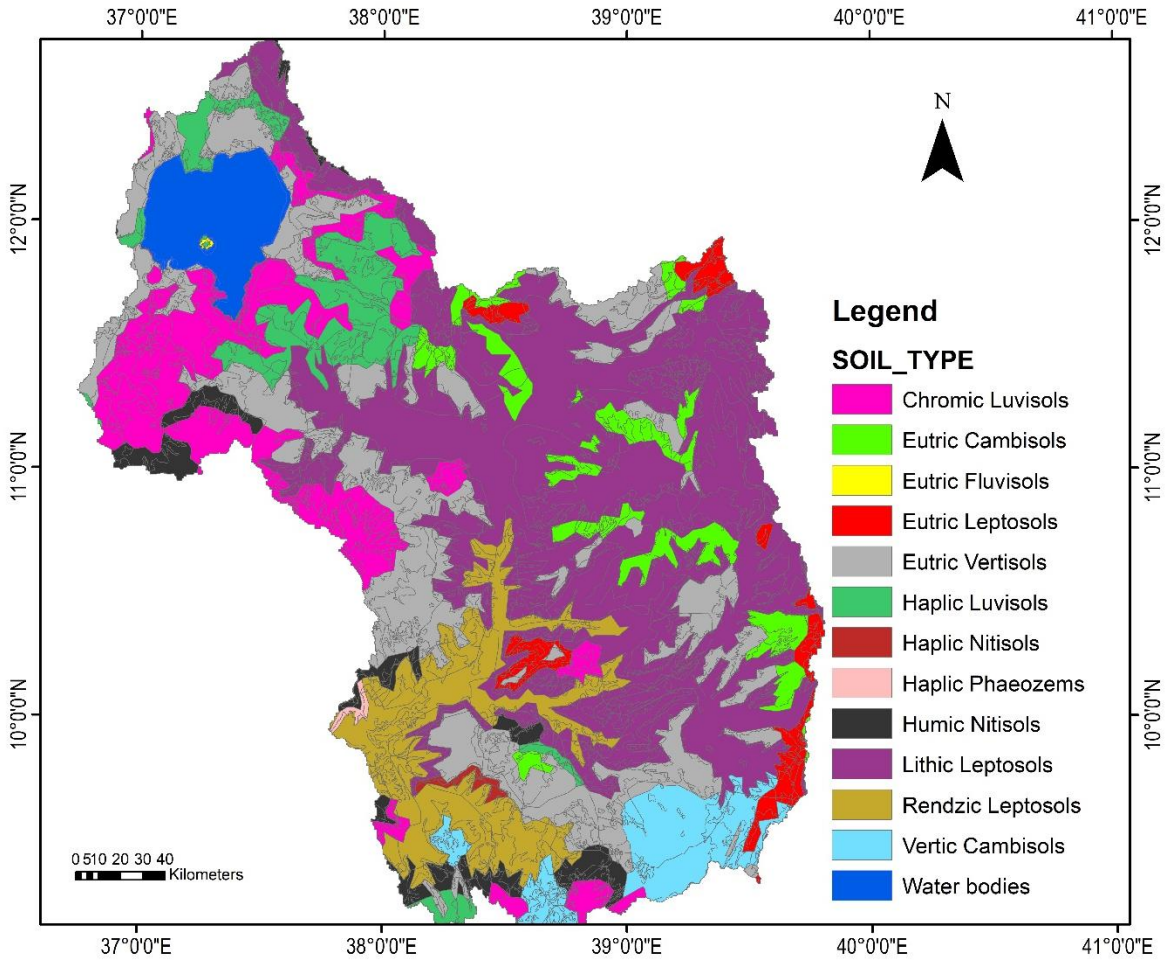

Figure 4-2 Soil types

The dominant LULC categories found within the Kessie watershed include farmland, grassland, barren terrain, bushland, and woodland. Based on the Water and Land Resource Center (WALRC), around half of the watershed area is covered by farmland. The dominant LULC in this watershed was farmland, which covered 50.69% of the watershed. Following agricultural land, the grassland and the bare land cover 12.41% and 10.50%, respectively. The area occupied by urban development is insignificant compared to the total LULC area, accounting for only 0.39% (Figure 4.3).

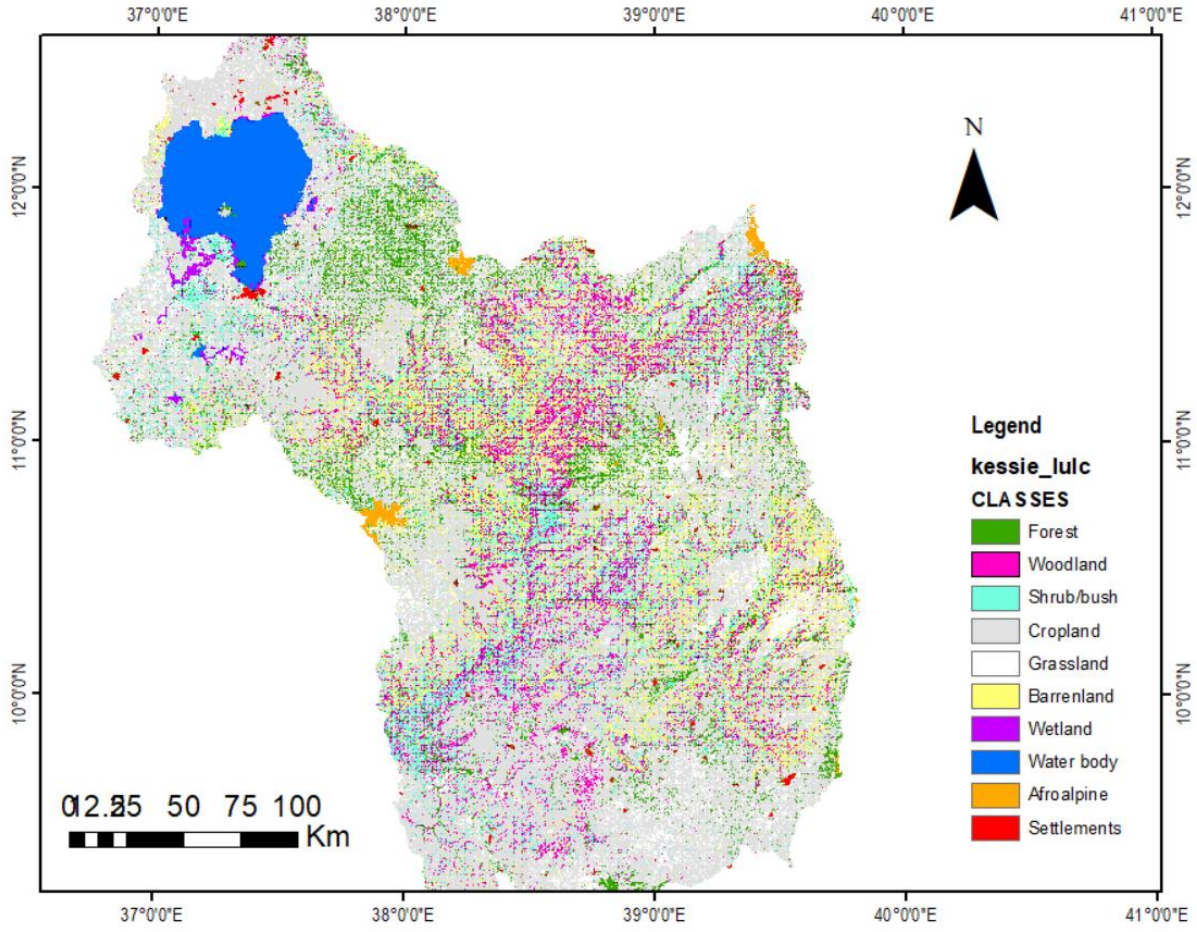

Figure 4-3 LULC map

4.2.2 Data type and sources

The climate condition of the watershed varies spatially due to the influences of the complex topography. Most of the areas have unimodal rainfall patterns and receive the maximum precipitation from June to September. The Digital Elevation Model is derived from the United States Geological Survey's (USGS) website. The daily streamflow data and meteorological data used in the seven case studies were obtained from the Department of Hydrology under the Ministry of Water and Energy and the Ethiopian Meteorology Institute, respectively. The study utilized data collected from approximately 30 weather monitoring stations located in the highland and mountainous regions. This study required spatial and temporal data to be used as input for the SWAT+ model. The spatial data, including soil and LULC information, was obtained from the Water and Land Resource Center (WLRC). Five weather data points were obtained from the

Ethiopian Meteorological Institute for this study. Additionally, hydrological information, including river flow and SSC (suspended sediment concentration), was gathered from the MoWE.

4.2.3 Observed data analysis

Computational areal rainfall: The areal rainfall for the study area is calculated using the Thiessen polygon method. This method involves selecting the weather stations relevant to the study area and using their point rainfall measurements to compute an average rainfall value for the overall study area.

Streamflow: For the purposes of streamflow calibration and validation, data from seven measured gauged stations located at the outlets of the watersheds were utilized. Due to gaps in the data, 16 years' worth of data was used for both the calibration and validation processes. The calibration and validation of streamflow and sediment yield simulations took place at Kessie, Megech, Ribb, Robi Gumero, Gumara, Gilgel Abbay, and Koga between 2000 and 2015.

Developing a sediment rating curve (SRC): The suspended sediment concentration (SSC) data obtained from the MoWE were inadequate for calibrating and validating the QSWAT+ model. This was because the recorded SSC data at the catchment outlets lacked continuous time-step measurements of the suspended sediment concentrations. To address this, the suspended sediment concentrations will be generated using a sediment rating equation. This equation establishes a relationship between the suspended sediment concentration in a river and the stream flow. The general form of this relationship is provided (Equation 4.1) (Augusto and Santos, 2008).

$$Q_S = c * {Q_W}^d \quad (4.1)$$

Where Qw is streamflow(m^3/sec), Qs is SSC (tons per day), and c and d are constant variables.

In this study, three different methods were used to develop the SSRC. These methods utilized the non-continuous sediment data and corresponding flow measurements. This indicates the SSC was modeled using several types of rating curve equations, encompassing both linear and non-linear formulations on logarithmic scales, with some curves also incorporating adjustment factors. The non-linear logarithm-suspended sediment rating curve relationships were calculated and fitted using the Solver Excel tool (Equation 4.2) (Asselman, 2000). The rating curve of different watersheds in the Kessie subbasin is shown in Table 4.2.

$$LogQ_S = a + b * Log(Q_W)^c \quad (4.2)$$

Where a, b, and c are constants

Table 4-2 Different watershed sediment rating curves

Station Name	a	b	R^2	Equation (LogQS)
Kessie	3.5439	1.0003	0.99	3.5439+1.0003logQW
GilgelAbbay	1.1826	1.5924	0.93	1.1826+1.5924logQW
Ribb	1.6215	1.527	0.91	1.6215+1.527logQW
Gumara	1.2649	1.5331	0.88	1.2649+1.5331logQW
Robigumero	1.1035	1.1836	0.94	1.1035+1.1836logQW
Koga	1.4788	1.3033	0.83	1.4788+1.3033logQW
Megech	1.5954	1.1861	0.89	1.5954+1.1861logQW

Table 4.2 revealed that the suspended sediment concentration (SSC) rating curve was developed using a log-log transformed relationship with relatively small data samples. Among the stations, Kessie had a larger dataset compared to the others, resulting in a more reliable and well-performing rating curve. In contrast, Koga station had fewer data points, which led to a model with lower performance compared to the others.

4.2.4 Description of the model

The hydrological simulation of flow and sediment for the UBNB was conducted using the revised SWAT+ model (version 60.5.4). QSWAT+ is the updated version of the SWAT model, and it is used to simulate surface runoff and sediment load from the watershed (Koltsida et al., 2021),(Arnold et al., 2018). The QSWAT+ model was used for this investigation because it accurately simulates watershed dynamics and corresponds to the hydrological aspects of the study area. The selection process includes a full examination of current modeling approaches, emphasizing their applicability to the unique climate and land-use features of the area. This is a widely used framework for projecting the consequences of altered soil conditions and land management strategies (e.g., deforestation or alternative agricultural practices) on water resources in a given region (Sab-basin and Daba, 2018). The QSWATPlus model allows for a detailed portrayal of the watershed's properties at the hydrologic response unit level. This design is broadly applicable on a worldwide scale, and the latest edition integrates terrain characteristics to help identify hotspot areas. Moreover, the results from the graphical interface are presented clearly, making them easy to understand.

The water balance equation shown in (Equation 4.3) forms the basis for the SWAT+ model, which is used to simulate surface runoff (Munoth and Goyal, 2019).

$$SW_t = SW_0 + \sum_{i=1}^{t} \left(R_{day} - Q_{sur} - E_a - W_{seep} - Q_{gw}\right) \quad (4.3)$$

Where SWt denotes the change in soil water storage at time t (mm), and SW0 is the soil water storage at the end of the previous day (mm). t is time in days. Rday is daily rainfall (mm); Qsur is surface runoff (mm); Ea represents losses due to evaporation and transpiration (mm); Wseep is water percolating into deeper soil layers (mm); and Qgw is groundwater flow returning to the soil (mm).

The SWAT+ model is powerful because it can not only predict how much water runs off the land (surface runoff) but also estimate how much soil erosion occurs (sediment loads) using the MUSLE equation. The MUSLE equation used in SWAT+ applies to the whole watershed and is derived from the pioneering soil loss equation developed by Wischmeier and Smith back in 1978 (Equation 4.4) (Taylor et al., n.d.), and (Vigiak et al., 2015).

$$Sed = 11.8(Q_{surf} * q_{peak} * area_{hru})\text{^}0.56\text{x}K_{USLE}xC_{USLE}xP_{USLE}xLS_{USLE}xCFRG \quad (4.4)$$

Sed: sediment loss (ton), Q_{sur}: the amount and rate of water runoff, $_{qpeak}$: the highest rate of water flow during a runoff event (m^3/sec), area $_{HRU}$: the size of an area of HRU (km^2), KUSLE: the soil erosion factor, C_{USLE}: the land cover and management factor, P_{USLE}: the conservation measure factor, LS_{USLE}: the topographic factor, and CFRG: the coarse fragment factor.

4.2.5 Model input

To build a QSWAT+ model, several types of information are required, including meteorological, hydrological, and physical variables. SWAT+ is a semi-distributed physical model, so it needs both spatial and temporal data as inputs. The main inputs required for the QSWAT+ model include digital elevation data, climate data, streamflow measurements, sediment data, soil information, and maps of LULC (Documentation, 2009). The DEM used in the study had a resolution of 30 meters, and it was obtained from http://srtm.csi.cgiar.org/strmdata/. The climate data comprised approximately 39 meteorological stations for the Kessie subbasin catchments.

4.2.6 Modeling approach

By using the QSWATPLUS model, the Kessie subbasin was divided into eighteen subbasins, 2500 HRUs, and 2500 channels. For calibration and validation, seven subbasins or watersheds were selected. The choice of these sub-basins was driven by data availability. The total streamflow and

sediment load for the Kessie watershed were calibrated and validated using measurements taken at the watershed outlet, located near the Millennium Bridge. For estimating evapotranspiration, the Hargreaves equation was used, and the Muskingum routing method was employed for channel routing. The QSWAT+ model (version 60.5.4) was set up and run using the QGIS software (version 3.30.2) interface. The model was configured to run on a daily time step, with a simulation period from 2000 to 2015 that included a one-year warm-up period.

4.2.7 Model performance, sensitivity analysis, calibration, and validation

The sensitive parameters in the QSWAT+ model have a considerable influence on various model outputs, including the rate of water volume, sediment load, percolation, groundwater movement, evaporation, and overall water yield. The QSWAT+ interface offers several well-established sensitivity analysis methods that can be used to evaluate the impact of the model's sensitive parameters. These sensitivity analysis techniques are used to understand how to alter the input setting parameters during the simulation of stream flow and sediment yield (Yen et al., 2019). The Sobol method was selected for the sensitivity analysis due to its common use in identifying significant sensitivity parameters. It was applied to the model and identified the most influential parameters in the model. The software automatically determined the sensitive parameters and ranked them in order from most to least significant (Hordofa et al., 2023). For example, to select Curve Number as a sensitive parameter, adjust its value while keeping other parameters constant and record the model efficiency metrics. Similarly, change the Available Water Content (AWC) values based on soil depth or moisture retention characteristics in set increments, and evaluate the model efficiency. If the model efficiency results during the calibration of streamflow and sediment yield show significant changes, it indicates that both parameters are sensitive.

Within the SWAT+ modeling framework, calibration and validation can be carried out using several different approaches, including the SWAT+ Toolbox, R-SWAT, and the SWAT+ Editor manual calibration method. The model calibration was conducted using the SWAT+ Toolbox version 1.05. Calibrating for runoff and sediment is easier and more effective with the SWAT+ Toolbox than with R-SWAT or the SWAT+ Editor (Hard et al., 2024). The calibration process is done using manual and automatic techniques. Finally, validating the simulation output is mandatory by using the different periods.

The model efficiency is measured by using statistical performance indicators; the most commonly used to evaluate model efficiency are the Coefficient of determination, Nash Sutcliffe, and Percent

Bias (Abbaspour et al., 2015). According to (Moriasi et al., 2007b), NSE >0.5, R2 >0.5, and PBIAS ≤ ±25 were used to assess the satisfactory performance of the model for simulating discharge and sediment yield.

4.2.8 Hotspot erosion area

Understanding the spatial distribution of sediment production and pinpointing areas prone to elevated erosion are vital considerations that need to be accounted for in order to implement effective watershed-scale management and conservation practices. The QSWAT+ model was used to identify and quantify the sediment erosion from the watershed. The average yearly sediment load for the various watersheds was classified according to the soil erosion rank established by Kidan et al. (Kidane et al., 2019). Based on this, the amount of erosion rate and the hotspot area are identified, as the spatial resolution. Quantifying the geographical variance of soil erosion across the watershed gives solid evidence of which areas should be prioritized for the deployment of management strategies. However, due to budgetary constraints, time limitations, and land resources in the study area, it is not feasible to implement watershed management practices across the entire catchment. This necessitates the prioritization of certain sub-watersheds or hotspot areas for the application of erosion control and sediment reduction measures.

4.2.9 Sediment reduction management scenarios

Developing and evaluating different sediment reduction scenarios was a beneficial approach for managing and implementing various practices within the upstream portions of the catchments. This allowed for an assessment of how different management strategies could impact sediment yields from the upstream areas of the watershed (Tesema and Leta, 2020). Various sediment management options were simulated using the QSWAT Plus model. This allowed for the identification of sub-catchments with high sediment yields, which helped determine the most appropriate approaches for managing and reducing the overall sediment load within the watershed. The modeling tool provided a means to evaluate different management strategies and their potential impacts on sediment transport (Jilo et al., 2019). It was used to simulate the implementation of various best management practices (BMPs) to evaluate their effectiveness in reducing sediment loads. Various BMP options were incorporated into the model, such as vegetative filter strips, contour tillage, terraces, grass waterways, stone soil bunds, check dams, and reforestation. Based on the simulated findings within the modeling tool, various types of BMPs were proven to be successful in controlling sediment loads at different watershed scales, as

recommended by previous studies. The modeling approach allowed for an assessment of how the implementation of these sediment control measures could impact sediment transport within the watershed (Leta et al., 2023), and (Risal and Parajuli, 2022). The selected scenarios for this work were the basin line scenario, contouring, filter strips, and terraces to manage the sediment load in the Kessie watershed found in the UBNB.

Baseline scenarios (BS): Using the QSWAT+ model, the baseline scenarios simulated the average sediment yield based on the current or actual conditions present within the watershed. For these baseline model runs, the calibrated parameter values of the QSWAT+ model were employed with no changes to the modeling inputs or parameters. This baseline scenario serves as a reference point for comparing the effectiveness and sediment reduction capability of the specified management strategies that were later simulated.

Filter strip (FS): Vegetative filter strips (FS) were simulated in the QSWAT Plus model as BMPs to reduce sediment load by decreasing soil loss. The impact of the filter strips (FS) was tested by investigating how increasing the width of the filter strips (FILTERW) influenced different land uses and landscape elements, such as agricultural areas, grasslands, pastures, soil types, and topography classes. These filter strip BMPs help to decrease runoff, reduce soil erosion, improve infiltration, and enhance sediment trapping. Based on recommendations from local studies conducted in the Ethiopian highlands, the filter strip widths were adjusted from 1 meter to 30 meters to assess the impact of a change in FS dimensions on sediment retaining efficiency (Betrie et al., 2011). Thus, for this study, a 5m wide filter strip is adopted.

In addition, two other structural best management practices (BMPs) assessed were terracing and contour farming. These practices were implemented to help control soil erosion within the catchment area. Contour farming involves tilling and planting crops along horizontal lines that follow the natural contours of the land, rather than up and down slopes. This allows more of the runoff to infiltrate into the soil instead of flowing downslope. The contoured tillage impounds the water, reducing its erosive potential (Dibaba et al., 2021). The contour farming scenario was assessed in the QSWAT Plus model by modifying two key parameters curve number (CN2) and the USLE Practice factor. These adjustments were made based on the watershed slope, recommendations from the publication, and guidelines provided in the QSWAT Plus user manual. By adjusting certain settings in the model (parameters), researchers were able to see how contour

farming techniques would reduce water runoff and soil erosion in the watershed's agricultural areas (Kefay et al., 2022).

Terracing: Terracing is a practice implemented to reduce soil erosion by constructing rigid platforms or steps on hillsides. In the QSWAT Plus model, the impacts of terracing were represented by modifying the parameters for both sediment concentration and runoff volume. Specifically, the parameters adjusted included the USLE-P, (CN2), and SLSUBBASIN. These parameter adjustments were based on the watershed slope characteristics to accurately represent the impacts of terracing on reducing sediment yield within the watershed.

The common method to assess BMP effectiveness calculates the percent reduction in a specific factor, such as sediment yield (Equation 4.5)

$$\text{The efficiency of the BMP} = \frac{\text{Pre BMPS} - \text{postBMPS}}{\text{Pre BMPS}} * 100 \quad (4.5)$$

The overall methodology of this study is outlined below in Figure 4.

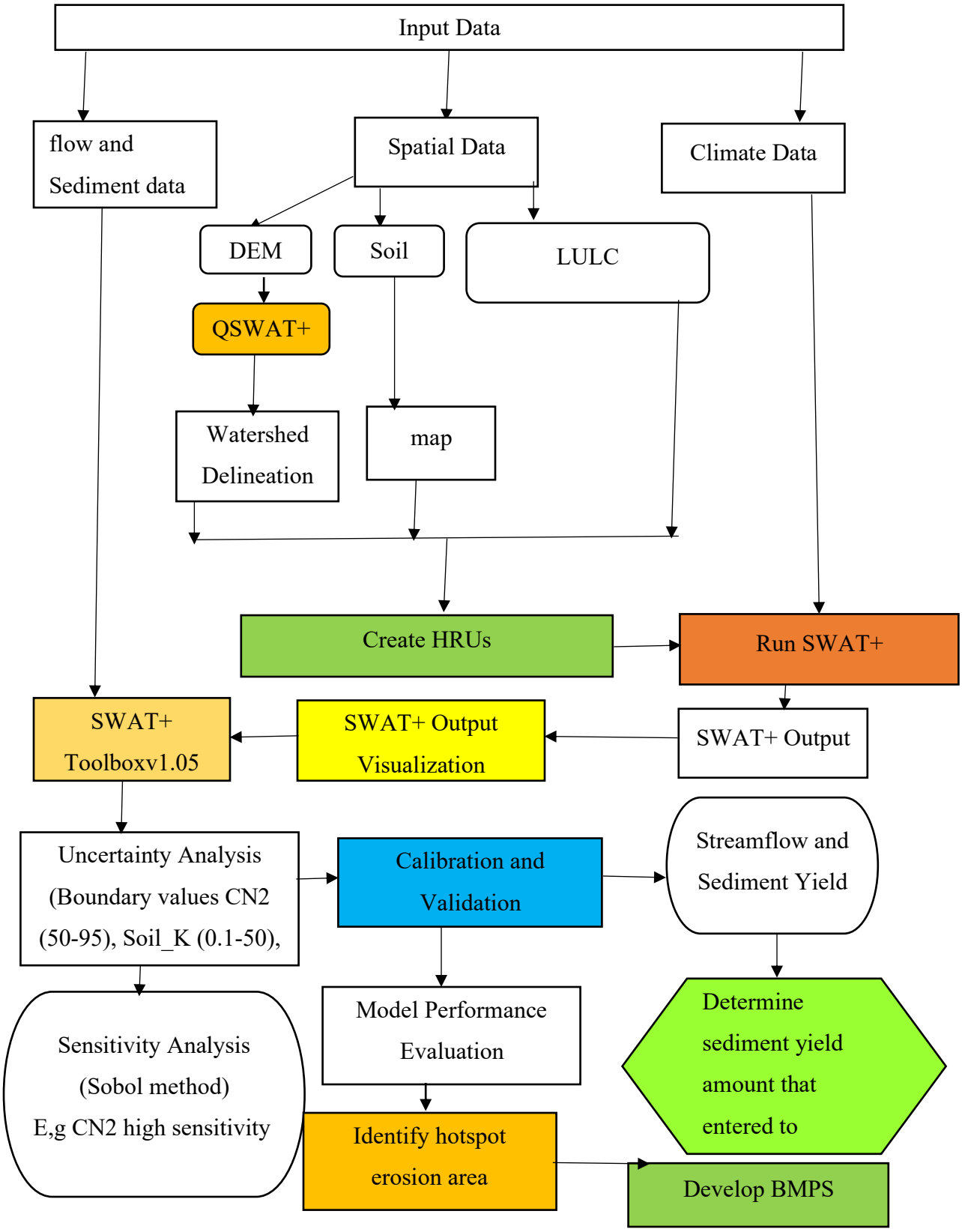

Figure 4-4 Flow chart showing the overall research methodology

4.3 RESULTS

This research paper utilized observed flow and suspended sediment concentration information (2000 to 2015) for model calibration, parameterization, uncertainty analysis, and validation. Where suspended sediment data were not available, an SRC was employed to calculate the suspended sediment data. The QSWAT+ model was developed using DEM, LULC information, soil type data, and slope characteristics of the Kessie watershed. This watershed was delineated into 18 smaller sub-basins and 2,500 HRUs, encompassing a total drainage area of 65,784 km^2.

The thorough calibration and validation process is crucial to minimize uncertainties in the simulation results. The study emphasized the importance of this comprehensive model setup and performance evaluation to ensure the reliability of the sediment yield estimates and BMP effectiveness assessments.

4.3.1 Sensitivity analysis for streamflow and sediment calibration

It is a useful tool for determining the most significant parameters in the model and how they influence the simulated output variations owing to changes in the input variables. For this study, an initial set of 13 parameters was included in the sensitivity analysis for both flow and sediment load.

The streamflow uncertainty analysis was conducted using 16 years of data, and the ranking of the parameters was determined based on the results of the automatic sensitivity analysis. The analysis using the QSWAT Plus model identified eight key parameters as sensitive in the simulation. These included factors related to surface runoff, such as curve number and moisture conditions, soil properties like available water content, evaporation compensation, and erodibility, as well as baseflow, water table depth, percolation, and management practice factors (Table 4.3). The results were like other findings that used the SWAT Plus model (Tumsa et al., 2022),(Konan-waidhet, 2023).

In the sediment simulation, eight parameters demonstrated very high sensitivity in the model, as shown in Table 4.4. As a result, a sensitivity analysis was performed to optimize the unknown variables, and the most sensitive parameters that had the greatest influence on sediment load in the model output were identified. The most sensitive parameters were identified as the slope of the subbasin, soil evaporation compensation factor, USLE equation support practice factor (USLE_P), Manning's "values for overland flow, sediment concentration in lateral and groundwater flow, plant uptake compensation factor (EPCO), linear parameter (SPCON), and exponent parameters.

The sensitivity analysis results for sediment calibration were like other studies conducted in the Ethiopian highlands (Bihonegn and Awoke, 2023), and (Tumsa et al., 2023).

Table 4-3 The streamflow calibration parameters and their corresponding fitted values

Rank	Parameters	Parameter Groups	Minimum value	Maximum value	Optimum value
1	awc	SOL	0.01	1	0.527
2	alpha	aqu	0	1	0.345
3	CN2	HRU	35	98	78
4	cn3_swf	HRU	0	1	0.384
5	usle_p	HRU	0	1	0.144
6	esco	HRU	0	1	0.37
7	revap_min	AQU	0	50	36.279
8	usle_k	SOL	0	0.65	0.618

Note: **SOL**- soil, **HRU** - hydrological response unit, **AQU** -aquifer

Table 4-4 The sediment calibration parameters and their optimized/fitted values

Rank	Parameters	Parameters group	Minimum value	Maximum value	Optimum value
1	slope	HRU	0.0001	0.9	0.071
2	esco	HRU	0	1	0.298
3	usle_p	HRU	0	1	0.658
4	ovn	HRU	0.01	30	4.407
5	lat_sed	HRU	0	5000	171.685
6	EPECO	HRU	0	1	0.354
7	SPCON	bsn	0.0001	0.01	0.001
8	SPEXP	bsn	1	1.5	1.07
9	cn2	hru	35	98	57.315

4.3.2 Streamflow and sediment yield calibration and validation

Streamflow and sediment load were calibrated at different Kessie sub-catchments from 2000 to 2010 and validated from 2011 to 2015. The overall goodness of fit for streamflow and sediment yield calibration was "very good" for the Kessie catchment with NSE= 0.85, R^2= 0.88, percent bias =-20.25, and NSE=0.79, R^2=0.8, and percent bias =9.63, respectively (Table 4.5 and Table 4.6). During the validation process, the model demonstrated good performance, with an NSE value of 0.65, an R-squared value of 0.69, and a PBIAS of -16.56. Other studies on streamflow and sediment modeling within the Kessie sub-catchment with other spatial data and short time series attained similar statistical results (Easton et al., 2010). As illustrated in Figures 4.5 (monthly sediment yield hydrograph) and 6 (monthly streamflow hydrograph), the predicted values for both flow and sediment load at the various watershed outlets were well-aligned with the observed values. The statistical values of model efficiency NSE, R^2, and PBias are shown in Tables 4.5 and 4.6. Tables 4.5 and 4.6 show the acceptable ranges of the static performance criteria for the model. As displayed in Figure 4.5 (**monthly sediment yield hydrograph)**, the simulated sediment data are greater than the observed values. Similarly, the simulated value of streamflow is greater than the observed value for each watershed. It showed that the model overestimated the streamflow and sediment yield. This result may have arisen due to data constraints, as the observed sediment data in the watershed is quite limited and relies on data generated by a sediment rating curve. Additionally, the model assumptions do not adequately capture the complex hydrological responses.

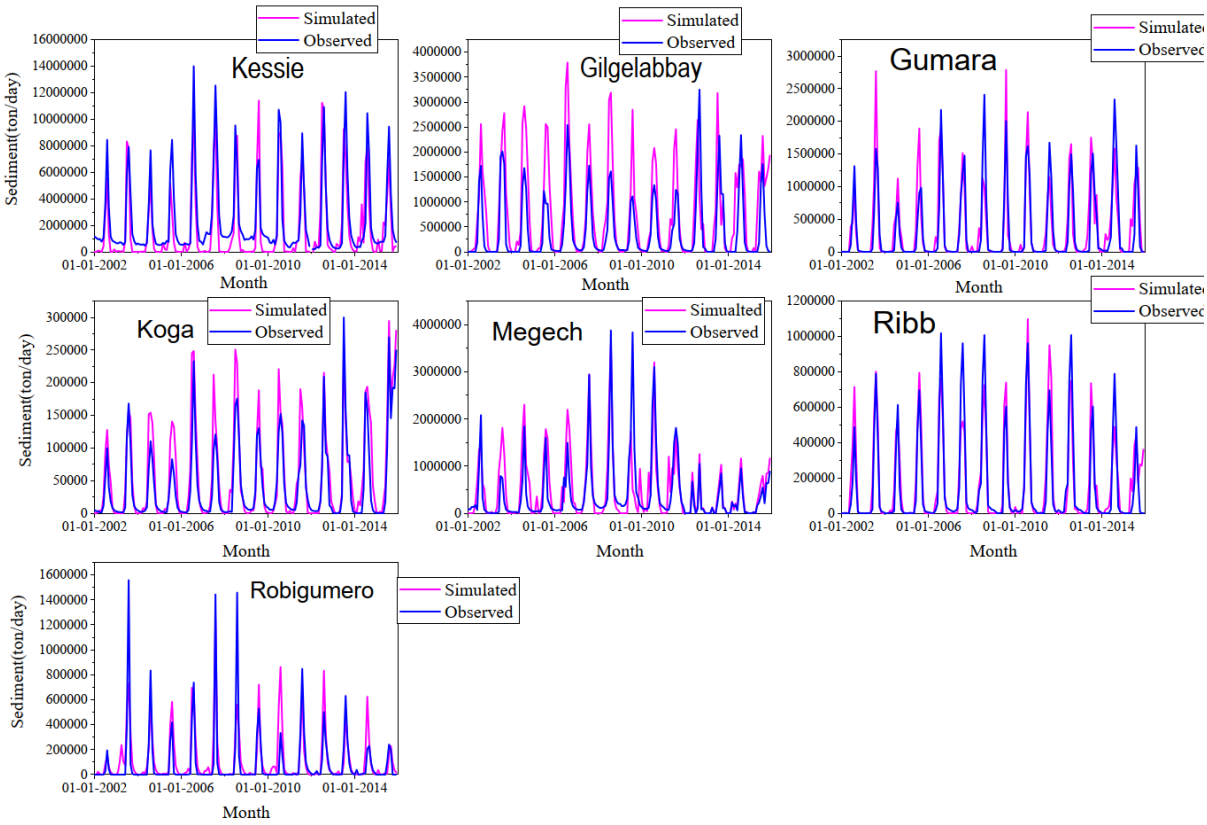

Figure 4-5 Monthly sediment yield hydrographs observed and simulated by the SWAT + model during calibration and validation between 2000 to 2015

The simulated and observed mean monthly streamflow values for Kessie, Megech, Ribb, Koga, Gumara, GilgelAbbay, and Robigumero was 774.49 m^3/sec and 650.9 m^3/sec, 8.86m^3/sec and 10.63m^3/sec, 44.02m^3/sec and 39.27m^3/sec,7.05m^3/sec and 6.36m^3/sec,34.41m^3/sec and 41.62m^3/sec, 48.71m^3/sec and 51.68m^3/sec, 8.92m^3/sec and 8.17m^3/sec, respectively. Similarly, the mean monthly simulated and observed sediment yield results are shown in Table 4.6.

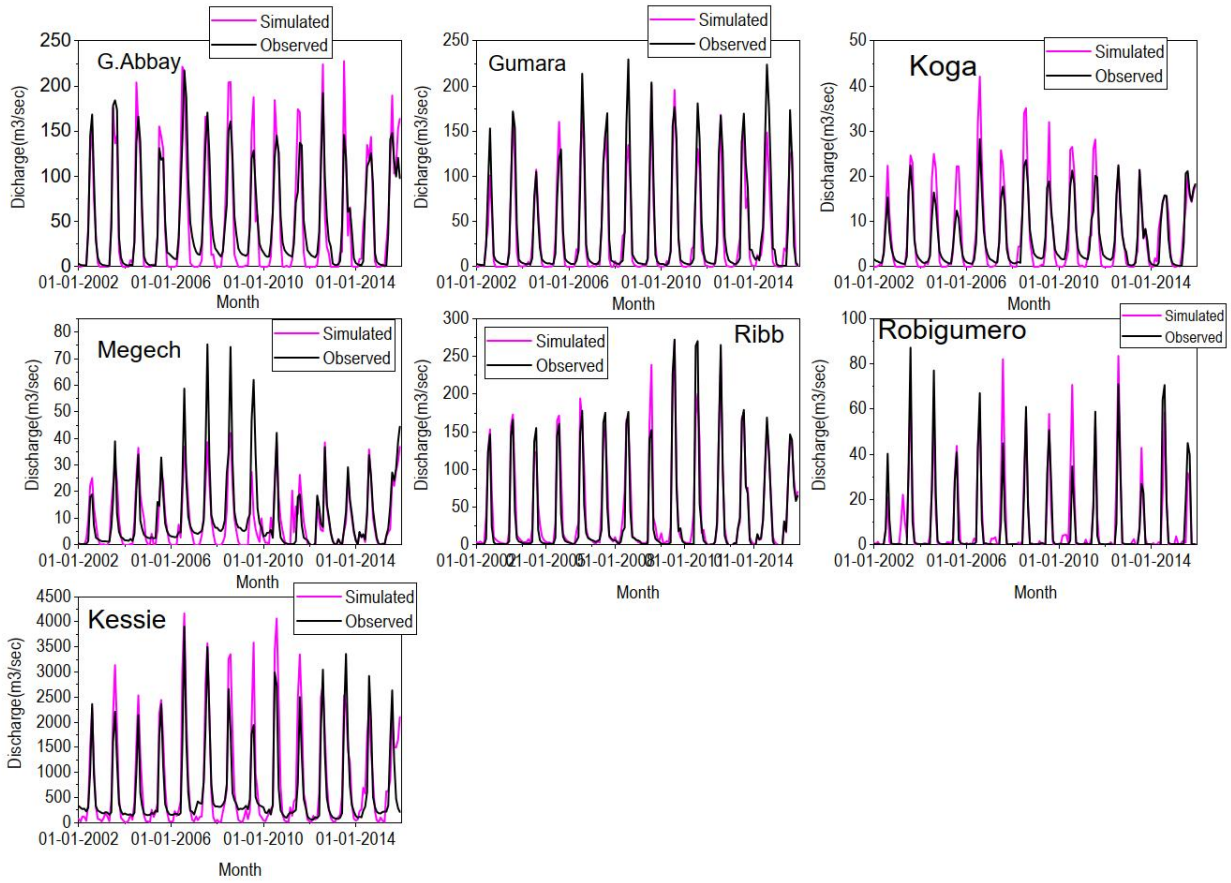

Figure 4-5 Monthly streamflow hydrographs observed and simulated by the SWAT + model during calibration and validation between 2000 to 2015

Table 4-5 SWAT+ model performance during streamflow calibration and validation with statistical parameters

Catchment	NSE		R2		PBIAS		Observed Mean Monthly Streamflow	Simulated Mean Monthly Streamflow
	Cal	Val	Cal	Val	Cal	Val	m^3/sec	m^3/sec
RobiGu.	0.79	0.79	0.81	0.79	17.7	8.25	8.17	8.92
Gumara	0.89	0.82	0.91	0.87	15.4	22.2	34.41	41.62
Gilgel.A	0.8	0.79	0.86	0.88	8.53	-1.3	48.71	51.68
Ribb	0.89	0.9	0.9	0.95	18.6	-1.0	39.27	44.02
Kessie	0.85	0.65	0.88	0.69	-20	-16	650.9	774.9

Koga	0.88	0.9	0.9	0.9	-17	3.58	10.63	8.86
Megech	0.73	0.7	0.75	0.71	17.7	13.1	6.36	7.05

Note: Cal: calibration, **Val**: validation

Table 4-6 SWAT+ model performance during sediment yield calibration and validation with statistical parameters

	NSE		R^2		PBIAS		Observed Mean Monthly Sediment Yield	Simulated Mean Monthly Sediment Yield
	Cal	Val	Cal	Val	Cal	Val	ton/day	ton/day
Robigumero	0.7	0.7	0.71	0.71	-25.3	-24.24	92,059.19	115,129.75
Gumara	0.73	0.69	0.75	0.7	-7.25	-12.38	318,192.59	346,614.25
GilgelAbbay	0.8	0.73	0.83	0.75	-8.75	-5.58	437,596.32	773,390.37
Ribb	0.85	0.7	0.87	0.74	-7.68	-12.1	151,458.41	164,852.24
Kessie	0.79	0.7	0.8	0.72	34.43	9.63	2,326,699.97	1,696,354.93
Koga	0.8	0.85	0.85	0.9	-24.5	23.4	43,620.47	56,776.40
Megech	0.8	0.82	0.85	0.89	-15.1	-13.5	412,914.40	485,824.01

4.3.3 Analysis of temporal variations in sediment discharge within the Kessie watershed

The QSWAT+ model analysis of soil erosion in the Kessie watershed (2000-2015) showed that winter months experience the most significant soil loss (as depicted in Figure 4.7). Approximately 90% of the total annual sediment yield occurred in the months of June, July, August, and September. The remaining months of the year contributed only 10% of the sediment yield.

Even though the most rain and the highest streamflow occurred in July, August saw the greatest average amount of soil erosion, reaching 145.54 t/km^2/yr. This was even though the mean monthly precipitation in July was 322.54 mm, and the corresponding mean monthly streamflow was 650.97 m^3/sec.

The peak streamflow occurred at the start of the rainy season, which is a pattern observed in other watersheds in the Ethiopian highlands region. Overall, the sediment yield output increased significantly by 30.25% between 2000 and 2015.

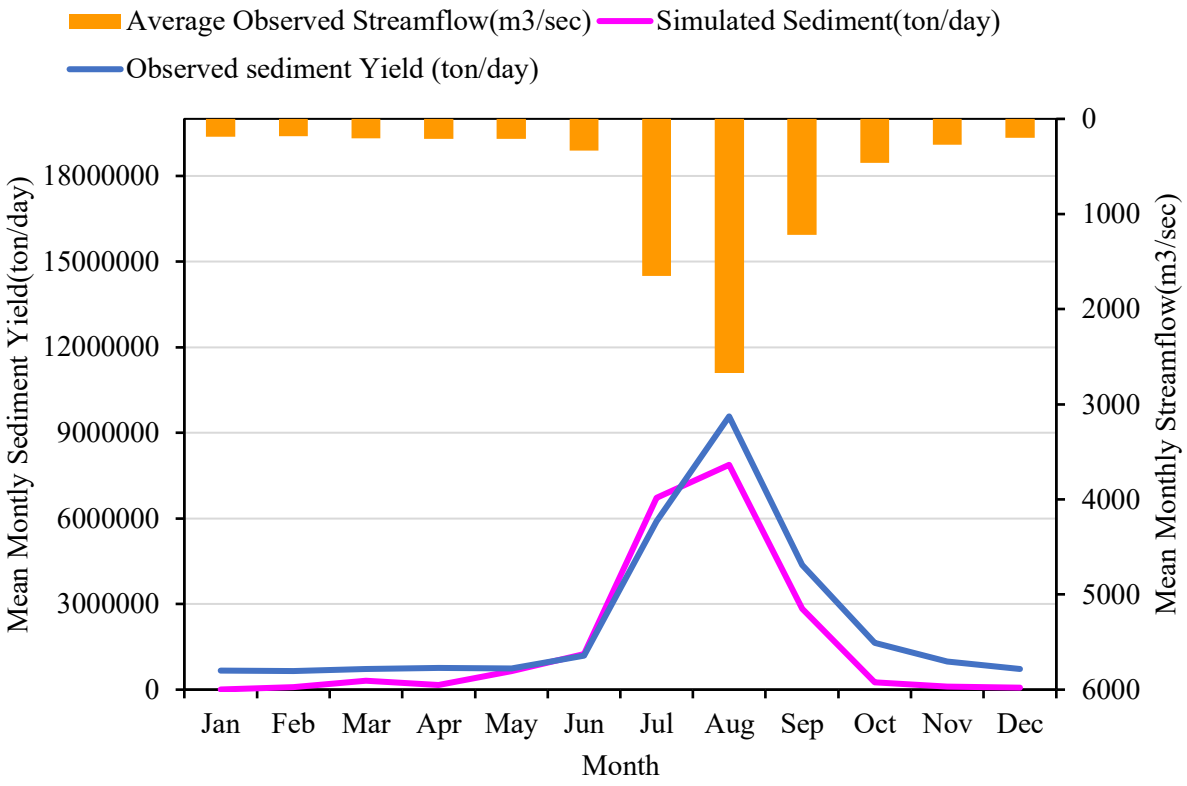

Figure 4-6 Mean Monthly Simulated Sediment yield, observed sediment, and streamflow of the Kessie watershed from 2002 to 2015

4.3.4 Mapping soil loss

A large area of the Kessie watershed experienced high rates of soil erosion. Table 4.7 shows that approximately 42.04% of the watersheds were designated as high sediment source areas. The spatial pattern of sediment yield showed that out of 18 subbasins' sediment-generating areas, 14 subbasins generated sediment yield ranging from 4.3 to 67.6 t/ha/yr, and the highest sediment load was found in the northern part of Gojam, some parts of the Beshilo subbasin, and partly the Jemma catchments.

The spatial map of how much sediment is produced in different parts of the Kessie watershed at a subbasin scale showed that there were areas more prone to erosion. Based on various literature sources, the erosion class of the watershed was categorized into five groups. A map (spatial variability map) showed two sub-basins experiencing very high erosion (9.5-67.6 t/ha/ yr), eight sub-basins with high erosion (4.3-9.5 t/ha/ yr), four with moderate erosion (2.1-4.3 t/ha /yr), and the remaining four having low to very low erosion rates (0-2.1 t/ha/yr) but still at risk from sediment buildup (Figures 4.9 and 10). A study of the middle Kessie watershed found severe soil

erosion throughout, with some areas experiencing very high rates. Fourteen sub-watersheds were identified as critical erosion zones, losing an average of 4.3 to 67.6 tons of soil per hectare each year. These hotspots cover a vast area, 70% of the watershed (43,647 km^2), and are dominated by agricultural activities on land with steeper slopes.

Table 4-7 Erosion rates in different areas of the Kessie watershed

Soil erosion class	Severity class	Subbasin number	Total area(km^2)	Area cover (%)
0-1	very low	138,286	12780.86	18.47
1-2.1	low	26,98	12754.90	18.44
2.1-4.3	moderate	22,249,254,261	14559.81	21.05
4.3-9.5	high	1,11,18,80,85,111,162,269	14600.35	21.10
9.5-67.6	very high	23,165	14486.93	20.94

According to the QSWAT+ model's calibration and validation results, the average annual sediment yield for the Kessie watershed during the period of 2000 to 2015 varied from 10.52 t/ha/yr to 55.77 t/ha/yr (Table 4.8). This showed that among the Kessie sub-catchments, Gilgel Abbay, Koga, Gumara, Ribb, and Megech had the largest sediment load. Therefore, the catchments need to be the best management practice intervention.

Table 4-8 Average annual sediment yield of different catchments

Catchment	Area(ha)	Sediment yield(t/ha/yr)
Koga	24400	27.92
Megech	46200	10.52
Robigumero	88200	15.58
Gumara	139400	29.84
Ribb	159200	12.43
Gilgel Abbay	166400	43.72
Kessie	6578400	55.77

4.3.5 Developing Sediment Reduction Scenarios

Baseline scenario: The QSWATPLUS model shows that sediment yield varies across the watershed. On average, the reach outlet yields 43.23 t/ha/yr, while the total yield for the entire

watershed is 284.987 million tons per year. The effectiveness of the sediment management measures was evaluated by comparing the results obtained after implementing these measures in sediment-prone areas to a scenario where no such measures were taken (baseline condition) (Figure 4.9).

Applying Filter Strips (Scenario I): The data in Figure 4.8 showed that using 5-meter filter strips significantly reduced soil erosion in critical subbasins. On average, these strips lowered yearly sediment loss from 11.5 t/ha/yr to 4.63 t/ha/yr, representing a decrease of 60%. The authors of (Zantet o et al., 2023) found that implementing 20m wide vegetated buffers in high-risk areas led to a 34.7 % to 65.6 % mean annual sediment yield reduction in those sub-basins compared to a baseline scenario.

Applying Contouring Farming (Scenario II): This management practice led to a significant decrease in the sediment yield rate. The average annual sediment yield was originally 11.51t/ha/yr. After implementing this practice, the sediment yield was reduced to 4.59 t/ha/year, which represents a 60.11% decrease, as shown in Table 4.9. Constructing contour structures on agricultural land, shrubland, and pastures increases the rate of water absorption into the soil. This is because the contours make the land surface less smooth and even, which allows more water to soak into the ground rather than run off the surface. By making the land rougher, contouring slows down runoff. This reduces the force of the runoff, which lessens its ability to erode the soil. The average amount of soil lost each year (mean annual sediment yield) was reduced by over 64%. Similarly, other studies (Dibaba et al., 2021) examined the impact of contour farming practices and buffer zones on environmental benefits and found that contour farming alone can reduce soil loss by around 63.8% on average each year in the Ethiopian highlands.

Applying Parallel Terracing (Scenario III): Building terraces in the identified critical erosion zones significantly reduced the average annual amount of soil erosion by 93.58%. According to the data presented in Table 4.9, the implementation of terraces in the identified hotspot areas significantly reduced the soil loss rates within those subbasins. The sediment output decreased from an original 11.51 t/ha/yr down to 0.76 t/ha/yr. At the entire watershed level, the model predictions indicated that the annual soil loss was lowered by 93.65% after implementing terraces in high-risk subbasins. The average sediment yield across the entire watershed decreased from 5.01 t/ha/yr to 0.32 t/ha/yr. Using parallel terracing is the most effective land management practice

in the Ethiopian highlands, compared to other best management approaches. (Kefay et al., 2022), (Gashaw et al., 2021), (Leta et al., 2023), and (Tesema and Leta, 2020).

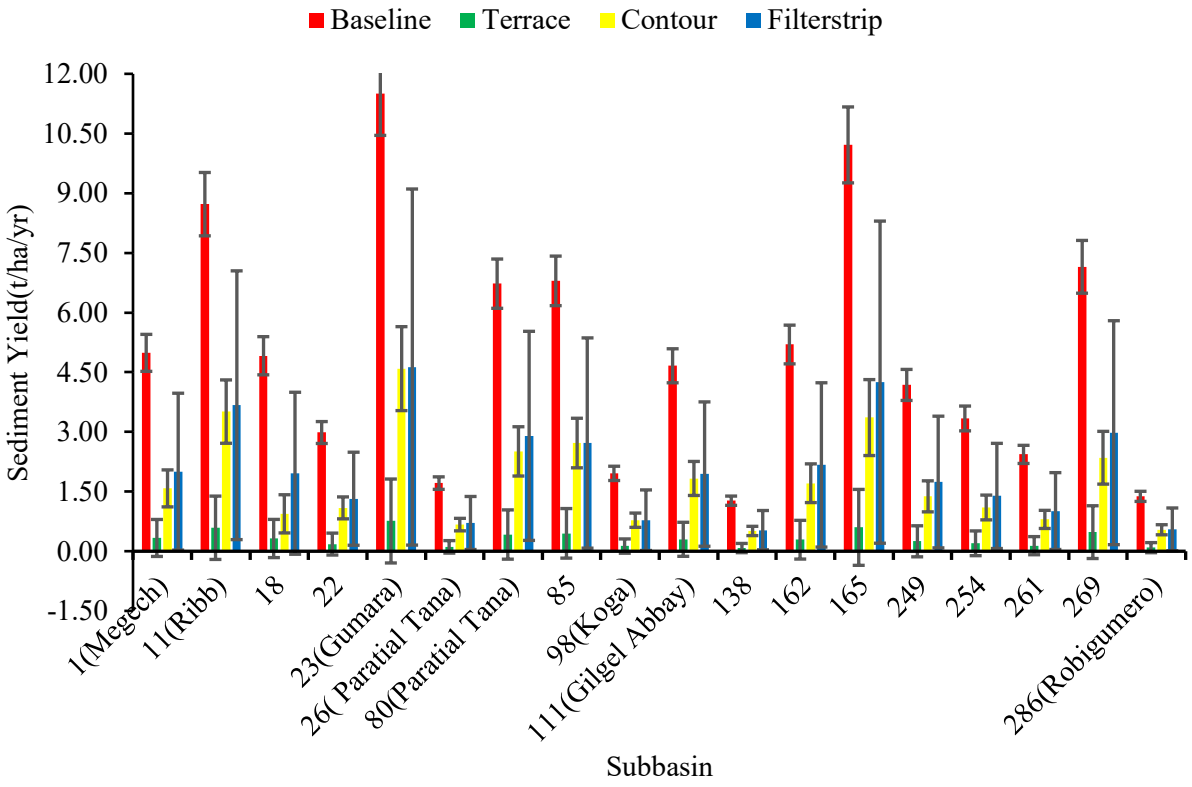

Figure 4-7: The average annual simulated sediment or soil loss for each management scenario at different sub-watersheds

Table 4-9 The best management practice scenario results

Subbasin	Sediment yield(t/ha)				Change in percentage		
	Baseline	Terrace	Contour	Filter strip	Terrace	Contour	Filter strip
1(Megech)	4.99	0.333835	1.58	2	93.31	68.31	59.89
11(Ribb)	8.72	0.59	3.51	3.67	93.24	59.77	57.93
18	4.91	0.32	0.94	1.96	93.49	80.87	60.12
22	2.98	0.18	1.09	1.32	93.97	63.47	55.77
23(Gumara)	11.51	0.76	4.59	4.63	93.40	60.11	59.77
26(Partial Tana)	1.71	0.11	0.67	0.71	93.58	60.88	58.54
80(Partial Tana)	6.73	0.42	2.51	2.90	93.76	62.68	56.88
85	6.80	0.45	2.72	2.72	93.38	59.98	59.98
98(Koga)	1.96	0.13	0.78	0.78	93.36	60.15	60.15
111(Gilgel Abbay)	4.66	0.30	1.83	1.94	93.56	60.74	58.38
138	1.27	0.08	0.51	0.53	93.70	59.85	58.28
162	5.20	0.29	1.71	2.17	94.42	67.10	58.24
165	10.21	0.60	3.36	4.25	94.13	67.10	58.39
249	4.18	0.25	1.38	1.74	94.02	66.99	58.38
254	3.34	0.20	1.10	1.39	94.01	67.05	58.36
261	2.43	0.14	0.80	1.01	94.25	67.14	58.51
269	7.15	0.480	2.35	2.98	93.29	67.13	58.32
286(Robigumero)	1.38	0.09	0.54	0.55	93.48	60.86	60.14

4.3.6 Evaluation of best management practices

This study tested different methods to reduce soil erosion in critical areas throughout a watershed. While 5-meter filter strips were implemented, they were the least effective, only achieving a modest decrease of around 59% in average annual sediment loss. In other words, these strips reduced soil erosion from an average of 5.01 t/ha/yr to 2.07 tons per hectare per year, representing a total decrease of 58.67% in sediment yield across the entire watershed. Compared to FS, the average effectiveness of contour farming in reducing soil loss for the critical subbasins was 64.46%. Contour farming was more effective at reducing soil loss than filter strips, but not as effective as the terracing approach, which achieved the highest 93.68% reduction. Implementing terracing in sub-basins 162, 261, 254, 165, 249, 22, and 23 led to significant reductions in sediment load, ranging from 93.4% to 94.42%. It reduced 93.68 % of the erosion-prone area of subbasins' annual soil loss rate from 5.01 t/ha/year to 0.32 t/ha/year. Furthermore, terracing was the most effective management practice for reducing sediment yield across all critical subbasins within the watershed region. The analysis concluded that terracing was a more effective management practice than others at reducing sediment in all the critical hotspot areas within this watershed region. Different literature also approved these results (Anteneh et al., 2023).

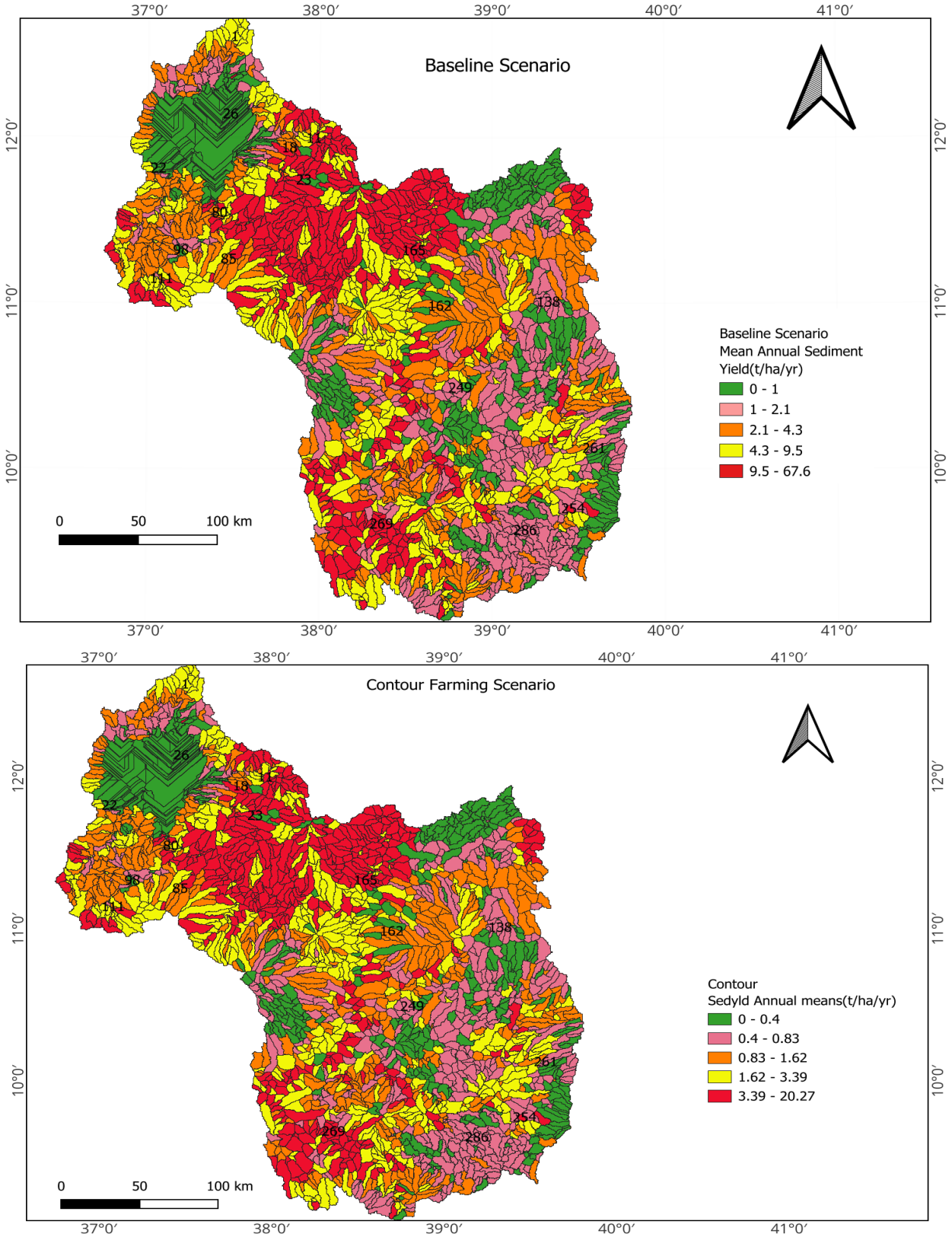

Figure 4-8 Spatial variability of soil erosion rate under baseline and contour farming scenario

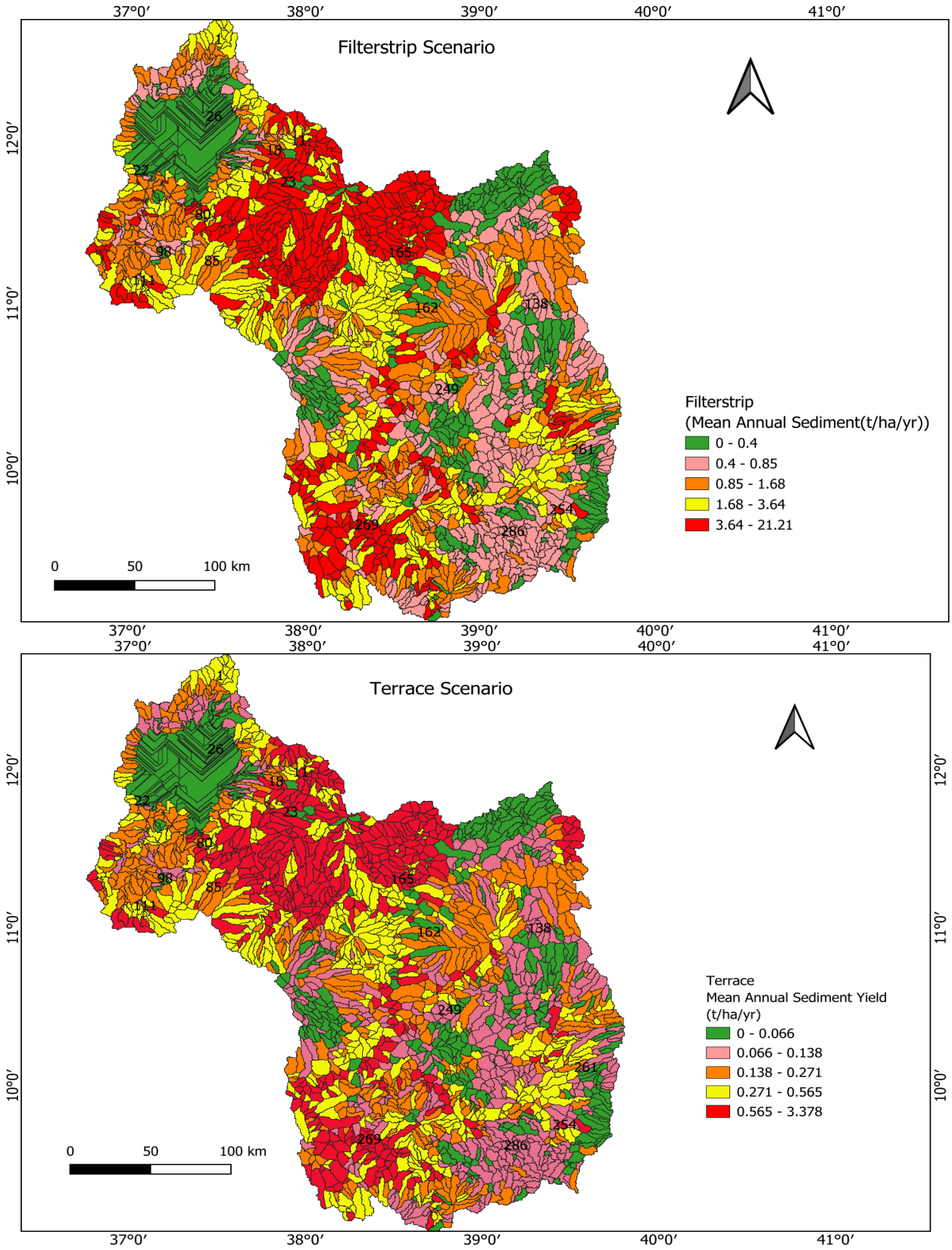

Figure 4-9 Spatial variability of soil erosion rate under filter strips and parallel terracing scenario

4.4 DISCUSSION

4.4.1 Modeling of sediment loading and runoff

The calibration and validation were conducted at the sub-watershed level using gauged streamflow and sediment concentration data between 2000 and 2015. The model simulation capability was satisfactory and at good performance when the model simulation results were calibrated and validated with the observed data within different sub-catchment outlets. The model efficiency at Koga, Ribb, Megech, Gumara, Robigumero, and Kessie watersheds was 0.88 and 0.85, 0.85 and 0.7, 0.8 and 0.82, 0.73 and 0.69, 0.7 and 0.7, and 0.79 and 0.7, during monthly time step calibration and validation, respectively. The results were similar to or beyond those of other studies conducted in similar study areas and used similar models. For instance, (Gebiaw T Ayele et al.,2021), (Ayele et al., 2021) found that the model efficiency results during calibration and validation at the Koga watershed outlet were 0.75 and 0.79, respectively. Therefore, the calibration and validation results of the QSWAT+ model demonstrated its effectiveness in comparison to other semi-distributed hydrological models.

The average annual soil erosion (sediment yield) for seven watersheds in Ethiopia over 16 years such as the Kessie watershed, Ribb watershed, Megech watershed, Gumara watershed, Koga, Gilgel Abbay, and Robigumero watershed was 59.42 tons per hectare per year, 12.43 t/ha/yr,10.52 t/ha/yr,29.84 t/ha/yr, 27.92 t/ha/yr, 55.77 t/ha/yr, and 15.58 t/ha/yr, respectively. These results are consistent with what other studies have found previously (Alebachew and Sewnet, 2024). For example, previous reports showed that sediment yield values in the Ribb watershed ranged from 0 to 16 t/ha/yr, with an average of 12.43 t/ha/yr (Sinshaw et al., 2021). The studies conducted in the Anjeb watershed region of northwestern Ethiopia found soil erosion rates ranging from 2.5 to 157 t/ha/yr. These soil loss rates were higher than the value observed in the current research, but the sediment yield was lower than the range reported in the northwestern Ethiopia study (Tsegaye and Bharti, 2021). Another study conducted in the BNB using the QSWATPLUS model estimated soil loss of around 27.5 t /ha/yr, which aligns with our findings(Gashaw et al., 2021). Several studies have estimated soil loss rates in different catchments and watersheds in Ethiopia using the RUSLE model and related approaches. For instance, in the Koga catchment the average soil loss was 27.5 t/ha/yr (Ayele et al., 2021), the Beshillo catchment in the BNB was 37.5 t/ha/yr (Yesuph and Dagnew, 2019), central Ethiopia was 23.4 t/ha/yr (Gessesse et al., 2015), the Gumara watershed

was 19.7 t/ha/yr (Gashaw et al., 2021), and the Gilgel Abbay watershed was varied from 9.8 t/ha/yr to 81.2 t/ha/yr (Gashaw et al., 2020).

4.4.2 Evaluate the variation in sediment output over the Upper Blue Nile basin

The spatial heterogeneity of sediment discharge within the study area was significant. This spatial variability was important in identifying the hot spot areas that were most in need of the best management practices. A wide section of the Kessie watershed was shown to experience substantial, accelerated, or excessive soil loss. Particularly, fourteen subbasins such as Gumara (23), Ribb (11), Koga (98), 249,254,261,11,80,85,162,269,165, and Gilgel Abbay (111) watersheds had high soil erosion rates. The study revealed that 42.04 % of the watershed area is a critical erosion region, and 39.48 % of the watershed is a subcritical region. Approximately 63.09% of the areas studied are estimated to be prone to erosion, with erosion rates exceeding 4.3 t/ha/yr. The sediment variability observed in the Upper Blue Nile basin ranged from 0 to 67.6 t/ha/yr across the different catchments in that region. The analysis shows that the Upper Blue Nile basin is currently experiencing a high rate of soil erosion, with a significant spatial variation. This ranges from zero tons per hectare per year in water bodies to as high as 67 t/ha/yr in areas with degraded slopes and intensive agricultural practices. Other similar reports have corroborated these findings (Haregeweyn et al., 2017). In general, the highest sediment loads are found in the North Gojjam, Beshilo sub-basins, and parts of the Jemma catchments. This high sediment concentration has impacted the storage capacity of several dam reservoirs in the region, including Koga, Ribb, Megech, and even the Grand Ethiopian Renaissance Dam. Unsustainable agricultural practices and increasing population demands are causing significant soil erosion in the UBNB. To address this issue and safeguard both agricultural productivity and the lifespan of downstream reservoirs, implementing land management practices like cover cropping or terracing, or constructing structures like check dams, might be necessary. Hence, implementing cost-effective and targeted soil erosion management strategies is essential to reduce erosion-prone areas.

4.4.3 Evaluating the effectiveness of optimal land management strategies in minimizing soil erosion

The successful application of the modeling approach has enabled the identification of specific soil erosion "hotspot" areas within the UBNB in Ethiopia. These high-risk erosion zones have been pinpointed at the subbasin level. The identification of the specific soil erosion hotspot areas within the Upper Blue Nile basin, at both the sub-basin and broader watershed scales, provides valuable

data that can be leveraged to prioritize and target necessary watershed management interventions. Over 41% of the sub-basins within the watershed were identified as major sediment source areas, generating higher than average sediment loads exceeding 22.85 t/ha/yr. This detailed quantitative information is essential for implementing cost-effective and targeted soil erosion management strategies. After identifying the hotspot areas within the watershed, the best management practice is to reduce the sediment load into reservoirs to maintain water quality. The best solutions for controlling soil erosion in each sub-basin will depend on several things, such as the type of erosion, cost, long-term benefits, effectiveness in reducing sediment loss, rainfall patterns, land use practices, and the steepness of the slopes.

The sediment yield from several erosion-prone sub-basins (1, 11, 18, 80, 85, 111, 162, 269, 165, and 23) was reduced by 55.77 % to 59.98 % in the first scenario, by 5-meter-wide filter strips as a best management practice. According to the simulation results, the total amount of sediment that flows out of the Kessie watershed has decreased significantly. Specifically, the soil loss rate at the watershed outlet has decreased from 5.01 t/ha/yr to 2.07 t/ha/yr, which represents a 58.6% decrease from the baseline conditions. The findings indicate that by increasing the width of the filter strips within the watershed, the efficiency of sediment reduction can be improved in the sub-basins that are prone to high sediment yields. In other words, expanding the filter strip areas can help capture and prevent more of the sediment from being transported out of those problematic sub-basins. The results of this study are similar to the findings from previous research conducted in other watersheds. Research consistently showed that installing wider strips of vegetation along waterways (filter strips) significantly reduces soil erosion. Studies by Bibi et al. (Zantet o et al., 2023) in the Gilo watershed and Abebe et al.(Tesema and Leta, 2020), in the Kesem Dam Watershed in Ethiopia, both found that wider filter strips led to substantial decreases in soil loss. The findings highlight the benefits of using filter strips, with reductions in soil erosion ranging from 22% to 80% depending on the initial width of the strip and specific location. Specifically, they reported that expanding the filter strip width from 5 meters to 10 meters resulted in sediment yield decreases ranging from 43.58% to 70.11%, and from 62.3% to 80%, respectively.

The practice of contour farming, which is considered another effective management technique, was found to result in a substantial decrease of up to 64.46% in the key metrics across all the sub-basins studied. Previous research has shown that the use of contour farming techniques resulted in a 68.1% reduction in the amount of sediment yield (Zantet o et al., 2023).

In addition to the advantages provided by contour farming, the study found that constructing a set of horizontal ridges or terraces on the hillsides and in the high rainfall sub-basins further reduced the sediment yield to 66.84 t/ha/yr from the overall watershed. This represents a substantial 93.68% decrease compared to the original baseline sediment levels. Furthermore, the study found that the terracing management practices achieved the greatest percentage reduction in sediment levels from the problematic, high-sediment sub-basins within the overall watershed. Therefore, utilizing terracing techniques provides a valuable solution for managing the sediment dynamics within the river basin. This finding is in line with the results reported in previous studies conducted by Negewo et al. (Negewo and Sarma, 2023), Leta et al. (Leta et al., 2023), and Kefay et al. (Kefay et al., 2022).

In general, the results of this study underscore the efficiency of various management techniques in mitigating sediment runoff. These results can help to inform future policy suggestions, such as promoting optimal management practices (BMPs), establishing educational initiatives, and incorporating erosion prevention strategies into land use planning.

4.5 Conclusion and Recommendation

Sediment yield resulting from soil erosion significantly affects water storage facilities such as dams and reservoirs. The buildup of sediment in riverbeds presents a significant obstacle for engineers and water resource professionals when conceptualizing, organizing, and executing water resource initiatives within watersheds (river basins). Appropriate upstream watershed management strategies are crucial to address this concern. The QSWATPLUS model was used in the Kessie watershed in Ethiopia to examine the spatial and temporal variability of sediment output at the sub-basin level. This was done to identify crucial erosion-prone sites and develop effective management techniques. It was calibrated from 2001 to 2010 and then verified the model from 2011 to 2015 using observed data to assess its suitability for modeling streamflow and sediment yield with the SWATPLUS TOOLBOX. The statistical indicator findings demonstrated very good performance, with R-squared values of 0.8 and 0.72, NSE = 0.79 and 0.7, and PBIAS = 34.43% and 9.63% for the calibration and validation periods, respectively.

In the baseline scenario, simulated sediment delivery volumes ranged from 0.0 to 67.60 t/ha/yr, with an average of 43.3 t/ha/yr. The highest sediment yield value was recorded in sub-basin 165, while the lowest was observed in sub-basin 22. The examination identified the critical erosion zones within the study region, which consisted of the sub-basins with modeled sediment yield

values exceeding 9.5 t/ha/yr. The designated subbasins deemed crucial for erosion were 1, 11, 18, 80, 85, 111, 162, 269, 23, and 165, representing 42. 04% of the total research area. The simulation results showed that implementing various management strategies in these critical sub-basins had variable effects on reducing sediment discharge. In particular, filter strips reduced sediment yield by 58. 67%, contour farming reduced it by 64. 46% and parallel terracing proved to be the most efficient, reducing sediment yield by 93. 68%. In general, the study determined that terracing was the most effective method for reducing sediment, as seen by the sediment reduction rates. From a temporal aspect, the research found that about 90% of the total annual sediment volume was reported during the winter months. These findings can help to inform future policy suggestions, such as promoting optimal management practices (BMPs), establishing educational initiatives, and incorporating erosion prevention strategies into land use planning.

The study also emphasized that areas with steep slopes and extensive agricultural practices are at high to very high risk of erosion. By categorizing erosion risk across sub-basins, the findings enable planners to prioritize areas requiring immediate soil conservation measures. The QSWATPLUS modeling approach proved valuable for identifying erosion hotspots and understanding the underlying causes of soil erosion, providing decision-makers with actionable insights for watershed management. The results can inform policy recommendations, such as promoting best management practices (BMPs), launching educational programs, and integrating erosion prevention strategies into land use planning.

The findings from the Kessie watershed have broader implications for other regions facing similar challenges. The simulated BMPs, particularly terracing, can serve as a model for reducing soil erosion in the Ethiopian highlands and other comparable watersheds worldwide. By identifying critical erosion zones and demonstrating the effectiveness of targeted interventions, the study offers a replicable framework for sustainable watershed management. This approach can guide policymakers and land use planners in implementing erosion control measures, ultimately contributing to the preservation of water storage infrastructure and the sustainable management of global watersheds.

4.6 Limitations of the study

This study centered on identifying critical erosion hotspots, recommending relevant BMP strategies, and analyzing sediment dynamics, but with the recognition that agricultural BMPs and cost-benefit perspectives should be the focus of further research going forward.

5. Developing Empirical Models to Estimate Suspended Sediment Yield in Ungauged Watersheds of the Ethiopian Highlands Using QSWATPLUS Model Parameters

Abstract

Lack of accurate sediment yield data and efficient sediment yield prediction methodology have contributed to poor planning and designing of reservoirs, which has led to increased reservoir sedimentation and loss of storage capacity. The estimation of suspended sediment yield in ungauged catchments is imperative, yet extant models have the potential to be more efficacious in predicting the suspended sediment yield. Furthermore, the scarcity of data represents a pervasive challenge in the field of sediment yield prediction. The present study, therefore, sought to develop an alternative empirical model using the QSWAT+ (Quantum Geography Information System Soil Water Assessment Tool Plus) conceptual model for a situation where data is scarce. The QSWAT+ model was used to divide the Kessie watershed into 18 sub-basins to determine the characteristics of each catchment and the basis for analyzing input variables. Data from six watersheds were collected over 11 years to test the performance of the newly established alternative model, which was assessed using model assessment statistics. Principal component analysis (PCA) was used to determine the significant variables that affected sediment yield. Through this analysis, seven significant variables were found among the 24 variables considered; the most significant included drainage area, slope of the stream, length of the main channel, rainfall, agricultural area coverage, forest area coverage, and streamflow. In general, climatic, geomorphological, and hydrological variables were found to be the key determinants of suspended sediment yield. The calibration and validation results demonstrated that six watersheds such as Robigumero, Gumara, Gilgel Abbay, Ribb, Kessie, Koga, and Megech achieved the following Nash-Sutcliffe Efficiency (NSE) values: (0.7, 0.7), (0.73, 0.69), (0.8, 0.73), (0.85, 0.7), (0.79, 0.7), (0.85, 0.8), and (0.8, 0.82), respectively. Following the calibration and validation of streamflow and suspended sediment yield data at the Kessie gauge station, a new empirical model was developed to estimate suspended sediment yield in ungauged catchments. The simulated suspended sediment yield estimated by the alternative empirical model aligned well with the observed values across all six watersheds. The model exhibited strong performance, with specific examples including Gumara ($R^2 = 0.84$), Ribb ($R^2 =$

0.71), and G. Abbay (R^2 = 0.61). The model's validity was further confirmed using 11 years of data, demonstrating its reliability and accuracy. This improves the model's accuracy and applicability in a variety of environmental scenarios, as well as its calibration and validation in places with little data. This approach could lead to better sediment management strategies and better planning for watershed conservation efforts. It is recommended that the model be evaluated in more basins, particularly with various soil properties.

Keywords: Empirical model, PCA, suspended sediment yield, QSWATPLUS, Reservoir sedimentation, Ungauged watershed, Kessie

5.1 Introduction

Reliable estimation of sediment yield is critical for effective reservoir management, environmental impact assessment, and understanding soil erosion and ecological health. Sediment is a ubiquitous issue in river catchments, affecting river flow, reservoir capacity, hydropower production, and dam structural integrity. Because the behavior of suspended sediment is non-linear, forecasting and predictive analysis must be performed using non-linear approaches. Accurate sediment prediction is critical because it has a substantial impact on hydraulic structures in rivers (Kisi and Çobaner, 2009).

In many countries, particularly in developing countries like Ethiopia, most rivers are ungauged to measure suspended sediment and streamflow data (Negatu et al., 2022). The lack of sediment data has resulted in inappropriate reservoir planning, resulting in rapid sedimentation and a loss of storage capacity (N. Haregeweyn et al., 2008). According to (N. Haregeweyn et al., 2008), the sedimentation problem is rather serious: six of the eleven reservoirs analyzed are experiencing significant sedimentation, which might reduce their economic lifespan to half of what was initially planned. Rapid sedimentation is mostly attributed to inadequate reservoir planning in terms of predicted sediment output during the design stage, which is caused by a lack of sediment yield data and appropriate sediment yield prediction tools.

Quantification of suspended sediment yield is vital for understanding the process of soil erosion, sediment transport, and their impacts on water resources. It is particularly problematic in ungauged basins with limited hydrological data. Specifically, the Ethiopian Highlands areas faced highly intensified soil erosion and sediment-laden rivers. This study presents the use of the QSWAT+

model, an extension of the Soil and Water Assessment Tool (SWAT), for building empirical models that will predict suspended sediment discharge in ungauged watersheds.

The QSWAT+ model, a QGIS interface for SWATPLUS, is gaining popularity due to its ease of use and increased power in hydrological and sediment modelling. The SWAT model, a physically based model, simulates sediment yield by taking into account topography, land cover, soil type, and meteorological conditions (Arnold et al., 1998). QSWAT+ expands these functionalities by its ability to integrate properly with geographical data, making it suited for data-poor areas.

Numerous studies have demonstrated the success of SWAT and QSWAT+ in sediment dynamics simulation. For instance, (Betrie et al., 2011) modeled sediment yield in the Blue Nile Basin with SWAT and illustrated the ability of the model in simulating regional and temporal sediment discharge. Similarly, (Dile et al., 2013) applied SWAT to quantify the effects of land use change on sediment processes in the Ethiopian Highlands. They showed the potential of QSWAT+ in sediment modeling in data-scarce conditions.

It has not been possible in the past to quantify sediment yield in ungauged catchments because the streamflow data monitored have been inadequate. Hence, several methods have been used, such as regionalization methods, remote sensing, and empirical models. Regionalization is defined as the transference of hydrological data from gauged to ungauged catchments based on physical similarity. Another study utilized remote sensing data, such as satellite data and digital elevation models (DEMs), for modelling sediment yield in data-poor regions (Ali et al., 2021).

The Ethiopian Highlands are one of the most erosion-susceptible areas, with average annual soil loss of over 100 tons/hectare in some areas (Hurni et al., 2015). Areas with steep topography, Steep slopes, high rainfall, and unsustainable land use are aspects that have made sediment yield in rivers like the Blue Nile basin. Empirical and process-based models, both of which have been employed in combination for the simulation of sediment transport in most research studies conducted within the basin.

For example, (Haregeweyn et al., 2008) estimated the sediment yield of ungauged catchments using an integration of remote sensing data and field measurements. Although these models have an important contribution, they should be validated and supplemented with more process-based, detailed models such as QSWAT+. (Setegn, 2014) Applied the SWAT model in the Lake Tana Basin and could verify its capability in simulating regional erosion and sediment yield. Similarly,(Tebebu et al., 2015), other researchers used SWAT to model the impact of conservation

measures on sediment yield in the Ethiopian Highlands. All these studies show the promise of QSWAT+ sediment simulation in the area, particularly with the best coupling of empirical data and modeling.

Empirical models, which are founded on statistical correlations among sediment yield and catchment characteristics, provide an appropriate option for process models in ungauged catchments. The Universal Soil Loss Equation (USLE), its revision (RUSLE), and sediment rating curves are a few of the notable examples of empirical models (Nawazuzzoha et al., 2024) and (Luvai et al., 2022). Empirical models are optimally applicable in environments with poor input data, resulting in a significant lack of data necessary for the application of process-based models. Empirical models have found wide application in the Ethiopian Highlands to estimate sediment yield. For instance,(Gelagay, 2016) applied RUSLE to estimate sediment yield and soil erosion within the Koga Reservoir catchment. However, empirical models are likely to be unable to represent temporal changes in sediment discharge, and hence integration with process-based models like QSWAT+ becomes inevitable.

Despite significant advancements in sediment modeling, some limitations remain in the application of QSWAT+ in estimating suspended sediment discharge in ungauged catchments, particularly in the Ethiopian Highlands. The limitations are the minimal availability of high-resolution input data for QSWAT+ and limited long-term suspended sediment data for calibration and validation.

The primary goal of this study is to develop an empirical model using the QSWAT+ model to estimate suspended sediment yield in ungauged catchments. The study also has two specific objectives: 1) identifying significant variables affecting suspended sediment yield using principal component analysis, and 2) developing alternative empirical models using the QSWAT+ model.

5.2 Study Area

5.2.1 Location and topography

The Kessie watershed is located in the Blue Nile Basin (BNB) and has a geographical extent between longitudes 36°43’55” to 39°49’12” E and latitudes 9°12’18” to 12°45’20” N (Figure 5.1). This watershed includes five of the 16 sub-basins of the Blue Nile, namely Bashilo, North Gojam, Tana, Welaka, and Jimma. The total area of these sub-basins provides about 25% of the total area of the Abbay Basin, covering approximately 65,784 km^2 with a total perimeter of about

2592.67 km. The elevation of the Kessie watershed ranges from 4,246 m a.m.s.l to 949 m a.m.s.l at the outlet, and the slope of the catchment ranges from 0% to 40%, having an average of 4%. The Kessie watershed plays an important role in the hydrology and ecology of the Blue Nile Basin by providing water resources, agricultural endeavors, and biodiversity. Its strategic and extensive coverage is critical in the continued functioning of the Nile River system. The flow of water, sediment transport, and diversity of upstream environments also provide watershed services needed for the continued nourishment of downstream ecosystems and human livelihoods. Thus, the Kessie watershed's management, conservation, and protection are of utmost significance in maintaining water supplies, climate change adaptation, and promoting regional development.

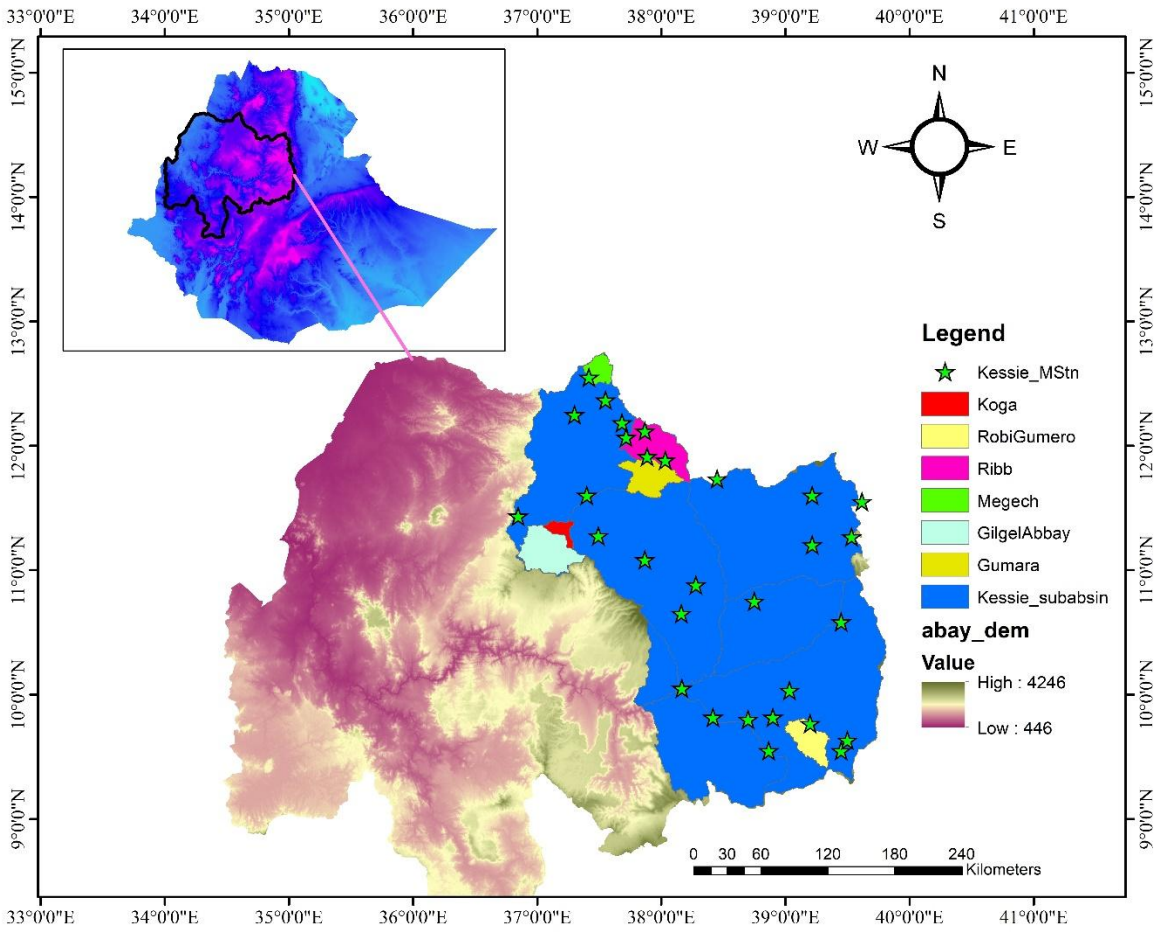

Figure 5-1 Study area location

The Kessie watershed covers a large area of the BNB and plays an important role in the region's hydrological and ecological processes. Several dams have previously been built in this watershed to facilitate water resource management, hydroelectric power generation, and agricultural

irrigation. In addition, various dam projects are planned to improve water utilization and meet the region's expanding energy and water demands. These changes underscore the Kessie watershed's critical role in maintaining the Blue Nile Basin's socioeconomic and environmental stability (see Figure 5.2).

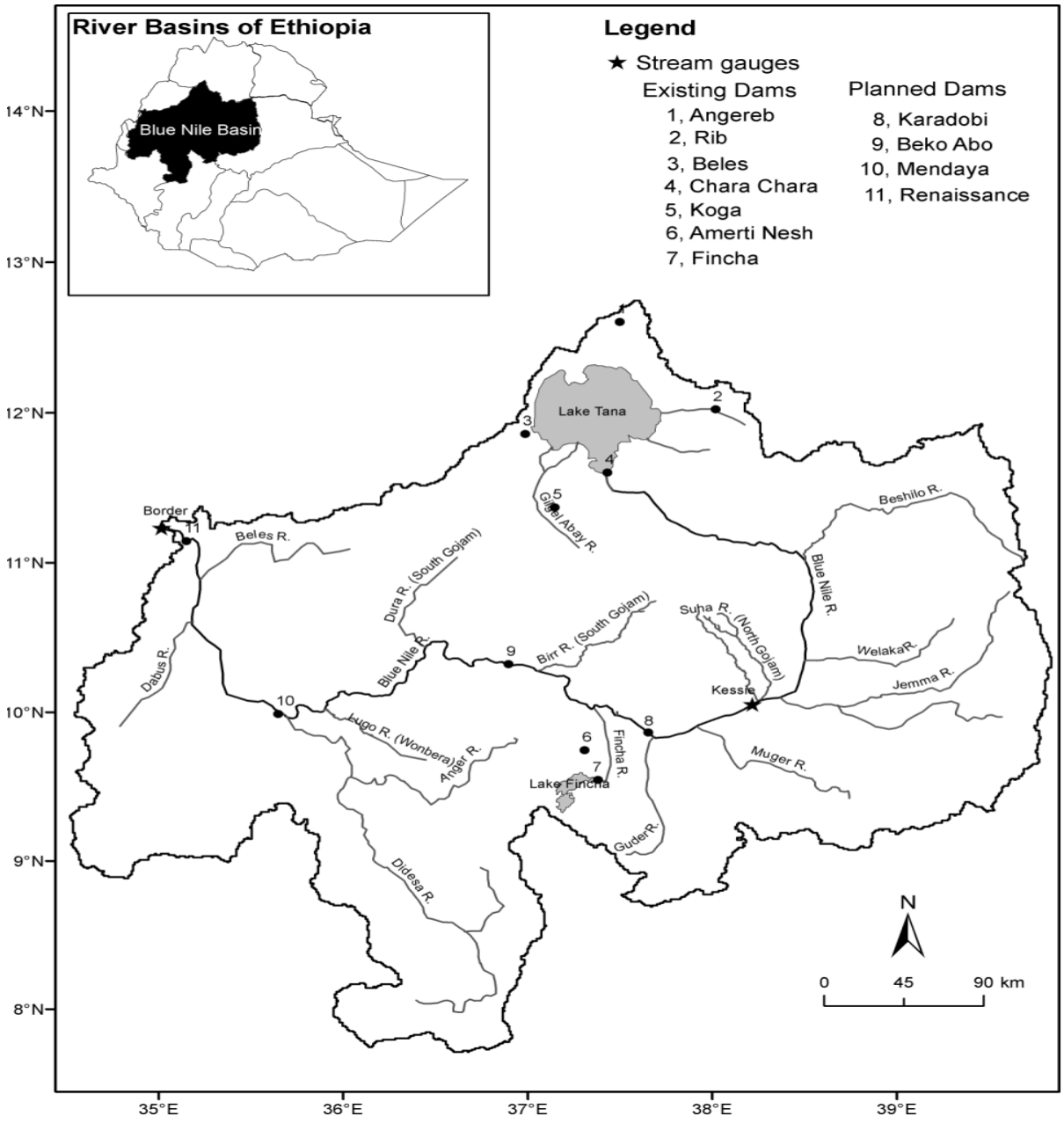

Figure 5-2 A map depicting the Blue Nile River and its sub-basins extending to the Sudanese border, illustrating the principal tributaries and the gauging stations located at Lake Tana, Kessie, and the border *(McCartney and Menker Girma, 2012)*

5.2.2 Climate and hydrology data

In the Kessie watershed, the weather conditions are varied in space with rough topography. Particularly in Ethiopia's highland areas, the rainfall patterns are unimodal, and receive the maximum rainfall from June to September. The climatic regime of the Kessie watershed is characteristic of the Ethiopian Highlands, as marked by the distinctive wet and dry seasons, controlled by the Intertropical Convergence Zone (ITCZ). The catchment gets 1,200-1,800 mm of mean annual precipitation with high spatial and temporal heterogeneity. Precipitation occurs predominantly from June to September under the influence of the summer monsoon and accounts for 70-90% of the annual total precipitation. The dry period with lesser rains is from October to May, particularly pronounced from the months of December to February. The Koga watershed had an average annual rainfall of 1475 mm during the period from 2000 to 2015, in addition to mean annual temperatures that ranged from 7 °C to 30 °C. The Kessie watershed, on the other hand, had a lower average annual rainfall of 1145 mm during this time. The other watersheds in the area have different patterns of rainfall: the Megech watershed has an average rainfall of 1177 mm, the Ribb watershed has 1428 mm, the Gilgel Abbay watershed has the highest rainfall of 1821 mm, while the Robigumero and Gumara watersheds have rainfall of 1266 mm and 1443 mm, respectively. These differences in rainfall indicate the heterogeneous climatic status of the watersheds in the area.

5.2.3 Soil and land use type

The dominant soil groups of the upper Blue Nile basin are vertisols, luvisols, and Leptosols (Easton et al., 2010). Specifically, the dominant soil categories of the Kessie watershed are Lithic Leptosols, Eutric Vertisols, and Chromic Luvisols occupying 44%, 24%, and 14% of the land, respectively. The soils significantly contribute to the hydrological processes, agriculture, and ecological interactions of the region. The Vertisols, which have high clay content, are particularly valuable for their water-holding properties, while shallow stony Leptosols are less fertile but otherwise contribute to the overall richness of the soil in the watershed. Luvisols with well-developed lower horizons must have the ability to sustain vegetation and agriculture. Conceptualization of the extent and character of these soils is relevant to successful management and conservation of the upper Blue Nile basin (Figure 5.3).

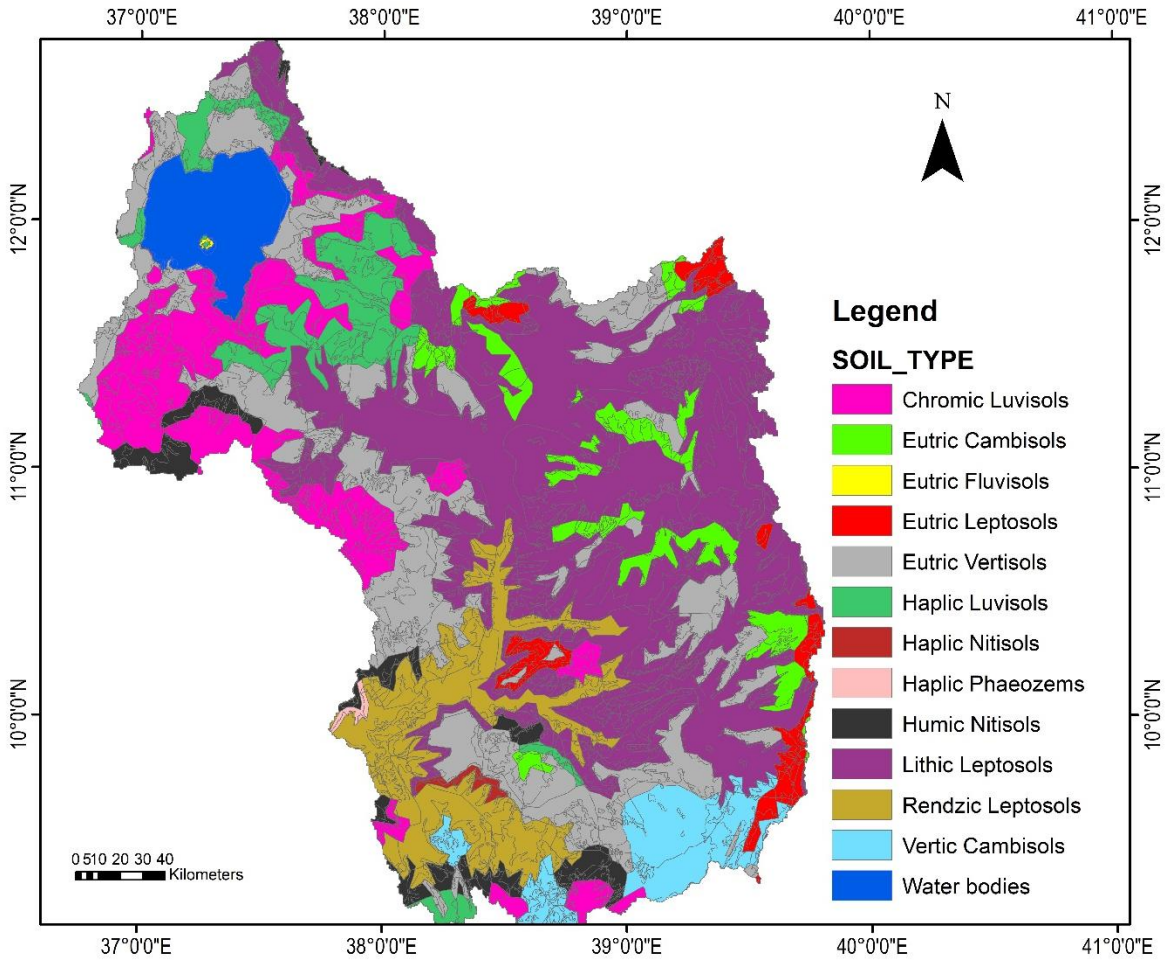

Figure 5-3 Soil Classification Categories

The most prevailing land use and land cover (LULC) classes in the Kessie watershed are agricultural land, grassland, bare land, shrubland, and woodland. The most prominent one is agricultural land, which occupies approximately 50.69% of the total area of the watershed, thereby representing the dominant land use. Grassland and bare land rank second and third, occupying 12.41% and 10.50% of the watershed, respectively. Woodland and shrubland do constitute some percentage of the landscape, although the specific percentages of these land types are not included in the data given. Urbanization, on the other hand, is a very small percentage of land use, comprising just 0.39% of the total area (Figure 5.4).

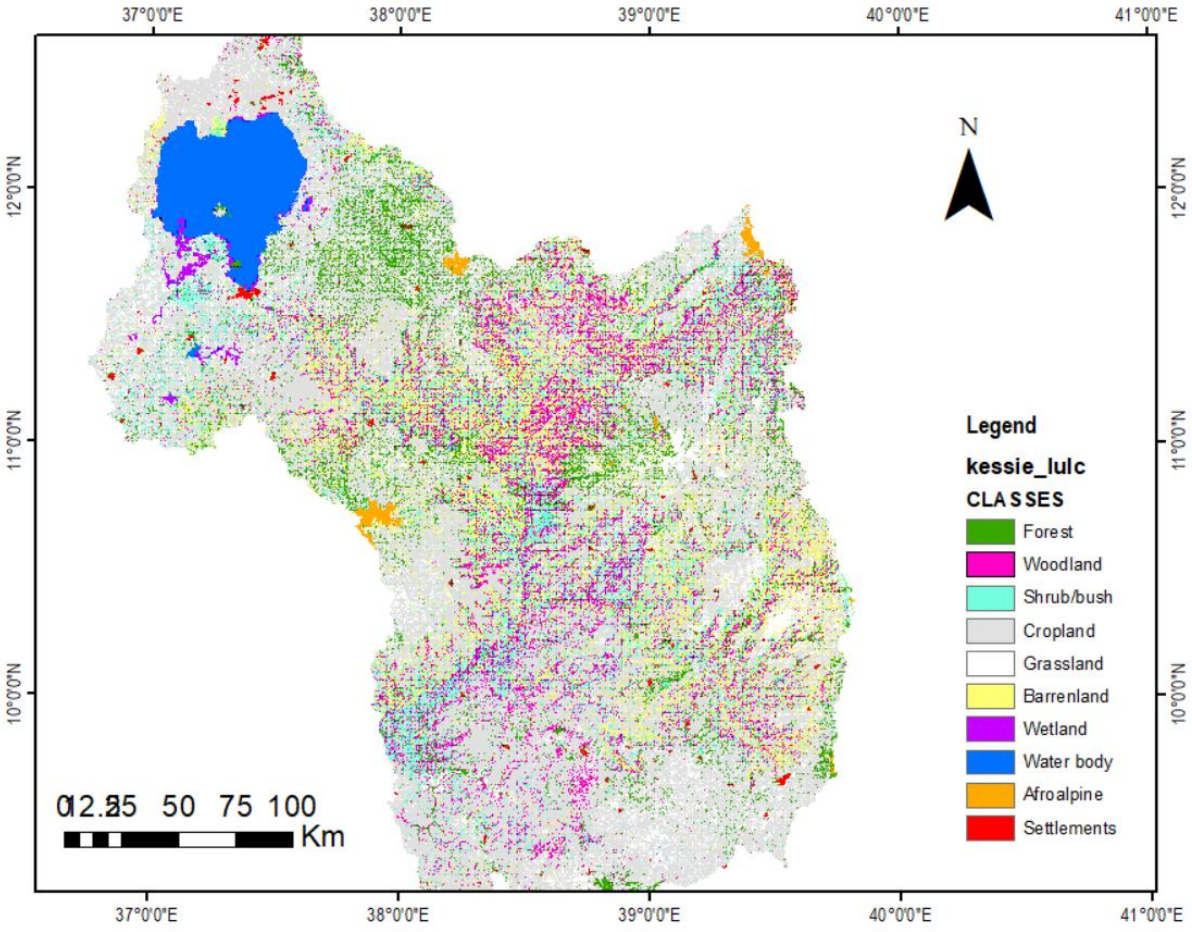

Figure 5-4 LULC map

5.3 Methodology

In river basins, sediment yield for specific sub-basins can be determined using two methods: direct measurement at each sub-basin outflow or conceptual/physical models. While direct measurement at sub-basin exits is regarded as the most dependable and precise method, it is frequently unfeasible due to its high cost, time requirements, and logistical obstacles. In instances when measured sediment data is scarce, physically based models provide a feasible alternative. These models can calculate sediment yields for each subbasin using sediment rating curves produced from restricted gauging station data. Furthermore, physically based models offer the advantage of splitting the entire watershed into smaller sub-basins, which allows for a more thorough geographical analysis. The QGIS-based Soil and Water Assessment Tool (QSWAT+) is a physically based model that has the ability to subdivide a basin into sub-basins and also model sediment yields for both gauged

and ungauged sections of the watershed. In this study, the QSWAT+ model was used because of its ability to integrate limited measurable data and generate detailed sediment yield predictions.

5.3.1 Sources of Data

The watershed has widely varied climatic conditions, the majority of which are influenced by the hilly terrain. The majority of the area experiences a unimodal rainfall regime with maximum precipitation between June and September. Topographical data were obtained from a Digital Elevation Model (DEM) uploaded by the United States Geological Survey. The Ethiopian Meteorological Institute provided daily weather data for the five research areas. The analysis included data from over 30 weather stations spread across the highlands and mountains. Spatial and temporal data were used as input to the SWAT+ model in this study. Spatial information, including land use/land cover (LULC) and soils, was obtained from the Water and Land Resource Center (WLRC). The Ministry of Water and Energy (MoWE) provided hydrological data in the form of river flow and suspended sediment concentration (SSC).

5.3.2 QSWAT+ Model Development

Hydrological modeling of flow and sediment for the Upper Blue Nile Basin (UBNB) was conducted with the most recent SWAT+ model (version 60.5.4). QSWAT+, an enhanced version of the SWAT model, was used to model surface runoff and sediment load within the watershed. The model incorporates enhanced features and capabilities that allow it to simulate hydrological processes and sediment dynamics in the study area. The use of QSWAT+ allowed the complete analysis of sediment and water transport, providing valuable information regarding the hydrological response of the basin (Koltsida et al., 2021), (Arnold et al., 2018). The QSWAT+ model was utilized for this research since it has the capability of appropriately simulating the dynamics of watersheds as well as conformity to the hydrological component of the research setting. Selection requires a full survey of all present modeling techniques on the basis of their adaptability to the region's unique climate and land uses. This is a broadly used model to predict the impact of altered land management and modified soil conditions (e.g., deforestation or other agricultural practices) on the water resources of a region (Daba, 2018). The QSWATPlus model allows for the complete characterization of the watershed properties at the hydrologic response unit level. It is a versatile design that can be applied globally, and the present edition includes terrain properties to allow for hotspot location identification. In addition, the graphical interface results are well presented and easy to understand.

The water balance equation in (5.1) forms the basis of the SWAT+ model used to compute surface runoff (Munoth and Goyal, 2019).

$$SW_t = SW_0 + \sum_{i=1}^{t} \left(R_{day} - Q_{sur} - E_a - W_{seep} - Q_{gw}\right) \quad (5.1)$$

Where SWt = variation of soil depth with time (mm), SW0 = initial amount stored in the soil one day back (mm), t = time (days), Rday = precipitation on a day basis (mm), Qsur = runoff water on the land surface (mm), Ea = loss of water through evaporation and transpiration (mm), Wseep = seepage of water from lower layers into the soil (mm), and Qgw = return flow of ground water to the soil (mm).

The SWAT+ model is also robust in the sense that it not only has the ability to estimate the quantity of water that flows over the ground (surface runoff) but also estimates the quantity of soil erosion that occurs (sediment loads) by applying the MUSLE equation. The MUSLE equation applied by SWAT+ is applied to the whole watershed and is a derivation of the revolutionary soil loss equation developed by Wischmeier and Smith way back in 1978(Vigiak et al., 2015)(see equation 5.2).

$$Sed = 11.8(Q_{surf} * q_{peak} * area_{hru})\text{^}0.56\text{x}K_{USLE}xC_{USLE}xP_{USLE}xLS_{USLE}xCFRG \quad (5.2)$$

Sed: sediment yield (ton), Qsur: runoff volume, qpeak: peak rate of runoff water (m3/sec), area HRU: size of an HRU (km2), KUSLE: soil erosion factor, CUSLE: land cover and management factor, PUSLE: conservation measure factor, LSUSLE: topographic factor, and CFRG: coarse fragment factor.

In order to develop a QSWAT+ model, different types of information, like meteorological, hydrological, and physical parameters, are required. SWAT+ is a semi-distributed physical model, and hence, spatial and temporal data must be provided as input. The main inputs required for the QSWAT+ model are digital elevation data, climate data, streamflow data, sediment data, soil data, and LULC maps (Documentation, 2009). The DEM used here was a resolution of 30 meters and was downloaded from http://srtm.csi.cgiar.org/strmdata/. Climatic information comprised approximately 39 meteorological stations for the catchments of the Kessie subbasin.

By using the QSWATPLUS model, the Kessie subbasin was divided into eighteen (18) subbasins, 2500 HRUs, and 2500 channels (Figure 5.5). Six subbasins or watersheds were selected for calibration and validation. The sub-basins were selected depending on data availability. The total streamflow and sediment load of the Kessie watershed were calibrated and validated using measurements at the watershed outlet, near the Millennium Bridge. For evapotranspiration

calculation, the Hargreaves formula was applied, and channel routing was done by the Muskingum routing method. The QSWAT+ model (60.5.4) was set up and run using the QGIS software interface (3.40.1).

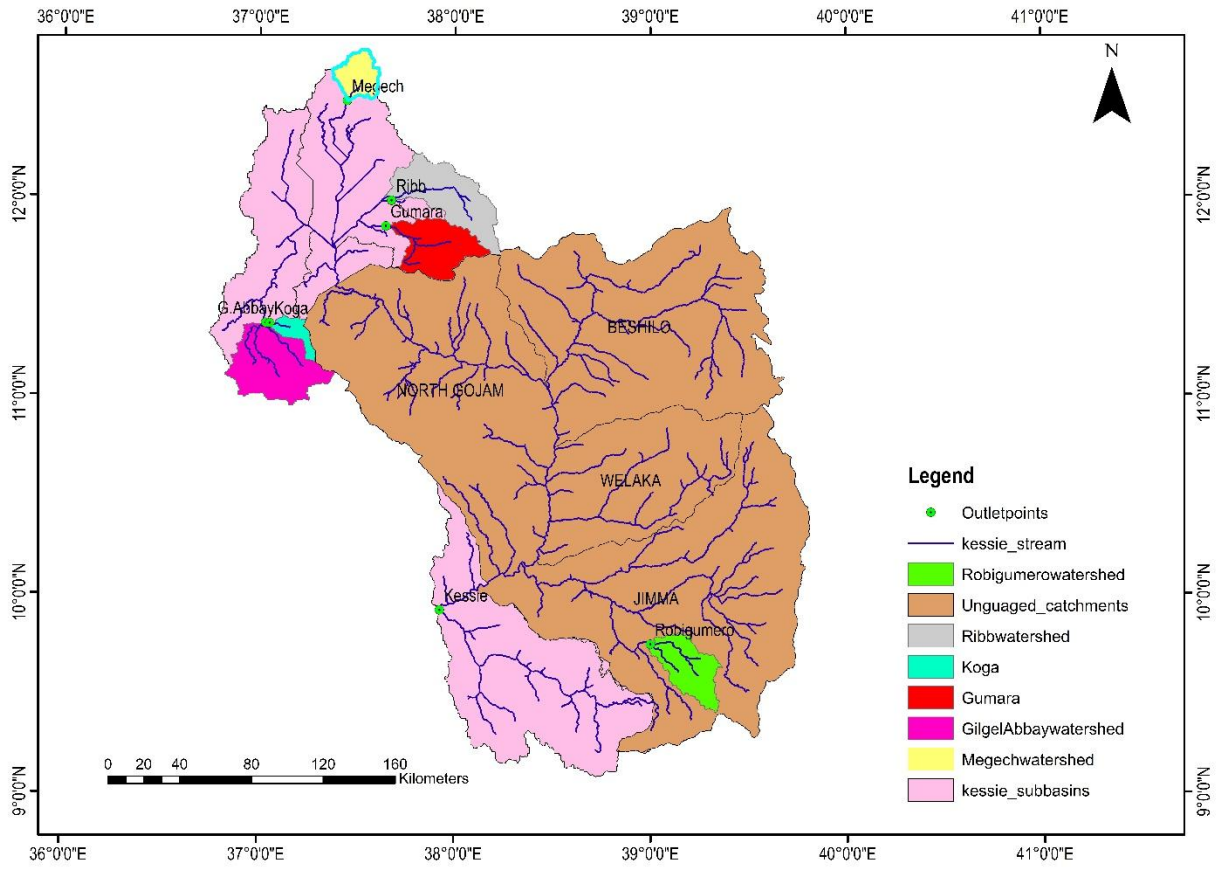

Figure 5-5 Delineated subbasins using the QSWATPLUs model, including gauged and ungauged catchments

5.3.3 Identification of the key parameters that significantly affect suspended sediment yield

The hydrology and geomorphology of a watershed have a significant impact on soil erosion in upland areas, as well as sediment deposition in lowlands and riverbanks. Geomorphology refers to the physical characteristics of a watershed, e.g., area, ratio of elongation, form factor, slope, and hypsometric integral. Geomorphological parameters were found and estimated using the QSWAT+ model. For measurements that were not feasible to derive directly from QSWAT+, QGIS spatial analysis was utilized to introduce additional information.

Each watershed's elevation values were derived from the research area's Digital Elevation Model (DEM). A contour map was created with QGIS spatial analysis tools, and the maximum, minimum,

and average elevations for each sub-watershed were calculated. These elevation values were subsequently utilized to compute basin relief (R), length of main river, perimeter of basin, mean elevation, area, slope, and length of watershed were obtained directly from the watershed configuration results in QSWAT+. In addition, sub-basin shape factors (Fs), drainage density (DD), circular ratio (CR), Ruggedness Number (RN), and elongation ratios (Re) were obtained by applying their respective mathematical formulas (Table 5.1).

Table 5-1 Standard computing morphometric parameters

S.No	Morphometric parameters	Formula	Reference
1	Drainage density (D)	D= Lu /A Where, D= Drainage, Lu=Total stream length of all orders, A= Area of the basin (km^2)	(Horton, 1955)
2	Relief ratio (Rh)	Rh = H/L Where, Rh = Relief ratio, H= Total Relief (Relative Relief) of the basin (km), Lb=Basic length	(Schumm , 1956)
3	Circularity ratio (Rc)	Rc=4π*A/P2 Where, Rc=Circulatory ratio, Pi=Pi value i.e., 3.14A= Area of the basin(km^2),P^2=Square of the perimeter	(Miller, 1953)
4	Elongation ratio (Re)	Re=(2/Lb)*(A/π) 0.5 Where. Re=Elongation ratio, A=Area of the basin(km^2),Lb= Basin length	(Schumm , 1956)
5	Length of overland flow (Lg)	Lg =1/D*2 where, Lg=Length of overland flow, D= Drainage Density	(Horton, 1955)
6	Ruggedness number (Rn)	Rn = Bh*D Where, D= Drainage density, H = Total Relief	(Singh and Singh, 1997)
7	Shape factor (Rs)	Rs = A/Lb, where A=Area of the basin(km^2), Lb= Basin length	(Horton, 1955)
8	Compactness coefficient (Cc)	Cc= 0.2821P/A 0.5 where A=Area of the basin (km^2), P= Basin perimeter	(Horton, 1955)

5.3.4 Principal Component Analysis

This study used PCA to identify the dominant parameters that influence suspended sediment yield. It is a DRT technique that attempts to obtain a few affected variables from a set of source variables. Variable or factor reduction in a data set can be an efficient approach to reduce the overall input data volume in modeling large data sets. Simplifying the input data complexity by limiting variables can make processing the modeling more efficient and practical (Ebrahimi-Khusfi et al., 2021). Also, in the present study, PCA has been used as a first or initial step in building a prediction model. PCA was used as an initial-stage technique to help prepare the data for the subsequent building of the prediction model (Haan, 2002). The key steps in the PCA process used by (Fernández et al., 2007) are summarized and described below:

1. Initially, select the initial variables that include 20 basin features, 1 climate, and 1 hydrology variable.
2. The suitability of data for PCA was assessed on the basis of Kaiser-Meyer-Olkin (KMO) measure of sample adequacy (Kaiser, 1974) and Bartlett's test of sphericity. The KMO test quantifies the proportion of item correlations to partial item correlations. If partial correlations are similar to raw correlations, it shows that the variable does not share much variance with other variables. This is a crucial condition since PCA is based on the assumption that obvious variance within the variables that are analyzed is due to latent common factors. KMO test scores range between 0 and 0.5; when the value of the score is 0.5, it is well noted and acceptable for PCA analysis. m 0 to 0.5; when the value of the score is 0.5, it is well noted and acceptable for PCA analysis. Bartlett's sphericity test is a key statistical test employed to check the hypothesis that the correlation matrix is an identity matrix, and hence all variables are uncorrelated. From the significance level derived through this test, it is possible to reject the null hypothesis and assert that the data set contains correlations appropriate for Principal Component Analysis. A Bartlett's test sphericity value of 95% ($p < 0.05$) is adequate enough to proceed with the PCA.
3. Using Principal Component Analysis (PCA) with Varimax rotation, the most important components of the dataset were determined. Kaiser's eigenvalues criterion was employed to select the principal factors, and only the principal factors with eigenvalues 1.0 and higher were retained for subsequent analysis as described in context-specific literature (Fernández et al., 2007) and other relevant sources (Sharma et al., 2015), and (Andrews et al., 2002).

The seven large criteria having the greatest contribution among 24 hydrological, meteorological, and land use parameters regulating sediment output were determined by employing Principal Component Analysis (PCA). The principal channel length (MCL), drainage area (DA), stream slope (SS), mean rainfall (Pr), farm area coverage (AA), forest areas (FA), and mean monthly stream flow (Qmean) are identified.

To develop an empirical formula for the estimation of the rate of sediment in the basin, the parameters that affect it were classified into two basic categories. The first one includes upland watershed factors, which consist of morphological characteristics (e.g., drainage area, length of the main channel, and stream slope, as shown in Table 5.1) and land use management methods (e.g., area of agricultural land and forest land areas). These parameters reflect the impact of topography and human activities on sediment generation and transport. The second group consists of instream parameters, including stream flow (e.g., mean monthly stream flow) and mean stream slope. These parameters are hydraulic and hydrodynamic conditions that affect sediment transport in the river channel. By separating the factors into these two categories, the empirical formula will be more likely to capture the intricate relationships between upland erosion mechanisms and in-stream sediment dynamics.

5.3.5 Empirical Model Development

The Sediment yield of a watershed can be predicted through various parameters of the hydrologic, climatic, and geomorphologic characteristics of the watershed. To develop a new empirical method for estimating sediment yield, the relation between sediment discharge and hydro-geomorphological factors was investigated for the Kessie River Basin. The basin was divided into 18 subbasins (Figure 5.5), and the streamflow and sediment yield were obtained from the calibrated QSWATPLUS model during the calibration and validation phases. For the development of an empirical model between sediment yield and certain parameters, DataFit software (version 9.0) was used. The software is suitable for nonlinear regression (curve fitting) and can also process statistical analysis along with data visualization. It can support to identification of the most significant variables that require multilinear sediment yield modeling.

Through the DataFit model, an empirical formula was obtained for sediment yield (SY) while determining watershed parameters. The nonlinear regression equation was used for the best-fit model within the boundary of sediment yield parameters as non-linear functions.

SY = function (geomorphology, climate, land use management practice, and hydrology)
Mathematically, the parameters in Equation (5.4) are equated as

$$SY = m(DA*MCL*SS) + n(Pr^{a}) + p(AA*FA) + q(Qmean^{b}) \quad (5.4)$$

Where SY stands for the mean monthly sediment yield of a sub-basin, in tons per day. It is computed with the following parameters:
DA (Drainage Area): The area of the sub-basin in square kilometers. MCL (Main Channel Length): The sub-basin main watercourse length, in kilometers. SS (Stream Slope): The stream slope, which influences water and sediment flow. Pr (Mean Monthly Rainfall): Average monthly rainfall in millimeters that affects erosion and runoff. Land Cover: Proportion of agricultural and forest cover, both of which affect the erodibility of the soil and the rates of erosion. Mean Monthly Stream Flow: Mean stream flow in cubic meters per second.
In addition, sediment yield can be estimated from a regression equation with empirical constants (m, n, p, and q). The model also contains two adjustment factors:
Rainfall Adjustment Factor: This is an adjustment factor for rainfall variability capable of influencing sediment mobilization.
Mean Monthly Flow Adjustment Factor: This factor adjusts for stream flow pattern variations, recognizing their effect on sediment transport efficiency.

For the development of the model, the hydrological and geomorphological characteristics such as stream slope, main channel length, watershed slope, mean monthly rainfall, agricultural land cover, forest cover, and drainage area of each of the 18 sub-basins, were extracted by using QGIS. The mean monthly average rainfall was calculated from Thiessen polygons using meteorological gauging station data available near each basin.

To obtain the mean stream slopes for every basin, we extracted elevation data of the outlet and inlet points of the streams from the Digital Elevation Model (DEM). This enabled us to calculate the slope accurately. Stream length was also calculated in QGIS directly.
The newly constructed alternative sediment yield prediction model was tested and validated rigorously to ensure its accuracy and reliability. The model performance was first checked by

comparing the predicted values of sediment yield with actual observed values using a collection of well-documented model evaluation statistics. These were the coefficient of determination (R^2), which quantifies the proportion of the variance in observed data explained by the model; the Nash-Sutcliffe efficiency (NSE), which is a test for the model's predictive capability against the mean of observed data; the root mean square error (RMSE), which computes the average size of the prediction errors; the observations standard deviation ratio (RSR), which scales RMSE to the standard deviation of observed data; and percent bias (PBIAS), which describes the average direction of the model to over- or under-predict the observed values. Together, these statistical metrics give a complete evaluation of the accuracy, precision, and bias of the model (Moriasi et al., 2007b).

In addition, the model was validated using an independent sub-basin and proved to be valid and applicable under various hydrological and geomorphological conditions. A two-stage testing framework like this not only enhances the validity of the model but also indicates its applicability in practical terms for various watersheds.

For testing the validity of the application of the model that has been developed, a study area for one of the BNB subbasins was selected. The Kessie subbasin, Gumara, Megech, Ribb, Robigumero, Koga, and Gilgel Abay were selected since they were among the available main subbasins with a daily river flow rate dataset maintained by the Ministry of Water and Energy (MoWE). These subbasins play a critical role in the hydrological and sediment transport process understanding in the region. In estimating daily sediment flow rates, sediment rating curves were applied, which establish a quantitative relationship between river discharge and sediment concentration (Aga et al., 2020).

5.4 Result and Discussion

5.4.1 The most influential variables on suspended sediment load yield

In this research, the Kaiser-Meyer-Olkin measure of the PCA method was 0.6, while Bartlett's test provided a significance value of 552.424. These measurements suggest that PCA is an appropriate method to ascertain the most dominant parameters in estimating suspended sediment yield (SSY). PCA analysis showed that four out of thirteen components were very active and explained 89.78% of the variation: DA (57.55%), SS (16.19%), ML (8.27%), Pr (8.12%), AA (8.11%), Qmean (8.05%), and FA (7.77%).

Varimax rotation of the correlation matrix PCA identifies four salient factors with eigenvalues > 1.00, accounting for a cumulative variance of 89.78%. The significance of variables listed in Table 5.2 is determined by the size of their eigenvalues.

Table 5.3 indicates PCA used variables and all principal components factor loadings, SS, DA, MCL, Pr, Qmean, AA, and FA are all variables with major loadings (≥ 0.60) on PC1. SF and ER constituted PC2, whereas PC3 only consisted of CR, and PC4 only comprised Bs. Suspended sediment load is well explained by PC1, which defines it and relates closely to drainage basin area and river flow. Suspended sediment yield will be related to the main channel length, total channel length, and periphery of the basin directly and will thus demonstrate that suspended sediment yield is affected by hydro-morphology directly. Hydrology, morphology, and topographic factors have been shown by principal component analysis in other studies to be important factors in regulating suspended sediment yield (Wuttichaikitcharoen and Babel, 2014).

Table 5-2 The principal components analysis of catchment characteristics and climate variables

PCs	Eigenvalues	Variances (%)	Cumulative Variances (%)
1	7.48	57.55	57.55
2	2.10	16.19	73.74
3	1.08	8.27	82.01
4	1.01	7.77	89.79
5	0.83	6.39	96.18
6	0.24	1.85	98.03

Table 5-3 Correlation matrix for the selected variables

	DA	BS	ML	TL	BP	BR	SF	ER	CR	TC	AASF	AASED	SSY
DA	1.0	0.1	**0.9**	**0.9**	**1.0**	**0.7**	0.2	0.2	-0.2	**0.9**	**1.0**	**1.0**	**0.6**
BS		1.0	0.1	0.0	0.0	-0.2	-0.2	-0.2	0.1	0.0	0.1	0.1	-0.1
ML			1.0	**0.9**	**1.0**	**0.8**	0.2	0.2	-0.2	**0.9**	**0.9**	**0.8**	0.4
TL				1.0	**1.0**	**0.8**	0.3	0.4	-0.2	**0.8**	**0.9**	**0.8**	0.4
BP					1.0	**0.7**	0.2	0.3	-0.3	**0.9**	**0.9**	**0.8**	0.5
BR						1.0	0.2	0.2	0.0	**0.6**	**0.7**	0.5	0.2
SF							1.0	**1.0**	0.1	0.0	0.2	0.0	0.2
ER								1.0	0.1	0.1	0.2	0.1	0.2
CR									1.0	-0.2	-0.3	-0.2	-0.1
TC										1.0	**0.9**	**0.8**	0.5
AASF											1.0	**1.0**	**0.6**
AASED												1.0	**0.7**
SSY													1.0

Notes: **Bolded values are correlation coefficients above 0.6; Kaiser-Meyer-Olkin measure of sample adequacy: 0.6; and Bartlett's test of sphericity: 552.42**

5.4.2 Sensitivity analysis for streamflow and sediment calibration

Sensitivity analysis is a helpful method for determining the most sensitive model parameters and their impact on simulated output due to variations in input variable values. A QSWAT Plus model generated eight parameters, ranking high sensitivity. These parameters were largely associated with surface runoff (e.g., curve number and soil moisture), soil properties (e.g., available water content, compensation for evaporation, and erodibility), baseflow, water table depth, percolation, and management practices (Table 5.4). These findings agree with previous research based on the SWAT Plus model (Tumsa et al., 2022),(Konan-waidhet, 2023).

Nine parameters were identified to be very sensitive to sediment simulation, based on Table 5.5. Sensitivity analysis was used to quantify missing parameters and identify those with the greatest impact on sediment load in the model response. The most sensitive parameters were the subbasin slope, compensation factor of the soil evaporation, USLE support practice factor (USLE_P),

Manning's "n" coefficients for overland flow, sediment concentration in lateral and groundwater flow, plant uptake compensation factor (EPCO), linear parameter (SPCON), and the exponent parameters. These findings are consistent with other reports in the Ethiopian highlands (Bihonegn and Awoke, 2023), and (Tumsa et al., 2023).

Table 5-4 Streamflow Calibration Parameters and Their Corresponding Fitted Values

Rank	Parameters	Parameter Groups	Minimum value	Maximum value	Optimum value
1	awc	Soil	0.01	1	0.527
2	alpha	Aquifer	0	1	0.345
3	CN2	Hydrological Response Unit	35	98	78
4	cn3_swf	Hydrological Response Unit	0	1	0.384
5	usle_p	Hydrological Response Unit	0	1	0.144
6	esco	Response Unit	0	1	0.37
7	revap_min	Aquifer	0	50	36.279
8	usle_k	Soil	0	0.65	0.618

Table 5-5 Sediment Calibration Parameters and Their Optimized/Fitted Values

Rank	Parameters	Parameters group	Minimum value	Maximum value	Optimum value
1	slope	Hydrological Response Unit	0.0001	0.9	0.071
2	esco	Hydrological Response Unit	0	1	0.298
3	usle_p	Hydrological Response Unit	0	1	0.658

4	ovn	Hydrological Response Unit	0.01	30	4.407
5	lat_sed	Hydrological Response Unit	0	5000	171.685
6	EPECO	Hydrological Response Unit	0	1	0.354
7	SPCON	Basin	0.0001	0.01	0.001
8	SPEXP	Basin	1	1.5	1.07
9	cn2	Hydrological Response Unit	35	98	57.315

5.4.3 Streamflow and sediment yield calibration and validation

Stream flow and sediment load were calibrated for each sub-catchment of the Kessie watershed for the period 2000-2011 and validated for the period 2011-2015. The model performed well in simulating streamflow and sediment yield during the calibration period, with Nash-Sutcliffe Efficiency (NSE) of 0.85 and 0.79, R-squared (R^2) of 0.88 and 0.8, and percent bias (PBIAS) of -20.25 and 9.63, respectively (Tables 5.6 and 5.7). During the validation period, the model also performed well with an NSE of 0.65, R^2 of 0.69, and PBIAS of -16.56. These results are comparable to those of other studies conducted in the Kessie sub-catchment with different spatial data and shorter time series (Easton et al., 2010). As is apparent in Figures 5.6 (monthly sediment yield hydrograph) and Figure 5.7 (monthly streamflow hydrograph), flow and sediment load values simulated at a number of watershed outlets compared well with the measured values. The statistical measures of model efficiency, i.e., NSE, R^2, and PBIAS, are given in Tables 5.6 and 5.7, which indicate that the model performance is satisfactory. However, the model tended to overestimate streamflow as well as sediment yield, as can be seen in Figure 6 (monthly sediment yield hydrograph). This overestimation may be attributed to data constraints because sediment data in the watershed are scarce and primarily derived from sediment rating curves, which can introduce uncertainties. The model assumptions may also not fully incorporate the complexity of hydrological processes and sediment transport processes in the watershed.

Despite these limitations, the model's overall performance is satisfactory and provides valuable information on the hydrology and sediment dynamics of the Kessie sub-catchment. The findings

indicate the necessity to improve data availability and more realistic model assumptions. The findings can serve as a foundation for further studies and inform sustainable water resources and sediment management in the region.

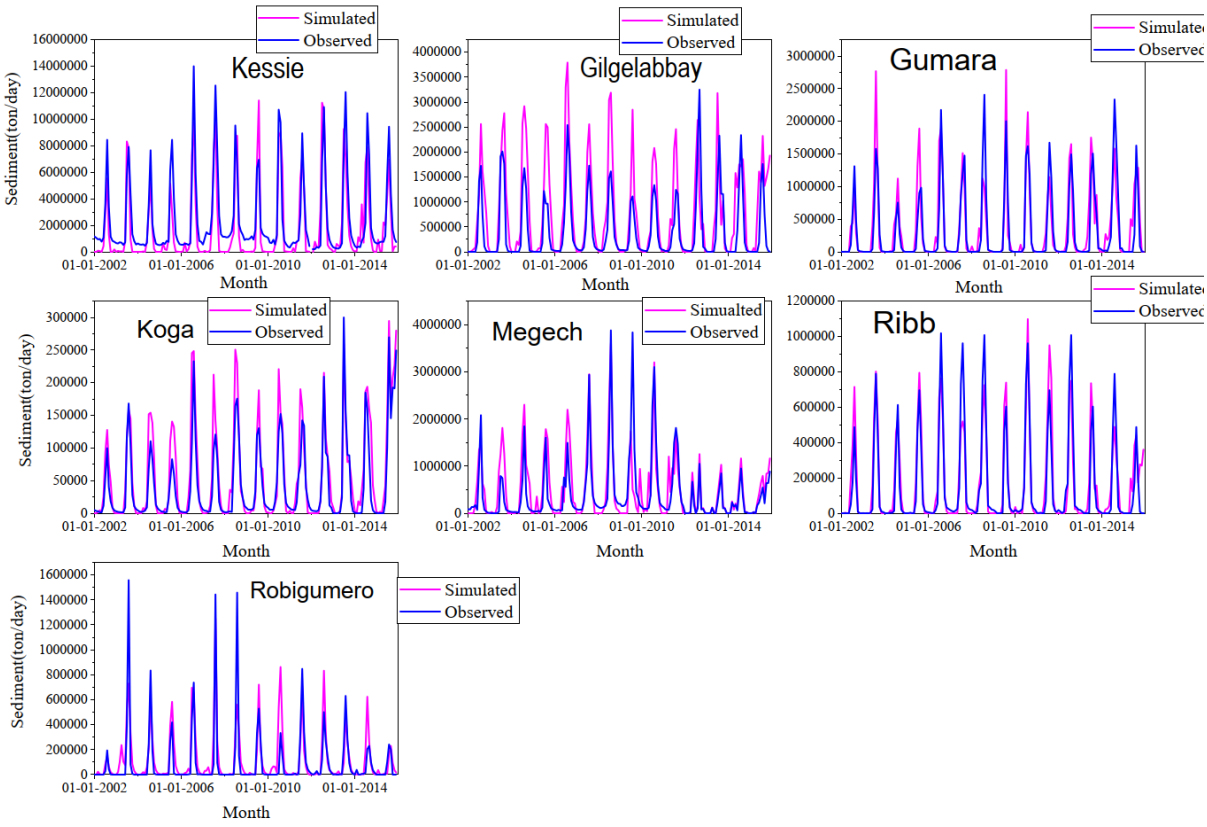

Figure 5-6 Observed and simulated monthly sediment yield hydrographs by the SWAT + model for the period of calibration and validation from 2000 to 2015

As seen in Table 5.6, the mean simulated streamflow at the various watershed gauging stations was higher than the mean observed flow, indicating that the model overestimates streamflow compared to the actual observed data. Overestimation may be due to factors such as input data constraints, model parameter uncertainties, or the inability of the model to capture localized hydrological processes. Similarly, the monthly average simulated and observed sediment yield results are shown in Table 5.7, depicting a comparison of sediment dynamics over the study area.

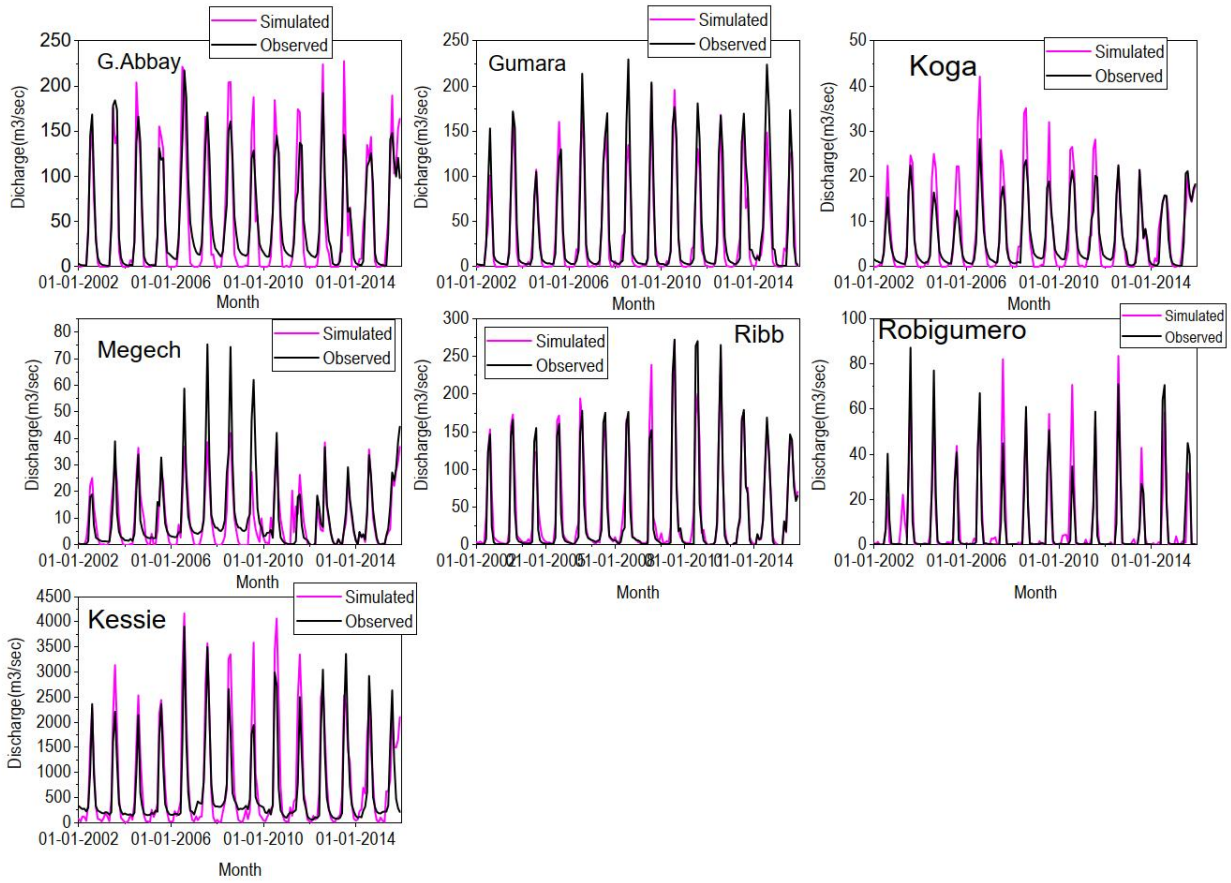

Figure 5-7 Observed and simulated monthly streamflow hydrographs by SWAT+ for calibration and validation from 2000 to 2015

The goodness-of-fit of streamflow and sediment yield during calibration and validation phases is presented in Tables 5.6 and 5.7. Calibration of the hydrological component of the model is acceptable, as suggested by the QSWAT+ developers (Santhi et al., 2001), if the following criteria are satisfied: $R^2 > 0.6$, NSE > 0.5, and RSR < 0.7. Also, according to the criterion given in (Moriasi et al., 2007b), the predictive performance of the model is very good. Thus, the output for stream flow and sediment yield is indeed credible and can be properly utilized in higher-order modeling development and calculations. Therefore, the good outcomes of the calibration validation aid in the development of an alternative empirical model that can estimate the suspended sediment yield in ungauged catchments.

Table 5-6 Performance of the SWAT+ model in streamflow calibration and validation using statistical parameters

Catchment	NSE		R2		PBIAS		Observed Mean Monthly Streamflow	Simulated Mean Monthly Streamflow
	Cal	Val	Cal	Val	Cal	Val	m^3/sec	m^3/sec
Robigumero	0.79	0.79	0.81	0.79	17.17	8.285	8.17	8.92
Gumara	0.89	0.82	0.91	0.87	15.34	22.22	34.41	41.62
GilgelAbbay	0.8	0.79	0.86	0.88	8.53	-1.399	48.71	51.68
Ribb	0.89	0.9	0.9	0.95	18.56	-1.065	39.27	44.02
Kessie	0.85	0.65	0.88	0.69	-20.27	-16.06	650.9	774.9
Koga	0.88	0.9	0.9	0.9	17.19	3.58	10.63	8.86
Megech	0.73	0.7	0.75	0.71	17.7	13.1	6.36	7.05

Note: Cal: calibration, **Val**: validation

Table 5-7 Performance of the SWAT+ model in sediment yield calibration and validation using statistical parameters

	NSE		R2		PBIAS		Observed Mean Monthly Sediment Yield	Simulated Mean Monthly Sediment Yield
	Cal	Val	Cal	Val	Cal	Val	ton/day	ton/day
Robigumero	0.7	0.7	0.71	0.71	-25.3	-24.24	92,059.19	115,129.75
Gumara	0.73	0.69	0.75	0.7	-7.25	-12.38	318,192.59	346,614.25

GilgelAbbay	0.8	0.73	0.83	0.75	-8.75	-5.58	437,596.32	773,390.37
Ribb	0.85	0.7	0.87	0.74	-7.68	-12.1	151,458.41	164,852.24
Kessie	0.79	0.7	0.8	0.72	34.43	9.63	2,326,699.97	1,696,354.93
Koga	0.8	0.85	0.85	0.9	-24.5	23.4	43,620.47	56,776.40
Megech	0.8	0.82	0.85	0.89	-15.1	-13.5	412,914.40	485,824.01

5.4.4 Alternative Empirical Model

Using a nonlinear regression approach, an alternative model for estimating sediment yield has been developed with the assistance of DataFit version 9.0.

$SY = 1.24(DA*MCL*SS) + 0.25(Pr^{a}) + 0.14\ (AA*FA) + 0.12\ (Qmean^{b})$

Whereas SY is the mean monthly subbasin sediment yield(ton/day), DA is drainage area(km^2), MCL, is main channel length (km), SS is stream slope, Pr is mean monthly rainfall (mm), AA is agricultural coverage area of subbasin (%), FA is forest area coverage (%), and Qmean is mean monthly streamflow (m^3/sec).

In the model, a and b are the mean monthly rainfall adjustment factor and mean monthly stream flow adjustment factor, respectively. The value of a varies between 1.85 and 3.51, with a mean value of 2.68, and b varies between 2.06 and 2.33, with the mean value of 2.19.

5.4.5 Validation of the newly developed empirical model

The newly developed empirical model was tested across six gauged watersheds within the Kessie subbasin. As depicted in Figure 5.8, the simulated suspended sediment yield estimated by the alternative empirical model aligned well with the observed values across all six watersheds. The model exhibited strong performance, with specific examples including Gumara ($R^2 = 0.84$), Ribb ($R^2 = 0.71$), and G. Abay ($R^2 = 0.61$). The model's validity was further confirmed using 11 years of data, demonstrating its reliability and accuracy. The newly developed alternative sediment estimation model was utilized to calculate the sediment outflow for the entire basin. The monthly sediment yield, using the alternate empirical model, was computed to assess sediment dynamics within the basin.

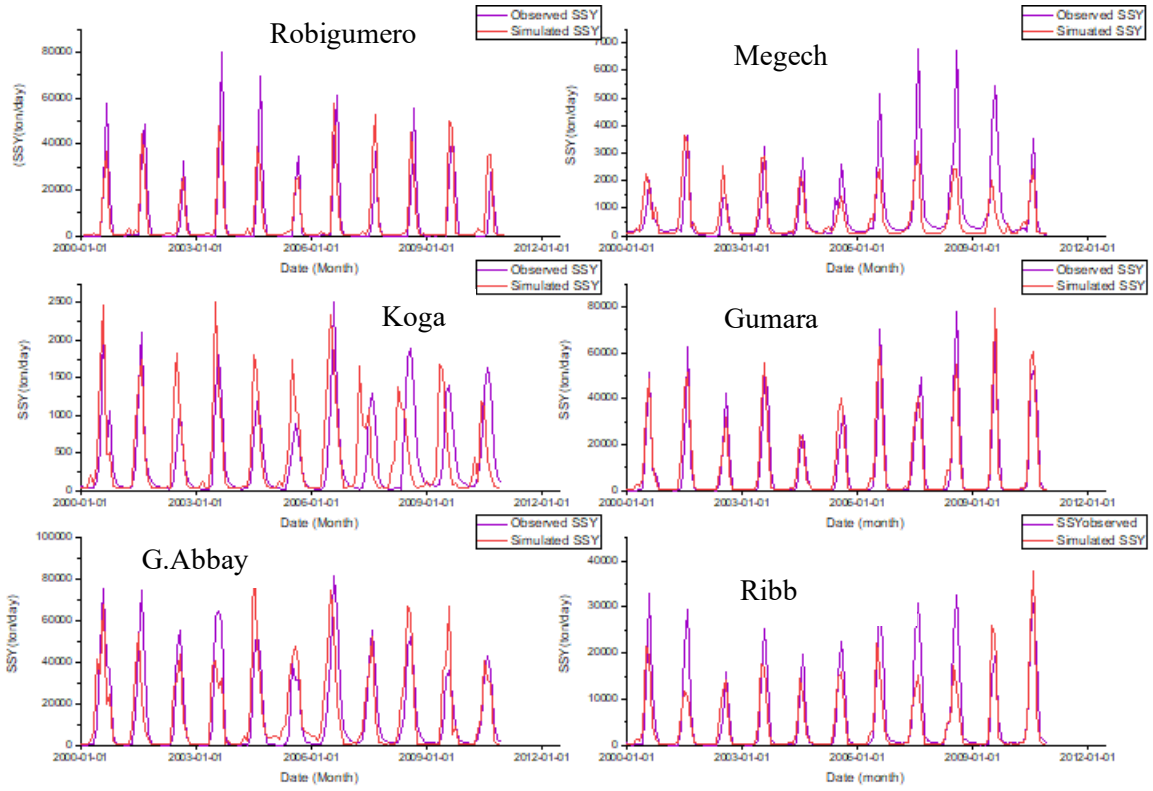

Figure 5-8 Verification of sediment yield derived from the alternative empirical model against measured suspended sediment data for various gauged watersheds

The time series plot (Figure 5.8) indicates the ratio of measured monthly sediment concentration to values predicted by the alternative empirical model, with high agreement for both dry and wet seasons in the various years.

5.4.6 Novelty of the newly developed empirical model

In predicting soil erosion, the Universal Soil Loss Equation (USLE) has a long history. The USLE was later adapted by (Williams, 1975) to obtain MUSLE, which is being widely used for sediment yield estimation in catchments. The MUSLE has been applied in most parts of the world for sediment yield prediction from agricultural and non-agricultural lands. In addition, it has been integrated into computer-based simulation models, e.g., QSWATPLUS, for the analysis of sediment yields at the basin and sub-basin levels (Arnold et al., 1995). The new model bears some resemblance to the USLE in that it also considers factors such as rainfall, land use, and slope characteristics of the watershed. However, unlike the USLE, the new model incorporates the influence of streamflow conditions on sediment transport. Moreover, it is able to assess

detachment-limited and transport-limited forms of erosion, offering a more comprehensive approach to erosion and sediment yield prediction.

In the Lake Zway basin, Ethiopia developed another empirical model was developed that has the potential to predict the sediment yield of the watershed. The developed model by (Aga et al., 2020) is shown as (Equation 5.6) :

$$SY = 0.04 \times (Qsb \times A \times Sb \times K) + 0.07 \times (qrd \times Sr), \quad (5.6)$$

Where SY is the sediment yield of a sub-basin in tons per month. It is estimated based on a series of factors: Qs, surface runoff in cubic meters per second (m^3/s); A, sub-basin area in square kilometers (km^2); Sb, the mean slope of the sub-basin in percentage (%); K, the soil erodibility factor; qr, streamflow in cubic meters per second (m^3/s); and Sr, the mean slope of the river in percentage (%). Here, b and d are adjustment factors for peak flow. The values of b commonly range between 0.01 and 0.621, with a mean of 0.31072, and those of d between 1.284 and 1.398, with a mean of 1.341. These constants are utilized to fine-tune the model for a better representation of the relationship between sediment yield and controlling variables.

As indicated in equation (5.6), the impact of climatic factors is not explicitly addressed in the model. Nevertheless, as indicated in the Universal Soil Loss Equation (USLE) and its derivatives, climate is a significant factor in the control of sediment transport in watersheds. In the discussion of their investigation (Aga et al., 2020), the researchers highlighted the need for further research directed towards the development of a more accurate sediment prediction model incorporating climatic variables specific to the watershed. Against this backdrop, the current research endeavors to alleviate the limitations identified in previous research and propose a more comprehensive approach to sediment yield estimation.

Another researcher also developed a model in northern Ethiopia that can be used to estimate the sediment yield of the watershed. The model developed by (Tamene, L., Park, S. J., Dikau, R., & Vlek, 2006) is shown as (Equation 5.7):

$$LogSY = 0.007 \times SBCG + 0.003 \times ELL + 0.002 \times RG - 0.007 \times BUSH + 2.33, \quad (5.7)$$

where LogSY is sediment yield in tons per square kilometer per year ($t\ km^{-2}\ yr^{-1}$), SBCG is normal bank collapse and gully erosion, ELL is the percentage of erodible lithology (%), RG is surface roughness, and BUSH is the percentage of bush or shrub cover (%).

It can be noted from the equation that the climatic variables are not included in this equation. However, climatic parameters like the intensity of rain are the main variables controlling soil erosion.

5.5 Conclusion and Recommendation

The newly developed alternative model for watershed sediment yield prediction involves geomorphologic, hydrologic, climatic, and hydraulic watershed characteristics. The model relies on the assumption that sediment delivered to the outlet of the basin is sourced by both the upland regions and stream channel reaches. For upland regions, the significant parameters governing sediment yield include basin area, slope, soil erodibility rate, and surface runoff. Similarly, for channel stream, stream flow rate and channel slope are identified as the main controlling factors of sediment yield. Based on these diverse parameters, the model presents a more comprehensive approach to predicting sediment yield, encompassing the complex relationships between different watershed constituents. An alternative empirical model was developed using the Kessie sub-basin, which covers an area of 65,784 km², and this sub-basin was further divided into 18 sub-basins, including both gauged and ungauged watersheds. After calibrating the model at the Kessie gauged station using observed streamflow and suspended sediment yield, the model was constructed utilizing hydrological, geomorphological, climatic, and land use data from the 18 sub-basins. The model was then tested with data from the gauged watersheds, and the performance indicators showed satisfactory results over eleven years of data. The performance of the model was validated by time-series plots comparing the recently estimated sediment yields from the model with observations. The outcome was that the alternative model strongly correlated with sediment yields at gauging stations. One major constraint to the use of physically-based models like QSWATPLUS is that measured sediment data is never available. The newly derived model addresses this issue in the study area. It is also recommended that this model be tested in other basins to further evaluate its applicability.

6. Developing an alternative regional suspended sediment yield estimation model for ungauged catchments: Ethiopia Highlands

Abstract

Accurate estimation of sediment discharge is crucial for designing and operating engineering structures such as dams, water treatment facilities, and erosion control systems. This study aimed to develop a regional model for estimating suspended sediment yield (SSY) for ungauged catchments using topographic, geomorphological, land use, climatic, and hydrological variables. However, including all these variables may hinder the model's performance. In order to select the most influential variables on suspended sediment output, data reduction techniques such as principal component analysis (PCA), the Gamma test (GT), classification and regression trees (CART), and stepwise regression (SR) were utilized. Furthermore, multiple linear regression (MLR) and artificial neural networks (ANN) models were used to develop a regional model for estimating SSY in an ungauged catchment. The analysis revealed that drainage area and overland flow length were the two most significant of the 22 variables affecting suspended sediment yield. This showed that the hydrology, morphology, and topography of the catchment area had a significant impact on the amount of suspended sediment yield. During calibration, the coefficient of determination (R^2), root mean square error (RMSE), and mean absolute error (MAE) were 99.9%, 12,631.6 t/yr, and 10,354.9 t/yr, respectively. During validation, these figures were 82%, 139,944 t/yr, and 136,036 t/yr, respectively. The performance indicators of the GT-ANN model revealed that it performed optimally during the calibration and validation phases. It revealed that the GT-ANN model outperformed all other ANN and MLR models. Overall, regional SSY estimation models developed using ANN outperformed MLR models. Ultimately, identifying the key factors influencing SSY and leveraging artificial intelligence technologies can empower water resource managers to swiftly evaluate SSY dynamics in ungauged catchments.

Keywords: Data reduction technique, Suspended sediment yield, regional model, Artificial Neural Network, Multiple linear regression

6.1 Introduction

Sediment yield is defined as the end product of soil erosion, which is the discharge of sediment load from the watershed or the concentration of sediment delivered to the point of interest in the

river network over a specified period of time (Melesse et al., 2011) and the net result of soil erosion and sediment deposition process (Haregeweyn et al., 2013). Sediment yield within a watershed includes soil degradation caused by terrain, inclines, channels, rivers, and landslides, minus sediment deposited after degradation but before reaching the area of interest. The process of sediment erosion, transport, and deposition in river systems is intricate and influenced by factors such as topography, weather patterns, watershed attributes, channel hydraulic characteristics, sediment properties, and both geology and land use /cover (S.L. Neitsch, J.G. Arnold, J.R. Kiniry, 2009). Reliable sediment yield data is essential for the planning, design, construction, management, commissioning, and operation of hydraulic structures in water resource projects (Heng and Suetsugi, 2013b),(Yadav et al., 2022b), and (Aga et al., 2020), for soil and water conservation practices in the watershed (Basin, 2017), for water management and environmental protection (Melesse et al., 2011), and for describing the water quality of aquatic ecosystems (Womber et al., 2021). However, it is challenging to obtain sediment yield data for rivers in many regions of the world, especially in underdeveloped countries and remote areas (Heng and Suetsugi, 2013a). In underdeveloped countries, the number of gauged sediment data is not only small but also not reliable (Haregeweyn et al., 2013). The lack of sediment yield makes it difficult to accurately quantify the total sediment load that will flow into new dam reservoirs during the planning processes. This can lead to reservoir designs that are either overly risky or not economically optimal (Haregeweyn et al., 2006). Therefore, estimating the amount of sediment transported from a catchment region is critical in the disciplines of water resources engineering, land resource management, and river engineering, as evidenced by the research conducted by (Melesse et al., 2011), and (Kisi et al., 2012). Furthermore, there is a vital need to develop effective methods for accurately predicting sediment yield in ungauged catchments that lack sufficient monitoring data.

Appropriate approaches for estimating erosion and sediment output at the watershed scale are extremely important for taking proper actions to prevent reservoir sedimentation and conserve water resources (Li and Wang, 2014). The application of a specific approach for estimating sediment output is dependent on the type and accessibility of data, time, and availability of finances. The most typical approach for estimating sediment yield in the ungauged catchment is to use the parameters from the hydrologically similar gauged catchment. This is known as the regionalization approach, and it involves transferring data from a gauged (measured) watershed to

an ungauged one. It is an alternative way to predict sediment load in the ungauged catchment (Swain and Patra, 2017), (Heng, S., Suetsugi, 2015). However, considering the fact of representing catchment characteristics, it is difficult to regionalize the parameters of observed to unobserved watersheds. In addition to the area-specific method, there are alternative techniques for modeling and estimating suspended sediment load in ungauged catchments. These include a physical-based model (e.g., unit stream power to directly model and estimate the sediment transport processes), a conceptual model (SWAT (USLE, RUSLE, MUSLE to conceptual represent and estimate sediment load), and a data-driven model (artificial neural network, sediment rating curve). The physical-based and process-based model approaches can be used universally to estimate the sediment load of a watershed. However, these models require intensive data concerning hydraulics, weather patterns, geology, and the characteristics of the sediment itself. It can be costly and time-consuming to gather spatial and temporal environmental data required for the calibration and validation of these models (Hamel et al., 2016), (Kisi et al., 2012). Because of the data-intensive nature of sediment transport processes and the high data consumption, the physically-based and process-based models rely on numerous simplifying assumptions and empirical correlations. As a result, when applied to catchments with restricted data availability, these models tend to produce highly unpredictable outcomes. As a result, these model types are often not feasible to apply in developing countries or rural places where the essential data may be lacking (Wicks and Bathurst, 1996). In contrast, the data-driven model is the preferred approach when data availability is limited. This is owing to the fact that data-driven models do not require extensive, comprehensive information about the entire erosion and sediment transport system. Artificial neural networks (ANN) are among the most well-known and effective data-driven or black-box models, particularly in scenarios with limited data. It is a type of machine-learning model inspired by the design and functionality of the human brain, and it has proven useful in describing and replicating hydrological processes (Kakaei Lafdani et al., 2013), (Wilby et al., 2003), (Nhu et al., 2020). Multiple studies have found that the ANN approach proved more effective in modeling and estimating sediment transport processes than standard physical-based models (Tayfur, 2009). Another comparative study conducted by (Haddadchi et al., 2013) examined various sediment transport models and found that an Artificial Neural Network (ANN) model significantly outperformed nine other hydrodynamic-based sediment transport formulas in estimating the suspended sediment yield of different watercourses in Iran. A study by (Singh et al., 2012)

examined the ability to predict monthly suspended sediment yield (SSY) for the Nagwa watershed in India. They found that an Artificial Neural Network (ANN) model performed better than the Modified Universal Soil Loss Equation (MUSLE) model. A similar study conducted by (Talebizadeh et al., 2010) indicated that ANN is superior to MUSLE in predicting low and medium values. (Melesse et al., 2011), and (Kheirfam and Mokarram-Kashtiban, 2018) demonstrated that an ANN model outperformed multiple linear regression, nonlinear regression, and autoregressive moving average models in predicting daily suspended sediment load. Overall, these studies suggest that ANN-based approaches are more effective than standard physical-based models for modeling and estimating sediment transport processes. While many studies have found ANN models effective for estimating sediment transport processes, there have been relatively few studies that addressed the use of ANN for estimating sediment data at ungauged basins. One such study was conducted by (Cigizoglu, 2005), which used an ANN model to predict suspended sediment concentration (SSC) at downstream locations based on upstream flow data; however, this is limited by the availability of gauged stations along the stream.

In addition to the ANN model, the regression analysis model is also a data-driven strategy that uses catchment characteristics, hydrology, and climate data as input variables to estimate longer-term expected sediment load (MYermolaev and Mukharamova, 2023). Thus, studies have attempted to explain sediment output by investigating the combined influence of numerous watershed factors, such as morphometric (physical dimensions), climatic, and hydrologic variables. Single or multiple linear regression models are widely used to express the correlations between sediment yield and basin parameters. Such models would allow for the calculation of suspended sediment load in the majority of rivers lacking measurement data (Wuttichaikitcharoen and Babel, 2014).

To this purpose, many methods have been employed to estimate suspended sediment load (SLY). Among the most prominent methodologies, artificial neural network (ANN) and multiple linear regression (MLR) methods are frequently recommended because of their high accuracy and ease of use(Kisi, 2008), (Barati, 2011), and (Samantaray and Ghose, 2018).

Several recent research studies have focused on developing and testing regional models that can be applied to estimate hydrological variables in ungauged catchments. For example, the study by (Kheirfam and Mokarram-Kashtiban, 2018) developed a regional model to estimate sediment load in an ungauged catchment using factors such as physical geography, climate, and hydrology. This

study found that an artificial neural network (ANN) model performed significantly better than a multiple linear regression model for this task. In another study, (Kamel et al., 2014) found that artificial neural networks (ANNs) were a promising approach for predicting suspended sediment yield in ungauged catchments in Algeria. In related studies, (Heng and Suetsugi, 2013a) used artificial neural networks (ANNs) to estimate monthly suspended sediment load at unmonitored sites in the Lower Mekong basin. They used climate data and streamflow data from seven hydrometric stations as inputs to the ANN model. (M. Atieh et al., 2015) Applied ANN models to estimate sediment transport in ungauged basins in Ontario, Canada. The researchers integrated data from 94 basins to estimate the parameters of the traditional sediment rating curve. They used input variables that physically characterize the basins, as well as climatic and hydrometric parameters, which led to satisfactory results for estimating sediment transport in the ungauged catchments. In a study by (Campos and Pedrollo, 2021), A regional artificial neural network (ANN)- based model was used to estimate suspended sediment concentrations (SSC) in ungauged, diverse catchments. This study showed that the proposed ANN-based methodology enables the regional extrapolation of SSC estimates to ungauged basins, even in heterogeneous regions, with very good predictive performance. In contrast, another study by (Wuttichaikitcharoen and Babel, 2014) attempted to estimate sediment yield in ungauged basins using principal component analysis and multiple regression analysis. The validation of the regression relationships for estimating suspended sediment yield showed errors ranging from -55% to +315% for suspended sediment yield, and -59% to +259% for area-specific suspended sediment yield. These results indicate relatively high errors compared to the ANN-based methods discussed in the previous examples.

This study focuses on the Ethiopian highlands, specifically the upper Blue Nile basin, which has been identified by the Ethiopian government as a region for irrigation and hydropower development, both of which are critical to Ethiopia's food security and economic growth (Ministry of Finance and Economic Development (MoFED), 2006). As a result, the Ethiopian government has allocated major financial resources to the development and construction of dams in the UBN region. However, there is a possibility that half of the dam reservoirs will not reach the end of their expected economic lifespan. This is owing to the lack of a thorough local database on sediment yield, as well as a suitable sediment yield.

The main objective of this study is to develop a viable regional model that can predict suspended sediment yield (SSY) in ungauged catchments in the Upper Blue Nile basin. In this study, the

researchers attempted to develop an appropriate regional model for estimating sediment load in watersheds without measured sediment data. They used input variable reduction techniques such as Principal Component Analysis (PCA), Gamma Test (GT), and Stepwise Regression (SR) to select the most important predictor variables. Additionally, they utilized Artificial Neural Networks (ANN) and Multiple Linear Regression (MLR) as modeling tools to predict sediment load in these ungauged watersheds.

6.2 Material and methods

6.2.1 Watershed characteristics and data sets

The study area is focused on the upper Blue Nile basin, covering the northwestern part of Ethiopia. The Blue Nile (Abbay) basin lies in the western part of Ethiopia between 7^0 45'-12^0 45' N and 34^0 05'-39^0 45' E. It is the largest of the 12 major river basins in Ethiopia with an area of about I76,000 km^2 at the border point with Sudan. It is a vital resource providing 45% of the country's surface water resources, sustaining 20% of its population, and occupying 17% of its landmass (Samy et al., 2019). The Upper Blue Nile Basin (UBNB) is a major agricultural production center in Ethiopia. Furthermore, this basin is where the Grand Ethiopian Renaissance Dam (GERD) is located. Furthermore, the basin makes a substantial contribution to Ethiopia's irrigation productivity and hydropower generation (Fenta Mekonnen and Disse, 2018). The Blue Nile basin plays a crucial role in the hydrology of the entire Nile River system, as it generates more than 62% of the total Nile River runoff that reaches Sudan and Egypt (Awulachew et al., 2008). The main tributaries of the Abay (Blue Nile) river in Ethiopia include Beshilo, Jemma, Fincha, Guder, Muger, Anger, Didessa, and Dabus on the left bank and Beles and small tributaries Chemoga, Temcha, and Bir on the right bank. Specifically, the research area encompasses 24 nested watersheds within the UBNB: Andit Tid, Anjenie, Selegi, RobiJida, Mugher, Muga, Angreb, Andessa, Chemoga, Fettam, Birr, Megech, Koga, and Robigumero (small), Ribb, Gilgel Abbay, Gudder, Mainbeles, and Gumara (middle), as well as Kessie, Didessa, Dabus, and Tana (large) (Figure 6.1).

The climate in the Upper Blue Nile Basin is predominantly tropical, with a rainy season from June to September and a dry season from October to May. The climate condition of the basin varies spatially with complex topographic influences. Most of the areas have unimodal rainfall patterns and receive the maximum precipitation from June to September. The mean annual rainfall of the

UBNB is 800 to 2200 mm in the range of 2000–2015, and the minimum and maximum temperatures are 11.4^0c °C and 24.7^0c respectively.

The land use and land cover of the basin are varied, ranging from cultivated lands, grasslands, and savannas in the north to dense tropical forests in the southern and eastern regions. The dominant LULC categories found within the upper Blue Nile basin include farmland, grassland, barren terrain, bushland, and woodland. Based on the Water and Land Resource Center (WALRC), the major dominant LULC in this watershed was farmland, which covered 37.47 % of the watershed. Following agricultural land, the woodland, shrub/bushland, grassland, and forest land cover 17.79%,14.73%,12.41% and 10.65%, respectively. The area occupied by Afroalpine is insignificant compared to the total LULC area, accounting for only 0.19%.

The majority of soil types in the basin include lithisols, nitisols, and vertisols. The soils in the basin are typically fertile. The Upper Blue Nile Basin is of critical importance to the economy and livelihoods of Ethiopia, as it supports a large population engaged in agriculture, livestock rearing, and hydropower generation. The basin is a major provider of water resources for irrigation, domestic use, and industrial development in Ethiopia and downstream countries, such as Sudan and Egypt.

The Upper Blue Nile Basin contains several existing and planned dams. The largest of these is the Grand Ethiopian Renaissance Dam (GERD), which is currently under construction on the Blue Nile River in Ethiopia. Another project is the Tana-Beles Hydropower Project, which helps regulate the flow of the Blue Nile and generate electricity for Ethiopia's national grid. The Finchaa Hydropower Project is located on the Finchaa River, a tributary of the Blue Nile. Additionally, the Chara Chara Weir is a small diversion structure situated on the Blue Nile near the outlet of Lake Tana. Beyond the existing dams, there are several other proposed or planned dam projects in the Upper Blue Nile Basin, including the Karadobi, Mandaya, and Border dams. Therefore, the Upper Blue Nile Basin plays a crucial role in water management, hydropower generation, and supporting the energy needs of Ethiopia, as well as having significant implications for the downstream countries that share the Nile River system. The basin's resources and development projects have a substantial impact on the region as a whole.

The raw data, such as climate and hydrology information, was obtained from Ethiopia's meteorological institute and the Ministry of Water and Energy. Twenty-four watersheds were selected for modeling suspended sediment loads (SSL), using a total of 23 climatic, hydrologic,

and physiographic variables (Table 6.1). Furthermore, the suspended sediment concentration is collected from different projects implemented by the Ministry of Water and Energy.

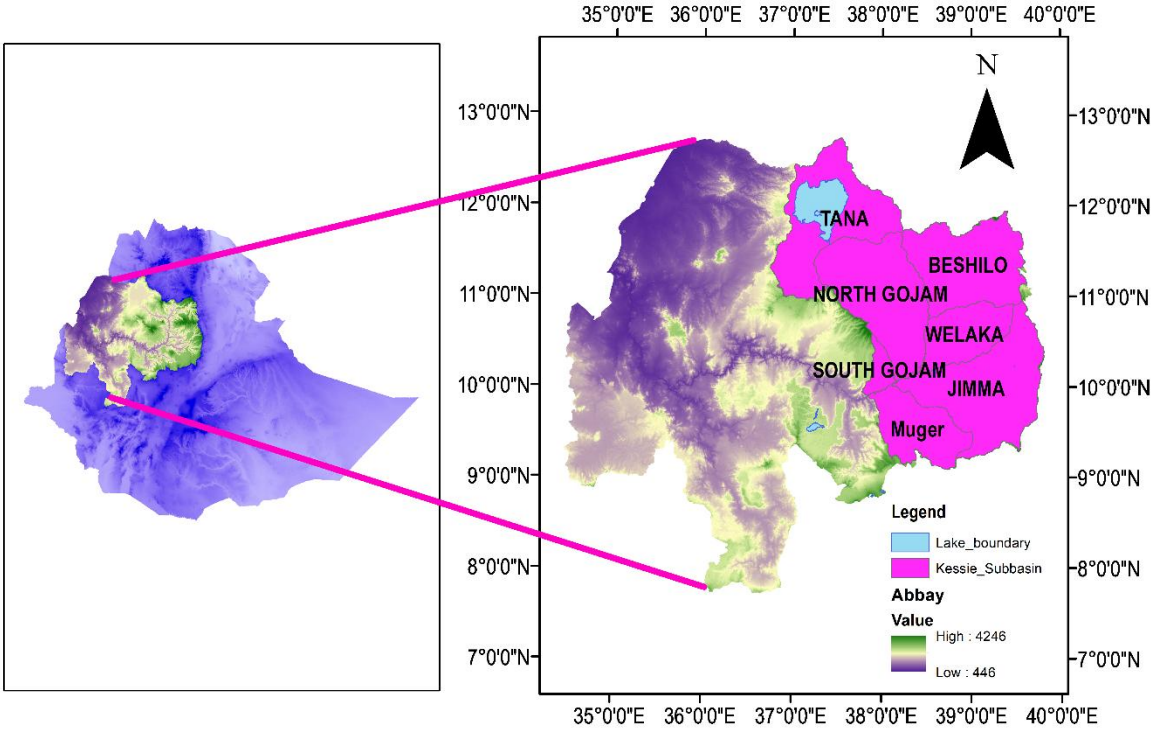

Figure 6-1 Overview study region

Table 6-1 Definitions and characteristics of the variables used for the 24 selected watersheds

No.	Variable	Definition	Unit	Mean	Minimum	Maximum
1	DA	Drainage area	km2	5094.96	1.13	65784.00
2	Qmean	Mean annual discharge	m3/sec	19451.04	8.28	237949.60
3	Pr	Mean annual rainfall	mm	1374.87	1079.50	1834.00
4	SS	Average stream slope	%	0.06	0.00	1.16
5	Sw	Watershed slope	%	0.19	0.01	0.48
6	MCL	Main channel length	km	101.42	3.10	558.02
7	TCL	Total channel length	km	301.30	1.57	1898.48
8	Pw	Watershed perimeter	km	406.13	8.20	2592.67
9	DD	Drainage density	km.km2	0.26	0.03	1.39
10	BR	Basin relief	m	1470.92	374.00	3297.00
11	RN	Ruggedness number		269.70	33.91	686.36

12	SF	Shape factor		0.20	0.08	0.39
13	RR	Relief ratio		30.88	1.74	238.22
14	ER	Elongation ratio		0.49	0.32	0.70
15	CR	Circularity ratio		0.21	0.04	0.46
16	CC	Compactness coefficient		0.19	0.06	0.76
17	LOF	Length of overland flow	km	4.29	0.36	17.33
18	TC	Time concentration	hr	52.68	0.30	416.65
19	AE	Average elevation	m	2349.39	1382.93	3220.89
20	AA	Agricultural Area	%	53.96	28.57	72.60
21	FA	Forest Area	%	10.16	0.40	33.63
22	VI	Vegetation Index		0.23	0.21	0.33

6.2.2 Input variable reduction

Data reduction techniques are essential for identifying the key variables that have a significant impact on sediment load values. Some commonly used approaches for this purpose include Principal Component Analysis (PCA), Classification and Regression Trees (CART), Gamma Test (GT), and Stepwise Regression (SR). These methods are used to reduce the number of variables that significantly influence sediment yield, and they have been applied worldwide (Hess and Hess, 2018),(Vanmaercke et al., 2011), (Mohammadi et al., 2018), and (Singh et al., 2018). To model sediment yield, four types of statistical analysis were performed. These methods used parameter sets that had been reduced from the original 22 variables related to physiography, hydrology, climatology, land use, geology, and soil.

6.2.2.1 Principal component analysis

This study used PCA to identify the primary parameters influencing suspended sediment yield. It is a data reduction approach that aims to extract a smaller number of derived variables from a larger set of source variables. Minimizing the number of variables or factors in a dataset can be a beneficial technique for reducing the overall volume of input data when modeling large datasets. Simplifying the complexity of the input data by limiting the variables can make the modeling process more efficient and practical (Ebrahimi-Khusfi et al., 2021). Additionally, in the present

study, PCA has been used as an initial or preliminary step in the process of developing a predictive model. PCA was employed as an early-stage technique to help prepare the data for the subsequent development of the prediction model (Haan, 2002). The key steps in the PCA process used by (Fernández et al., 2007) are summarized and described below:

1. The initial set of variables selected for the study area included a group of 22 basin characteristics and 1 climate-related factor.
2. The suitability of the data for conducting PCA was evaluated using the Kaiser-Meyer-Olkin (KMO) measure of sampling adequacy (Kaiser, 1974) and Bartlett's test of sphericity. The KMO test examines the ratio of the item correlations to the partial item correlations. If the partial correlations are similar to the raw correlations, it indicates that the variable does not share much variance with the other variables. This is an important criterion, as PCA assumes that common factors are the source of the observed variance in the variables being analyzed. The KMO score ranges from 0.0 to 1.0, but a minimum value of 0.50 is generally considered acceptable for conducting a reliable PCA. Bartlett's test of sphericity is used to examine the hypothesis that the correlation matrix is an identity matrix, which would indicate that all the variables are uncorrelated. The significance value from this test allows us to reject the null hypothesis and conclude that there are correlations present in the dataset that are suitable for conducting Principal Component Analysis (PCA). A Bartlett's test of sphericity score with a significance level of 95% ($p < 0.05$) is considered appropriate for proceeding with the PCA.
3. To determine the dominant factors, a Principal Component Analysis (PCA) with Varimax rotation was performed to identify the principal components (PCs) or subsets within the larger data set. For selecting the dominant factors, the Kaiser's criterion or eigenvalues rule was used, where only components with eigenvalues of 1.0 or greater were retained for further investigation, as described in (Fernández et al., 2007) and other relevant sources (Sharma et al., 2015), and (Andrews et al., 2002).

6.2.2.2 Gamma test

The Gamma Test (GT) is another dimensionality reduction technique, which can be achieved through the use of the winGamma software. To identify the most effective input variables, all the variables are first uploaded to the software. Then, one variable is eliminated from the main set, and the Gamma value of this run is recorded. For the next run, the eliminated variable is added

back to the main set, and the second variable is eliminated. This process is repeated for all the variables, with the Gamma values recorded each time. Finally, the variables with the highest Gamma values, as determined through this elimination procedure, are selected as the input variables. Unlike stepwise regression (SR), classification and regression trees (CART), and principal component analysis (PCA), the Gamma Test (GT) is a nonlinear technique (Moghaddamnia et al., 2009). More detailed methodological and functional descriptions of these techniques were provided in our previous research (Hossein, 2015).

6.2.2.3 Stepwise regression

Stepwise regression (SR) is a general statistical method that combines forward and backward techniques, using a step-by-step algorithm to select the most effective variables based on a linear regression model. After adding all the independent variables one by one, they are sorted according to their correlation coefficients (R) with the output variable. The variables with the optimum R values are then selected as the input variables for the model (Sharma and Yu, 2015).

6.2.2.4 Classification and regression trees

Classification and Regression Tree (CART) models use tree-building algorithms to create a set of if-then rules or split conditions. These rules allow the model to predict outcomes or classify cases into different categories (Razi and Athappilly, 2005). CART was initially developed to handle clinical data due to its ability to simultaneously manage combinations of categorical variables and continuous information, and to search for the best way to split the range of continuous variables into two groups (Leo Breiman, Jerome Friedman, R.A. Olshen, 1984). The tree structure is created by splitting at different points or nodes until the end or leaf node is reached. CART can address both linear and regression problems, and can be used for linear, logistic, and additive logistic models in classification problems. The binary recursive partitioning technique is used to split the sequential data into homogeneous subsets until a certain condition is fulfilled. Each split depends on the value of a specific variable and divides the data into two subsets, generating a binary tree structure. The key features of the CART model construction include the selection of binary splits of the measurement space, the decision to create a node or continue splitting, and the assignment of each terminal node to a class. The classification components involve dependent variables, independent variables, a learning dataset, and a future dataset. The regression components include prior probabilities from each outcome and a cost matrix.

The progress of CART models has been relatively slow in some cases due to the complexity of the analysis. However, these models are effective in understanding complex interactions between predictors, compared to traditional multivariate techniques. CART can handle highly skewed data and categorical data, deal with missing data by using surrogate variables, require little input for analysis, and are relatively straightforward to interpret (Tao et al., 2021).

6.2.3 Sediment yield modeling techniques

Sediment yield modeling is a technique used to estimate the amount of sediment transported from a watershed or catchment area over a given period. This information is crucial for understanding and managing processes related to soil erosion, sedimentation, and water quality.

6.2.3.1 Artificial Neural Network (ANN)

Artificial neural networks (ANNs) are complex models that consist of interconnected nodes (neurons) and their associated connection weights. The fundamental architecture of an ANN includes an input layer, one or more hidden layers, and an output layer. Each of these layers is composed of interconnected neurons. The ANN algorithm works by taking the input data and passing it through the hidden layer neurons, which apply an activation function to produce nonlinear outputs. These hidden neuron outputs are then combined and used to calculate the final outputs in the output layer. In essence, ANNs are powerful "black box" models that can learn and approximate intricate functions without the need for explicit programming. The hidden layers and neurons within the network act as an intermediate representation that enables the ANN to transform the inputs into the desired outputs. ANNs have been the most widely used machine learning models for sediment yield simulation over the past 20 years (Kheirfam and Mokarram-Kashtiban, 2018), (Kamel et al., 2014), (Sokchhay, 2013), and (Heng and Suetsugi, 2014b).

The ANN system often utilizes sigmoid transfer functions, which are connected in a multi-layered structure known as a multilayer perceptron (MLP). This multilayer configuration allows the ANN to capture and model complex nonlinear relationships between the input and output data. It is a type of artificial neural network (ANN) that is the most commonly used classical machine-learning architecture in the field of hydrology (Oyebode and Stretch, 2019). To predict sediment yield, the MLP has been identified as a recommended type of artificial neural network (ANN) architecture (Kişi, 2010), and (Heng and Suetsugi, 2013a). Feed-forward multilayer perceptron (MLP) is a widely used architecture in the field of hydrology research and literature (Zounemat-Kermani et al., 2016). A multilayer perceptron (MLP) consists of three primary layers: an input layer, a hidden

layer, and an output layer. By adding more hidden layers, the network becomes deeper and can extract more complex, higher-order statistical patterns. A three-layer MLP configuration is commonly used in hydrological time series modeling (Nacar et al., 2018).

A typical diagram of a single node (the jth node) in an artificial neural network is shown in Figure 6.2. Depending on the layer location, the series of inputs form an input vector X = (x1, xi, ..., xn). The corresponding series of weights fitted to each input forms a weight vector Wj = (w1j, wij, ..., wnj). The output (Yj) for node j is calculated using the value of a function (f) with the inner product of the input vector (X) and the weight vector (Wj), minus a bias term (bj). The described operation can be expressed mathematically as follows in equation (6.1) (Committee, 2000):

$$Y_j = f\left(X.W_j - b_j\right) \tag{6.1}$$

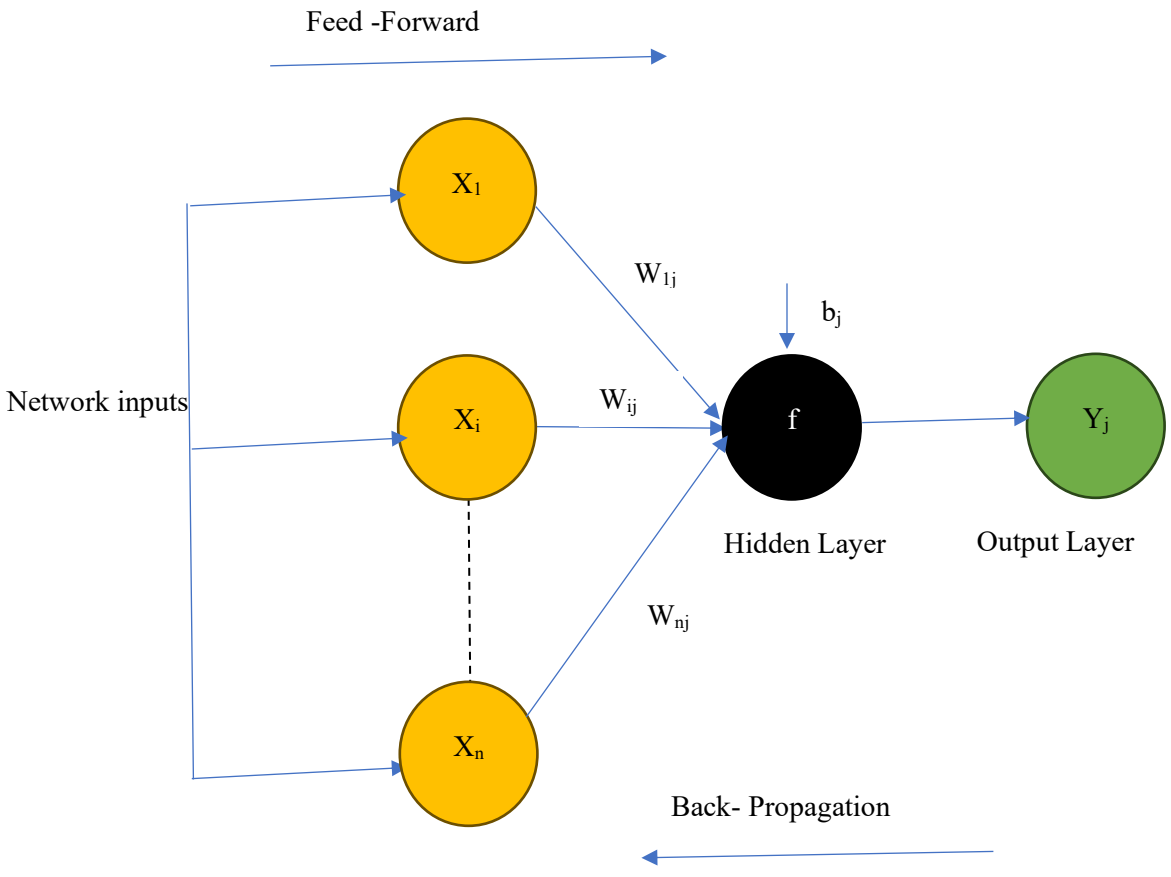

Figure 6-2 : Schematic diagram of MLP for node j

6.2.3.2 Multiple linear regression

Multiple Linear Regression (MLR) is a statistical method that is suitable for modeling the linear relationship between a dependent variable and one or more independent variables, especially when the sample size is small (Razi and Athappilly, 2005). MLR aims to model the relationship between two or more predictor variables and a target or outcome variable. It does this by fitting a linear mathematical equation to the observed data (Leo Breiman, Jerome Friedman, R.A. Olshen, 1984). The regression relationships between sediment yield and the key factors identified through principal component analysis, gamma tests, stepwise regression, and data reduction techniques—specifically biophysical and climate factors—were formulated using Equation (1). To prevent negative lower bounds in the estimates, a logarithmic transformation was applied. The regression coefficients were derived using ordinary least squares linear regression on the logarithmic values of the response and predictor variables. Ultimately, a back-transformed relationship was established in the following form (Equation 6.2).

$$Y = \beta_0 {X_1}^{\beta_1} {X_2}^{\beta_2} {X_3}^{\beta_3} \quad (6.2)$$

Where Y represents the response variable (suspended sediment yield), while X1, X2, …, Xp denote the predictor variables (factors affecting suspended sediment yield). The constants β0, β1, β2, …, βp are obtained through multiple linear regression analysis. The typical method for identifying the optimal regression equation is stepwise linear regression analysis, utilizing an F probability threshold of 0.05 for the chosen factors.

The size of the drainage area plays a crucial role in determining both suspended sediment yield and area-specific suspended sediment yield. However, this relationship is influenced by various factors, including rainfall, vegetation cover, sediment texture, and land use. To assess the impact of these key factors on suspended sediment yield across different basin sizes, regression models were developed using four data groups: (1) 11 sub-basins with drainage areas under 500 km² (small basins); (2) 5 sub-basins with drainage areas between 500 km² and 1000 km² (medium basins); (3) 10 sub-basins with drainage areas over 1000 km² (large basins); and (4) all 26 sub-basins, regardless of their drainage area size.

6.2.4 Model validation

Out of the 37 samples from the selected stations, 30 were utilized to develop the multiple regression model, while the remaining 7 samples were randomly excluded based on drainage area size for model validation. Additionally, the jackknife technique was employed to assess the

validity of the developed regression models. This method involves excluding one sub-basin at a time from the total and then fitting a regression model based on the remaining sub-basins. The suspended sediment yield (SSY) or area-specific suspended sediment yield (ASSY) for the excluded sub-basin was estimated using this test model. This process was repeated for each sub-basin, and the coefficient of determination for the test model was calculated. Furthermore, the Pearson product-moment correlation coefficient was also computed to compare the predicted SSY or ASSY from both the general and test models.

6.2.5 Model performance evaluation

To assess the performance of the regional SLY estimation models, 80% of the watersheds were randomly selected for the calibration (training) phase, while the remaining 20% were allocated for validation (testing). The models were then evaluated using relative error (RE), root mean square error (RMSE), coefficient of determination (R^2), and bias (BIAS) as follows:

$$RE = \frac{1}{N}\sum_{i=1}^{N}\left|\frac{O_{Si} - M_{Si}}{O_{Si}}\right| * 100 \tag{6.3}$$

$$RMSE = \sqrt{\sum_{i=1}^{N}\frac{(O_{Si}-M_{Si})^2}{N}} \tag{6.4}$$

$$R^2 = \frac{\left[\sum_{i=1}^{N}(O_{Si}-O_m)(M_{Si}-M_m)\right]^2}{\sum_{i=1}^{N}(O_{Si}-O_m)^2\sum_{i=1}^{N}(M_{Si}-M_m)^2} \tag{6.5}$$

$$BIAS = \frac{1}{N}\sum_{i=1}^{N} O_{Si} - M_{Si} \tag{6.6}$$

Where Osi and Msi represent the ith observed and estimated mean annual SLY, respectively; Om and Mm denote the average values of Osi and Msi, respectively; and N indicates the total number of observed data points.

6.3 Results and Discussion

6.3.1 The most influential variables on suspended sediment load yield

In this study, the KMO value for the PCA approach was 0.6, and Bartlett's test yielded a significance level of 552.424. These findings indicate that PCA is a suitable method for determining the most effective factors for sediment load yield (SLY) modeling. The PCA analysis revealed that four of the 13 factors were significantly effective, accounting for 89.78% of the variability: DA (57.55%), BS (16.19%), ML (8.27%), and TL (7.77%).

The PCA findings from the correlation matrix analysis using Varimax rotation reveal four main components with eigenvalues exceeding 1.00, accounting for a total cumulative variance of 89.78%. Table 6.2 shows the significance of these variables is ranked based on the size of their eigenvalues.

Table 6.3 displays the different variables analyzed in the PCA, as well as their factor loadings for each principal component. TCL, DA, MCL, BP, SSY, BR, TC, Qmean, and ASSY are the variables having significant loadings (≥ 0.60) on PC1. PC2 includes SF and ER, PC3 includes CR, and PC4 contains BS. From PC1, it was observed that the suspended sediment load is strongly correlated with the drainage basin area and flow of the river. Area-specific sediment yield is proportional to the main channel length, total channel length, and basin perimeter, demonstrating that hydro-morphology has a direct impact on area-specific suspended sediment yield. We selected eleven factors to develop a regression model for estimating suspended and area-specific sediment production. Other studies found that hydrology, morphology, and topographic characteristics were significant variables in determining suspended sediment yield using principal component analysis (Wuttichaikitcharoen and Babel, 2014).

Table 6-2 Principal components (PCs) for basin characteristics and climatic factors

PCs	Eigenvalues	Variances (%)	Cumulative Variances (%)
1	7.48	57.55	57.55
2	2.10	16.19	73.74
3	1.08	8.27	82.01
4	1.01	7.77	89.79
5	0.83	6.39	96.18
6	0.24	1.85	98.03

Table 6-3 Correlation matrix for the selected variables

	DA	BS	ML	TL	BP	BR	SF	ER	CR	TC	AASF	AASED	SSY
DA	1.0	0.1	**0.9**	**0.9**	**1.0**	**0.7**	0.2	0.2	-0.2	**0.9**	**1.0**	**1.0**	**0.6**
BS		1.0	0.1	0.0	0.0	-0.2	-0.2	-0.2	0.1	0.0	0.1	0.1	-0.1
ML			1.0	**0.9**	**1.0**	**0.8**	0.2	0.2	-0.2	**0.9**	**0.9**	**0.8**	0.4

TL	1.0	**1.0**	**0.8**	0.3	0.4	-0.2	**0.8**	**0.9**	**0.8**	0.4
BP		1.0	**0.7**	0.2	0.3	-0.3	**0.9**	**0.9**	**0.8**	0.5
BR			1.0	0.2	0.2	0.0	**0.6**	**0.7**	0.5	0.2
SF				1.0	**1.0**	0.1	0.0	0.2	0.0	0.2
ER					1.0	0.1	0.1	0.2	0.1	0.2
CR						1.0	-0.2	-0.3	-0.2	-0.1
TC							1.0	**0.9**	**0.8**	0.5
AASF								1.0	**1.0**	**0.6**
AASE									1.0	**0.7**
D										
SSY										1.0

Notes: Bold values indicate correlation coefficients above 0.6; Kaiser–Meyer–Olkin measure of sampling adequacy: 0.6; Bartlett's test of sphericity: 552.42;

Along with the PCA, GT analysis was conducted using WinGamma software to identify the influencing variables based on their gamma values. The following variables were selected: AE (Gv = 0.266), RN (Gv = 0.257), MCL (Gv = 0.249), BR (Gv = 0.242), DD (Gv = 0.242), LOF (Gv = 0.242), BS (Gv = 0.241), CC (Gv = 0.240), AA (Gv = 0.240), TCL (Gv = 0.240), RR (Gv = 0.239), Qmean (Gv = 0.238), SS (Gv = 0.236), DA (Gv = 0.234), CR (Gv=0.233), and TC (Gv = 0.232). The topography and geomorphology variables had the highest Wingamma value. We identified fifteen variables as being the most important in influencing suspended sediment load. Similarly, numerous studies have revealed that hydrological and geomorphological elements are significant (Noori et al., 2011).

Besides PCA and GT, CART (Classification and Regression Trees) was employed to identify the significant variables. The selected variables include DA, MCL, TCL, BP, DD, BR, SF, ER, LOF, AE, Pr, and Qmean.

In addition to PCA, CART, and GT, the SR (Stepwise Regression) technique was employed as a linear approach to identify significant variables for modeling SLY in the examined watersheds based on their R^2 results. Using the SR approach, we found climate, hydrology, and geomorphology data that affected suspended sediment production, including TCL, SF, ER, Pr, and Qmean.

6.3.2 Regression analysis to estimate suspended sediment yield

After identifying the key variables using PCA, SR, GT, and CART, stepwise multiple regression analysis was conducted to develop a regional suspended sediment load model. As illustrated above, the selected variables varied across the different methods: PCA, SR, CART, and GT. The Multiple stepwise regression analysis was performed based on the class intervals of watershed areas. Multiple stepwise regression analyses revealed that mean annual flow, overland flow length, time of concentration, average basin elevation, and shape factor were all highly associated with area-specific suspended sediment output and suspended sediment load across all data reduction techniques. This indicated that streamflow, hydro morphology, and catchment characteristics were significant factors influencing suspended sediment yield. For areas under 500 km², elevation watersheds were selected; for the 500-1000 km² range, five watersheds were chosen; and for those above 1000 km², ten watersheds were included. The study area had watersheds ranging from 1.13 km2 to 65,784 km^2 in size. As illustrated in Table 6.4, for watershed areas of less than 500 km², more than 1,000 km², and combined (all), there were no correlations in the area-specific suspended sediment yield with the given factor variables. Whereas, the area-specific suspended sediment output in watersheds ranging from 500 to 1000 km² was significantly correlated with the shape factor and time of concentration. Across all watershed area class intervals, the GT-MLR model combination proved to be the most effective regression model. This suggests that the gamma test data reduction strategy is the most successful for identifying the key parameters that influence suspended sediment yield.

Based on the stepwise regression analysis, the ANOVA shows a significance level of less than 0.001 for all equations using the F-test. However, some cases show no relationships due to statistical insignificance. From the R^2 and the standard error of estimation, it can be concluded that suspended sediment yield (SSY) is more closely related to the selected dominant factors than area-specific suspended sediment yield (ASSY) for all watershed area class intervals. Moreover, across all different watershed areas, predictions for SSY are more accurate than those for ASSY. It indicates that both the small and the large basin areas contribute to the ASSY modeling with additional complexity and uncertainty. Among the different combinations utilizing data reduction methods followed by regression analysis models, the GT-MLR model is strongly correlated and dominates the others.

To investigate the impact of predictor factors on suspended sediment amount, it was discovered that DA, TC, Qmean, LOF, BR, BP, AA, RN, DD, SF, and AE are relevant in estimating SSY. In contrast, TC and SF are relevant for ASSY estimates. Therefore, it was concluded that the main factors influencing suspended sediment levels are basin size, channel network characteristics, topography and slope, land use and vegetation cover, hydrology, geomorphology, and basin steepness. In watersheds under 500 km², hydrology is significantly correlation to suspended sediment yield (SSY), but morphology, channel characteristics, and basin size have less correlation to area-specific suspended sediment yield (ASSY). In medium-sized watersheds (500-1000 km²), time of concentration and geomorphology have a greater impact on ASSY while, drainage size, elevation, hydrology, and agricultural areas, are more sensitive to SSY. In large watersheds, geomorphology, hydrology, drainage size, topography, and channel characteristics have a greater relationship with SSY. Taking into account all data samples (irrespective of basin size), the relationships illustrated in Equations (6.11)and (6.14) reveal noteworthy findings, indicating that the amount of suspended sediment is influenced by topography, streamflow conditions, land use and vegetation cover, and geomorphological factors. (Golshan et al., 2020) found that geomorphology, land use, climate, and geology all have a substantial influence on suspended sediment output in the Garehsoo River basin.

Table 6-4 Regression model at different classes of drainage area

Watershed area class	**No of subbasin**	**Model combination**	**Regression model**	**Equation No.**	**R^2**	**Standard error**
<500 km²	11	PCA-MLR	$SSY=272.270*Qmean^{0.916}$	(1)	0.85	0.584
			No correlation for ASSY			
		GT-MLR	$SSY=2275.097*LOF^{0.690}$	(2)	0.86	0.571
			No correlation for ASSY			
		SR-MLR	$SSY=272.270*Qmean^{0.916}$	(3)	0.85	0.584
			No correlation for ASSY			
		CART-MLR	$SSY=272.270*Qmean^{0.916}$	(4)	0.85	0.584
			No correlation for ASSY			
500-1000	5	PCA-MLR	$SSY=9.16E+10*TC^{-4.24}$	(5)	0.95	0.209
			$ASSY=2E+06*TC^{-4.76}$	(6)	0.94	0.259

km^2		GT-MLR	$SSY=301.301*TC^{-5.234}*AE^{2.92}$	(7)	0.95	0.064
			$ASSY=2E+06*TC^{-4.76}$	(8)	0.94	0.259
		SR-MLR	$SSY=39.719*SF^{-4.165}$	(9)	0.91	0.263
			$ASSY=3.75E-05*SF^{-4.841}$	(10)	0.94	0.260
		CART-MLR	$SSY=9.572*E+17.98*(DA^{-2.765})*(SF^{-0.078})*(BP^{-1.969})*(DD^{0.166})$	(11)	0.95	0.101
			$ASSY= 0.0000375*SF^{-4.841}$	(12)	0.94	0.260
>1000 km^2	10	PCA-MLR	$SSY=0.488652*Qmean^{1.502}$ No correlation for ASSY	(13)	0.65	1.215
		GT-MLR	$SSY=2.0654E-38*Qmean^{0.851}*AE^{31.166}*AA^{-19.862}*BR^{-8.450}*RN^{-0.962}$ No correlation for ASSY	(14)	0.96	0.299
		SR-MLR	$SSY=0.488652*Qmean^{1.502}$ No correlation for ASSY	(15)	0.65	1.215
		CART-MLR	$SSY=0.488652*Qmean^{1.502}$ No correlation for ASSY	(16)	0.65	1.215
All	26	PCA-MLR	$SSY= 154.5254*(Qmean^{0.930})$ No correlation for ASSY	(17)	0.72	0.873
		GT-MLR	$SSY=28.9068*Qmean^{1.755}*LOF^{-0.723}$ No correlation for ASSY	(18)	0.78	0.801
		SR-MLR	$SSY= 154.5254*(Qmean^{0.930})$ No correlation for ASSY	(19)	0.72	0.873
		CART-MLR	$SSY= 154.5254*(Qmean^{0.930})$ No correlation for ASSY	(20)	0.72	0.873
		OR-MLR	$SSY= 28.907*Qmean^{1.855}*LOF^{-0.713}$ No correlation for ASSY	(21)	0.78	0.801

Note: Standard error*: the unit for SSY is tons per year, while for ASSY it is tons per square kilometer per year.

According to Table 6.5 and statistical analysis, the minimum, maximum, average, standard deviation, and coefficient of variation of input data over the calibration period were 1507.1 t/yr, 850431703.3 t/yr, 36639016 t/yr, 173347433 t/yr, and 473.12%, respectively. These statistical criteria can provide important information regarding the accuracy or errors of the presented models.

Table 6-5 Summary statistical values of the MLR model during calibration

Model	Statistics							
	Minimum (t/yr)	Maximum (t/yr)	Average (t/yr)	Standard deviation (t/yr)	Coefficient of variation (%)	R^2	RMSE	MAE
Input	1507.1	850431703.3	36639016	173347433	473.12%			
PCA-MLR	1103.49	15457162.85	1378487.7	3168118.1	229.83%	0.9	293651.7	206581
GT-MLR	1690.18	38082460.65	2416517.4	7684549.1	318%	0.98	264564.2	186082
CART-MLR	1103.49	15457203.86	1378487.7	3168118.1	229.83%	0.9	293652.2	206581
SR-MLR	1103.49	15457203.86	1378491.3	3168126.5	229.83%	0.9	293652.2	206581
OR-MLR	1690.18	38082460.65	2416517.4	7684549.1	318%	0.98	262707.7	187840

6.3.3 Multiple regression model validation

Table 6.6 displays the model validation results for the regression method, which uses the jackknife methodology. Each model combination was cross-validated using the jackknife approach (France et al., 2018). All regression models performed well in validation, although equations 13, 14, 15, and 16 for watersheds larger than 1000 km² had poor performance. Whereas Equations 1, 2, 3, 4, 5, 6, 7, 17, 18, 19, 20, and 21 demonstrated that the calibration and validation results were very similar.

Table 6-6 Results of model validation using the jackknife technique

	R^2		Correlation Coefficient, R,
Equation No.	Calibration	Test Model	between calibration and Test Model
1	0.85	0.86	0.99
2	0.86	0.86	0.999

3	0.85	0.85	0.999
4	0.85	0.85	0.999
5	0.97	0.98	0.99
6	0.96	0.98	0.99
7	0.95	0.95	0.999
8	0.94	0.77	0.81
9	0.91	0.396	0.44
10	0.94	0.398	0.42
11	0.95	0.593	0.62
12	0.94	0.594	0.63
13	0.65	0.18	0.28
14	0.96	0.17	0.17
15	0.65	0.16	0.25
16	0.65	0.16	0.25
17	0.72	0.73	0.99
18	0.78	0.78	0.999
19	0.72	0.72	0.999
20	0.72	0.72	0.999
21	0.78	0.78	0.999

6.3.4 Develop ANN structures

We developed an artificial neural network model after identifying the essential variables using PCA, GT, SR, and CART data reduction methods. Table 6.9 shows the ANN structures for several model combinations depending on area-specific suspended sediment yield and total suspended sediment yield. The configuration showed that the designs vary from each other as a result of differences in factors. The largest variables are included under the Original-ANN combination (ORG-ANN), and the smallest combination is SR-ANN. The largest hidden layer of the ANN structures, as presented below, was 14, and the lowest hidden layer was 8, which showed that they were capable of capturing more complex relationships in the data. Furthermore, the artificial neural network provides a nonlinear combination of dependent and independent variables. The network is supported by a set of interconnected layers of processing elements.

Table 6-7 The model structures using ANN

Model	Observation	ANN Structures
PCA-ANN	SSY	11 input layer nodes, 10 hidden layer nodes, and 1 output layer node
	ASSY	11 input layer nodes, 8 hidden layer nodes, and 1 output layer node
CART-ANN	SSY	12 input layer nodes, 14 hidden layer nodes, and 1 output layer node
	ASSY	12 input layer nodes, 14hidden layer nodes, and 1 output layer node
GT-ANN	SSY	15 input layer nodes, 11 hidden layer nodes, and 1 output layer node
	ASSY	15 input layer nodes, 11hidden layer nodes, and 1 output layer node
SR-ANN	SSY	5 input layer nodes, 12 hidden layer nodes, and 1 output layer node
	ASSY	5 input layer nodes, 10hidden layer nodes, and 1 output layer node
ORG-ANN	SSY	22 input layer nodes, 14hidden layer nodes, and 1 output layer node
	ASSY	22 input layer nodes, 9 hidden layer nodes, and 1 output layer node

6.3.5 Training and testing the ANN model

The training approach for the ANN model is similar to that for calibration. The model performed well throughout training in all combinations. The average statistical values of area-specific suspended sediment yield showed the most significant correlations among the model combinations. Table 6.10 demonstrates the model's effectiveness in relation to these average statistical figures.

Table 6-8 Statistical summary of the ANN model during training

Model	Statistics							
	Minimum (t/yr)	Maximum (t/yr)	Average (t/yr)	Standard deviation (t/yr)	Coefficient of variation (%)	R^2	RMSE	MAE
Input	1507.096	8.5E+08	3663906	1.73E+08	473.12%			
PCA-ANN	104012	2916943	887076	740385.9	83.40%	0.9	24817.9	17390.5
GT-ANN	7712.077	2567126	540805.9	706806.3	130.70%	0.9	13517.1	12090.6
CART-ANN	200984.2	3466704	817510	675740	82.60%	0.9	143.08	20471.9
SR-ANN	325698.8	2960918	539764.2	727542.3	134.78%	0.9	6470.2	4912.24
OR-ANN	-1918.14	2595660	539297.2	712465.5	132.21%	0.9	14147.5	10746.6

Testing the ANN model helps to validate its training. Table 6.9 shows the model's performance and summary statistical values, which indicate strong correlations between the input and different model combinations.

Table 6-9 Statistical summary of the ANN model during testing

Model	Statistics							
	Minimum (t/yr)	Maximum (t/yr)	Average (t/yr)	Standard deviation (t/yr)	Coefficient of variation (%)	R^2	RMSE	MAE
Input	1507	$9x10^8$	36639016	$2x10^8$	473%			
PCA-ANN	-34585	$1x10^6$	431979	$4x10^5$	101%	0.7	255366	215656
GT-ANN	-102482	$3x0^5$	94156	$2x10^5$	189%	0.8	135822	134008

CART-ANN	157275	$1x10^6$	578424	$4x10^5$	73%	0.7	343714	310561
SR-ANN	330248	$6x10^5$	475485	$1x10^5$	20%	0.6	339094	304392
OR-ANN	-77621	$4x10^5$	175146	$2x10^5$	129%	0.6	176329	136193

6.3.6 Develop a regional suspended sedimentation model

After identifying the important factors using PCA, SR, and GT, ANN and MRL were used to generate individual regional models for each dataset. The performance of the developed model was assessed using statistical performance indicators, which also helped to select the most suitable regional sediment load yield model (SLY). The structure of the ANN and MLR model is presented in Table 6.10, and the evaluation results of model performance and statistical values are presented in Table 6.11. According to Table 6.11 and the statistical analysis, the input data for the calibration period had a minimum of 1,507.1 t/yr, a maximum of 850,431,703.3 t/yr, an average of 36,639,016 t/yr, a standard deviation of 173,347,433 t/yr, and a coefficient of variation of 473.12%. These statistical criteria can provide useful information on the accuracy and error of the proposed models. In the calibration period, both the ANN and MLR models could estimate the maximum suspended sediment loads; however, the average value from the two models was lower than the observed value. Furthermore, the ANN model using the original input data failed to estimate low values, as it underestimated the low values of observed SLY. However, when data other than the original input was used, the ANN model accurately forecasted both the minimum and maximum sediment loads. During the validation period, Table 6.12 and the statistical analysis show that the ANN model, which used the original input data, PCA input, and GT input, failed to estimate the lowest value. Compared to the ANN model, the average value of the MLR model is relatively close to the observed average during the calibration period. This showed that a higher number of variables typically leads to increased complexity and potential fluctuation in suspended sediment yield, whereas fewer variables can result in more stable and predictable outcomes. The nature and interactions of the variables involved will determine the specific relationship. In contrast, during the validation period, the average value of the ANN model is quite close to the average observed value. Meanwhile, in ORG-MLR, GT-MLR, PCA-MLR, SR-MLR, and CART-MLR models, the estimated low values of SLY were very close to the observed values. Furthermore, in the original dataset, the MLR model provided the most accurate estimation compared to the ANN model during the calibration period. However, for validation purposes, the ANN model yielded the best estimation for the original dataset. For higher values, the OR-MLR and GT-MLR models provided the most accurate estimations among the models considered. The variables that estimated the suspended sediment values included mean annual flow and the length of overland flow.

Table 6-10 ANN structure and equation in multiple linear regression (MLR) models for estimating regional SLY

Model	ANN structure or and MLR equation
OR-MLR[1]	$SSY= 28.907*Qmean^{1.855}*LOF^{-0.713}$
PCA-MLR[2]	$SSY= 154.5254*(Qmean^{0.930})$
GT-MLR[3]	$SSY=28.9068*Qmean^{1.755}*LOF^{-0.723}$
SR-MLR[4]	$SSY= 154.5254*(Qmean^{0.930})$
CART-MLR[5]	$SSY= 154.5254*(Qmean^{0.930})$
ORG-ANN[6]	22 input layer nodes, 14 hidden layer nodes, and 1 output layer node
PCA-ANN[7]	11 input layer nodes, 10 hidden layer nodes, and 1 output layer node
GT-ANN[8]	15 input layer nodes, 11 hidden layer nodes, and 1 output layer node
SR-ANN[9]	5 input layer nodes, 12 hidden layer nodes, and 1 output layer node
CART-ANN[10]	12 input layer nodes, 14 hidden layer nodes, and 1 output layer node

Note: [1] indicates the original data set as input for MLR, [2] indicates PCA output data set as input for MLR, [3] indicates GT output data set as input for MLR, [4] means SR output data set as input for MLR, [5] indicates CART output data set as input for MLR, [6] means original data set as input for ANN, [7] indicates PCA output data set as input for ANN, [8] indicates GT output data set as input for ANN, [9] means SR output data set as input for ANN, [10] means output CART output data set as input for ANN and SSY means suspended sediment yield (t/year).

Table 6-11 Summary of statistics for regional SLY estimate models during calibration

Model	Statistics							
	Minimum (t/yr)	Maximum (t/yr)	Average (t/yr)	Standard deviation (t/yr)	Coefficient of variation (%)	R^2(%)	RMSE	MAE
Input	1507	$9x10^8$	$4x10^7$	$2x10^8$	473%			
ORG-MLR	1686	$4x10^7$	$3x10^6$	$9x10^6$	315%	98	262708	$2x10^5$
ORG-ANN	404665	$9x10^8$	$5x10^7$	$2x10^8$	415%	90	14148	10747

PCA-MLR	1134	$2x10^7$	$1x10^6$	$3x10^6$	230%	91	293652	$2x10^5$
PCA-ANN	101095	$8x10^6$	$2x10^6$	$2x10^6$	115%	99	24818	17390
GT-MLR	1686	$4x10^7$	$3x10^6$	$9x10^6$	315%	98	264564	$2x10^5$
GT-ANN	129029	$8x10^8$	$6x10^7$	$2x10^8$	370%	99	13517	12091
SR-MLR	417	$6x10^6$	$5x10^5$	$1x10^6$	230%	90	293652	$2x10^5$
SR-ANN	354960	$9x10^8$	$6x10^7$	$2x10^8$	354%	99	6470.2	4912
CART-MLR	417	$6x10^6$	$5x10^5$	$1x10^6$	230%	90	293652	$2x10^5$
CART-ANN	29094	$8x10^6$	$1x0^6$	$2x10^6$	128%	99	143.08	20472

Table 6-12 Summary of statistics for regional SLY estimate models during validation

Model	Statistics							
	Minimum (t/yr)	Maximum (t/yr)	Average (t/yr)	Standard deviation (t/yr)	Coefficient of Dispersion (%)	R^2	RMSE	MAE
Input	15143.7	396530.9	178097	197774	111%			
ORG-MLR	2306.3	1.55E+08	7301414	31430352	430%	30.00	387297	350000
ORG-ANN	21554.7	294990.2	155506	97092	62%	35.00	127095	106874
PCA-MLR	31276.7	269244.3	147654	101712	69%	51.00	331247	337521
PCA-ANN	25370.3	1011753	526172	397560	76%	46.00	328748	269968
GT-MLR	32216.3	1369483	441180	547335	124%	60.00	617790	292859
GT-ANN	23652.7	384566	194822	130800	67%	73.00	69038	40819
SR-MLR	30161.5	266015.6	147758	101357	69%	50.00	178300	156925

SR-ANN	145028.8	248762.5	207725	41696	20%	28.00	133220	117438
CART-MLR	31569.2	254112.9	142078	93825	66%	51.00	143352	133177
CART-ANN	208263.3	1528590	641078	516008	80%	82.00	139944	136036

The evaluation of regional SLY estimating models shown in Tables 6.13 and 6.14 shows that the ANN models outperformed the MLR models during both calibration and validation. Furthermore, ANN models outperformed MLR models in terms of daily SLY estimation (Melesse et al., 2011), (Pektas and Cigizoglu, 2017), (Yadav et al., 2022a), and (Heng and Suetsugi, 2013a). Among the ANN models, the GT-ANN model proved to be the most effective for regional SLY estimation. The R^2, RMSE, and MAE values for the calibration periods were 99.9%, 13,517.11 t/year, and 12,090.76 t/year, while for the validation period, they were 79%, 135,822.4 t/year, and 134,007.8 t/year. Although the PCA-ANN, CART-ANN, and SR-ANN models also yielded acceptable estimation results, the ORG-ANN model faced a significant limitation due to its high input data requirements. According to various research findings (Noori et al., 2011),(Kakaei Lafdani et al., 2013),(Mohammadi et al., 2018), and (Sharifi Garmdareh et al., 2018), preprocessing the most influential input variables improves the accuracy of both black-box and gray-box models, which is consistent with the findings of the current study. Unlike PCA, CART, and SR, the GT approach functioned as a nonlinear evaluator for determining the effectiveness of variables on the dependent (Chang and Heinemann, 2018). As a result, it is well-suited to assessing a high-volatility dataset like SLY.

Figures 5.11–5.12 show the fitting of the estimated and observed SLY values for all models. These findings show that ANN models, particularly those combining GT and PCA approaches, produced the greatest fitting results.

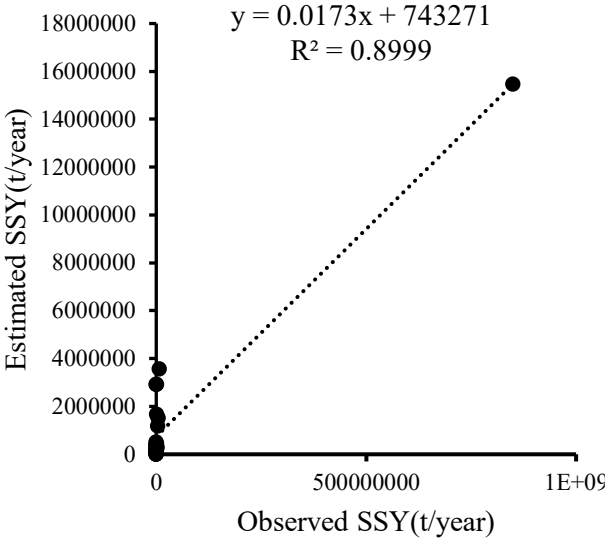

a) CART-MLR

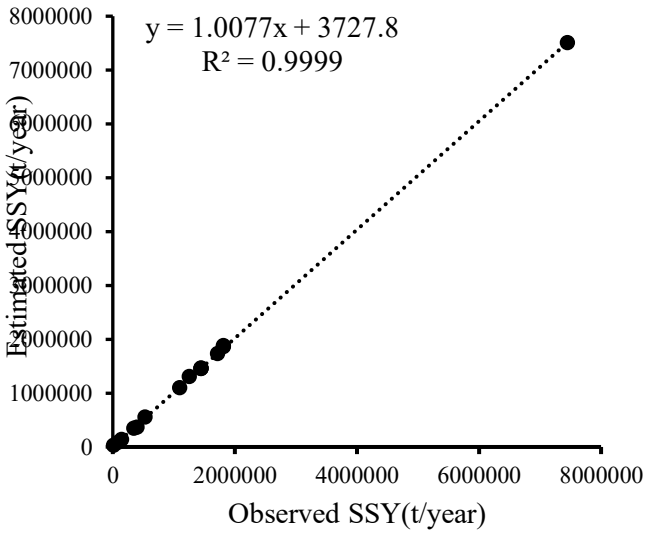

b) CART-ANN

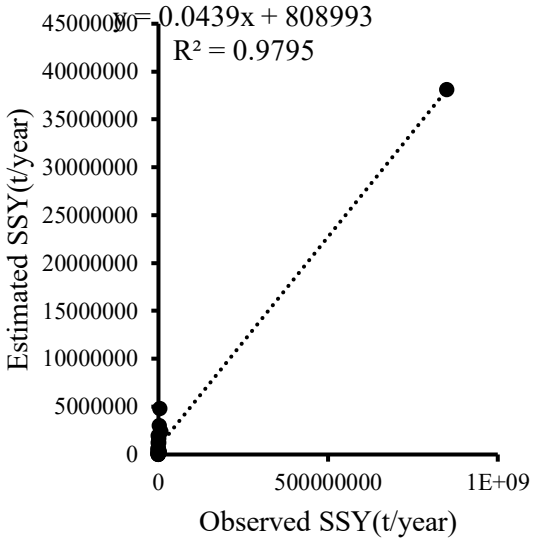

c) GT-MLR

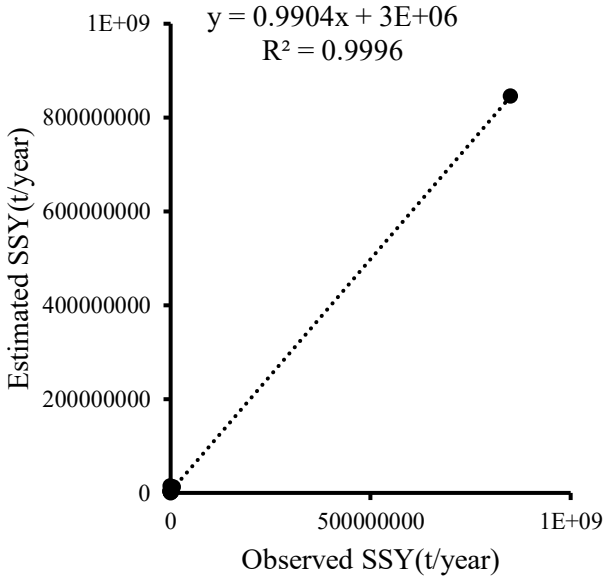

d) GT-ANN

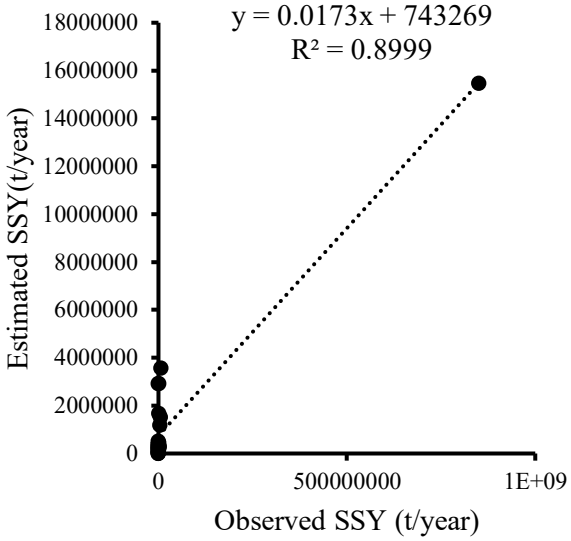

E) PCA-MLR

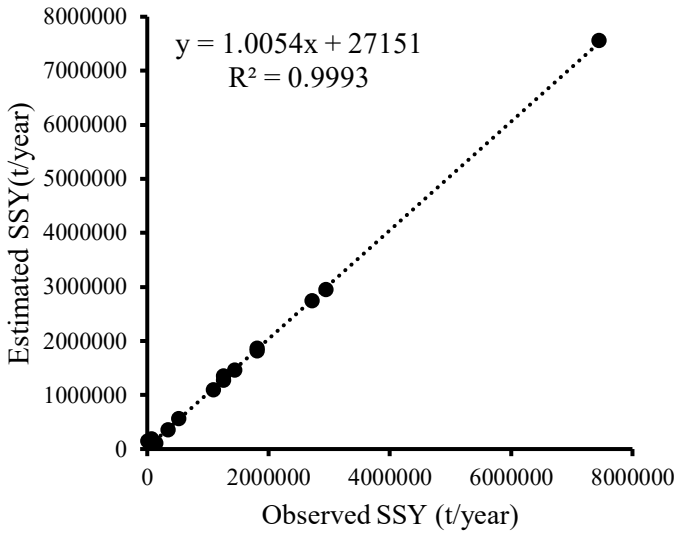

F) PCA-ANN

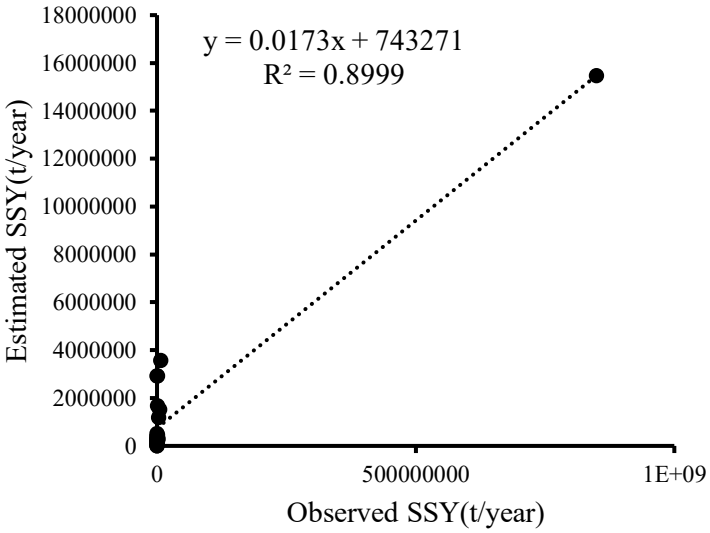

G) SR-MLR

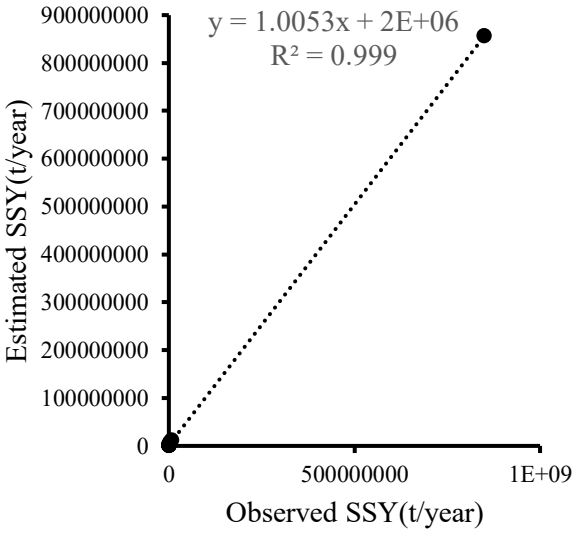

H) SR-ANN

Figure 6-3 Fitting the estimated and observed SLY values using CART-MLR, CART-ANN, GT-MLR, GT-ANN, PCA-MLR, PCA-ANN, SR-MLR, and SR-ANN models during the calibration period

.

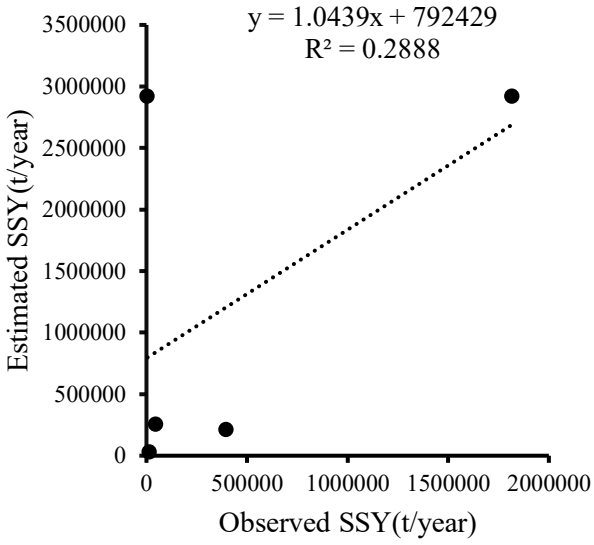

i)CART-MLR

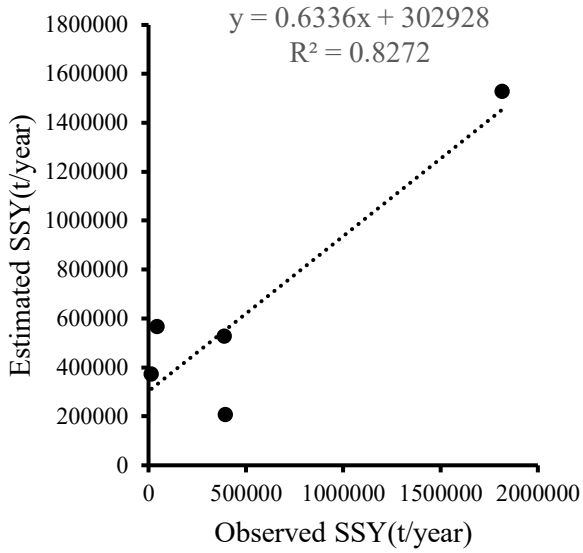

ii) CART-ANN

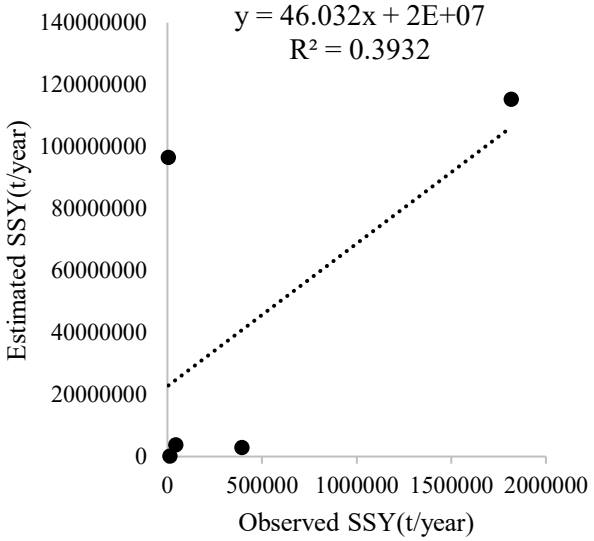

iii) GT-MLR

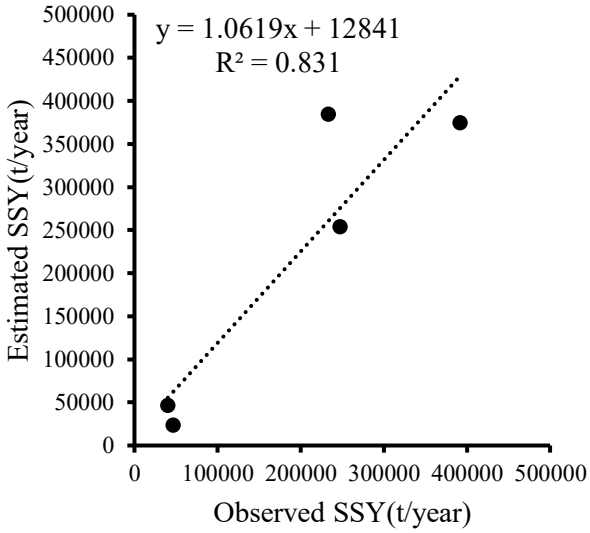

iv) GT-ANN

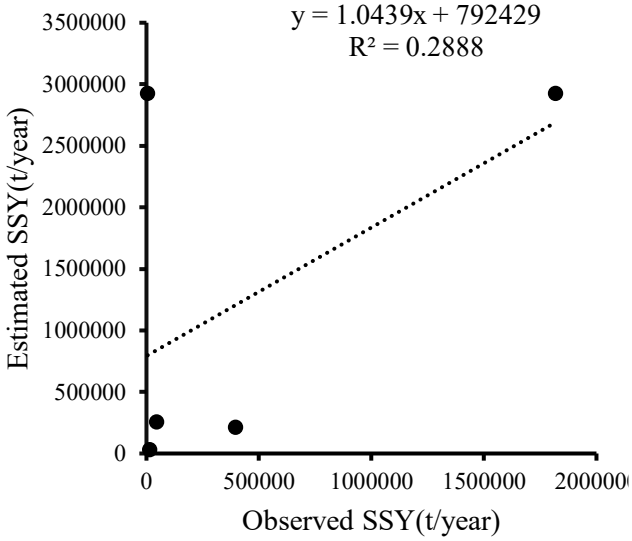

V) PCA-MLR

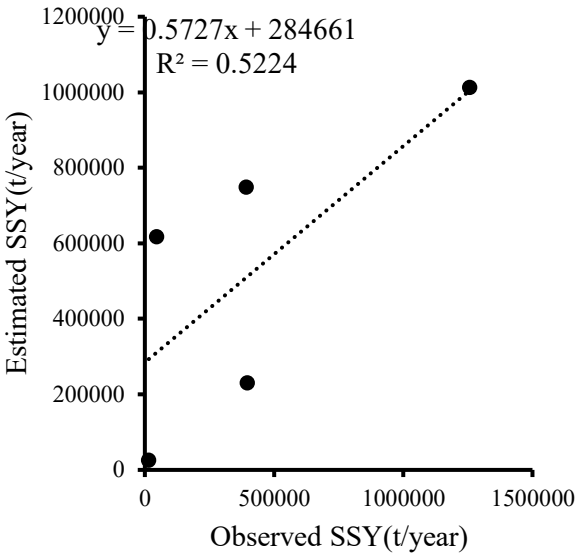

VI) PCA-ANN

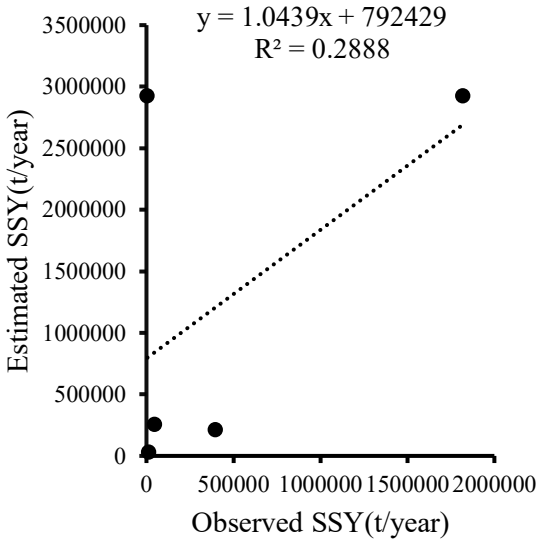

VII) SR-MLR

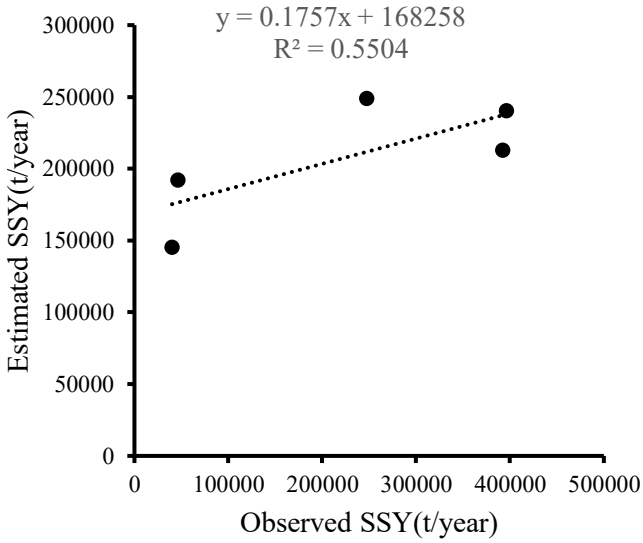

VIII) SR-ANN

Figure 6-4 :Fitting the estimated and observed SLY values using CART-MLR, CART-ANN, GT-MLR, GT-ANN, PCA-MLR, PCA-ANN, SR-MLR, and SR-ANN models during the validation period

6.4 Conclusion and Recommendation

Data reduction techniques (DRT) are essential for simplifying datasets, which serve as the input data for model development intended for estimation purposes. PCA, GT, CART, and SR data reduction techniques were used to identify the important variables influencing suspended sediment output in catchments. As a result, 11, 15, 12, and 5 influential variables were selected from the 22 input variables using PCA, GT, CART, and SR, respectively. According to the four data reduction techniques (DRT), three of the 22 input variables, mean annual flow (Qmean), drainage area (DA), and overland flow length, had the most effect on the determination of suspended sediment yield in the upper Awash and Upper Blue Nile basins. GT outperformed the other data reduction techniques (DRT) in determining the most effective input variables for both the ANN and MLR models used to estimate suspended sediment yield (SSY).

In the MLR analysis, various watershed area class intervals were tested, particularly the 500-1000 km² range, which exhibited the best performance in the regression analysis. Smaller and larger ranges demonstrated low performance. The regression models increased predictability for suspended sediment yield and area-specific sediment yield in basins with drainage sizes of 500-1000 km². Overall, a set of equations was proposed to estimate suspended sediment yield and area-specific suspended sediment yield for basins of various sizes while maintaining an acceptable estimation error range. However, the suspended sediment equation had a correlation with input factors only for watersheds ranging from 500 to 1000 km². The Artificial Neural Network (ANN) model was only applied to the entire watershed; hence, it was not evaluated at different watershed area intervals.

Among the various combinations of multiple linear regression models, the GT-MLR model showed the best performance in estimating suspended sediment yield (SSY). Similarly, the GT-ANN model excelled in the ANN model combinations for estimating suspended sediment yield. Overall, ANN models were more effective than MLR models in SSY estimation. In multiple linear regression analysis, the model result showed that the simulated average value varies from the observed average value. The ANN model demonstrated a comparatively strong relationship with the observed average values. This accuracy stemmed from the iterative training method used, which improved estimations for both individual and overall data sets. Both models were developed to estimate the average annual suspended sediment yield in ungauged catchments. These equations, which are based on easily quantifiable input elements, might help estimate sediment

yield in ungauged basins during the planning and design phases of water and land development projects in Ethiopia's highlands. However, it is crucial to note that the estimation error for suspended sediment is rather significant, owing to difficulties in sediment collection and measurement, particularly during high discharge or flood events, as well as the development of sediment-discharge rating curve equations. As a result, these methods can be regarded as as cost-effective, appropriate, and trustworthy for predicting suspended sediment output in ungauged watersheds. Future research should use monthly and daily input data and investigate additional deep learning models.

7. Conclusion and Recommendation

The overall examination of sediment yield dynamics in Ethiopian watersheds, specifically the Koka Dam and Kessie basins, highlights the paramount interaction between human activities, land use/land cover (LULC) transformation, and inherent geomorphological processes in inducing soil erosion. Agricultural development (7.31%) and urban growth (6.34%) in the Koka Dam catchment over 16 years (2005–2015) significantly altered hydrological processes, leading to an increase in surface runoff by 12.68% and sediment yield by 8.84%, with average annual sediment loading of 28.33 t/ha/yr in 2015. Intensive agriculture and steep slopes (>15%) led to subbasin sediment yield rates of more than 105 t/ha/yr, threatening dam operation and water security. Likewise, in the Kessie watershed, QSWATPLUS modelling revealed subbasins such as 165 with sediment yields as high as 67.6 t/ha/yr, where 42% of the study area is under high risk from erosion-prone slopes and unsustainable agriculture. Such trends portend the susceptibility of Ethiopia's highland ecosystems, where seasonal rainfall regimes compound sediment transport, with 90% of yearly sediment loads in winter months, to further stress water infrastructure and agricultural productivity.

To address these challenges, a multi-faceted approach that blends intensive best management practices (BMPs), robust policy frameworks, and local solutions is critical. Terracing is the best solution, reducing sediment yields by 86–93% in risk-prone locations, particularly in steep slopes and highly cultivated areas. Combined with filter strips (58–60% reduction) and contour farming (64–65% reduction), synergistic reductions in up to 94% sediment are possible, as shown in the Koka watershed. Spatial targeting of these BMPs utilizing QSWATPLUS-generated erosion risk maps is required, with top priority areas being subbasins such as 165 and 269 in Kessie, where sediment yields are disproportionately high. Policy interventions need to impose LULC rules to limit deforestation and urbanization, and encourage sustainable activities by providing subsidies on terracing or tax incentives to farmers who apply agroforestry. In the meantime, the incorporation of erosion risk zoning into national land-use planning can deflect agricultural growth and infrastructure development from risk areas.

Enhancing data infrastructure is also critical; the installation of automated sediment sensors in high-yielding subbasins and during floods will strengthen sediment-discharge rating curves, mitigating current estimation biases from sparse monitoring. Hybrid modeling techniques—

integrating QSWATPLUS for scenario creation and the empirical model (tested in Kessie's data-poor subbasins)—provide an upscaleable strategy for ungauged areas worldwide, e.g., the Himalayan foothills or Andean highlands. Local participation continues to be a success factor: farmer-initiated conservation activities, including participatory field workshops on low-cost stone terracing and agroforestry, alongside education on the economic rewards of sediment reduction (e.g., extended dam life, lower irrigation costs), can promote local ownership. Climate resilience initiatives also need to adjust to seasonal cycles, such as pre-rainy season strengthening of temporary check dams and silt fences to intercept sediment loads during winter and encourage climate-smart crops to minimize runoff pressure.

Future studies need to investigate deep-learning models such as LSTM networks to increase the temporal resolution of sediment predictions and examine sediment-nutrient interactions in an attempt to synchronize erosion control with soil fertility objectives.

References

Abbaspour, K.C., Rouholahnejad, E., Vaghefi, S., Srinivasan, R., Yang, H., Kløve, B., 2015. A continental-scale hydrology and water quality model for Europe: Calibration and uncertainty of a high-resolution large-scale SWAT model. J. Hydrol. 524, 733–752. https://doi.org/10.1016/j.jhydrol.2015.03.027

Abdelwahab, O.M.M., Bingner, R.L., Milillo, F., Gentile, F., 2014. Effectiveness of alternative management scenarios on the sediment load in a Mediterranean agricultural watershed. J. Agric. Eng. 45, 125–136. https://doi.org/10.4081/jae.2014.430

Abebe, T., Gebremariam, B., 2019. Modeling runoff and sediment yield of Kesem dam watershed , Awash basin , Ethiopia. SN Appl. Sci. 1, 1–13. https://doi.org/10.1007/s42452-019-0347-1

Abiye, W., Waltner, I., Kindie, H., 2023. Spatiotemporal dynamics of soil erosion response to land use land cover dynamics and climate variability in Maybar watershed , Awash basin , Ethiopia. Geol. Ecol. Landscapes 00, 1–23. https://doi.org/10.1080/24749508.2023.2256542

Adugna, T.M., Cherie, D.A., 2023. A Review on Reservoirs Sedimenation Problems in Ethiopia A Review on Reservoirs Sedimenation Problems in Ethiopia. https://doi.org/10.9734/ajarr/2021/v15i330372

Aga, A.O., Melesse, A.M., Chane, B., 2020. An alternative empirical model to estimate watershed sediment yield based on hydrology and geomorphology of the basin in data-scarce rift VALLEY lake regions, Ethiopia. Geosci. 10. https://doi.org/10.3390/geosciences10010031

Ahmed, A.A., Haileselassie, A., Denekew Yilma, A., Bashar, K.E., Mccartney, M., Steenhuis, T., Erkossa, T., Shiferaw, Y.S., Easton, Z., 2010. CPWF Project Report Improved water and land management in the Ethiopian highlands and its impact on downstream stakeholders dependent on the Blue Nile Project Number 19 Seleshi Bekele Awulachew (Project Leader) International Water Management Institute Wit.

Alebachew, M., Sewnet, A., 2024. Remote Sensing Applications : Society and Environment Modeling the impact of land use land cover change on the estimation of soil loss and sediment export using InVEST model at the Rib watershed of Upper Blue Nile Basin , Ethiopia. Remote Sens. Appl. Soc. Environ. 34, 101177. https://doi.org/10.1016/j.rsase.2024.101177

Ali, M.G., Ali, S., Arshad, R.H., Nazeer, A., Waqas, M.M., Waseem, M., Aslam, R.A., Cheema, M.J.M., Leta, M.K., Shauket, I., 2021. Estimation of potential soil erosion and sediment yield: A case study of the transboundary chenab river catchment. Water (Switzerland) 13, 1–23. https://doi.org/10.3390/w13243647

Amasi, A., Wynants, M., Blake, W., Mtei, K., 2021. Drivers, impacts and mitigation of increased sedimentation in the hydropower reservoirs of East Africa. Land 10. https://doi.org/10.3390/land10060638

An overview of reservoir sedimentation in some African river basins, 1993. 93–100.

Anamika, Ratwan, P., Dalal, D.S., Magotra, A., 2021. International Journal of Agriculture Extension and Social Development. Int. J. Agric. Ext. Soc. Dev. 7, 34–42.

Andrews, S.S., Mitchell, J.P., Mancinelli, R., Karlen, D.L., Hartz, T.K., Horwath, W.R., Pettygrove, G.S., Scow, K.M., Munk, D.S., 2002. On-farm assessment of soil quality in California's Central Valley. Agron. J. 94, 12–23. https://doi.org/10.2134/agronj2002.0012

Aneseyee, A.B., Elias, E., Soromessa, T., Feyisa, G.L., 2020. Land use/land cover change effect on soil erosion and sediment delivery in the Winike watershed, Omo Gibe Basin, Ethiopia. Sci. Total Environ. 728, 138776. https://doi.org/10.1016/j.scitotenv.2020.138776

Ang, R., Kinouchi, T., Zhao, W., 2023. Sediment load estimation using a novel regionalization sediment-response similarity method for ungauged catchments, Journal of Hydrology. https://doi.org/10.1016/j.jhydrol.2023.129198

Anteneh, Y., Alamirew, T., Zeleke, G., Kassawmar, T., 2023. Modeling runoff - sediment influx responses to alternative BMP interventions in the Gojeb watershed , Ethiopia , using the SWAT hydrological model. Environ. Sci. Pollut. Res. 22816–22834. https://doi.org/10.1007/s11356-022-23711-4

Arnold, J., Srinivasan, R., Muttiah, R., Williams, J.R., 1998. Large area hydrologic modeling and assessment part I: model development. J. Am. Water Resour. Assoc. 34, 73–89.

Arnold, J.G., Bieger, K., White, M.J., Srinivasan, R., Dunbar, J.A., Allen, P.M., 2018. Use of decision tables to simulate management in SWAT+. Water (Switzerland) 10, 1–10. https://doi.org/10.3390/w10060713

Arnold, J.G., Williams, J.R., Maidment, D.R., 1995. Continuous-Time Water and Sediment-Routing Model for Large Basins. J. Hydraul. Eng. 121, 171–183. https://doi.org/10.1061/(asce)0733-9429(1995)121:2(171)

Asselman, N.E.M., 2000. Fitting and interpretation of sediment rating curves. J. Hydrol. 234, 228–248. https://doi.org/10.1016/S0022-1694(00)00253-5

Assfaw, A.T., 2020. Modeling Impact of Land Use Dynamics on Hydrology and Sedimentation of Megech Dam Watershed, Ethiopia. Sci. World J. 2020. https://doi.org/10.1155/2020/6530278

Atieh, Gharabaghi, B., Rudra, R., 2015. Entropy-based neural networks model for flow duration curves at ungauged sites. J. Hydrol. 529, 1007–1020. https://doi.org/10.1016/j.jhydrol.2015.08.068

Atieh, M., Mehltretter, S.L., Gharabaghi, B., Rudra, R., 2015. Integrative neural networks model for prediction of sediment rating curve parameters for ungauged basins. J. Hydrol. 531, 1095–1107. https://doi.org/10.1016/j.jhydrol.2015.11.008

Augusto, C., Santos, G., 2008. No Title 2. https://doi.org/10.4090/juee.2008.v2n1.021027

Aumann, C.A., 2007. A methodology for developing simulation models of complex systems. Ecol. Modell. 202, 385–396. https://doi.org/10.1016/j.ecolmodel.2006.11.005

Awulachew, S.B., Mccartney, M., Steenhuis, T.S., Ahmed, A.A., 2008. A Review of Hydrology , Sediment and Water Resource Use in the Blue Nile Basin, IWMI Working Paper 131.

Awulachew, S.B., Yilma, A.D., Loulseged, M., Loiskandl, W., Ayana, M., Alamirew, T., 2007. Wp123.

Ayele, G.T., Kuriqi, A., Jemberrie, M.A., Saia, S.M., Seka, A.M., Teshale, E.Z., Daba, M.H., Ahmad Bhat, S., Demissie, S.S., Jeong, J., Melesse, A.M., 2021. Sediment yield and reservoir sedimentation in highly dynamic watersheds: The case of koga reservoir, ethiopia. Water (Switzerland) 13, 1–20. https://doi.org/10.3390/w13233374

Ayele, G.T., Teshale, E.Z., Yu, B., Rutherfurd, I.D., Jeong, J., 2017. Streamflow and sediment yield prediction for watershed prioritization in the upper Blue Nile river basin, Ethiopia. Water (Switzerland) 9. https://doi.org/10.3390/w9100782

Bachiller, A.R., Rodríguez, J.L.G., Sánchez, J.C.R., Gómez, D.L., 2019. Specific sediment yield model for reservoirs with medium-sized basins in Spain: An empirical and statistical approach. Sci. Total Environ. 681, 82–101. https://doi.org/10.1016/j.scitotenv.2019.05.029

Bai, J., Shen, Z., Yan, T., 2017. RESEARCH ARTICLE A comparison of single- and multi-site calibration and validation : a case study of SWAT in the Miyun Reservoir watershed , China 11, 592–593. https://doi.org/10.1007/s11707-017-0656-x

Barati, R., 2011. River sus- pended sediment load prediction: Application of ANN and Wavelet conjunction model 16, 946–954. https://doi.org/10.1061/(ASCE)HE

Bashar, K.E., Eltahir, E.O., Fattah, S.A., Ali, A.S., Musnad, M., S, I.O., By, C., Advisor, S., 2010. Nile Basin Reservoir Sedimentation Prediction and Mitigation 49.

Basin, R., 2017. Modelling river suspended sediment load using artificial neural network and multiple linear regression : Vamsadhara River Basin , India.

Basson, G.R., 2009. Sediment Yield Prediction Based on Analytical Methods and Mathematical Modeling 168PP.

Bekele, D., Alamirew, T., Kebede, A., Zeleke, G., Assefa, M., 2018. Land use and land cover dynamics in the Keleta watershed , Awash River basin , Ethiopia 7891. https://doi.org/10.1080/17477891.2018.1561407

Belay, T., Mengistu, D.A., 2019. Land use and land cover dynamics and drivers in the Muga watershed, Upper Blue Nile basin, Ethiopia. Remote Sens. Appl. Soc. Environ. 15, 100249. https://doi.org/10.1016/j.rsase.2019.100249

Betrie, G.D., Mohamed, Y.A., Van Griensven, A., Srinivasan, R., 2011. Sediment management modelling in the Blue Nile Basin using SWAT model. Hydrol. Earth Syst. Sci. 15, 807–818. https://doi.org/10.5194/hess-15-807-2011

Bezak, N., Lebar, K., Bai, Y., Rusjan, S., 2025. Using Machine Learning to Predict Suspended Sediment Transport under Climate Change. Water Resour. Manag.

Bieger, K., Arnold, J.G., Rathjens, H., White, M.J., Bosch, D.D., Allen, P.M., 2019. Representing the Connectivity of Upland Areas to Floodplains and Streams in SWAT+. J. Am. Water Resour. Assoc. 55, 578–590. https://doi.org/10.1111/1752-1688.12728

Bieger, K., Arnold, J.G., Rathjens, H., White, M.J., Bosch, D.D., Allen, P.M., Volk, M., Srinivasan, R., 2017. Introduction to SWAT+, A Completely Restructured Version of the Soil and Water Assessment Tool. J. Am. Water Resour. Assoc. 53, 115–130. https://doi.org/10.1111/1752-1688.12482

Bihonegn, B.G., Awoke, A.G., 2023. Evaluating the impact of land use and land cover changes on sediment yield dynamics in the upper Awash basin, Ethiopia the case of Koka reservoir. Heliyon 9, e23049. https://doi.org/10.1016/j.heliyon.2023.e23049

Billi, P., 2015. Landscapes and landforms of Ethiopia, Choice Reviews Online. https://doi.org/10.5860/choice.192361

Bingner, R.L., Theurer, F.D., Yuan, Y., Taguas, E. V., 2018. AnnAGNPS Technical Process Version 5.5 163.

Bishaw, D., Kedir, Y., 2015. Determining sediment load of Awash River entering into Methara sugarcane irrigation scheme in Ethiopia. J. Environement Earth Sci. 5, 110–117.

Boru, N., Adugna, M., Debele, A., 2022. Ecohydrology & Hydrobiology Impacts of Management Scenarios on Sediment Yield Simulation in Upper and Middle Awash River Basin , Ethiopia. Ecohydrol. Hydrobiol. 22, 269–282. https://doi.org/10.1016/j.ecohyd.2021.11.003

Briak, H., Moussadek, R., Aboumaria, K., Mrabet, R., 2016. International Soil and Water Conservation Research Assessing sediment yield in Kalaya gauged watershed (Northern Morocco) using GIS and SWAT model. Int. Soil Water Conserv. Res. 4, 177–185. https://doi.org/10.1016/j.iswcr.2016.08.002

Buyukyildiz, M., Kumcu, S.Y., 2017. An Estimation of the Suspended Sediment Load Using Adaptive Network Based Fuzzy Inference System, Support Vector Machine and Artificial Neural Network Models. Water Resour. Manag. 31, 1343–1359. https://doi.org/10.1007/s11269-017-1581-1

Calsamiglia, A., Fortesa, J., García-Comendador, J., Lucas-Borja, M.E., Calvo-Cases, A., Estrany, J., 2018. Spatial patterns of sediment connectivity in terraced lands: Anthropogenic controls of catchment sensitivity. L. Degrad. Dev. 29, 1198–1210. https://doi.org/10.1002/ldr.2840

Campos, J.A., Pedrollo, O.C., 2021. A regional ANN-based model to estimate suspended sediment concentrations in ungauged heterogeneous basins. Hydrol. Sci. J. 66, 1222–1232. https://doi.org/10.1080/02626667.2021.1918695

Carter, J., Owens, P.N., Walling, D.E., Leeks, G.J.L., 2003. Fingerprinting suspended sediment sources in a large urban river system. Sci. Total Environ. 314–316, 513–534. https://doi.org/10.1016/S0048-9697(03)00071-8

Chang, F., Heinemann, P.H., 2018. Optimizing prediction of human assessments of dairy odors using input variable selection. Comput. Electron. Agric. 150, 402–410. https://doi.org/10.1016/j.compag.2018.05.017

Chelkeba Tumsa, B., 2023. The Response of Sensitive LULC Changes to Runoff and Sediment Yield in a Semihumid Urban Watershed of the Upper Awash Subbasin Using the SWAT+ Model, Oromia, Ethiopia. Appl. Environ. Soil Sci. 2023. https://doi.org/10.1155/2023/6856144

Chen, Y., Song, L., Liu, Y., Yang, L., Li, D., 2020. A review of the artificial neural network models for water quality prediction. Appl. Sci. 10. https://doi.org/10.3390/app10175776

Choto, M., Fetene, A., 2019. Impacts of land use/land cover change on stream flow and sediment yield of Gojeb watershed, Omo-Gibe basin, Ethiopia. Remote Sens. Appl. Soc. Environ. 14, 84–99. https://doi.org/10.1016/j.rsase.2019.01.003

Cigizoglu, H.K., 2005. Application of Generalized Regression Neural Networks to Intermittent Flow Forecasting and Estimation. J. Hydrol. Eng. 10, 336–341. https://doi.org/10.1061/(asce)1084-0699(2005)10:4(336)

Cigizoglu, H.K., 2004. Estimation and forecasting of daily suspended sediment data by multi-layer perceptrons. Adv. Water Resour. 27, 185–195. https://doi.org/10.1016/j.advwatres.2003.10.003

Committee, A.., 2000. Application of Artificial Neural Networks in Hydrology 1. J. Hydrol. Eng. 5, 115–123.

Contador L.F.J., Schnabel S., G.G.A. and F.P.., 2009. Mapping Sensitivity To Land Degradation in. L. Degrad. Dev. 144, 129–144. https://doi.org/10.1002/ldr

Cooper, M., 2010. Advanced Bash-Scripting Guide An in-depth exploration of the art of shell scripting Table of Contents. Okt 2005 Abrufbar uber httpwww tldp orgLDPabsabsguide pdf Zugriff 1112 2005 2274, 2267–2274. https://doi.org/10.1002/hyp

Daba, M.H., 2018. Sensitivity of SWAT simulated runoff to temperature and rainfall in the Upper Awash Sab-Basin, Ethiopia. Hydrol. Curr. Res. 9, 1–7.

Daba, M.H., You, S., 2022. Quantitatively Assessing the Future Land-Use/Land-Cover Changes and Their Driving Factors in the Upper Stream of the Awash River Based on the CA–Markov Model and Their Implications for Water Resources Management. Sustain. 14. https://doi.org/10.3390/su14031538

Daba, M.H., You, S., 2020. Assessment of climate change impacts on river flow regimes in the

upstream of awash basin, ethiopia: Based on ipcc fifth assessment report (ar5) climate change scenarios. Hydrology 7, 1–22. https://doi.org/10.3390/hydrology7040098
Daliakopoulos, I.N., Coulibaly, P., Tsanis, I.K., 2005. Groundwater level forecasting using artificial neural networks. J. Hydrol. 309, 229–240. https://doi.org/10.1016/j.jhydrol.2004.12.001
Devi, R., 2008. Assessment of siltation and nutrient enrichment of Gilgel Gibe dam , Southwest Ethiopia 99, 975–979. https://doi.org/10.1016/j.biortech.2007.03.013
Dibaba, W.T., Demissie, T.A., Miegel, K., 2021. Evaluation of Best Management Practices in Highland Ethiopia , Finchaa Catchment.
Dile, Y.T., Berndtsson, R., Setegn, S.G., 2013. Hydrological Response to Climate Change for Gilgel Abay River, in the Lake Tana Basin - Upper Blue Nile Basin of Ethiopia. PLoS One 8, 12–17. https://doi.org/10.1371/journal.pone.0079296
Documentation, T., 2009. Soil & Water Assessment Tool Theoretical Documentation Version 2009.
Duru, U. (Department of G.-C.S.U., 2015. Modeling Sediment Yield and Deposition Using the Swat Model :
Dutta, S., Sen, D., 2018. Application of SWAT model for predicting soil erosion and sediment yield. Sustain. Water Resour. Manag. 4, 447–468. https://doi.org/10.1007/s40899-017-0127-2
E., H., M., A., 2012. The Impact of Land Use Change on the Hydrology of the Angereb Watershed, Ethiopia. Int. J. Water Sci. 1. https://doi.org/10.5772/56266
Easton, Z.M., Fuka, D.R., White, E.D., Collick, A.S., Biruk Ashagre, B., McCartney, M., Awulachew, S.B., Ahmed, A.A., Steenhuis, T.S., 2010. A multi basin SWAT model analysis of runoff and sedimentation in the Blue Nile, Ethiopia. Hydrol. Earth Syst. Sci. 14, 1827–1841. https://doi.org/10.5194/hess-14-1827-2010
Ebrahimi-Khusfi, Z., Taghizadeh-Mehrjardi, R., Mirakbari, M., 2021. Evaluation of machine learning models for predicting the temporal variations of dust storm index in arid regions of Iran. Atmos. Pollut. Res. 12, 134–147. https://doi.org/10.1016/j.apr.2020.08.029
Edossa, D.C., Babel, M.S., Gupta, A. Das, 2010. Drought analysis in the Awash River Basin, Ethiopia. Water Resour. Manag. 24, 1441–1460. https://doi.org/10.1007/s11269-009-9508-0
El-Sayed, M.E.M., Zumwalt, K.W., 1991. Comparison of two different approaches for making design sensitivity analysis an integrated part of finite element analysis. Struct. Optim. 3, 149–156. https://doi.org/10.1007/BF01743071
Endalew, L., Mulu, A., 2022. Estimation of reservoir sedimentation using bathymetry survey at Shumburit earth dam, East Gojjam zone Amhara region, Ethiopia. Heliyon 8, e11819. https://doi.org/10.1016/j.heliyon.2022.e11819
Ermias, A., Solomon, A., Ejerta, A., 2014. Small-scale reservoir sedimentation rate analysis for a reliable estimation of irrigation schemes economic lifetime (A case study of Adigudom area, Tigray, northern Ethiopia. ResearchGate 1–10.
Farhan, Y., Nawaiseh, S., 2015. Spatial assessment of soil erosion risk using RUSLE and GIS techniques. Environ. Earth Sci. 74, 4649–4669. https://doi.org/10.1007/s12665-015-4430-7
Fazzini, M., Bisci, C., Billi, P., 2015. The Climate of Ethiopia. World Geomorphol. Landscapes 65–87. https://doi.org/10.1007/978-94-017-8026-1
Fenta Mekonnen, D., Disse, M., 2018. Analyzing the future climate change of Upper Blue Nile River basin using statistical downscaling techniques. Hydrol. Earth Syst. Sci. 22, 2391–

2408. https://doi.org/10.5194/hess-22-2391-2018
Ferdowsi, A., Piadeh, F., Behzadian, K., Mousavi, S.-F., Ehteram, M., 2024. Urban water infrastructure: A critical review on climate change impacts and adaptation strategies. Urban Clim. 58, 102132. https://doi.org/10.1016/j.uclim.2024.102132
Ferguson, R.I., 1986. L = forCQ dt. Water Resour. 22, 74–76.
Fernández, C., Vega, J.A., Fonturbel, T., Pérez-Gorostiaga, P., Jiménez, E., Madrigal, J., 2007. Effects of Wildfire , Salvage Logging and Slash. L. Degrad. Dev. 607, 591–607. https://doi.org/10.1002/ldr
Feyissa Negewo, T., Kumar Sarma, A., 2021. Spatial and temporal variability evaluation of sediment yield and sub-basins/hydrologic response units prioritization on Genale Basin, Ethiopia. J. Hydrol. 603, 127190. https://doi.org/10.1016/j.jhydrol.2021.127190
France, S.L., Sharif Vaghefi, M., Batchelder, W.H., 2018. FlexCCT: A Methodological Framework and Software for Ratings Analysis and Wisdom of the Crowd Applications. IEEE Trans. Comput. Soc. Syst. 5, 358–370. https://doi.org/10.1109/TCSS.2018.2798624
Francke, T., López-Tarazón, J.A., Schröder, B., 2008. Estimation of suspended sediment concentration and yield using linear models, random forests and quantile regression forests. Hydrol. Process. 22, 4892–4904. https://doi.org/10.1002/hyp.7110
Gashaw, T., Dile, Y.T., Worqlul, A.W., Bantider, A., Zeleke, G., Bewket, W., Alamirew, T., 2021. Evaluating the Effectiveness of Best Management Practices On Soil Erosion Reduction Using the SWAT Model: for the Case of Gumara Watershed, Abbay (Upper Blue Nile) Basin. Environ. Manage. 68, 240–261. https://doi.org/10.1007/s00267-021-01492-9
Gashaw, T., Tulu, T., Argaw, M., Worqlul, A.W., 2017. Evaluation and prediction of land use/land cover changes in the Andassa watershed, Blue Nile Basin, Ethiopia. Environ. Syst. Res. 6. https://doi.org/10.1186/s40068-017-0094-5
Gashaw, T., Worqlul, A.W., Dile, Y.T., Addisu, S., Bantider, A., Zeleke, G., 2020. Evaluating potential impacts of land management practices on soil erosion in the Gilgel Abay watershed, upper Blue Nile basin. Heliyon 6, e04777. https://doi.org/10.1016/j.heliyon.2020.e04777
Gelagay, H.S., 2016. RUSLE and SDR Model Based Sediment Yield Assessment in a GIS and Remote Sensing Environment; A Case Study of Koga Watershed, Upper Blue Nile Basin, Ethiopia. J. Waste Water Treat. Anal. 7. https://doi.org/10.4172/2157-7587.1000239
Gessesse, B., Bewket, W., Bräuning, A., 2015. Model-Based Characterization and Monitoring of Runoff and Soil Erosion in Response to Land Use/land Cover Changes in the Modjo Watershed, Ethiopia. L. Degrad. Dev. 26, 711–724. https://doi.org/10.1002/ldr.2276
Getachew, H.E., Melesse, A.M., 2012. International Journal of Water Sciences. Int. J. Water Sci.
Goaba, G.B., 2022. Sediment Yield Estimation and Identifying the Soil Erosion Prone Areas in Koysha Dam Watershed of Omo-Gibe Basin. Civ. Environ. Res. 14, 1–14. https://doi.org/10.7176/cer/14-2-01
Golshan, M., Kavian, A., Esmali, A., Ziegler, A.D., 2020. Runoff and sediment yield modeling in data-sparse catchments in the Garehsoo River basin, northern Iran. Environ. Earth Sci. 79. https://doi.org/10.1007/s12665-020-09084-2
Guideline, A., 2005. Community Based Participatory Watershed Development A Guideline.
Gull, S., Shah, S.R., 2022. Hydrological modeling for streamflow and sediment yield simulation using the SWAT model in a forest-dominated watershed of north-eastern Himalayas of Kashmir Valley, India. J. Hydroinformatics 00, 1–16. https://doi.org/10.2166/hydro.2022.042

Gupta, H.V., Sorooshian, S., Yapo, P.O., 1999. Status of Automatic Calibration for Hydrologic Models: Comparison with Multilevel Expert Calibration. J. Hydrol. Eng. 4, 135–143. https://doi.org/10.1061/(asce)1084-0699(1999)4:2(135)

Gwapedza, D., Hughes, D.A., Slaughter, A.R., Mantel, S.K., 2023. Simulating daily sediment transport using the Water Quality and Sediment Model (WQSED). Model. Earth Syst. Environ. 9, 3759–3775. https://doi.org/10.1007/s40808-023-01726-1

Gwapedza, D., Nyamela, N., Hughes, D.A., Slaughter, A.R., Mantel, S.K., van der Waal, B., 2021. Prediction of sediment yield of the Inxu River catchment (South Africa) using the MUSLE. Int. Soil Water Conserv. Res. 9, 37–48. https://doi.org/10.1016/j.iswcr.2020.10.003

Haan, C.T., 2002. Statistical methods in hydrology. lowa State Press 2nd ed.

Haddadchi, A., Movahedi, N., Vahidi, E., Omid, M.H., Dehghani, A.A., 2013. Evaluation of suspended load transport rate using transport formulas and artificial neural network models (Case study: Chelchay Catchment). J. Hydrodyn. 25, 459–470. https://doi.org/10.1016/S1001-6058(11)60385-6

Hailemariam, K., 1999. Impact of climate change on the water resources of Awash River Basin, Ethiopia. Clim. Res. 12, 91–96. https://doi.org/10.3354/cr012091

Hailu Estifanos, T., Gebremariam, B., 2019. Modeling-impact of Land Use/Cover Change on Sediment Yield (Case Study on Omo-gibe Basin, Gilgel Gibe III Watershed, Ethiopia). Am. J. Mod. Energy 5, 84. https://doi.org/10.11648/j.ajme.20190506.11

Hamel, P., Falinski, K., Sharp, R., Auerbach, D.A., Sánchez-canales, M., Dennedy-frank, P.J., 2016. Science of the Total Environment Sediment delivery modeling in practice : Comparing the effects of watershed characteristics and data resolution across hydroclimatic regions. Sci. Total Environ. https://doi.org/10.1016/j.scitotenv.2016.12.103

Haque, M.B., Karmakar, S., Datta, S., Sajid, A.P., Mamun, M.M.A. Al, Hoque, M.E., Hossain, M.M., Alam, M.S., 2024. Discharge and sediment load modeling using rating curve-based missing data management. Hydrol. Res. 55, 959–975. https://doi.org/10.2166/nh.2024.165

Hard, E., Zy, R., Hiroshi, I., Kazuyoshi, S., Jun, M., 2024. Uncorrected Proof Multi-gauge calibration comparison for simulating stream fl ow across the Major River Uncorrected Proof 00. https://doi.org/10.2166/nh.2024.188

Haregeweyn et al., 2008. Sediment yield variability in Northern Ethiopia: A quantitative analysis of its controlling factors. Catena 75, 65–76. https://doi.org/10.1016/j.catena.2008.04.011

Haregeweyn, N., Melesse, B., Tsunekawa, A., Tsubo, M., Meshesha, D., Balana, B.B., 2012a. Reservoir sedimentation and its mitigating strategies: A case study of Angereb reservoir (NW Ethiopia). J. Soils Sediments 12, 291–305. https://doi.org/10.1007/s11368-011-0447-z

Haregeweyn, N., Melesse, B., Tsunekawa, A., Tsubo, M., Meshesha, D., Balana, B.B., 2012b. Reservoir sedimentation and its mitigating strategies: a case study of Angereb reservoir (NW Ethiopia). J. Soils Sediments 12, 291–305. https://doi.org/10.1007/s11368-011-0447-z

Haregeweyn, N., Nyssen, J., Poesen, J., Schu, B., 2015a. Soil erosion and conservation in Ethiopia : A review. https://doi.org/10.1177/0309133315598725

Haregeweyn, N., Poesen, J., Nyssen, J., De Wit, J., Haile, M., Govers, G., Deckers, S., 2006. Reservoirs in Tigray (Northern Ethiopia): Characteristics and sediment deposition problems. L. Degrad. Dev. 17, 211–230. https://doi.org/10.1002/ldr.698

Haregeweyn, N., Poesen, J., Nyssen, J., Govers, G., Verstraeten, G., de Vente, J., Deckers, J., Moeyersons, J., Haile, M., 2008. Sediment yield variability in Northern Ethiopia: A quantitative analysis of its controlling factors. Catena 75, 65–76.

https://doi.org/10.1016/j.catena.2008.04.011
Haregeweyn, N., Poesen, J., Tsunekawa, A., Tsubo, M., Nyssen, J., Deckers, J., Meshesha, D., 2013. Reservoir sedimentation and its mitigation strategies : a case study of the Ethiopian highlands 1–8.
Haregeweyn, N., Tsunekawa, A., Poesen, J., Tsubo, M., Nyssen, J., Vanmaercke, M., Zenebe, A., Meshesha, D.T., Adgo, E., 2015b. Reservoir sedimentation Channel stabilization 227–238. https://doi.org/10.1007/978-94-017-8026-1
Haregeweyn, N., Tsunekawa, A., Poesen, J., Tsubo, M., Tsegaye, D., Almaw, A., Nyssen, J., Adgo, E., 2017. Science of the Total Environment Comprehensive assessment of soil erosion risk for better land use planning in river basins : Case study of the Upper Blue Nile River. Sci. Total Environ. 574, 95–108. https://doi.org/10.1016/j.scitotenv.2016.09.019
Hathaway, T., 2008. What Cost Ethiopia ' s Dam Boom ? Int. Rivers 26.
Hayicho, H., Alemu, M., Kedir, H., 2019. Assessment of Land-Use and Land Cover Change Effect on Melka Wakena Hydropower Dam in Melka Wakena Catchment of Sub-Upper Wabe-Shebelle Watershed, South Eastern Ethiopia. Agric. Sci. 10, 819–840. https://doi.org/10.4236/as.2019.106063
Heng, S., Suetsugi, T., 2015. Regionalization of sediment rating curve for sediment yield prediction in ungauged catchments Sokchhay Heng and Tadashi Suetsugi 26–39. https://doi.org/10.2166/nh.2013.090
Heng, S., Suetsugi, T., 2014a. Comparison of regionalization approaches in parameterizing sediment rating curve in ungauged catchments for subsequent instantaneous sediment yield prediction. J. Hydrol. 512, 240–253. https://doi.org/10.1016/j.jhydrol.2014.03.003
Heng, S., Suetsugi, T., 2014b. Development of a regional model for catchment-scale suspended sediment yield estimation in ungauged rivers of the Lower Mekong Basin. Geoderma 235–236, 334–346. https://doi.org/10.1016/j.geoderma.2014.07.030
Heng, S., Suetsugi, T., 2013a. Using Artificial Neural Network to Estimate Sediment Load in Ungauged Catchments of the Tonle Sap River Basin, Cambodia. J. Water Resour. Prot. 05, 111–123. https://doi.org/10.4236/jwarp.2013.52013
Heng, S., Suetsugi, T., 2013b. An approach to the model use for measuring Suspended Sediment Yield in ungauged catchments. Am. J. Environ. Sci. 9, 367–376. https://doi.org/10.3844/ajessp.2013.367.376
Hess, A.S., Hess, J.R., 2018. Principal component analysis. Transfusion 58, 1580–1582. https://doi.org/10.1111/trf.14639
Hordofa, A.T., Leta, O.T., Alamirew, T., Chukalla, A.D., 2023. Climate Change Impacts on Blue and Green Water of Meki River Sub-Basin. Water Resour. Manag. 37, 2835–2851. https://doi.org/10.1007/s11269-023-03490-4
Horton, R.E., 1955. Erosional development of streams and their drainage basins, hydrophysical approach to quantitative morphology. Nihon Ringakkai Shi/Journal Japanese For. Soc. 37, 555–558. https://doi.org/10.1130/0016-7606(1945)56
Hossein, K. et al., 2015. Assessment of some homogeneous methods for the regional analysis of suspended sediment yield in the south and southeast of the Caspian Sea. J. Earth Syst. Sci. 124, 1247–1263. https://doi.org/10.1007/s12040-015-0604-7
Houghton-Carr, H., Matt, F.R.Y., 2006. The decline of hydrological data collection for development of integrated water resource management tools in Southern Africa. IAHS-AISH Publ. 51–55.
Hurni, H., Tato, K., Zeleke, G., 2005. The implications of changes in population, land use, and

land management for surface runoff in the Upper Nile Basin Area of Ethiopia. Mt. Res. Dev. 25, 147–154. https://doi.org/10.1659/0276-4741(2005)025[0147:TIOCIP]2.0.CO;2
Hurni, K., Zeleke, G., Kassie, M., Tegegne, B., Kassawmar, T., Teferi, E., Moges, A., Tadesse, D., Ahmed, M., Degu, Y., Kebebew, Z., Hodel, E., Amdihun, A., Mekuriaw, A., Debele, B., Deichert, G., Hurni, H., 2015. The Economics of Land Degradation. Ethiopia Case Study. Soil Degradation and Sustainable Land Management in the Rainfed Agricultural Areas of Ethiopia: An Assessment of the Economic Implications. Rep. Econ. L. Degrad. Initiat. 94.
Jackisch, C., Zehe, E., Samaniego, L., Singh, A.K., 2014. Expérience de jaugeage d'un bassin versant non jaugé: évaluation rapide des données et modélisation éco-hydrologique dans un bassin versant rural pauvre en données. Hydrol. Sci. J. 59, 2103–2125. https://doi.org/10.1080/02626667.2013.870662
Jilo, N.B., Gebremariam, B., Harka, A.E., Woldemariam, G.W., Behulu, F., 2019. Evaluation of the Impacts of Climate Change on Sediment Yield from the Logiya Watershed, Lower Awash Basin, Ethiopia. Hydrology 6, 81. https://doi.org/10.3390/hydrology6030081
Kaiser, H.F., 1974. An index of factorial simplicity. Psychometrika 39, 31–36. https://doi.org/10.1007/BF02291575
Kakaei Lafdani, E., Moghaddam Nia, A., Ahmadi, A., 2013. Daily suspended sediment load prediction using artificial neural networks and support vector machines. J. Hydrol. 478, 50–62. https://doi.org/10.1016/j.jhydrol.2012.11.048
Kamel, K., Mahmoud, T., Le Bissonnais, Y., Mahmoud, T., 2014. Assessment of the artificial neural networks to geomorphic modelling of sediment yield for ungauged catchments, Algeria. J. Urban Environ. Eng. 8, 175–185. https://doi.org/10.4090/juee.2014.v8n2.175185
Kefay, T., Abdisa, T., Tumsa, B.C., 2022. Prioritization of Susceptible Watershed to Sediment Yield and Evaluation of Best Management Practice: A Case Study of Awata River, Southern Ethiopia. Appl. Environ. Soil Sci. 2022. https://doi.org/10.1155/2022/1460945
Keshtegar, B., Piri, J., Hussan, W.U., Ikram, K., Yaseen, M., Kisi, O., Adnan, R.M., Adnan, M., Waseem, M., 2023. Prediction of Sediment Yields Using a Data-Driven Radial M5 Tree Model. Water.
Kheirfam, H., Mokarram-Kashtiban, S., 2018. A regional suspended load yield estimation model for ungauged watersheds. Water Sci. Eng. 11, 328–337. https://doi.org/10.1016/j.wse.2018.09.008
Kidane, M., Bezie, A., Kesete, N., Tolessa, T., 2019. The impact of land use and land cover (LULC) dynamics on soil erosion and sediment yield in Ethiopia. Heliyon 5, e02981. https://doi.org/10.1016/j.heliyon.2019.e02981
Kisi, 2008. Constructing neural network sediment estimation models using a data-driven algorithm 79, 94–103. https://doi.org/10.1016/j.matcom.2007.10.005
Kişi, Ö., 2010. River suspended sediment concentration modeling using a neural differential evolution approach. J. Hydrol. 389, 227–235. https://doi.org/10.1016/j.jhydrol.2010.06.003
Kisi, Ö., Çobaner, M., 2009. Modeling river stage-discharge relationships using different neural network computing techniques. Clean - Soil, Air, Water 37, 160–169. https://doi.org/10.1002/clen.200800010
Kisi, O., Dailr, A.H., Cimen, M., Shiri, J., 2012. Suspended sediment modeling using genetic programming and soft computing techniques. J. Hydrol. 450–451, 48–58. https://doi.org/10.1016/j.jhydrol.2012.05.031
Kisi, O., Shiri, J., 2012. River suspended sediment estimation by climatic variables implication: Comparative study among soft computing techniques. Comput. Geosci. 43, 73–82.

https://doi.org/10.1016/j.cageo.2012.02.007
Koltsida, E., Mamassis, N., Kallioras, A., 2021. Hydrological modeling using the SWAT Model in urban and peri- urban environments : The case of Kifissos experimental sub-basin 1–24.
Konan-waidhet, A.B., 2023. Using the SWAT + model to assess the conditions of water inflow to a reservoir in an uncontrolled agricultural catchment . Case Study of the Nanan Reservoir in the Lake Taabo catchme ... Ecohydrol. Hydrobiol. https://doi.org/10.1016/j.ecohyd.2023.08.002
Koneti, S., Sunkara, S.L., Roy, P.S., 2018. Hydrological modeling with respect to impact of land-use and land-cover change on the runoff dynamics in Godavari river basin using the HEC-HMS model. ISPRS Int. J. Geo-Information 7. https://doi.org/10.3390/ijgi7060206
Kuma, H.G., Chinasho, E.M., Tolke, A.A., 2024. Assessment of sediment yield and accumulation in reservoir: The case of Gibe One Reservoir, Southwestern Ethiopia. Heliyon 10, e36315. https://doi.org/10.1016/j.heliyon.2024.e36315
Kuma, H.G., Feyessa, F.F., Demissie, T.A., 2023. Assessing the impacts of land use / land cover changes on hydrological processes in Southern Ethiopia : The SWAT model approach Assessing the impacts of land use / land cover changes on hydrological processes in Southern Ethiopia : The SWAT model approach. Cogent Eng. 10. https://doi.org/10.1080/23311916.2023.2199508
Lee, F.-Z., Du, Y.-Y., 2025. Desilting Efficiency Assessment Under Four Hydraulic Sediment Prevention Operations. Water Resour. Manag. https://doi.org/10.1007/s11269-025-04161-2
Lemma, H., Adgo, E., Poesen, J., Nyssen, J., 2019a. Identifying erosion hotspots in Lake Tana Basin from a multisite Soil and Water Assessment Tool validation : Opportunity for land managers 1449–1467. https://doi.org/10.1002/ldr.3332
Lemma, H., Frankl, A., van Griensven, A., Poesen, J., Adgo, E., Nyssen, J., 2019b. Identifying erosion hotspots in Lake Tana Basin from a multisite Soil and Water Assessment Tool validation: Opportunity for land managers. L. Degrad. Dev. 30, 1449–1467. https://doi.org/10.1002/ldr.3332
Leo Breiman, Jerome Friedman, R.A. Olshen, C.J.S., 1984. Classification and Regression Trees. Mathematics & Statistics.
Leta, M.K., Waseem, M., Rehman, K., Tränckner, J., 2023. Sediment yield estimation and evaluating the best management practices in Nashe watershed, Blue Nile Basin, Ethiopia. Environ. Monit. Assess. 195. https://doi.org/10.1007/s10661-023-11337-z
Li, X., Wang, H. et al., 2014. Soil erosion and sediment yield prediction at the basin scale in the upstream watershed of the Miyun reservoir. https://doi.org/10.1061/(ASCE)HE.1943-5584.0001098
Liu, Y., Yang, W., Yu, Z., Lung, I., Gharabaghi, B., 2015. Estimating Sediment Yield from Upland and Channel Erosion at A Watershed Scale Using SWAT. Water Resour. Manag. 29, 1399–1412. https://doi.org/10.1007/s11269-014-0729-5
Luvai, A., Obiero, J., Omuto, C., 2022. Soil Loss Assessment Using the Revised Universal Soil Loss Equation (RUSLE) Model. Appl. Environ. Soil Sci. 2022. https://doi.org/10.1155/2022/2122554
Mariye, M., Mariyo, M., Changming, Y., Teffera, Z.L., Weldegebrial, B., 2022. Effects of land use and land cover change on soil erosion potential in Berhe district: a case study of Legedadi watershed, Ethiopia. Int. J. River Basin Manag. 20, 79–91. https://doi.org/10.1080/15715124.2020.1767636
McCartney, M.P., Menker Girma, M., 2012. Evaluating the downstream implications of planned

water resource development in the Ethiopian portion of the Blue Nile River. Water Int. 37, 362–379. https://doi.org/10.1080/02508060.2012.706384
Mekonnen, M., Keesstra, S.D., Baartman, J.E., Ritsema, C.J., Melesse, A.M., 2015. EVALUATING SEDIMENT STORAGE DAMS : STRUCTURAL OFF-SITE SEDIMENT TRAPPING MEASURES IN NORTHWEST ETHIOPIA 41, 7–22. https://doi.org/10.18172/cig.2643
Melesse, A.M., Abtew, W., Setegn, S.G., 2013. Nile River Basin: Ecohydrological challenges, climate change and hydropolitics. Nile River Basin Ecohydrol. Challenges, Clim. Chang. Hydropolitics 1–718. https://doi.org/10.1007/978-3-319-02720-3
Melesse, A.M., Ahmad, S., McClain, M.E., Wang, X., Lim, Y.H., 2011. Suspended sediment load prediction of river systems: An artificial neural network approach. Agric. Water Manag. 98, 855–866. https://doi.org/10.1016/j.agwat.2010.12.012
Mersha, A.N., Masih, I., de Fraiture, C., Wenninger, J., Alamirew, T., 2018. Evaluating the impacts of IWRM policy actions on demand satisfaction and downstream water availability in the Upper Awash Basin, Ethiopia. Water (Switzerland) 10. https://doi.org/10.3390/w10070892
Miller, V.C., 1953. A quantitative geomorphic study of drainage basin characteristic in the clinch, Mountain area, Verdinia and Tennesser, Project NR 389-042, Tech. Rept. 3 Columbia Univ. Dep. Geol. ONR, Geogr. Branch, New York.
Ministry of Finance and Economic Development (MoFED), 2006. Plan for Accelerated and Sustained Development to End Poverty (2005/06-2009/10): Plan for Urban Development and Urban Good Governance. Plan Accel. Sustain. Dev. to End Poverty I, 278.
Moghaddamnia, A., Ghafari Gousheh, M., Piri, J., Amin, S., Han, D., 2009. Evaporation estimation using artificial neural networks and adaptive neuro-fuzzy inference system techniques. Adv. Water Resour. 32, 88–97. https://doi.org/10.1016/j.advwatres.2008.10.005
Mohammadi, A.A., Yousefi, M., Soltani, J., Ahangar, A.G., Javan, S., 2018. Using the combined model of gamma test and neuro-fuzzy system for modeling and estimating lead bonds in reservoir sediments. Environ. Sci. Pollut. Res. 25, 30315–30324. https://doi.org/10.1007/s11356-018-3026-7
Moriasi, D.N., Arnold, J.G., Liew, M.W. Van, Bingner, R.L., Harmel, R.D., Veith, T.L., 2007a. M e g s q a w s 50, 885–900.
Moriasi, D.N., Arnold, J.G., Liew, M.W. Van, Bingner, R.L., Harmel, R.D., Veith, T.L., 2007b. MODEL EVALUATION GUIDELINES FOR SYSTEMATIC QUANTIFICATION OF ACCURACY IN WATERSHED SIMULATIONS. Am. Soc. Agric. Biol. Eng. ISSN 0001−2351 885 50, 885–900.
Moriasi, D.N., Wilson, B.N., Arnold, J.G., Gowda, P.H., 2012. H w q m : u , c , v 55, 1241–1247.
Mosbahi, M., Benabdallah, S., 2020. Assessment of land management practices on soil erosion using SWAT model in a Tunisian semi-arid catchment. J. Soils Sediments 20, 1129–1139. https://doi.org/10.1007/s11368-019-02443-y
Munoth, P., Goyal, R., 2019. Impacts of land use land cover change on runoff and sediment yield of Upper Tapi River Sub-Basin ,. Intl. J. River Basin Manag. 0, 1–13. https://doi.org/10.1080/15715124.2019.1613413
MYermolaev, O., Mukharamova, S., 2023. Statistical Analysis and Modeling of Suspended Sediment Yield Dependence on Environmental Conditions. Water (Switzerland) 15. https://doi.org/10.3390/w15142639

Nacar, S., Hınıs, M.A., Kankal, M., 2018. Forecasting Daily Streamflow Discharges Using Various Neural Network Models and Training Algorithms. KSCE J. Civ. Eng. 22, 3676–3685. https://doi.org/10.1007/s12205-017-1933-7

Nadew', B., Chaniyalew, E., Tsegaye, T., 2019. Runoff Sediment Yield Modeling and Development of Management Intervention Scenarios, Case Study of Guder Watershed, Blue Nile Basin, Ethiopia. Hydrol. Curr. Res. 9, 0–16. https://doi.org/10.4172/2157-7587.1000306

Nash, J.E., Sutcliffe, J. V., 1970. River flow forecasting through conceptual models part I - A discussion of principles. J. Hydrol. 10, 282–290. https://doi.org/10.1016/0022-1694(70)90255-6

Nawazuzzoha, M., Rashid, M.M., Mishra, P.K., Abdelrahman, K., Fnais, M.S., Naqvi, H.R., 2024. Empirical Modeling of Soil Loss and Yield Utilizing RUSLE and SYI: A Geospatial Study in South Sikkim, Teesta Basin. Land 13, 1–17. https://doi.org/10.3390/land13101621

Nda, M., Adnan, M.S., Azlan, M., Mohd, B., Nda, R.M., 2023. An Overview of Machine Learning Techniques for Sediment Prediction †. 4th Int. Electron. Conf. Appl. Sci. 1–10.

Negatu, T.A., Zimale, F.A., Steenhuis, T.S., 2022. Establishing Stage–Discharge Rating Curves in Developing Countries: Lake Tana Basin, Ethiopia. Hydrology 9, 1–26. https://doi.org/10.3390/hydrology9010013

Negewo, T.F., Sarma, A.K., 2023. Sustainable and Cost-Effective Management of Degraded Sub-Watersheds using Ecological Management Practices (EMPs) for Genale Basin, Ethiopia. J. Hydrol. 619, 129289. https://doi.org/10.1016/j.jhydrol.2023.129289

Nhu, V.H., Khosravi, K., Cooper, J.R., Karimi, M., Kisi, O., Pham, B.T., Lyu, Z., 2020. Monthly suspended sediment load prediction using artificial intelligence: testing of a new random subspace method. Hydrol. Sci. J. 65, 2116–2127. https://doi.org/10.1080/02626667.2020.1754419

Nkwasa, A., Chawanda, C.J., van Griensven, A., 2022. Regionalization of the SWAT+ model for projecting climate change impacts on sediment yield: An application in the Nile basin. J. Hydrol. Reg. Stud. 42, 101152. https://doi.org/10.1016/j.ejrh.2022.101152

Noori, R., Karbassi, A.R., Moghaddamnia, A., Han, D., Zokaei-Ashtiani, M.H., Farokhnia, A., Gousheh, M.G., 2011. Assessment of input variables determination on the SVM model performance using PCA, Gamma test, and forward selection techniques for monthly stream flow prediction. J. Hydrol. 401, 177–189. https://doi.org/10.1016/j.jhydrol.2011.02.021

Nyssen, J., Poesen, J., Moeyersons, J., Deckers, J., Haile, M., Lang, A., 2004. Human impact on the environment in the Ethiopian and Eritrean highlands — a state of the art 64, 273–320. https://doi.org/10.1016/S0012-8252(03)00078-3

Olyaie, E., Banejad, H., Chau, K.W., Melesse, A.M., 2015. A comparison of various artificial intelligence approaches performance for estimating suspended sediment load of river systems: a case study in United States. Environ. Monit. Assess. 187. https://doi.org/10.1007/s10661-015-4381-1

Oyebode, O., Stretch, D., 2019. Neural network modeling of hydrological systems: A review of implementation techniques. Nat. Resour. Model. 32, e12189. https://doi.org/https://doi.org/10.1111/nrm.12189

Pandey, A., Himanshu, S.K., Mishra, S.K., Singh, V.P., 2016. Physically based soil erosion and sediment yield models revisited. Catena 147, 595–620. https://doi.org/10.1016/j.catena.2016.08.002

Pektas, A.O., Cigizoglu, H.K., 2017. Investigating the extrapolation performance of neural

network models in suspended sediment data. Hydrol. Sci. J. 62, 1694–1703. https://doi.org/10.1080/02626667.2017.1349316
Perera, D., Williams, S., Smakhtin, V., 2023. Present and Future Losses of Storage in Large Reservoirs Due to Sedimentation: A Country-Wise Global Assessment. Sustain. 15. https://doi.org/10.3390/su15010219
Praskievicz, S., Luo, C., 2020. Assessment of flow–ecology relationships for environmental flow standards: a synthesis focused on the southeast USA. Hydrol. Sci. J. 65, 571–582. https://doi.org/10.1080/02626667.2020.1714051
Ramsankaran, R., Kothyari, U.C., Ghosh, S.K., Malcherek, A., Murugesan, K., 2013. Modèle distribué à bases physiques d'érosion des sols et de production de sédiments (DREAM) pour la simulation d'événements particuliers. Hydrol. Sci. J. 58, 872–891. https://doi.org/10.1080/02626667.2013.781606
Razi, M.A., Athappilly, K., 2005. A comparative predictive analysis of neural networks (NNs), nonlinear regression and classification and regression tree (CART) models. Expert Syst. Appl. 29, 65–74. https://doi.org/10.1016/j.eswa.2005.01.006
Risal, A., Parajuli, P.B., 2022. Evaluation of the Impact of Best Management Practices on Streamflow, Sediment and Nutrient Yield at Field and Watershed Scales. Water Resour. Manag. 36, 1093–1105. https://doi.org/10.1007/s11269-022-03075-7
Roba, N.T., Kassa, A.K., Geleta, D.Y., Harka, A.E., 2021. Streamflow and sediment yield estimation, and area prioritization for better conservation planning in the Dawe River watershed of the Wabi Shebelle River Basin, Ethiopia. Heliyon 7, e08509. https://doi.org/10.1016/j.heliyon.2021.e08509
Roth, V., Nigussie, T.K., Lemann, T., 2016. Model parameter transfer for streamflow and sediment loss prediction with SWAT in a tropical watershed. Environ. Earth Sci. 75. https://doi.org/10.1007/s12665-016-6129-9
S.L. Neitsch, J.G. Arnold, J.R. Kiniry, J.R.W., 2009. Soil & Water Assessment Tool Theoretical Documentation Version 2009.
Sab-basin, U.A., Daba, M.H., 2018. Sensitivity of SWAT Simulated Runoff to Temperature and Rainfall in the 9, 1–7. https://doi.org/10.4172/2157-7587.1000293
Samantaray, S., Ghose, D.K., 2018. Evaluation of suspended sediment concentration using descent neural networks. Procedia Comput. Sci. 132, 1824–1831. https://doi.org/10.1016/j.procs.2018.05.138
Samy, A., Ibrahim, M.G., Mahmod, W.E., Fujii, M., Eltawil, A., Daoud, W., 2019. Statistical assessment of rainfall characteristics in upper Blue Nile basin over the period from 1953 to 2014. Water (Switzerland) 11. https://doi.org/10.3390/w11030468
Santhi, C., Arnold, J.G., Williams, J.R., Dugas, W.A., Srinivasan, R., Hauck, L.M., 2001. Validation of the SWAT model on a large river basin with point and nonpoint sources. J. Am. Water Resour. Assoc. 37, 1169–1188. https://doi.org/10.1111/j.1752-1688.2001.tb03630.x
Schumm, S.A., 1956. Geological Society of America Bulletin EVOLUTION OF DRAINAGE SYSTEMS AND SLOPES IN BADLANDS AT PERTH AMBOY , NEW JERSEY. Bull. Geol. Soc. Am. 67, 597–646. https://doi.org/10.1130/0016-7606(1956)67
Setegn, S.G., 2014. H YDROLOGICAL AND S EDIMENT YIELD M ODELLING IN L AKE T ANA B ASIN ,.
Setegn, S.G., Dargahi, B., Srinivasan, R., Melesse, A.M., 2010. MODELING OF SEDIMENT YIELD FROM ANJENI-GAUGED 46, 514–526.

Sharifi Garmdareh, E., Vafakhah, M., Eslamian, S.S., 2018. Regional flood frequency analysis using support vector regression in arid and semi-arid regions of Iran. Hydrol. Sci. J. 63, 426–440. https://doi.org/10.1080/02626667.2018.1432056
Sharma, M.J., Yu, S.J., 2015. Stepwise regression data envelopment analysis for variable reduction. Appl. Math. Comput. 253, 126–134. https://doi.org/10.1016/j.amc.2014.12.050
Sharma, S.K., Gajbhiye, S., Tignath, S., 2015. Application of principal component analysis in grouping geomorphic parameters of a watershed for hydrological modeling. Appl. Water Sci. 5, 89–96. https://doi.org/10.1007/s13201-014-0170-1
Shawul, A.A., Chakma, S., 2019. Spatiotemporal detection of land use/land cover change in the large basin using integrated approaches of remote sensing and GIS in the Upper Awash basin, Ethiopia. Environ. Earth Sci. 78, 0. https://doi.org/10.1007/s12665-019-8154-y
Shiau, J.T., Chen, T.J., 2015. Quantile Regression-Based Probabilistic Estimation Scheme for Daily and Annual Suspended Sediment Loads. Water Resour. Manag. 29, 2805–2818. https://doi.org/10.1007/s11269-015-0971-5
Singh, A., Imtiyaz, M., Isaac, R.K., Denis, D.M., 2012. Comparison of soil and water assessment tool (SWAT) and multilayer perceptron (MLP) artificial neural network for predicting sediment yield in the Nagwa agricultural watershed in Jharkhand, India. Agric. Water Manag. 104, 113–120. https://doi.org/10.1016/j.agwat.2011.12.005
Singh, R.K., Panda, R.K., Satapathy, K.K., Ngachan, S. V., 2011. Simulation of runoff and sediment yield from a hilly watershed in the eastern Himalaya, India using the WEPP model. J. Hydrol. 405, 261–276. https://doi.org/10.1016/j.jhydrol.2011.05.022
Singh, S., Singh, M.C., 1997. Morphometric analysis of Kanhar river basin. Natl. Geogr. J. india 43, 31–43.
Singh, V.K., Kumar, D., Kashyap, P.S., Kisi, O., 2018. Simulation of suspended sediment based on gamma test, heuristic, and regression-based techniques. Environ. Earth Sci. 77, 1–14. https://doi.org/10.1007/s12665-018-7892-6
Sinshaw, B.G., Belete, A.M., Mekonen, B.M., Wubetu, T.G., 2021. Watershed-based soil erosion and sediment yield modeling in the Rib watershed of the Upper Blue Nile Basin , Ethiopia Watershed-based soil erosion and sediment yield modeling in the Rib watershed of the Upper Blue Nile Basin , Ethiopia. Energy Nexus 3, 100023. https://doi.org/10.1016/j.nexus.2021.100023
Sokchhay, H., 2013. Investigation on Applicability of Data-Driven Models in Ungauged Catchments: Sediment Yield Prediction. Earth Resour. 1, 37. https://doi.org/10.12966/er.07.01.2013
Sušanj Čule, I., Ožanić, N., Volf, G., Karleuša, B., 2025. Artificial Neural Network (ANN) Water-Level Prediction Model as a Tool for the Sustainable Management of the Vrana Lake (Croatia) Water Supply System. Sustain. 17. https://doi.org/10.3390/su17020722
Swain, J.B., Patra, K.C. et al., 2017. Streamflow estimation in ungauged catchments using regionalization techniques. J. Hydrol. 554, 420–433. https://doi.org/10.1016/j.jhydrol.2017.08.054
Talebizadeh, M., Morid, S., Ayyoubzadeh, S.A., Ghasemzadeh, M., 2010. Uncertainty analysis in sediment load modeling using ANN and SWAT model. Water Resour. Manag. 24, 1747–1761. https://doi.org/10.1007/s11269-009-9522-2
Tamene, L., Park, S. J., Dikau, R., & Vlek, P.L.G., 2006. Reservoir siltation in the semi-arid highlands of northern ethiopia: sediment yield–catchment area relationship and a semi-quantitative approach for predicting sediment yield. Earth Surf. Process. Landforms 31,

1364–1383. https://doi.org/https://doi.org/10.1002/esp.1338
Tamene, L., Adimassu, Z., Aynekulu, E., Yaekob, T., 2017. Estimating landscape susceptibility to soil erosion using a GIS-based approach in Northern Ethiopia. Int. Soil Water Conserv. Res. 5, 221–230. https://doi.org/10.1016/j.iswcr.2017.05.002
Tamene, L., Vlek, P.L.G., 2008. Soil erosion studies in Northern Ethiopia. L. Use Soil Resour. 73–100. https://doi.org/10.1007/978-1-4020-6778-5_5
Tamene, L., Vlek, P.L.G., 2007. Assessing the potential of changing land use for reducing soil erosion and sediment yield of catchments: A case study in the highlands of northern Ethiopia. Soil Use Manag. 23, 82–91. https://doi.org/10.1111/j.1475-2743.2006.00066.x
Tao, H., Al-Khafaji, Z.S., Qi, C., Zounemat-Kermani, M., Kisi, O., Tiyasha, T., Chau, K.W., Nourani, V., Melesse, A.M., Elhakeem, M., Farooque, A.A., Pouyan Nejadhashemi, A., Khedher, K.M., Alawi, O.A., Deo, R.C., Shahid, S., Singh, V.P., Yaseen, Z.M., 2021. Artificial intelligence models for suspended river sediment prediction: state-of-the art, modeling framework appraisal, and proposed future research directions. Eng. Appl. Comput. Fluid Mech. 15, 1585–1612. https://doi.org/10.1080/19942060.2021.1984992
Tayfur, G., 2009. Artificial neural networks for sheet sediment transport 6667. https://doi.org/10.1080/02626660209492997
Taylor, P., Chandra, P., Patel, P.L., Porey, P.D., Gupta, I.D., n.d. ISH Journal of Hydraulic Engineering Estimation of sediment yield using SWAT model for Upper Tapi basin 37–41. https://doi.org/10.1080/09715010.2014.902170
Tebebu, T.Y., Abiy, A.Z., Zegeye, A.D., Dahlke, H.E., Easton, Z.M., Tilahun, S.A., Collick, A.S., 2010. Surface and subsurface flow effect on permanent gully formation and upland erosion near Lake Tana in the northern highlands of 2207–2217. https://doi.org/10.5194/hess-14-2207-2010
Tebebu, T.Y., Steenhuis, T.S., Dagnew, D.C., Guzman, C.D., Bayabil, H.K., Zegeye, A.D., Collick, A.S., Langan, S., MacAlister, C., Langendoen, E.J., Yitaferu, B., Tilahun, S.A., 2015. Improving efficacy of landscape interventions in the (sub) humid Ethiopian highlands by improved understanding of runoff processes. Front. Earth Sci. 3, 1–13. https://doi.org/10.3389/feart.2015.00049
Tesema, T.A., Choy Lam, K., GebreMariam, B., Tefere, W.M., 2021. Multi-site calibration of SWAT for the spatial distribution of sediment yield, Middle Awash Dam watershed, Ethiopia. Malaysian J. Soc. Sp. 17, 256–273. https://doi.org/10.17576/geo-2021-1704-18
Tesema, T.A., Leta, O.T., 2020. Sediment Yield Estimation and Effect of Management Options on Sediment Yield of Kesem Dam Watershed, Awash Basin, Ethiopia. Sci. African 9, e00425. https://doi.org/10.1016/j.sciaf.2020.e00425
Tessema, N., Kebede, A., Yadeta, D., 2021. Modelling the effects of climate change on streamflow using climate and hydrological models: the case of the Kesem sub-basin of the Awash River basin, Ethiopia. Int. J. River Basin Manag. 19, 469–480. https://doi.org/10.1080/15715124.2020.1755301
Tessema, Y.M., Zimale, F.A., Kebedew, M.G., 2024. Understanding sedimentation trends to enhance sustainable reservoir management in the Angereb reservoir, Upper Blue Nile Basin, Ethiopia. Front. Water 6. https://doi.org/10.3389/frwa.2024.1387915
Tibebe, D., Bewket, W., 2011. Surface runoff and soil erosion estimation using the SWAT model in the Keleta Watershed, Ethiopia. L. Degrad. Dev. 22, 551–564. https://doi.org/10.1002/ldr.1034
Tsegaye, L., Bharti, R., 2021. Soil erosion and sediment yield assessment using RUSLE and

GIS-based approach in Anjeb watershed, Northwest Ethiopia. SN Appl. Sci. 3, 1–19. https://doi.org/10.1007/s42452-021-04564-x
Tumsa, B.C., Feyessa, F.F., Tullu, K.T., Guder, A.C., 2023. Spatiotemporal changes of land use in response to runoff and sediment yield for environmental sustainability in the upper Blue Nile Basin, Oromiyaa, Ethiopia. H2Open J. 6, 551–575. https://doi.org/10.2166/h2oj.2023.072
Tumsa, B.C., Kenea, G., Tola, B., 2022. Heliyon The application of SWAT þ model to quantify the impacts of sensitive LULC changes on water balance in Guder catchment , Oromia , Ethiopia. Heliyon 8, e12569. https://doi.org/10.1016/j.heliyon.2022.e12569
Vanmaercke, M., Poesen, J., Verstraeten, G., de Vente, J., Ocakoglu, F., 2011. Sediment yield in Europe: Spatial patterns and scale dependency. Geomorphology 130, 142–161. https://doi.org/10.1016/j.geomorph.2011.03.010
Vigiak, O., Malagó, A., Bouraoui, F., Vanmaercke, M., Obreja, F., Poesen, J., Habersack, H., Fehér, J., Grošelj, S., 2017. Modelling sediment fluxes in the Danube River Basin with SWAT. Sci. Total Environ. 599–600, 992–1012. https://doi.org/10.1016/j.scitotenv.2017.04.236
Vigiak, O., Malagó, A., Bouraoui, F., Vanmaercke, M., Poesen, J., 2015. Adapting SWAT hillslope erosion model to predict sediment concentrations and yields in large Basins. Sci. Total Environ. 538, 855–875. https://doi.org/10.1016/j.scitotenv.2015.08.095
Ward, P.J., de Ruiter, M.C., Mård, J., Schröter, K., Van Loon, A., Veldkamp, T., von Uexkull, N., Wanders, N., AghaKouchak, A., Arnbjerg-Nielsen, K., Capewell, L., Carmen Llasat, M., Day, R., Dewals, B., Di Baldassarre, G., Huning, L.S., Kreibich, H., Mazzoleni, M., Savelli, E., Teutschbein, C., van den Berg, H., van der Heijden, A., Vincken, J.M.R., Waterloo, M.J., Wens, M., 2020. The need to integrate flood and drought disaster risk reduction strategies. Water Secur. 11. https://doi.org/10.1016/j.wasec.2020.100070
Welde, K., Gebremariam, B., 2017. Effect of land use land cover dynamics on hydrological response of watershed: Case study of Tekeze Dam watershed, northern Ethiopia. Int. Soil Water Conserv. Res. 5, 1–16. https://doi.org/10.1016/j.iswcr.2017.03.002
Wicks, J.M., Bathurst, J.C., 1996. SHESED: A physically based, distributed erosion and sediment yield component for the SHE hydrological modelling system. J. Hydrol. 175, 213–238. https://doi.org/10.1016/S0022-1694(96)80012-6
Wilby, R.L., Abrahart, R.J., Dawson, C.W., 2003. Detection of conceptual model rainfall-runoff processes inside an artificial neural network. Hydrol. Sci. J. 48, 163–181. https://doi.org/10.1623/hysj.48.2.163.44699
Williams, J.R., 1975. Sediment-Yield Prediction with Universal Equation Using Runoff Energy Factor. In: Present and Prospective Technology for Predicting Sediment Yield and Sources. US Dep. Agric. Agric. Res. Serv. Washingt. DC Vol.6, 244–252.
Womber, Z.R., Zimale, F.A., Kebedew, M.G., Asers, B.W., Deluca, N.M., Guzman, C.D., Tilahun, S.A., Zaitchik, B.F., 2021. Estimation of Suspended Sediment Concentration from Remote Sensing and in Situ Measurement over Lake Tana, Ethiopia. Adv. Civ. Eng. 2021. https://doi.org/10.1155/2021/9948780
Wu, J., Yen, H., Arnold, J.G., Yang, Y.C.E., Cai, X., White, M.J., Santhi, C., Miao, C., Srinivasan, R., 2020. Development of reservoir operation functions in SWAT+ for national environmental assessments. J. Hydrol. 583, 124556. https://doi.org/10.1016/j.jhydrol.2020.124556
Wuttichaikitcharoen, P., Babel, M.S., 2014. Principal component and multiple regression

analyses for the estimation of suspended sediment yield in ungauged basins of Northern Thailand. Water (Switzerland) 6, 2412–2435. https://doi.org/10.3390/w6082412
Yadav, A., Chithaluru, P., Singh, A., Joshi, D., Elkamchouchi, D.H., P, C.M., Anand, D., 2022a. An Enhanced Feed-Forward Back Propagation Levenberg – Marquardt Algorithm for Suspended Sediment Yield Modeling.
Yadav, A., Hasan, M.K., Joshi, D., Kumar, V., 2022b. Optimized Scenario for Estimating Suspended Sediment Yield Using an Artificial Neural Network Coupled with a.
Yasarer, L.M.W., Sturm, B.S.M., 2016. Potential impacts of climate change on reservoir services and management approaches. Lake Reserv. Manag. 32, 13–26. https://doi.org/10.1080/10402381.2015.1107665
Yen, H., Park, S., Arnold, G., Srinivasan, R., Chawanda, C.J., Wang, R., Feng, Q., Wu, J., Miao, C., Bieger, K., Daggupati, P., Griensven, A. Van, Kalin, L., Lee, S., 2019. IPEAT + : A Built-In Optimization and Automatic Calibration Tool of SWAT + 1–17.
Yesuph, A.Y., Dagnew, A.B., 2019. Soil erosion mapping and severity analysis based on RUSLE model and local perception in the Beshillo Catchment of the Blue Nile Basin, Ethiopia. Environ. Syst. Res. 8, 1–21. https://doi.org/10.1186/s40068-019-0145-1
Zalaki-badil, N., Eslamian, S., Sayyad, G., Hosseini, S., 2017. Using SWAT Model to Determine Runoff, Sediment Yield in Maroon-Dam Catchment. Int. J. Res. Stud. Agric. Sci. 3, 31–41. https://doi.org/10.20431/2454-6224.0312004
Zantet, M., Sambeto, T., Abdulkerim, E., 2023. Heliyon Evaluation of best management practices to reduce sediment yield in the upper Gilo watershed , Baro akobo basin , Ethiopia using SWAT. Heliyon 9, e20326. https://doi.org/10.1016/j.heliyon.2023.e20326
Zantet o, M., Takele, S., A, E., 2023. Evaluation of best management practices to reduce sediment yield in the upper Gilo watershed, Baro akobo basin, Ethiopia using SWAT. Heliyon 9, e20326. https://doi.org/10.1016/j.heliyon.2023.e20326
Zema, D.A., Bingner, R.L., Denisi, P., Govers, G., Licciardello, F., Zimbone, S.M., 2010. EVALUATION OF RUNOFF , PEAK FLOW AND SEDIMENT YIELD FOR EVENTS SIMULATED BY THE ANNAGNPS MODEL IN A BELGIAN AGRICULTURAL WATERSHED y.
Zhang, D., Lu, G., 2004. Review of shape representation and description techniques. Pattern Recognit. 37, 1–19. https://doi.org/10.1016/j.patcog.2003.07.008
Zinabu, E., Kelderman, P., van der Kwast, J., Irvine, K., 2019. Monitoring river water and sediments within a changing Ethiopian catchment to support sustainable development. Environ. Monit. Assess. 191. https://doi.org/10.1007/s10661-019-7545-6
Zounemat-Kermani, M., Kişi, Ö., Adamowski, J., Ramezani-Charmahineh, A., 2016. Evaluation of data driven models for river suspended sediment concentration modeling. J. Hydrol. 535, 457–472. https://doi.org/10.1016/j.jhydrol.2016.02.012

Appendix

Satellite image of the Koka watershed from 2005,2010 and 2015

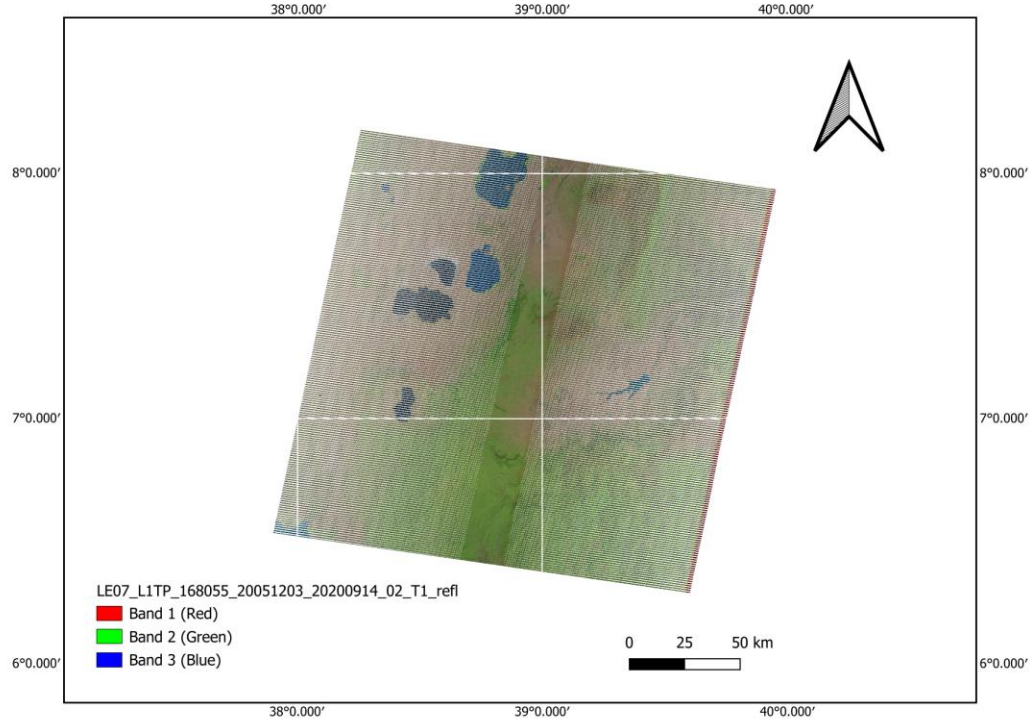

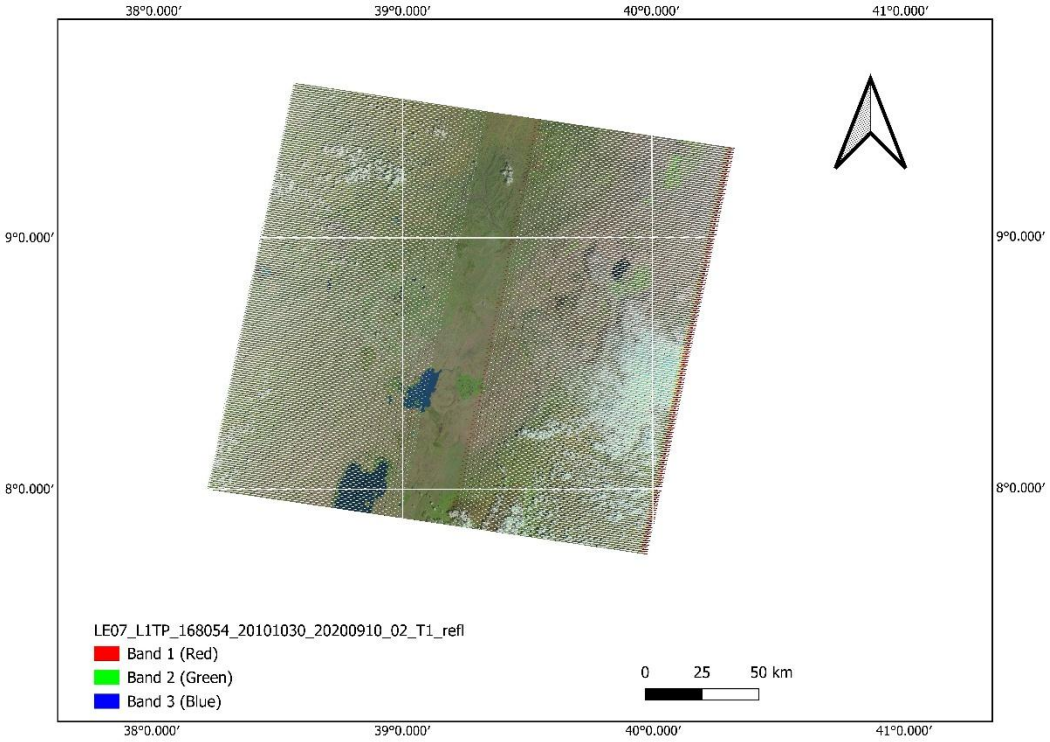

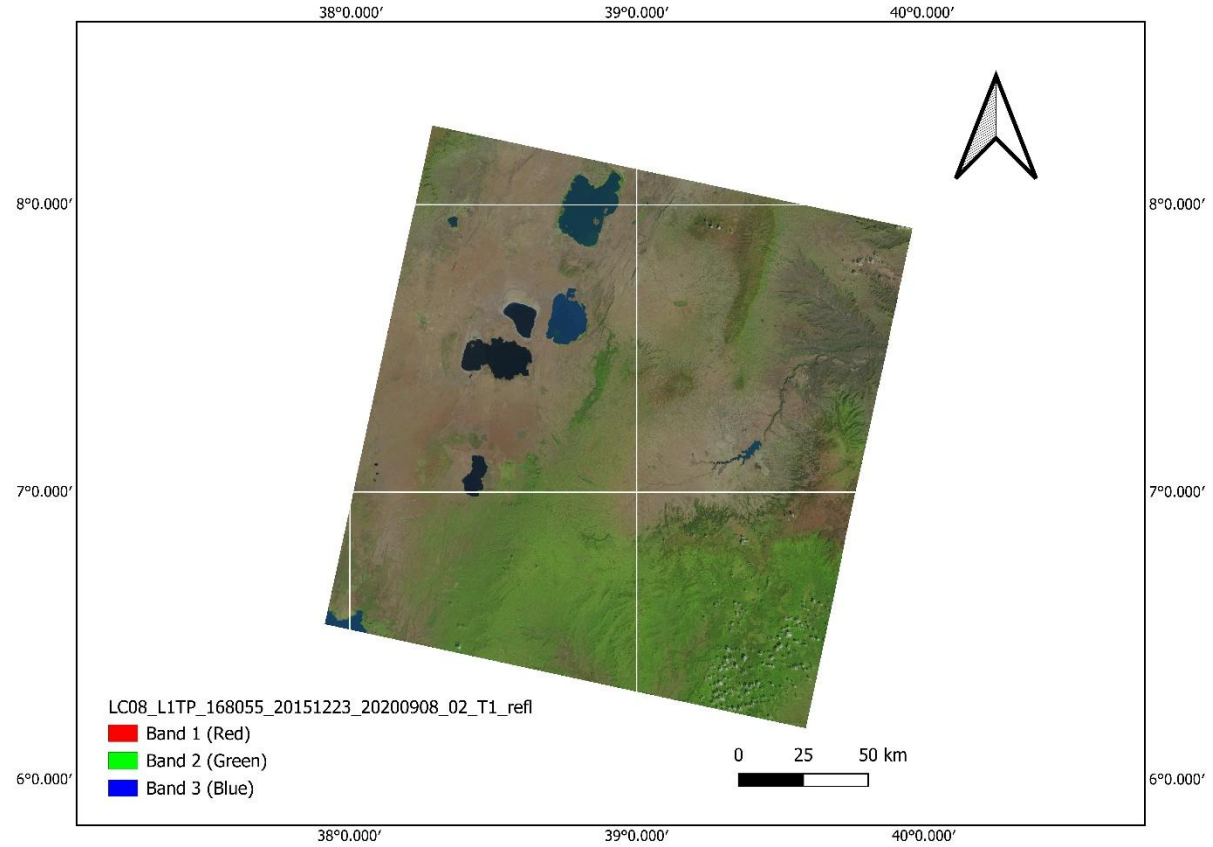

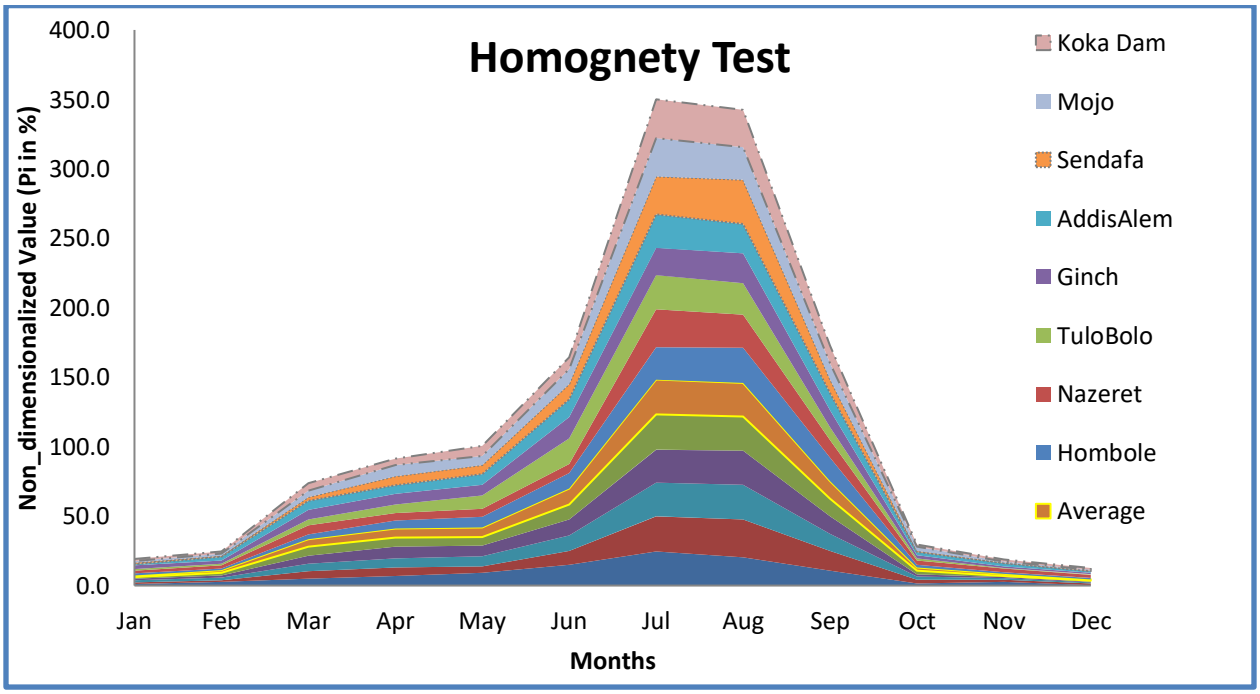

Testing the homogeneity of rainfall contributions to the Koka watershed

Annual precipitation that contributed to the Kessie watershed starting from 2000 to 2016

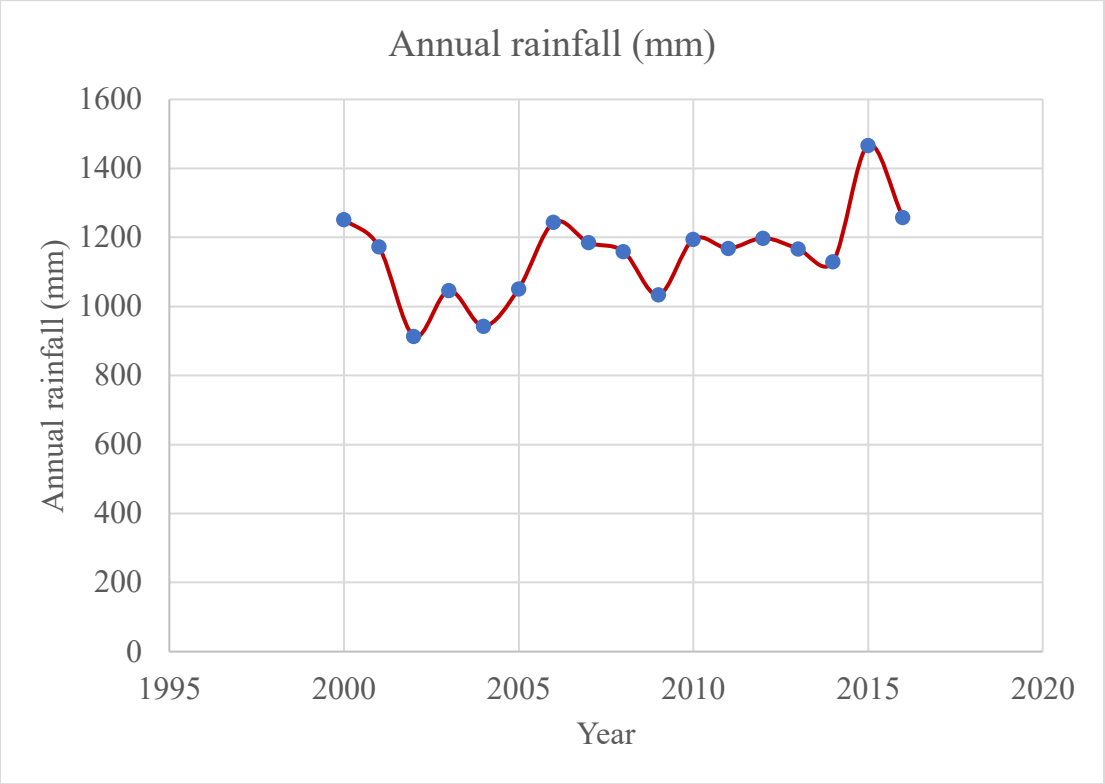

Flow data at Kessie gauge stations

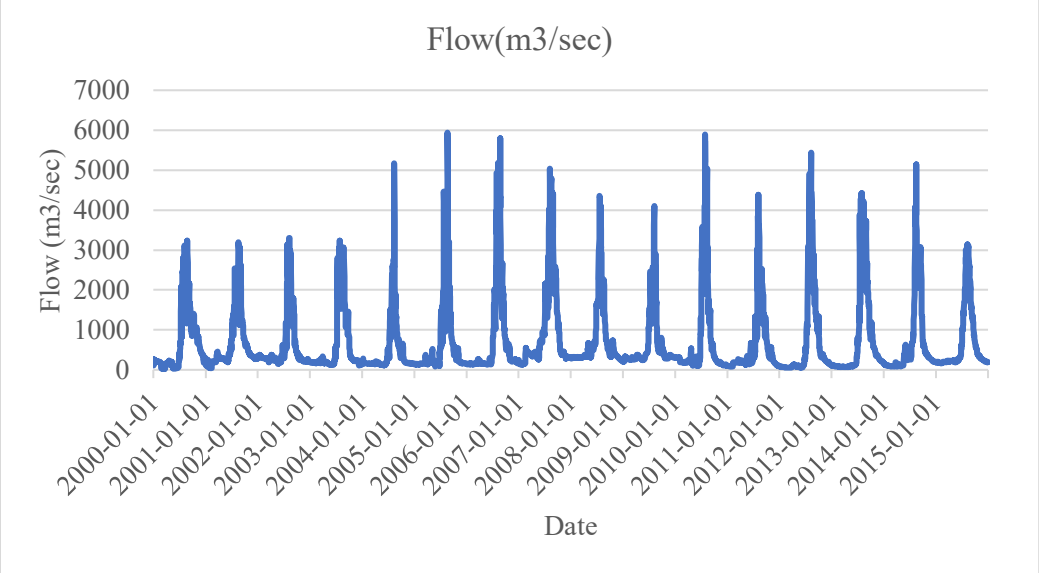

Sediment data at Kessie gauge stations